

**STUDIES ON THERMAL DECOMPOSITION
OF SOME INORGANIC BROMATES BY DYNAMIC
THERMOGRAVIMETRY**

**Thesis submitted to the University of Calicut
in partial fulfilment of the requirement for the
degree of**

***DOCTOR OF PHILOSOPHY*
in
*CHEMISTRY***

by

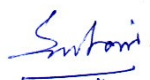
DEVADASAN K K

**Department of Chemistry
University of Calicut, Kerala - 673635**

July 2009

Certificate

This is to certify that the thesis entitled *Studies On Thermal Decomposition Of Some Inorganic Bromates By Dynamic Thermogravimetry* bound herewith is an authentic record of the research work carried out by Sri. Devadasan K.K under our supervision in partial fulfillment of the requirement for the degree of **Doctor of Philosophy** in Chemistry of the University of Calicut and further that this work or part thereof has not been presented earlier for the award of any other degree.



Dr. S. Madhavankutty Nair
Retd. Professor, Department of Chemistry
University of Calicut
(Supervising Teacher)




Dr. M. S. Krishnan
Retd. Reader, Department of Chemistry
University of Calicut
(Supervising Teacher)

Declaration

*It is hereby declared that the results of the investigations reported in this thesis entitled **Studies on Thermal Decomposition of Some Inorganic Bromates by Dynamic Thermogravimetry** have not been presented previously for the award of any other degree.*

Department of Chemistry
University of Calicut
10 July 2009

A handwritten signature in blue ink, appearing to read 'Devadasan K K', is written over a horizontal blue line.

Devadasan K K

Acknowledgement

I have great pleasure to record my sincere and heartfelt gratitude to my supervising teachers Dr. S. Madhavankutty Nair, Retired Professor, Department of Chemistry, University of Calicut and Dr. M.S. Krishnan, Retired Reader, Department of Chemistry, University of Calicut for the valuable guidance, sustained help, expert discussions, constant encouragement and kind blessings without which this work would not have been completed.

I express my sincere gratitude to Dr. Muhammed Shafi, Professor and Head, Department of Chemistry, University of Calicut, Dr. K.K. Aravindakshan, Professor and former Head, Department of Chemistry, University of Calicut and other faculty members and research scholars of the Department for their support.

I am extremely glad to express my sincere gratitude to Dr. Lisa Sreejith, Senior Lecturer, Department of Chemistry, NIT Calicut and Dr. Sreejith M. Nair and Dr. Sheeba P.S of the Department of Chemistry of Malabar Christian College, Calicut for the kind help and inspiration.

I also wish to express my heartfelt thanks to Smt. A. Parvathy, Retired Professor and Head of the Department of Chemistry, Govt. Arts and Science College, Calicut for the blessings and support.

Special thanks are to Dr. G. Unnikrishnan, Asst. Professor and Head, Department of Chemistry, NIT Calicut, Dr. N. Seetharaman, Retired Professor, NIT Calicut and Dr. Soney Varghese, NIT Calicut for valuable suggestions and help.

I also wish to express my sincere thanks to Dr. P.K. Indira, Dr. T. S. Sahish and Sri . P.N. Sathyanathan for their help.

I am very grateful to Sri. Sooraj Varma, Sri. Mallikarjuna Rao, Sri. Sudheesh, Smt. Jinu George, Sri. Sharafudheen, Miss. Prajila, Mrs. Vindhya Ramesh and Mr. Shinu for the timely help.

Special thanks to Sri. Anil Kumar of NIIST, Thiruvananthapuram for the kind help in getting the XRD studies done and discussions relating to that.

I wish to acknowledge my sincere thanks to Department of Chemistry, NIT Calicut, RSIC, Nagpur and STIC, Cochin University of Science & Technology for the thermograms.

My sincere thanks to my wife and children for their prayers and support.

Finally, I acknowledge my thanks to Sri. Sugeesh and Sri. Beljith for the care they have taken in typing, setting and binding the thesis.

Devadasan K K

Preface

The thesis reports results of an original investigation carried out independently by the author on the kinetics and mechanism of thermal decomposition of bromates of barium, nickel, neodymium and yttrium and a comparative study of the effects of addition of intentional impurities on the thermal decomposition of these bromates by dynamic thermogravimetry.

Chapter I gives an introduction to the topic, theories of solid state decomposition and the application of thermogravimetric methods in studying kinetic parameters of solid state decomposition. A review of the work done in the field is given and wherever required due acknowledgement has been made.

Details relating to materials used and experimental methods adopted for the investigation are included in Chapter II.

A brief account of the results of the investigation along with necessary data, tables, graphs and figures are presented in chapter III.

Chapter IV gives discussion of the results, the findings, the inferences, the author's views and conclusions arising out of the findings.

The last section of the thesis gives a list of references made in connection with the investigation.

Summary

In material science and condensed matter research solid state decomposition studies are of paramount importance and a lot of research has been done in this field in the past few decades. Such studies have brought to light a good deal of information concerning the kinetics and mechanism of solid state reactions. A number of theoretical models have been proposed to substantiate and interpret the results of these studies.

Studies on solid state reactions have shown that crystal imperfections of various kinds do play a very significant role in deciding the reactivity of solids. Processes such as irradiation, precompression, crushing, doping and addition of impurities increase the lattice imperfections in solids. This will profoundly influence the formation and growth of reaction nuclei in the solid matrix and thereby enhance the reactivity.

Considerable amount of work has been done on the thermal decomposition of alkali and alkaline earth metal bromates.¹⁻¹² It was of interest therefore to extend the studies to other bromates. Nickel bromate, yttrium bromate and neodymium bromate were taken for the investigations in a program of comparative study of the thermal decomposition behaviour of metal bromates.

Thermal decomposition reactions are very sensitive to the presence of impurities.¹³⁻¹⁸ Impurities can produce vacancies¹⁹ or act as electron traps²⁰ and can affect the thermal decomposition reaction. It was of interest therefore to study the variation of the decomposition behaviour of barium bromate, nickel bromate, yttrium bromate and neodymium bromate due to the addition of intentional impurities.

All bromates required for the studies (barium bromate, strontium bromate, magnesium bromate, zinc bromate, cadmium bromate, nickel bromate, yttrium bromate and neodymium bromate) were synthesized by the method of Bancroft and Gesser.^{1,21-24} Crystals of bromates containing intentional impurities were prepared by slow evaporation of solutions containing the host bromate and the one used as impurity in the mole fraction range 10^{-3} to 10^{-1} .

The untreated barium bromate, yttrium bromate, nickel bromate and neodymium bromate and samples of barium bromate containing NaBrO_3 , KBrO_3 , $\text{Mg}(\text{BrO}_3)_2$, $\text{Sr}(\text{BrO}_3)_2$, $\text{Zn}(\text{BrO}_3)_2$, $\text{Cd}(\text{BrO}_3)_2$, $\text{Ni}(\text{BrO}_3)_2$, $\text{Nd}(\text{BrO}_3)_3$, $\text{Y}(\text{BrO}_3)_3$, KBr , SrBr_2 as intentional impurities, samples of nickel bromate containing $\text{Zn}(\text{BrO}_3)_2$, $\text{Nd}(\text{BrO}_3)_3$, $\text{Y}(\text{BrO}_3)_3$ as intentional impurities, samples of neodymium bromate containing $\text{Ni}(\text{BrO}_3)_2$, $\text{Ba}(\text{BrO}_3)_2$ as intentional impurities and samples of yttrium bromate containing $\text{Ni}(\text{BrO}_3)_2$, $\text{Ba}(\text{BrO}_3)_2$ as intentional impurities were subjected to dynamic thermogravimetric analysis. 52 samples were used in all in the form of fine powder (200-240 mesh). Some samples were subjected to XRD studies with a view to get information concerning the samples containing the impurities.

Analysis of the TG curves shows that the addition of impurities do not alter the pattern of the TG curve to any significant extent though it does alter the initial temperature of decomposition(T_i), final temperature(T_f) and peak temperature(T_s) characteristic of the decomposition. In general lowering of T_i , T_f and T_s is observed in samples containing impurities.

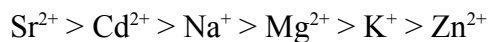
Earlier studies have shown that the thermal decomposition of barium bromate is a first order process¹⁹ and hence the kinetic parameters viz., energy of activation(E), frequency factor(Z) and entropy of activation(ΔS) were calculated using the Coats-Redfern²⁵, the Freeman-Carroll²⁶ and the Horowitz-Metzger²⁷ methods in the form applicable to first order process. For nickel bromate, neodymium bromate and yttrium bromate and for all the samples containing intentional impurities the kinetic parameters were calculated by the above methods. The E and Z values obtained by the three methods show good agreement within ± 10 percent in all cases.

XRD studies indicate no new phase formation in samples containing intentional impurities except in two cases.

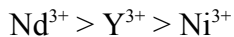
Thermal decomposition of barium bromate occurs with an initial loss of water of hydration followed by the decomposition of anhydrous bromate to bromide. In the case of bromates of Ni, Nd and Y loss of water of hydration occurs in two steps followed by the decomposition of bromate into bromide and oxide.

The thermal stability of barium bromate decreased on adding the impurities. In the case of samples of barium bromate containing intentional impurities the effect of

lowering of activation energy was the highest in the case of barium bromate containing $\text{Sr}(\text{BrO}_3)_2$ and the effect decreased in the order



and for barium bromate samples containing $\text{Ni}(\text{BrO}_3)_2$, $\text{Nd}(\text{BrO}_3)_3$, $\text{Y}(\text{BrO}_3)_3$ as impurities, the lowering of activation energy was in the order



The higher susceptibility of the bromates containing the intentional impurities towards thermal decomposition is attributed to the presence of lattice defects generated. The extent of the lattice defects depends on the valency, size, surface charge density and concentration of the added impurity. In general the intensity of the lattice defects increases with increase in concentration of the impurity. The enhancement of the decomposition in the presence of the added Br^- ion is due to eutectic formation between Br^- and BrO_3^- as proposed by Jach.²⁸

In the case of Nd, Y and Ni bromates the decomposition yields oxides which, as is well known, are compounds with very good catalytic properties. So the enhancement of decomposition may also be due to the catalyzing effect of the oxide apart from the lattice defects and eutectic formation.

Addition of zinc bromate and yttrium bromate to nickel bromate decreases the activation energy while addition of neodymium bromate increases the activation energy. This may be probably due to the greater thermal stability of neodymium bromate. Addition of nickel bromate and barium bromate to yttrium bromate decreases the activation energy of decomposition of yttrium bromate. Z and ΔS were also lowered in the samples containing impurities.

The mechanism of decomposition was established by following the non-isothermal method by Sestak and Berggren²⁹ and Satava³⁰. For the decomposition of barium bromate, neodymium bromate and yttrium bromate fairly good correlation was obtained for the “*Contracting Cube Model*”³¹

$$1 - (1 - \alpha)^{1/3} = kt$$

where α is the fractional decomposition and k is the rate constant. This correlation suggests that the rate controlling process is a phase boundary reaction assuming spherical symmetry. For nickel bromate the data fit well with other mechanistic equations also. However, the activation energy obtained with the contracting cube model is in better agreement with the experimental results obtained by the Coats-Redfern method.²⁵ Thus it is concluded that the decomposition of nickel bromate also follows the contracting cube equation. It is also found that the activation energies calculated for the samples containing intentional impurities using the above model fairly agree with those obtained by non-mechanistic equations. These findings conclusively prove that the presence of impurities, though does tune the rate of decomposition, does not alter the mechanism of decomposition of barium bromate, nickel bromate, neodymium bromate and yttrium bromate.

.....
References :

1. Bancroft G. M and Gesser H.D. , *J. Inorg. Nucl. Chem.*, 27, 1545 (1965).
2. Erdey L. , Simon J. and Gal S., *Talanta.*, 15, 653 (1968).
3. Arnikaar H.J and Patnaik S.K, *J. Univ. Poona Sci. Technol.*, 50, 163-70 (1977).
4. Nair S.M.K, Malayil Koshykunju, Daisamma Jacob P., *Thermochim. Acta.*, 141, 61-80 (1989).
5. Nair S.M.K and James C. *Thermochim. Acta.*, 96(1), 27-36 (1985).
6. Diefallah, EL.H.M., Basahl, Suliman N, Obaid Abdullah Y, *J. Radioanal. Nucl. Chem.* 109(1) 177-81(1987).
7. Solymosi. F. and Bansagi T., *J. Phys. Chem.*, 74, 15 (1970).
8. Bhattamisra. S.D and Mohanty S.R, *Indian J. Chem.* 15A, 350 (1977).
9. Bhattamisra. S.D and Mohanty S.R, *Inorg. Nucl. Chem.*, 39(12), 2103-09 (1977).
10. Mohanty S.R. and Satapathy M., *Radio Chem., Radioanal. Lett.*, 37, 345 (1979).
11. Jena B., Mohanty S.R and Satapathy M., *Indian J. Chem.*, 19A, 1139 (1980).
12. Das B.C., Patnaik D., *J. Them. Anal. and Calorimetry*, vol 61, 879-883 (2000).
13. Bhatta D., Sahoo M.K, Jena B., *Thermochim Acta*, 132, 7-13 (1988).
14. Das B.C, Sethi K.K, *J. Teach. Res. Chem.*, 6(2), 41-46 (1999).

15. Sahu K.K., Bose S., Bhatta D., *React. Kinet. Catal. Lett*, 52(1), 149-54 (1994).
16. Bhatta D., Mishra S, Sahu K.K, *J. Them. Anal.*, 39(3), 275-80 (1993).
17. Shoba U.S. and Udupa M.R, *Proc. Natl. Symp. Them. Anal.*, 9th 395-8 (1993).
18. Shoba U.S. and Udupa M.R, *Thermochim Acta.*, 242(1-2), 215-21 (1994).
19. Delbeeq C.J, Hayes W. and Yuster P.H, *Phys. Rev.*, 121, 1043 (1961).
20. Johnson P.D. and Williams F.E., *Phys. Rev.*, 117, 964 (1960).
21. Nair S.M.K. and Daisamma Jacob P, *Thermochim Acta*, 179, 273-280 (1991).
22. Abbasi, A, Eriksson L, *Acta Crystallogr. Ser. E.* , 62, p.m. 126 (2006).
23. Abbasi, Alireza; Badiei, Alireza., *Iran J. Chem. Chem. Eng*, Research note, Vol 26, No 4 (2007).
24. A. Chatterji, K.N. Chattopadhyay, D. Neogy, P. Paul, Reba Chatterjee, S. Chatterjee., *Journal of Magnetism and Magnetic materials*, 271, 1-8 (2004).
25. Coats A. W and Redern J.P, *Nature*, 201, 68 (1964).
26. Freeman E.S. and Carroll B., *J. Phys. Chem.*, 62,394 (1958).
27. Horowitz H.H. and Metzger. G., *Anal. Chem.*, 35,1464 (1963).
28. Jach J., *Reactivity of Solids*(Ed. De Boer J.H.) Elsevier Publication Co., Amsterdam, p. 334 (1961).
29. Sestak J. and Berggren G., *Thermochim Acta*, 3,1 (1971).
30. Satava V., *Thermochim Acta*, 2,423 (1971).
31. M. Avrami, *J.Chem. Phys.*, 7,103 (1939).

• • •

CONTENTS

	Page No.
Certificate	i
Declaration	ii
Acknowledgement	iii
Preface	iv
Summary	v-ix
CHAPTER I : INTRODUCTION	
1.1 Thermal Decomposition of Inorganic Salts	
1.1.1 Introduction	2
1.1.2 Types of solid state reactions	2
1.1.3 Decomposition curve and its features	2
1.1.4 Theories of solid state decomposition	4
1.1.5 The laws of nucleus formation	5
1.1.5.1 Instantaneous nucleation	
1.1.5.2 Exponential law	
1.1.5.3 Linear law	
1.1.5.4 Power law	
1.1.6 Laws of nucleus growth	8
1.1.6.1 Power law	
1.1.6.2 Exponential law	
1.1.6.3 Avrami- Erofeyev equation	
1.1.6.4 Prout – Tompkins equation	
1.1.6.5 Deceleratory equations	
1.1.6.6 Unimolecular decay – first order equation	
1.2 Crystal Defects and their Role in the Thermal Decomposition of Solids	
1.2.1 Point defects	12
i) Interstitial	
ii) Schottky defect	
iii) Frenkel defect	
iv) Substitutional impurity	
1.2.2 Line defects or dislocations	12
i) Edge dislocation or Taylor’s dislocation	
ii) Screw dislocation or Burger’s dislocation	

1.2.3	Plane defects	13
	i) Lineage boundary	
	ii) Grain boundary	
	iii) Stacking fault	
1.2.4	Electronic imperfections	13
1.2.5	Excitation states of crystals	13
1.2.6	Transient imperfections	14
1.3	Review of Studies on Thermal Decomposition of Bromates	
1.3.1	Pathways of decomposition	14
1.3.2	Bromates of monovalent cations	15
1.3.3	Bromates of divalent cations	17
1.3.4	Bromates of transition metals	18
1.3.5	Thermal decomposition of rare earth bromates	18
1.3.6	Effect of doping on the thermal decomposition of bromates	19
1.3.7	Effect of additives on the thermal decomposition of bromates	21
1.3.8	Effect of precompression on the thermal stability of solids	22
1.3.9	Effect of irradiation on the thermal decomposition of bromates	22
1.4	Thermal Methods of Analysis	
1.4.1	Introduction	24
1.4.2	Thermogravimetry	25
1.4.3	Methods used in thermogravimetry	26
1.4.4	Factors affecting thermogravimetry	27
	1.4.4.1 Instrumental factors	
	1.4.4.2 Sample characteristics	
	1.4.4.3 Effect of heating rate and heat transfer	
	1.4.4.4 Furnace atmosphere	
	1.4.4.5 Rate of recording TG curve	
	1.4.4.6 Sample holder and its geometry	
	1.4.4.7 Effects due to sample characteristics	
1.4.5	Study of reaction kinetics by thermogravimetry	30
1.4.6	Calculation of kinetic parameters from TG traces	31
	1.4.6.1 Freeman-Carroll method - Differential method	
	1.4.6.2 Coats-Redfern equation - Integral method	
	1.4.6.3 Horowitz-Metzger method – Approximation method	

1.4.6.4 Relative merits of the methods

1.5 The Scope of the Present Investigation

35

CHAPTER II : MATERIALS AND EXPERIMENTAL METHODS

2.1 Materials

2.1.1	Preparation of barium bromate	38
2.1.2	Preparation of nickel bromate	38
2.1.3	Preparation of yttrium bromate	38
2.1.4	Preparation of neodymium bromate	39
2.1.5	Preparation of Mg, Sr, Zn and Cd bromates	39
2.1.6	Preparation of samples of barium bromate, nickel bromate, neodymium bromate and yttrium bromate containing intentional impurities	39

2.2 Analysis of Bromates - Iodometric Method 40

2.3 Thermogravimetric Studies 40

2.4 XRD Studies 41

2.5 FTIR Studies 41

CHAPTER III : RESULTS

3.1 TG Curves 43

3.2 XRD Results 62

3.3 FTIR Spectra 65

3.4 Evaluation of Kinetic Parameters 69

3.4.1 The Coats- Redfern method 69

3.4.2 The Freeman-Carroll method 70

3.4.3 The Horowitz-Metzger method 70

CHAPTER IV : DISCUSSION

4.1 Thermal Decomposition Patterns 127

4.1.1 Thermal decomposition of barium bromate 127

4.1.2 Thermal decomposition of nickel bromate 142

4.1.3 Thermal decomposition of neodymium bromate and yttrium bromate 147

4.1.4 XRD results 148

4.1.5 FTIR results 148

4.2 Mechanism of Thermal Decomposition 149

4.3 Conclusion 163

CONTENTS – TABLES

Table No.		
Page No.		
1(i)	Thermal decomposition of barium bromate - 1(i) Analysis of data by using Coats- Redfern , Freeman-Carroll and Horowitz-Metzger methods	71
1(ii)	Thermal decomposition of barium bromate - 1(ii) Analysis of data by using Coats- Redfern , Freeman-Carroll and Horowitz-Metzger methods	72
2	Thermal decomposition of barium bromate containing sodium bromate ($10^{-3}M$) Analysis of data by using Coats- Redfern , Freeman-Carroll and Horowitz-Metzger methods	73
3	Thermal decomposition of barium bromate containing sodium bromate ($10^{-2}M$) Analysis of data by using Coats- Redfern , Freeman-Carroll and Horowitz-Metzger methods	74
4	Thermal decomposition of barium bromate containing sodium bromate ($10^{-1}M$) Analysis of data by using Coats- Redfern , Freeman-Carroll and Horowitz-Metzger methods	75
5	Thermal decomposition of barium bromate containing potassium bromate ($10^{-3}M$) Analysis of data by using Coats- Redfern , Freeman-Carroll and Horowitz-Metzger methods	76
6	Thermal decomposition of barium bromate containing potassium bromate ($10^{-2}M$) Analysis of data by using Coats- Redfern , Freeman-Carroll and Horowitz-Metzger methods	77
7	Thermal decomposition of barium bromate	78

	containing potassium bromate ($10^{-1}M$) Analysis of data by using Coats- Redfern , Freeman-Carroll and Horowitz-Metzger methods	
8	Thermal decomposition of barium bromate containing magnesium bromate ($10^{-3}M$) Analysis of data by using Coats- Redfern , Freeman-Carroll and Horowitz-Metzger methods	79
9	Thermal decomposition of barium bromate containing Magnesium bromate ($10^{-2}M$) Analysis of data by using Coats- Redfern , Freeman-Carroll and Horowitz-Metzger methods	80
10	Thermal decomposition of barium bromate containing strontium bromate ($10^{-3}M$) Analysis of data by using Coats- Redfern , Freeman-Carroll and Horowitz-Metzger methods	81
11	Thermal decomposition of barium bromate containing strontium bromate ($10^{-2}M$) Analysis of data by using Coats- Redfern , Freeman-Carroll and Horowitz-Metzger methods	82
12	Thermal decomposition of barium bromate containing strontium bromate ($10^{-1}M$) Analysis of data by using Coats- Redfern , Freeman-Carroll and Horowitz-Metzger methods	83
13	Thermal decomposition of barium bromate containing zinc bromate ($10^{-3}M$) Analysis of data by using Coats- Redfern , Freeman-Carroll and Horowitz-Metzger methods	84
14	Thermal decomposition of barium bromate containing zinc bromate ($10^{-2}M$) Analysis of data by using Coats- Redfern , Freeman-Carroll and Horowitz-Metzger methods	85

15	Thermal decomposition of barium bromate containing zinc bromate (10^{-1} M) Analysis of data by using Coats- Redfern , Freeman-Carroll and Horowitz-Metzger methods	86
16	Thermal decomposition of barium bromate containing cadmium bromate (10^{-3} M) Analysis of data by using Coats- Redfern , Freeman-Carroll and Horowitz-Metzger methods	87
17	Thermal decomposition of barium bromate containing cadmium bromate (10^{-2} M) Analysis of data by using Coats- Redfern , Freeman-Carroll and Horowitz-Metzger methods	88
18	Thermal decomposition of barium bromate containing cadmium bromate (10^{-1} M) Analysis of data by using Coats- Redfern , Freeman-Carroll and Horowitz-Metzger methods	89
19	Thermal decomposition of barium bromate containing potassium bromide (10^{-3} M) Analysis of data by using Coats- Redfern , Freeman-Carroll and Horowitz-Metzger methods	90
20	Thermal decomposition of barium bromate containing potassium bromide (10^{-2} M) Analysis of data by using Coats- Redfern , Freeman-Carroll and Horowitz-Metzger methods	91
21	Thermal decomposition of barium bromate containing potassium bromide (10^{-1} M) Analysis of data by using Coats- Redfern , Freeman-Carroll and Horowitz-Metzger methods	92
22	Thermal decomposition of barium bromate containing strontium bromide (10^{-3} M) Analysis of data by using Coats- Redfern ,	93

	Freeman-Carroll and Horowitz-Metzger methods	
23	Thermal decomposition of barium bromate containing strontium bromide (10^{-2} M) Analysis of data by using Coats- Redfern , Freeman-Carroll and Horowitz-Metzger methods	94
24	Thermal decomposition of barium bromate containing strontium bromide (10^{-1} M) Analysis of data by using Coats- Redfern , Freeman-Carroll and Horowitz-Metzger methods	95
25	Thermal decomposition of barium bromate containing nickel bromate (10^{-3} M) Analysis of data by using Coats- Redfern , Freeman-Carroll and Horowitz-Metzger methods	96
26	Thermal decomposition of barium bromate containing nickel bromate (10^{-2} M) Analysis of data by using Coats- Redfern , Freeman-Carroll and Horowitz-Metzger methods	97
27	Thermal decomposition of barium bromate containing nickel bromate (10^{-1} M) Analysis of data by using Coats- Redfern , Freeman-Carroll and Horowitz-Metzger methods	98
28	Thermal decomposition of barium bromate containing neodymium bromate (10^{-3} M) Analysis of data by using Coats- Redfern , Freeman-Carroll and Horowitz-Metzger methods	99
29	Thermal decomposition of barium bromate containing neodymium bromate (10^{-2} M) Analysis of data by using Coats- Redfern , Freeman-Carroll and Horowitz-Metzger methods	100
30	Thermal decomposition of barium bromate containing neodymium bromate (10^{-1} M)	101

	Analysis of data by using Coats- Redfern , Freeman-Carroll and Horowitz-Metzger methods	
31	Thermal decomposition of barium bromate containing yttrium bromate (10^{-3} M) Analysis of data by using Coats- Redfern , Freeman-Carroll and Horowitz-Metzger methods	102
32	Thermal decomposition of barium bromate containing yttrium bromate (10^{-2} M) Analysis of data by using Coats- Redfern , Freeman-Carroll and Horowitz-Metzger methods	103
33-1	Thermal decomposition of barium bromate containing yttrium bromate (10^{-1} M) Analysis of data by using Coats- Redfern , Freeman-Carroll and Horowitz-Metzger methods– Stage 1	104
33-2	Thermal decomposition of barium bromate containing yttrium bromate (10^{-1} M) Analysis of data by using Coats- Redfern , Freeman-Carroll and Horowitz-Metzger methods– Stage 2	105
34	Thermal decomposition of nickel bromate Analysis of data by using Coats- Redfern , Freeman-Carroll and Horowitz-Metzger methods	106
35	Thermal decomposition of nickel bromate containing zinc bromate (10^{-3} M) Analysis of data by using Coats- Redfern , Freeman-Carroll and Horowitz-Metzger methods	107
36	Thermal decomposition of nickel bromate containing zinc bromate (10^{-2} M) Analysis of data by using Coats- Redfern , Freeman-Carroll and Horowitz-Metzger methods	108
37	Thermal decomposition of nickel bromate containing zinc bromate (10^{-1} M)	109

	Analysis of data by using Coats- Redfern , Freeman-Carroll and Horowitz-Metzger methods	
38	Thermal decomposition of nickel bromate containing neodymium bromate (10^{-3} M) Analysis of data by using Coats- Redfern , Freeman-Carroll and Horowitz-Metzger methods	110
39	Thermal decomposition of nickel bromate containing neodymium bromate (10^{-2} M) Analysis of data by using Coats- Redfern , Freeman-Carroll and Horowitz-Metzger methods	111
40	Thermal decomposition of nickel bromate containing neodymium bromate (10^{-1} M) Analysis of data by using Coats- Redfern , Freeman-Carroll and Horowitz-Metzger methods	112
41	Thermal decomposition of nickel bromate containing yttrium bromate (10^{-3} M) Analysis of data by using Coats- Redfern , Freeman-Carroll and Horowitz-Metzger methods	113
42	Thermal decomposition of nickel bromate containing yttrium bromate (10^{-2} M) Analysis of data by using Coats- Redfern , Freeman-Carroll and Horowitz-Metzger methods	114
43	Thermal decomposition of nickel bromate containing yttrium bromate (10^{-1} M) Analysis of data by using Coats- Redfern , Freeman-Carroll and Horowitz-Metzger methods	115
44	Thermal decomposition of neodymium bromate Analysis of data by using Coats- Redfern , Freeman-Carroll and Horowitz-Metzger methods	116
45	Thermal decomposition of neodymium bromate containing nickel bromate (10^{-2} M)	117

	Analysis of data by using Coats- Redfern , Freeman-Carroll and Horowitz-Metzger methods	
46	Thermal decomposition of neodymium bromate containing nickel bromate (10^{-1} M)	118
	Analysis of data by using Coats- Redfern , Freeman-Carroll and Horowitz-Metzger methods	
47	Thermal decomposition of neodymium bromate containing barium bromate (10^{-2} M)	119
	Analysis of data by using Coats- Redfern , Freeman-Carroll and Horowitz-Metzger methods	
48	Thermal decomposition of neodymium bromate containing barium bromate (10^{-1} M)	120
	Analysis of data by using Coats- Redfern , Freeman-Carroll and Horowitz-Metzger methods	
49	Thermal decomposition of yttrium bromate	121
	Analysis of data by using Coats- Redfern , Freeman-Carroll and Horowitz-Metzger methods	
50	Thermal decomposition of yttrium bromate containing nickel bromate (10^{-2} M)	122
	Analysis of data by using Coats- Redfern , Freeman-Carroll and Horowitz-Metzger methods	
51	Thermal decomposition of yttrium bromate containing nickel bromate (10^{-1} M)	123
	Analysis of data by using Coats- Redfern , Freeman-Carroll and Horowitz-Metzger methods	
52	Thermal decomposition of yttrium bromate containing barium bromate (10^{-1} M)	124
	Analysis of data by using Coats- Redfern , Freeman-Carroll and Horowitz-Metzger methods	
53.	FTIR Spectral Data-Prominent Vibrational Absorption Frequencies	

54.	Kinetic parameters of decomposition of barium bromate and barium bromate containing sodium bromate and potassium bromate as intentional impurities calculated using Coats-Redfern, Freeman-Carroll and Horowitz-Metzger methods	129
55.	Kinetic parameters of decomposition of barium bromate and barium bromate containing magnesium bromate and strontium bromate as intentional impurities calculated using Coats-Redfern, Freeman-Carroll and Horowitz-Metzger methods	130
56.	Kinetic parameters of decomposition of barium bromate and barium bromate containing zinc bromate and cadmium bromate as intentional impurities calculated using Coats-Redfern, Freeman-Carroll and Horowitz-Metzger methods	131
57.	Kinetic parameters of decomposition of barium bromate and barium bromate containing potassium bromide and strontium bromide as intentional impurities calculated using Coats-Redfern, Freeman-Carroll and Horowitz-Metzger methods	132
58.	Kinetic parameters of decomposition of barium bromate and barium bromate containing nickel bromate, neodymium bromate and yttrium bromate as intentional impurities calculated using Coats-Redfern, Freeman-Carroll and Horowitz-Metzger methods	133
59.	Kinetic parameters of decomposition of nickel bromate and nickel bromate containing zinc bromate, neodymium bromate and yttrium bromate as intentional impurities calculated using Coats-Redfern, Freeman-Carroll and Horowitz-Metzger methods	134
60.	Kinetic parameters of decomposition of neodymium bromate and neodymium bromate containing nickel bromate and barium bromate as intentional impurities calculated using Coats-Redfern, Freeman-Carroll and	135

Horowitz-Metzger methods

61.	Kinetic parameters of decomposition of yttrium bromate and yttrium bromate containing nickel bromate and barium bromate as intentional impurities calculated using Coats-Redfern, Freeman-Carroll and Horowitz-Metzger methods	136
62.	Ionic radii and surface charge densities of ions	137
63.	Computation of E & Z using the mechanism based equation for barium bromate.	150
64.	Computation of E & Z using the mechanism based equation for nickel bromate.	151
65.	Computation of E & Z using the mechanism based equation for neodymium bromate	152
66.	Computation of E & Z using the mechanism based equation for yttrium bromate	153
67.	Solid state decomposition – Mechanistic Equations	155
68-73.	Kinetic parameters calculated using the mechanism based equation $1 - (1 - \alpha)^{1/3} = kt$	156 - 161

CONTENTS – FIGURES

Fig . No.		Page No.
1.	Decomposition curve	2
2.	TG curves of barium bromate and samples of barium bromate containing sodium bromate	44
3.	TG curves of barium bromate and samples of barium bromate containing potassium bromate	45
4.	TG curves of barium bromate and samples of barium bromate containing magnesium bromate	46
5.	TG curves of barium bromate and samples of barium bromate containing strontium bromate	47
6.	TG curves of barium bromate and samples of barium bromate containing zinc bromate	48
7.	TG curves of barium bromate and samples of barium bromate containing cadmium bromate	49
8.	TG curves of barium bromate and samples of barium bromate containing potassium bromide	50
9.	TG curves of barium bromate and samples of barium bromate containing strontium bromide	51
10.	TG curves of barium bromate and samples of barium bromate containing nickel bromate	52
11.	TG curves of barium bromate and samples of barium bromate containing neodymium bromate	53
12.	TG curves of barium bromate and samples of barium bromate containing yttrium bromate	54
13.	TG curves of nickel bromate and samples of nickel bromate containing zinc bromate	55
14.	TG curves of nickel bromate and samples of nickel bromate containing neodymium bromate	56
15.	TG curves of nickel bromate and samples of	57

	nickel bromate containing yttrium bromate	
16.	TG curves of neodymium bromate and samples of neodymium bromate containing nickel bromate	58
17.	TG curves of neodymium bromate and samples of neodymium bromate containing barium bromate	59
18.	TG curves of yttrium bromate and samples of yttrium bromate containing nickel bromate	60
19.	TG curves of yttrium bromate and samples of yttrium bromate containing barium bromate.	61
20.	XRD plots for barium bromate, neodymium bromate and barium bromate containing neodymium bromate($10^{-1}M$)	62
21.	XRD plots for neodymium bromate, nickel bromate and neodymium bromate containing nickel bromate($10^{-1}M$)	63
22.	XRD plots for nickel bromate, zinc bromate and nickel bromate containing zinc bromate($10^{-1}M$)	63
23.	XRD plots for yttrium bromate, nickel bromate and yttrium bromate containing nickel bromate($10^{-1}M$)	64
24.	XRD plots for barium bromate, yttrium bromate and barium bromate containing yttrium bromate($10^{-1}M$)	64
25.	FTIR Spectra of neodymium bromate and nickel bromate containing $10^{-1}M$ neodymium bromate	66
26.	FTIR Spectra of nickel bromate, zinc bromate and nickel bromate containing $10^{-3}M$ zinc bromate	67
27.	FTIR Spectra of nickel bromate containing $10^{-1}M$ yttrium bromate and nickel bromate containing $10^{-2}M$ neodymium bromate	68
28.	Variation of E with concentration of impurities – barium bromate containing Na, K, Mg, Sr, Zn, Cd bromates and K and Sr bromides – Coats- Redfern Method	139
29.	Variation of E with concentration of impurities –	140

	barium bromate containing Na, K, Mg, Sr, Zn, Cd bromates and K and Sr bromides – Freeman-Carroll Method	
30	Variation of E with concentration of impurities – barium bromate containing Na, K, Mg, Sr, Zn, Cd bromates and K and Sr bromides – Horowitz-Metzger Method	141
31.	Variation of E with concentration of impurities – barium bromate containing Ni, Nd and Y bromates - Coats- Redfern ,Freeman-Carroll and Horowitz-Metzger Methods	143
32.	Variation of E with concentration of impurities – nickel bromate containing Zn, Nd and Y bromates - Coats- Redfern ,Freeman-Carroll and Horowitz-Metzger Methods	144
33.	Variation of E with concentration of impurities – neodymium bromate containing Ni and Ba bromates - Coats- Redfern ,Freeman-Carroll and Horowitz-Metzger Methods	145

Chapter I

Introduction

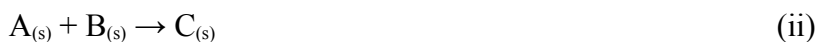
1.1 Thermal Decomposition of Inorganic Salts

1.1.1 Introduction

The advancement in solid state science and related technologies in the last few decades have been amazing. Investigations relating to chemical transformations of solids are of paramount importance in modern solid state technologies. Studies of kinetics of solid state reactions especially thermal decomposition studies of various inorganic salts, coordination complexes, polymers and polymer blends have been extensively undertaken in the recent past and a good deal of information has been brought to light relating to the kinetics and mechanisms of many solid state transformations. Theories substantiating the results of such studies have also been developed. This, of course, is an area which has immense potential for further research.

1.1.2 Types of solid state reactions

Most of the solid state reactions of inorganic compounds are decomposition reactions of the following types.



Of these the reactions of the type (i) are the most common.

1.1.3 Decomposition curve and its features

Kinetics of solid state decomposition is often studied by monitoring the fractional decomposition either from the mass loss of the reactant or from the pressure of the evolved gas as a function of time at a series of temperature. Fractional decomposition (α) is given by

$$\alpha = \frac{\text{mass loss}}{\text{theoretical maximum mass loss at the completion of the reaction}} \quad 1.1$$

or

$$\alpha = \frac{\text{pressure of the gaseous product(s)}}{\text{theoretical maximum pressure developed at the completion of the reaction}} \quad 1.2$$

The plot of fractional decomposition (α) versus time (t) is called decomposition curve¹ which is sigmoidal in nature and is characterized by the following features (Fig. 1).

- i) An initial rapid evolution of gas – this stage corresponds to 0.1 to 1.5% decomposition and is usually of first order with an activation energy of 3-5 Kcal mol⁻¹.
- ii) An induction period – a period of slow evolution of gas.

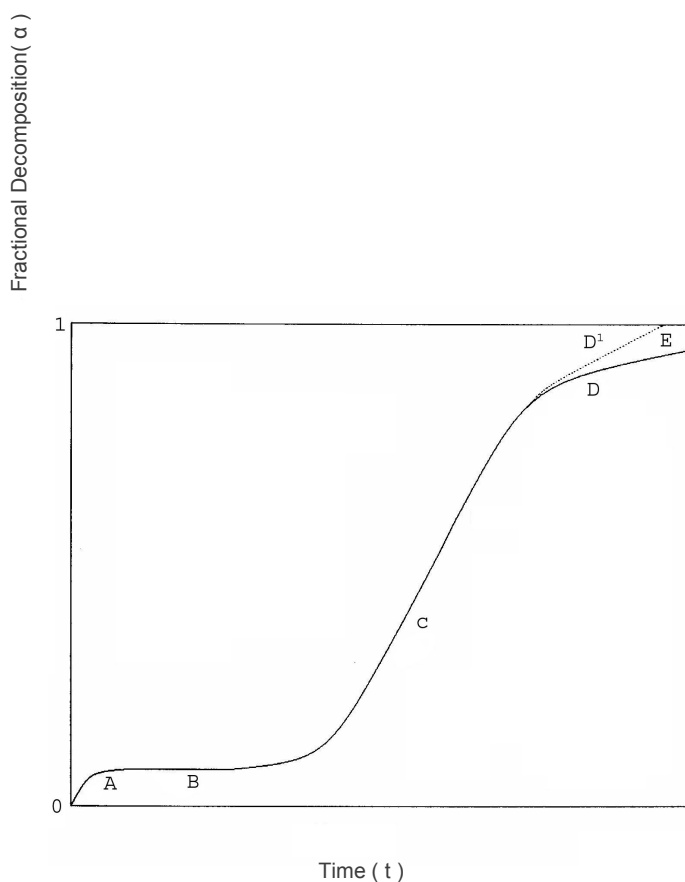


Fig : 1 – Decomposition curve

A - initial rapid evolution of gas B - induction period
C - acceleratory period D – decay period

- iii) An acceleratory period – the most informative and intensively studied part of the curve which satisfies one of the equations of the type²

$$\alpha = f(\exp kt) \quad (1.3)$$

or

$$\alpha = f(kt^n) \quad (1.4)$$

or

$$\alpha = f(t - t_0)^n \quad (1.5)$$

where k is the rate constant and t_0 is an adjustable parameter. This part of the curve represents the period of maximum rate.

- iv) A decay period – this part of the curve is less informative and more difficult to analyse as it depends to a large extent on the details of the particle distribution. At stages with $\alpha > 0.98$ there is difficulty, in most cases, in the reproducibility of the decay period (as exemplified by the dotted line in the curve Fig. 1). Their reproducibility arises from a combination of particle size effects, the reduction of chemical reactivity due to poisoning or sintering or due to the adsorption of the product gas on the solid product³.

1.1.4 Theories of solid state decomposition

As early as 1916 Langmuir⁴ put forward the idea that solid state decompositions occur only at the boundary between the reactant and product phases. This was followed by the concept of *internal surfaces* due to Hinshelwood and Bowen⁵. According to them calculation of activation energy from temperature coefficient of reaction should take into consideration the variations in the extent of the reaction interface which not only includes the external surface of the crystal but also the “internal surface” which are continuously being generated during the course of a reaction.

A revolutionary concept in this connection was proposed by Macdonald and Hinshelwood⁶ in 1925 which has been universally accepted in explaining solid state reactions. According to their theory called *theory of nucleation* the mechanism of decomposition involves two major steps.

- i) the formation of reaction nuclei

ii) the growth of reaction nuclei

The onset of the reaction involves the formation of aggregates of the product (B) within the matrix of the reactant (A). This will preferentially take place at the sites of lattice imperfections such as point defects. The generation of a new and more stable phase B within the parent phase is called *nucleation*. Nucleation tends to cause local deformations in the lattice of A as the lattice parameters of B will not be the same as that of A. Only aggregates of a critical size tend to grow while others redisperse. Nucleation may occur on the particle surface or throughout the particle volume. Slow nucleation forms a single domain on each particle while a fast surface nucleation causes the reacting particle to be covered by a thin layer of the product and the rate determining process becomes the propagation of the reacting interface towards the centre of the particle controlled either by diffusion or phase boundary reaction. If the rate of nucleation and the rate of growth of reaction nuclei are comparable, the overlapping of growing nuclei occurs and the mathematical treatment of the problem becomes more complicated.

Indirect evidence for the theory of nucleation was obtained from the decomposition of silver oxalate⁶ which was found to be autocatalytic. The autocatalytic activity, they suggested, could either be due to increase in the surface area of the solid or due to the presence of nuclei of the product. The theory was confirmed by the work of Roginskii and Schultz⁷ in 1928 on the basis of their studies on thermal decomposition of potassium permanganate.

The kinetics of the acceleratory periods of many decompositions could be explained by the concept of nucleation and growth of nuclei by an interfacial mechanism. Satisfactory evidence for the existence of nuclei was provided by the works of Kohlschütter⁸ and Garner⁹. Their work showed that nuclei are formed on the crystal surface and grow at constant rates above a critical dimension. The rate of nucleation may be zero, constant, proportional to time or proportional to the square of time.

Bradley, Colvin and Hume¹⁰ could get photographs illustrating nucleus formation in potassium chlorate and interfacial reactions in anhydrous potassium oxalate. A given solid

state decomposition or one of its steps may be described by a given rate law. A general mathematical treatment is not possible because the individual participating processes of nucleation and growth are functionally different.

1.1.5 The laws of nucleus formation

Most of the laws have been formulated on the basis of the idea that nucleation is favoured at definite localized spots of least activation energy. Such potential nucleus forming sites in a crystal are associated with lattice imperfections like vacancies, interstitials, dislocations, grain boundaries etc. Dislocations are characterized by a strain energy and nucleation at such sites or surface is energetically more favourable. Interfacial strain energy is of the order of 1 Kcal mol⁻¹ for a typical reactant which is adequate to account for the slow growth of small nuclei. Lattice defects introduced during crystal growth profoundly influence the characteristic features of the crystal and transform its properties to varying extents. The movement of defects is responsible for diffusion in crystals which also plays an important role in solid state decomposition. The various laws of nucleus formation are given below:

1.1.5.1 Instantaneous nucleation

In this case nucleation is complete at zero time. A number of germ nuclei are situated at regions of defects such as sites of emergence of dislocations, at vacancies, interstitials or impurity clusters or at the meeting points of high angle grain boundaries. All such sites may be called potential sites of nucleus formation. The reactant molecules at these sites are less well coordinated in the crystal than are molecules in the normal surface and will decompose more readily because fewer bounds per molecule is required to be broken.

If N_0 represents the number of such potential sites and N is the number of nuclei formed at t , then

$$N_0 = N \text{ at } t = 0$$

or,

$$\frac{dN}{dt} = 0 \text{ or negligible} \quad 1.6$$

for instantaneous nucleation. Under this condition the overall kinetic law can be directly related to the shape of the nuclei and the rate of growth.

1.1.5.2 Exponential law

When the nucleus formation involves a single surface chemical reaction, the rate of nucleation will be directly proportional to the number of sites available for nucleation. If N_0 is the number of available sites at which nucleation may take place and N is the number of nuclei present at time t , then the rate of nucleation is given by

$$\frac{dN}{dt} = k_n (N_0 - N) \quad 1.7$$

where k_n is the rate constant for nucleation.

Integrating,

$$N = N_0 [1 - \exp(-k_n t)]$$

or,

$$N_0 - N = N_0 \exp(-k_n t) \quad 1.8$$

Substituting in 1.7 we get

$$\frac{dN}{dt} = k_n N_0 \exp(-k_n t) \quad 1.9$$

1.1.5.3 Linear law

When $k_n t$ is very small which is the case with the early stages of the reaction, $\exp(-k_n t)$ in equation 1.9 can be expanded and the power terms neglected, then the exponential law reduces to the form

$$\frac{dN}{dt} = k_n N_0 \quad 1.10$$

or

$$N = k_n N_0 t \quad 1.11$$

The nucleation proceeds at a constant rate leading to a linear increase in the number of nuclei with time^{11,12}.

1.1.5.4 Power law

Instead of a linear increase in the number of nuclei with time, in certain reactions, the number of nuclei increases as a higher power of time. In the study of barium azide crystals,¹³ extrapolation of direct microphotographic measurements of the size and number of visible nuclei as a function of time showed that

$$N = (k_n t)^3 \quad 1.12$$

This observation was explained by Bagdassarian¹⁴ as due to the involvement of several successive decomposition steps in the formation of a stable nucleus. Thomas and Tompkins¹⁵ explained the same thing as due to a bimolecular process involving the combination of a given number of active intermediates. If β successive steps of equal probability occur at the potential nucleus forming sites before it can function as active growth nucleus, then

$$\frac{dN}{dt} = k(k_n t)^{\beta-1} \quad 1.13$$

where k is the rate constant for nucleation and k_n is that for the individual step.

Integrating 1.13, we get

$$\begin{aligned} N &= \frac{k(k_n)^{\beta-1} t^\beta}{\beta} \\ &= D t^\beta \end{aligned} \quad 1.14$$

where D includes k , k_n and β . This equation has been found to be valid for the decomposition of nickel sulphate heptahydrate and barium azide for which $\beta = 2$ and 3 respectively.

1.1.6 Laws of nucleus growth

The advancement of the reactant-product interface in a direction normal to the surface is called nucleus growth. The rate of growth in different directions depends on several factors such as the structure of the reactant, the product and the interface. Another factor influencing the rate of growth in a particular direction is the diffusion of product gases away from the reactant along cracks at the interface. Except in some cases, especially with small nuclei, growth occurs at constant rate. Generally small nuclei appear to grow more slowly than larger ones. A well documented case of departure is that of chrome alum¹⁶ in which small nuclei are sometimes observed to grow faster than large nuclei. This deviation is due to detailed changes in the interfacial conditions. Slow growth appears to be important in the case of hydrates and azides. The shape of the growing nucleus may be different for different compounds. The laws of nucleus growth are summarized below.

1.1.6.1 Power law

This law is applicable to those solid decompositions in which nucleation proceeds according to a power law and the nucleus growth is normal. Assuming a constant rate of growth, the fractional decomposition (α) at time t is given by

$$\alpha = Ct^m \quad 1.15$$

where C is constant and m is a possible integer. This equation is found to fit satisfactorily well for early stages of a reaction before appreciable overlap of nuclei takes place, for example slow growth in hydrates.

1.1.6.2 Exponential law

Garner¹⁷ considered growth of nuclei as linear branching chains similar to branching chain reactions involving free radicals in gas phase reactions. Under such conditions the net rate of production of nuclei is given by

$$\frac{dN}{dt} = k_n N_0 + k_b N \quad 1.16$$

where k_n and k_b are the rate constants for the formation and branching of nuclei respectively. Starting with equation 1.16, the following equation can be arrived at

$$\alpha = C' \exp(k_b t) \quad 1.17$$

where C' is a constant which contains the rate constants for nucleation, nucleus growth and branching. This law has been found to be valid for silver oxalate upto $\alpha = 0.3$.

1.1.6.3 Avrami – Erofeyev equation

With a view to account for the overlap of growth nuclei and ingestion of germ nuclei into active growth nuclei, Avrami, Mampel and Kholmogorov developed a more general kinetic equation for nucleus growth. According to them, as nuclei grow, the overall rate of reaction may be reduced via

- i) cessation of reaction at those regions of contact formed by coalescence of the reaction interface – where the growth of two adjoining nuclei have resulted in a common boundary
- ii) removal of potential nucleus forming sites on the surface through the interference created by such regions into the growth of the existing nuclei.

Giving appropriate allowances for these two effects. Avrami and Erofeyev^{18, 19} derived the equation

$$\alpha = 1 - \exp(-kt^n) \quad 1.18$$

The differential form of the equation can be written as

$$\frac{d\alpha}{dt} = nk^n [-\ln(1-\alpha)]^{1-\frac{1}{n}} (1-\alpha) \quad 1.19$$

which on expansion, approximation and rearrangement gives

$$\frac{d\alpha}{dt} = k'\alpha^a (1-\alpha)^b \quad 1.20$$

where k' is the new rate constant where a and b are constants associated with given values of n . From the above equation a more generalized and simplified equation was derived in the form

$$-\ln(1-\alpha) = (kt)^n \quad 1.21$$

where $n = 2, 3$ or 4 . This is one of the most popular equations in solid state kinetics and has been used to explain a number of solid state reactions, for example decomposition of ammonium perchlorate, potassium permanganate and barium azide. Kinetics of nickel formate, nickel oxalate and sodium azide also conform to this equation.

1.1.6.4 Prout-Tompkins equation

Prout and Tompkins²⁰ visualized the mechanism of solid state decomposition as a chain branching process similar to certain gas phase reactions involving radicals. In such a case the chain termination by radical recombination has also to be taken into account. This was accounted by adding the term $-k_t N$ in the Garner's¹⁷ equation (1.16) to get the expression

$$\frac{dN}{dt} = k_n N_0 + k_b N - k_t N \quad 1.22$$

where k_n , k_b and k_t are the rate constants for nucleation, branching and chain termination. Assuming the rate of decomposition to be proportional to the number of nuclei present, we can write

$$\frac{dN}{dt} = k'N \quad 1.23$$

Integrating equations 1.22 and 1.23 and after making reasonable approximations, the following equation could be derived

$$\ln[\alpha/(1-\alpha)] = k_b t + C \quad 1.24$$

where C is a constant.

This is one of the most commonly used equations in solid state kinetics and has been successfully applied to decompositions of a large number of compounds such as potassium permanganate, lead oxalate, nickel formate, potassium chlorate, potassium bromate, potassium periodate etc.

1.1.6.5 Deceleratory equations

In certain solid decompositions an initial acceleratory period is not observed. For solids with instantaneous nucleation over the entire surface the rate progressively decreases since the interface progresses towards the centre of the crystal resulting in a decrease in interfacial area. The equations which have been found fit for such deceleratory situations are

- i) The '*contracting cube*' equation or '*contracting sphere*' equation

$$1 - (1 - \alpha)^{1/3} = k t \quad 1.25$$

This equation fits well in cases where the initial nucleation step occurs rapidly over all surfaces for a single cube of reactant and interface established contracts in the direction of the centre of the crystal. High temperature decomposition of ammonium perchlorate, dehydration of copper sulphate pentahydrate etc follow this equation.

- ii) The '*contracting square*' equation

$$1 - (1 - \alpha)^{1/2} = k t \quad 1.26$$

This is applicable to decomposition reaction that proceeds with decrease in interfacial contact area. Such behaviour is seen in solids with layer lattices.

1.1.6.6 Unimolecular decay or first order equation

In the case of some solids the decomposition behaviour is markedly influenced by the particle nature²¹. The powdered sample of the solid may obey equation of the type

$$-\ln(1 - \alpha) = k t \quad 1.27$$

The sample contains particles of similar size, each particle nucleated with equal probability. This type of kinetics has been found with the decomposition of powdered samples of barium azide and many metal carbonates.

1.2 Crystal Defects and their Role in Thermal Decomposition of Solids

A lot of information has been made available relating to the significant role of crystal imperfections in modifying the properties of a crystal ^{22,23,24}. A perfect crystal consists of a perfectly periodic array of atoms or ions whose arrangement has symmetry of one kind or the other. Theoretically the state of perfect order and of lowest energy is predicted at 0 K and above 0 K, departure from the perfect order is inevitable. Deviation from an orderly arrangement is termed as imperfection or defect. Defects are responsible for many of the characteristic properties of crystals. Apart from inherent defects in the crystal, it is possible to generate defects in crystals. Defects are also responsible for chemical reactivity of the crystal. An ideal crystal is quite unreactive. The sites of reactivity are those points or sites where there is a defect or fault in the perfect order. These defects can be point defects, dislocations, stacking faults of atomic order or high angle grain boundaries. A brief description of the different kinds of defects in crystals may be mentioned in this connection.

1.2.1 Point defects

If the deviation from regularity is confined to a very small region of only several atoms, it is called a point defect. The following types of point defects have been noticed in the case of crystals.

i) Interstitial

In this case there is present an extra atom (molecule or ion) somewhere in the interstice of the crystal lattice. This may be an impurity atom (interstitial impurity defect) or an atom of the substance itself (self interstitial).

ii) Schottky defect

This is a defect in which an atom or ion is found to be missing from its normal position creating a vacancy. In ionic crystals, equal number of cations and anions would be missing.

iii) Frenkel defect

Frenkel defect arises when an atom or ion leaves its normal site and occupies an interstice. Frenkel defect, in fact, characterizes two imperfections – vacancy and interstitial.

iv) Substitutional impurity

This defect is characterized by the presence of impurity atom or ion in a lattice position.

1.2.2 Line defects or dislocations

Deviations extending through microscopic regions producing discontinuity in the lattice are called lattice imperfections. If the lattice imperfection propagates as lines in a crystal it is called line defect or dislocation. It is a region of strain in a crystal in which part of the lattice has undergone a shearing strain. There are two types of dislocations.

i) Edge dislocation or Taylor's dislocation

In this case periodicity of the atomic lattice array is interrupted along certain directions for example by missing a half plane of atoms.

ii) Screw dislocation or Burger's dislocation

It is a type of dislocation in which dislocation plane is parallel to the slip direction and it has a row of atoms about which a normal crystallographic plane appears to be spiral.

1.2.3 Plane defects

A cluster of line defects in a plane is called plane defect which are of three types.

i) Lineage boundary

It is a boundary between two adjacent perfect regions in the same crystal which are slightly tilted with respect to each other.

ii) Grain boundary

Sometimes a bulk crystal may be a polycrystalline form in which many crystals are stacked together in a random way. The boundary between two crystals in a polycrystalline solid is called grain boundary.

iii) Stacking fault

These are mistakes occurring in the stacking sequence of close packed structures in solids. The plane separating two incorrectly juxtaposed layers is called stacking fault.

1.2.4 Electronic Imperfections

By electronic imperfections is meant the errors in the charge distribution or energy in solids. At temperatures above 0 K the electrons from valence bands are thermally released into higher conduction bands. The released electrons are conduction electrons and correspondingly 'positive holes' are generated in the valence band. These defects are on a subatomic scale and are responsible for many electrical and magnetic properties of solids.

1.2.5 Excitation states of crystals

The following excitation states of crystals are, in a way, defects.

- i) Phonons and magnons-they are quantized lattice vibrations and space waves respectively.
- ii) Conduction electrons and holes which are excited thermally from filled bands or impurity levels.
- iii) Excitons- they are quantized electron-hole pairs.
- iv) Quantized plasma waves.

1.2.6 Transient imperfections

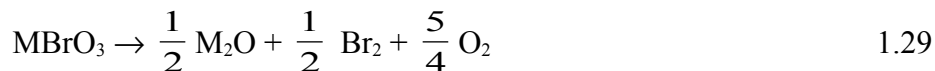
As mentioned earlier, defects may be inherent in crystals but defects can be generated or introduced into crystal by various methods. In fact many of the electrical and magnetic properties of solids may be manipulated by generating defects of a given kind to a given extent.

The imperfections introduced into the crystal from external sources are collectively called transient imperfections. Irradiation of crystals with photons, high energy charged particles like electrons, protons, alpha particles etc and high energy uncharged particles like neutrons can produce defects in crystals. Studies on the influence of lattice imperfections or nucleation during the solid decomposition reaction on a series of crystals of barium azide¹³ revealed that the concentration of nuclei in the imperfect region was many times greater than that in the perfect region. The degree of imperfection can be enhanced by crushing, grinding²⁵, addition of impurities, doping of ions or irradiation. In general the greater the degree of imperfection the greater the ease of formation of nuclei.

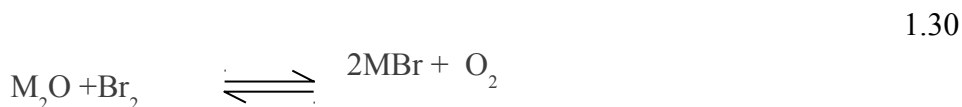
1.3 Review of Studies on Thermal Decomposition of Bromates

1.3.1 Pathways of decomposition

There have been quite a number of studies on the thermal decomposition of metal bromates. Bromates decompose to give a residue of either the oxide, the bromide or a mixture of both. Thus the following two overall reactions are possible²⁶.



The deviation from stoichiometry of products in the case of decomposition of some bromates has been explained as due to equilibrium between oxide and bromide¹⁸.



Markowitz²⁷ suggested that the path of decomposition (1.28 or 1.29) could be predicted only from a knowledge of the free energies ΔG , for the formation of bromide and oxide. If ΔG_f (metal bromide) - ΔG_f (metal oxide) is negative, then thermodynamically the bromide should form; if it is positive the oxide should form. This method, however, considers only the relative stabilities of the final products in predicting the decomposition products and is not a correct deciding principle if the reaction is kinetically controlled. In most cases studied so far the decompositions are mostly irreversible and therefore the kinetics should play a significant role in determining the decomposition products.

Markowitz²⁷ was able to predict the decomposition products of perchlorates using thermodynamic principle. In the case of bromates of lithium, calcium, cadmium, cobalt, nickel and zinc ΔH_f (bromide) - ΔH_f (oxide) values are very small²⁶ coming in between -15 Kcal and +5 Kcal, showing that the exact course of decomposition can be better arrived at from kinetic studies.

1.3.2 Bromates of monovalent cations

The decomposition occurs in accordance with the stoichiometry.



Oxide formation was noted to a small extent in the case of LiBrO_3 . The thermal stability decreases in the order $\text{Li} > \text{Na} > \text{K} > \text{Cs} > \text{Rb}$ which is same as the order of their melting points²⁶.

Calculation of activation energy by the Horowitz and Metzger method²⁸ gave unusually high values for lithium and potassium bromates. Derivatographic studies have shown that the decomposition of sodium and potassium bromates²⁹ begin after fusion. Thermogravimetric studies prove that alkali metal bromates do not contain water of hydration^{29,30}. The decomposition of NaBrO₃ was reported as a five stage process³¹ viz. small initial gas evolution, induction period, a slow linear reaction, acceleratory and decay stages:

Decomposition of potassium bromate crystals takes place without an induction period. The initial rapid gas evolution is followed by an exponential decay equation which is preceded by an acceleratory process. At high temperature, the crystals melted below the melting point due to eutectic formation between potassium bromide and potassium bromate³². The bromide formed on the surface affects the decomposition of bromate catalytically. The catalytic effect of the bromide ion is explained by Jach³² as due to the donation of an electron by it to an oxygen atom of a still undecomposed bromate ion thereby enhancing the cleavage of the latter.

Studies on solid decomposition of potassium bromate³³ showed that increase of temperature and exposure to X-rays enhanced the decomposition. Manganese dioxide catalysed decomposition of potassium bromate³⁴ and the decomposition of irradiated and unirradiated samples of sodium bromate³⁵ and potassium bromate³⁶⁻³⁸ were seen to obey the equation of contracting cube(1.25) and the rate controlling process has been shown to be a phase boundary reaction assuming spherical symmetry³⁶.

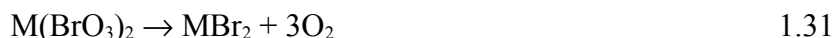
$$1 - (1 - \alpha)^{1/3} = kt \quad 1.25$$

Cesium bromate³⁹ also showed a similar behaviour. Among other monovalent bromates thallium (I) bromate⁴⁰ has been studied in some detail. In this case the decomposition begins with a rapid evolution of oxygen obeying first order kinetics followed by a slow process of constant rate and then by an autocatalytic stage⁴¹. Silver (I) bromate⁴² decomposition is also autocatalytic and it follows Prout-Tompkins equation (1.24).

Ammonium bromate⁴³ is much less stable than other bromates; however it has been studied in the temperature range 32-50°C in vacuum. The decomposition curve consisted of three parts (i) a short acceleratory period, (ii) a fairly long constant rate process and (iii) a deceleratory reaction. The short acceleratory period obeyed Garner's relation (1.16 and 1.17) and the deceleratory stage obeyed the equation of unimolecular decay (1.27).

1.3.3 Bromates of divalent cations

Thermal decomposition of bromates of divalent metals Mg, Ca, Sr, Ba was studied by Bancroft and Gesser²⁶. All of them form hydrated crystals and the water of hydration is lost on heating and in majority of cases they decompose to bromide and oxygen according to the equation



In the case of magnesium bromate, oxide formation took place to a notable extent. Physicochemical analysis of magnesium bromate hexahydrate⁴⁴ was done by X-ray diffraction, IR spectroscopy, NMR technique and thermal analysis. In the temperature range 293-770K there was no structural phase transition detected.

The initial stages in the thermal decomposition of barium bromate^{33,45-48} and calcium bromate⁴⁹ obey the equation(1.32) and the acceleratory and decay stages both have been analysed⁵⁰ by the Prout –Tompkins equation (1.24) or by the simplified equation

$$\alpha = kt + C \quad 1.32$$

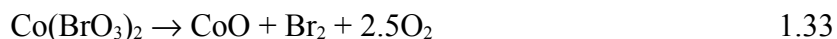
Thermogravimetric studies of calcium⁵¹ and magnesium⁵² bromate revealed the rate controlling process of the reaction to be a phase boundary reaction assuming spherical symmetry.

The decomposition of lead bromate⁵³ is somewhat similar to that of alkaline earth bromates and has also been analysed by Prout-Tompkins equation(1.24). The decomposition of zinc bromate⁵⁴ was found to fit well with Avrami-Erofeyev equation (1.18). For cadmium bromate^{55,56}, the slow linear reaction was found to be missing while the decay stage appeared

lengthy. The acceleratory and decay stages were best explained by Avrami-Erofeyev model.^{18,19}

1.3.4 Bromates of transition metals

Not much has been reported about the thermal decomposition of transition metal bromates. There are some studies on silver bromate⁴², cobalt bromate²⁶ and nickel bromate²⁶. Sufficient literature is available relating to the decomposition of zinc⁵⁴ and cadmium bromates^{55,56} (already cited in the previous section) which, however, behave like other non-transition divalent bromates. Both cobalt and nickel bromate crystallize as hexahydrates. They lose water of hydration on heating and decompose to the corresponding oxide and bromide. Bancroft and Gesser²⁶ reported that cobalt bromate decomposition involves the evolution of Br₂ and water vapour and a major percentage decomposed to oxide and only a small amount of bromide was obtained.

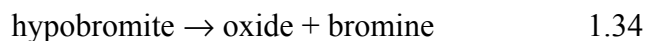


1.3.5 Thermal decomposition of rare earth bromates

Thermal analysis of not many rare earth bromates have been studied in detail. Yukiku Mishimura⁵⁷ had prepared rare earth bromates and made an extensive study of many of their thermodynamic properties in solution. Bancroft and Gesser²⁶ had prepared bromates of neodymium, praseodymium and yttrium and had estimated their composition. In a recent study Abbasi⁵⁸ and Badiei⁵⁹ had determined the composition of yttrium bromate in detail.

Major and Glassner⁶⁰ had investigated the routes of thermal decomposition of rare earth bromates and suggested the following scheme.

Hydrated bromate → anhydrous bromate →



The decompositions begin without a time lag and the curves were best analysed by the equation

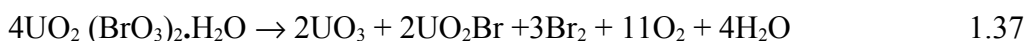
$$\alpha = 1 - e^{-kt^n} \quad 1.35$$

or

$$[-\ln(1-\alpha)]^{\frac{1}{n}} = k't \quad 1.36$$

which, in general, described reaction upto 85%. The latter equation corresponds to the sigmoidal rate equations as given by Avrami and Erofeyev.^{18,19}

Thermal decomposition studies on uranyl bromate $\text{UO}_2(\text{BrO}_3)_2 \cdot \text{H}_2\text{O}$ was studied by Weigel and Engelhardt⁶¹ by Sartorius thermogravimetric method. A mass loss accompanied by a loss of bromine was observed at 203°C. The total mass was 41.96% which corresponds to the reaction



1.3.6 The effect of doping on the thermal decomposition of bromates

In section 1.2 the role of various types of crystal defects in the decomposition of solids has been discussed briefly. The population or concentration of defects in crystals can be altered by doping. As the kinetics of solid state decomposition depends on the formation and growth of nuclei and for the formation of nuclei the occurrence of defects of some kind is inevitable, it follows that the rate, kinetics and mechanism of decomposition may change with the addition of dopants.

Doping of sodium bromate with potassium bromate or sodium bromide⁶², zinc bromate with nickel bromate⁵⁴, potassium bromate with rubidium bromate⁶³ and potassium bromate with cesium bromate⁶³ enhances the decomposition and decreases the energy of activation. The effect increases with increase in concentration of the dopant. The effect is explained as due to the bond rupture induced by the steady accumulation of strain resulting from the introduction of vacancies and defects by doping. However the mechanism of decomposition is not altered by doping.

Studies on the effect of doping on the thermal decomposition of NaBrO_3 ³¹ show that doping shortens the induction period, enhances the rate of reaction in the acceleratory and decay stages. It is reported that the activation energy of the acceleratory period decreases while that of the decay stage increases due to doping.

The effect of adding KBr on the thermal decomposition of KBrO_3 has been reported⁶⁴. At a given temperature the rate constant of the initial slow first order process increases while that of the subsequent faster first order process is practically unchanged.

Studies⁶⁵ were made on the isothermal decomposition of KBrO_3 as a function of concentration of the dopants SO_4^{2-} and Ba^{2+} by isothermal thermogravimetry in the temperature range 668-683 K. The rate law and the activation energies remained unaltered by doping. Das et al.⁶⁶ has studied the effects of anion doping on potassium bromate and found that structural defects introduced by way of doping the anions Cl^- (monovalent) and SO_4^{2-} (divalent) did influence the decomposition. The effect was more pronounced in the case of SO_4^{2-} than in the case of Cl^- .

In a study of the role of dopant cations Al^{3+} and Th^{4+} ⁶⁷ on the kinetics of thermal decomposition of γ -irradiated KBrO_3 , it is reported that the sensitizing effect of the dopant ions is more prominent during the initial period of the decomposition than the subsequent stages of acceleration and decay. The activation energies are not much affected by doping with trivalent and tetravalent ions. Studies on the role of both cationic and anionic dopants on the thermal decomposition of barium bromate⁶⁸⁻⁷¹ revealed that both the dopants shortened the induction period and enhanced the rate constants in the linear, acceleratory and decay stages.

The influence of dopants on the thermal decomposition of strontium bromate^{72,73} was studied using KBrO_3 , $\text{Mg}(\text{BrO}_3)_2$, $\text{Al}(\text{BrO}_3)_3$ and KBr in 10^{-4} to 10^{-1} mole percentages. It was found that doping enhanced the decomposition and decreased the energy of activation in samples doped with $\text{Al}(\text{BrO}_3)_3$ and KBr whereas KBrO_3 and $\text{Mg}(\text{BrO}_3)_2$ increase the thermal stability of $\text{Sr}(\text{BrO}_3)_2$. It was suggested that the greater susceptibility to thermal decomposition observed in the case of strontium bromate containing potassium bromide arises due to the formation of the eutectic between the bromate and bromide.

An interesting case reported is that of CsBrO_3 ⁷⁴ which is immune to thermal decomposition in the pure state but does decompose in the presence of dopants. In a sample of CsBrO_3

doped with Ba^{2+} the presence of two decay stages (one short and one long) are seen, the short decay stage diminishes with increase in temperature and is virtually absent at 673K. The data best fitted with a power law model where the energies of activation for the decay stages are higher than that of the acceleratory stage. Microscopic observation reveals that the reaction begins essentially on the surface with the rapid formation of an interface and is followed by penetration of the interface into the crystallite.

1.3.7 Effect of additives on the thermal decomposition of bromates

The influence of additives such as CuO , Cr_2O_3 , TiO_2 and Al_2O_3 on the thermal decomposition of barium bromate has been studied⁷⁵. In all cases additives shorten the duration of the induction period. CuO and TiO_2 being p and n type semiconductors respectively enhances the rate constants of the linear and acceleratory stages. CuO retards the rate of the decay period whereas TiO_2 does not affect it. The p type semi-conducting oxide Cr_2O_3 decelerates the rate of all the stages. Al_2O_3 being an insulator has only a marginal effect on the reaction rates.

Effect of additives CuO and MnO_2 ⁷⁶ on the thermal decomposition of potassium bromate was studied at 638K and 648K. Analysis of data using various kinetic models showed that the decomposition best fitted with Prout-Tompkins model²⁰ and Avrami-Erofeyev model.^{18,19}

In a study of the effect of Dy_2O_3 ⁷⁷ on the thermal decomposition of sodium bromate, it was found that Dy_2O_3 being a p type semiconductor accelerates the decomposition by favouring the electron transfer reaction involved in the process.

Similar studies on the role of rare earth semiconductors of the p type Gd_2O_3 and Dy_2O_3 in catalytic amounts on the thermal decomposition of barium bromate have been reported.⁷⁸ Both catalysed the reaction without affecting the induction and linear periods. The presence of the additives enhanced the nucleation which occurs in a chain branching manner obeying Prout-Tompkins equation²⁰ and also following a two dimensional growth of nuclei which follows Avrami – Erofeyev equation.^{18,19}

Certain interesting effects of some additives such as transition metal oxides^{79,80} on the thermal decomposition of potassium bromate have been reported. It is observed that KBrO_3 in the presence of Cr_2O_3 undergoes decomposition and chemically interacts in the mole ratio 2:1 to form $\text{K}_2\text{Cr}_2\text{O}_7$ at 180-320°C and in 4:1 mole ratio to form K_2CrO_4 at 180-340°C.

1.3.8 Effect of precompression on the thermal stability of solids

In a comparative study of the effect of precompression^{81,82} on the thermal stabilities of potassium bromate, ammonium perchlorate and potassium permanganate it was found that the rates of isothermal decomposition of these solids were significantly modified by precompression without affecting the mechanism of decomposition. The rate of decomposition increased with increase in the applied pressure in the case of ammonium perchlorate and potassium permanganate but the rate dramatically decreased in the case of potassium bromate. The reports are explained as due to precompression sensitising electron transfer reaction as a result of an increase in the dislocations whereas it desensitizes diffusion controlled reactions as a result of the densification of the solid matrix. The method of precompression is suggested as a quick and simple tool for testing whether a decomposition is diffusion controlled or not.

1.3.9 Effect of irradiation on the thermal decomposition of bromates

In a study of the effect of γ -irradiation on the kinetic parameters of thermal decomposition of KBrO_3 it was found that radiation causes a decrease in activation energy and frequency factor at a rate which is large at small doses but decreases at higher doses. The results showed that the increase in the concentration of decomposition nuclei tends to be more important than the increase in the porous character of the solid in deciding the kinetics of decomposition.

Effect of doping and irradiation on thermal decomposition of NaBrO_3 ³¹ was reported as a five stage process—small initial gas evolution, induction period, a slow linear reaction, acceleratory and decay stages. The acceleratory stage fitted with Prout-Tompkins equation²⁰ and Avrami – Erofeyev equation.^{18,19} Irradiation as well as doping shorten the induction period, enhance the rate of the reaction in the acceleratory and decay stages. The combined

treatment eliminates the induction period and increases the extent of decomposition to a remarkable extent.

Effect of γ -irradiation on the thermal decomposition of KBrO_3 ⁸³ and KBrO_3 doped with 2.5% KBr was investigated within the temperature range 653-683K. The catalytic effect of KBr on decomposition becomes more pronounced upon irradiation. The value of the rate constant increased with the increase in the radiation dose. Activation energies did not change much. A similar study on γ -irradiated CsBrO_3 ^{84,85} in the temperature range 633-673 K also showed that the activation energy of either acceleratory or decay stage is not affected. When Ba^{2+} doped CsBrO_3 ³⁹ was subjected to thermal decomposition, the initial rapid gas evolution representing 1-2% reaction is completely eliminated. The doped irradiated samples indicated two decay stages –one short and the other long – the short decay diminishes with increase in temperature and virtually remains absent at 673 K. The acceleratory and decay periods of the samples were analysed by Prout-Tompkins equation(1.24), Avrami Erofeyev equation (1.18) and contracting square model(1.26). The energy of activation for the acceleratory stages of both doped and doped and irradiated samples was nearly the same irrespective of the kinetic model employed. In a different experiment⁸⁶ of radiolysis as well as annealing of radiolytic damage entities in γ - irradiated Ba^{2+} doped CsBrO_3 it was observed that cationic vacancies generated by doping with a divalent ion enhanced both processes. Analysing the data in the light of theories of diffusion controlled mechanism indicated that hypobromite (OBr) and bromite (BrO_2^-) recovered by a combination of one first order process and one second order process. In another study it was found that preannealing⁸⁷ influences the thermal decomposition of γ - irradiated CsBrO_3 .

Studies on thermal decomposition of γ - irradiated strontium bromate⁸⁸ revealed that irradiation enhances the decomposition and decreases the energy of activation but does not change the mechanism of decomposition. In another study^{89,90} the role of lattice defects introduced by crushing and doping on the annealing of chemical radiation damage in $\text{Sr}(\text{BrO}_3)_2$ has been investigated. Crushing of irradiated crystals produces direct recovery and also accelerates the subsequent thermal annealing. The initial damage and susceptibility to

thermal annealing are greater in the doped crystals than in the untreated samples. Similar studies on strontium bromate have also been reported^{89,91}.

In a study of the effect of γ - irradiation on the thermal decomposition of zinc bromate⁹² by dynamic thermogravimetry, it was found that irradiation enhanced the decomposition and the effect increased with the irradiation dose. The activation energy in this case however, decreased with irradiation. Irradiation did not alter the mechanism.

Irradiation and doping shorten the induction period, facilitates the acceleratory and decay stages in the case of sodium bromate at temperatures 613-653 K.^{93,94,95} Interestingly the combined effect of the two pretreatments doping and irradiation eliminates the induction period and increases the extent of decomposition remarkably. The irradiated and unirradiated samples followed Prout-Tompkins model (1.24) exploring that nucleation occurs by a branching chain mechanism.

In a comparative study of radiation induced thermal decomposition of lithium perchlorate and barium bromate^{96, 97} it was reported that lithium perchlorate decomposed with melting and barium bromate without melting. In both cases irradiation enhanced decomposition.

Studies on the effect of γ - irradiation in zinc bromate⁹² and magnesium bromate⁹⁸ have also been undertaken. It was found that irradiation enhances the decomposition and the effect increases with the irradiation dose. The activation energy decreases on irradiation. In both cases the decomposition of the unirradiated salt as well as irradiated salt followed Avrami-Erofeyev model (1.18) indicating that the rate controlling process is a phase boundary reaction assuming spherical symmetry. Similar results have been reported for cadmium bromate⁵⁶ also.

1.4 Thermal Methods of Analysis

1.4.1 Introduction

Among the different analytical methods of investigation, thermal methods of analysis have assumed paramount importance. Methods of thermal analysis, in general may be defined as a

group of analytical techniques in which the parameters of any physical properties of substances are monitored as a function of temperature. Thermogravimetry (TG), derivative thermogravimetry (DTG), differential thermal analysis (DTA) and differential scanning calorimetry (DSC) are the most widely used thermo analytical techniques. In fact thermogravimetry has been most potent and traditionally used method for investigating thermal decomposition of solids.

1.4.2 Thermogravimetry

Of the different methods of thermal analysis thermogravimetric analysis (TGA) is probably the most powerful and popular thermo analytical technique used in connection with the study of thermal decomposition of solids and it involves the study of the change in mass of a substance as a function of temperature⁹⁹. The thermogravimetric curve (TG curve) which expresses the dependence of the mass change on temperature gives information on the sample composition, its thermal stability, the stages of its thermal decomposition and information on the products formed on heating. TG curves normally express the dependence of the sample mass (w) on temperature (T) or time (t)

$$w = f(T \text{ or } t) \quad 1.38$$

whereas derivative thermogravimetry (DTG) curve gives the change in mass with time

$\left(\frac{dw}{dt}\right)$ as a function of temperature or time.

$$\frac{dw}{dt} = f(T, \text{ or } t) \quad 1.39$$

In the present day equipments both these can be mentioned simultaneously to give TG and DTG curves in the same graph.

The history of thermogravimetry can be traced back to 1905 when Brill¹⁰⁰ studied the mass loss during heating of CaCO_3 . The method assumed status of an analytical technique with the development of the first thermobalance by Honda (1915). The credit of the successful evolution of thermogravimetric equipment from the original primitive device to the present highly technical and most advanced apparatus goes to Guichard, Chevanard and Dual¹⁰¹. The first commercially produced thermobalance was due to Chevanard. In his book published in

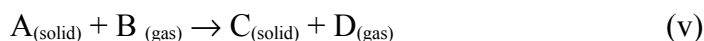
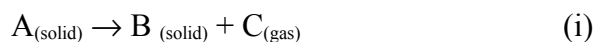
1953 Dual¹⁰¹ narrates the study of a large number of analytical precipitates by thermogravimetry. With the publication of papers by Simons and Newkirk¹⁰² and Freeman and Carroll¹⁰³ in which interpretation of TG curves were exhaustively discussed, TGA became one of the most widely used methods for the investigation of kinetics of solid state decompositions. The method became user friendly with the automation of TGA by Bradley and Wendlandt¹⁰⁴.

1.4.3 Methods used in thermogravimetry

There are three types of thermogravimetry.

- i) Isothermal or static thermogravimetry in which the sample mass is recorded as a function of time at constant temperature.
- ii) Quasistatic thermogravimetry in which the sample is heated to a constant mass at each of a series of increasing temperatures.
- iii) Non-isothermal or dynamic thermogravimetry in which the sample mass is recorded as a function of temperature at a constant heating rate.

The curve representing the mass change versus temperature is called thermogram and provides quantitative information concerning the thermal stability and composition of the initial sample, the thermal stability and composition of any intermediate compounds that may be formed and the composition of the residue, if any. The technique is employed in the study of the following types of solid state reactions which involve formation of volatile or gaseous products.



One very important thing about thermogravimetry is that except for mass change, much of the information obtained from a TG curve is of an empirical nature since the curve transition temperatures are procedurally obtained temperatures (dependent on the instrument and sample parameters) and are not fundamental to the compound.

Thermogravimetry has grown as a very widely and successfully used analytical tool in chemistry for the investigation of thermal behaviour of compounds, of new compounds suitable for gravimetry, to ascertain purity of compounds, in the study of dehydration and decomposition reactions etc. It is exhaustively used in the field of inorganic chemistry in the study of minerals, ceramics, metals, alloys, sintered carbides, glass, catalysts, construction materials etc and in organic chemistry in the analysis of drugs, plastics, explosives, detergents, dyes, textile fibres, fuels, polymers, composites and soft materials.

According to Hill¹⁰⁵, thermal analytical techniques have a diversity of applications unmatched by other conventional techniques and thermodynamic data derived from such studies are of prime significance in the rationalization of physical and chemical phenomena.

1.4.4 Factors affecting thermogravimetry

Thermogravimetry has a large number of variables because of the dynamic nature of the temperature change of the sample. A number of factors must be controlled carefully if useful and reproducible thermogravimetric curves are to be obtained. These factors include the features and design of the experimental setup, the quality and physical properties of the sample, the type of the working atmosphere and the method of heating etc.

The factors which influence a TG curve are:

1.4.4.1 Instrumental factors

- i) Furnace heating rate
 - ii) Nature of heating
 - iii) Rate of recording the curve
 - iv) Furnace atmosphere
 - v) Composition of the sample container
 - vi) Geometry of the sample holder and furnace
 - vii) Sensitivity for the balance and the recording mechanism etc
- and

1.4.4.2 Sample characteristics

- i) Amount of the sample
- ii) Solubility of the evolved gas in the sample
- iii) Particle size
- iv) Heat of reaction
- v) Nature of the sample and packing
- vi) Thermal conductivity etc

The factors such as sample holder geometry, recording speed, balance sensitivity and sample container buoyancy are fixed with any given thermobalance whereas factors such as particle size, packing, solubility of evolved gas in the sample, furnace convection currents and electrostatic effects are variable and are very difficult to reproduce. Effects arising from the materials used for the construction of the TG equipment can be avoided by carefully designing the instrument. Modern thermobalances and accessories are free from errors due to electrostatic effects on the weighing mechanism and inaccuracies in the recording and weighing mechanism. Some of the factors may be examined in detail.

1.4.4.3 Effect of heating rate and heat transfer

A number of reports^{101-104, 106-109} are available in literature relating the effect of heating rate and heat transfer in thermogravimetry. As thermogravimetry requires heating and weighing of the sample simultaneously there must be no contact between the sample and the furnace wall. A temperature gradient is formed between the sample and furnace wall and this introduces errors in the measurement of the sample temperature and determination of the range of temperature of reaction being studied. Coats and Redfern¹⁰⁶ have found that the rate of heating can affect the decomposition of the sample. For a given temperature interval, the extent of decomposition is greater at a slow rate of heating than when the sample is heated at a faster rate. If the decomposition is exothermic, the sample temperature will rise above that of the furnace and this causes faster rate of heating. In certain cases, the appearance of a point of inflection in a TG curve at a faster heating rate may resolve itself into a small horizontal plateau at a slower heating rate.

1.4.4.4 Furnace atmosphere

The nature of the surrounding atmosphere can have a profound effect upon the temperature of a decomposition stage. Normally the function of the atmosphere is to remove the gaseous products evolved during thermogravimetry, in order to ensure the nature of the surrounding gas remains as constant as possible throughout the experiment. There are three atmospheres most commonly used.

Static air : air from the surroundings flows through the furnace

Dynamic air : compressed air from a cylinder is passed through the furnace at a measured flow rate

Nitrogen : oxygen free nitrogen which provides an inert atmosphere

Dynamic air¹¹⁰, being an oxidizing atmosphere the tendency for cation or anion to get oxidized cannot be ruled out. The decomposition occurring at a lower temperature in air can be due to the active role of the corresponding metal ions in promoting the anion break down (as in the thermal decomposition of metal oxalates¹¹¹).

In other study the kinetic parameters calculated using the mass loss data indicate a higher value of activation energy in dynamic air in oxalate samples of certain transition metals than in static air. The ΔS values were also higher in such cases indicating a more disordered transition state in atmospheric air. This leads to the conclusion that magnitudes of E calculated from TG traces do not provide a measure of absolute reactivity at least in some cases¹¹²⁻¹¹⁴.

1.4.4.5 Rate of recording TG curve

The rate of recording of the TG curve has an appreciable effect on its shape and clarity. The slope of the curve is dependent both on the recording rate and on the scale used for the mass change. A more rapid movement may lead to an undesirable distortion of the curve.

1.4.4.6 Sample holder and its geometry

Sample holders range from flat plates to deep crucibles made of glass, alumina, metals, alloys or ceramics. Simons and Newkirk¹¹⁵ and Garn and Kessler¹¹⁶ had studied the effect of sample holder geometry, size etc in detail and according to them sample holders should be

designed to supply the heat of reaction of the sample as rapidly as possible. A flat plate shaped crucible is generally preferred to a high form cone shaped because of the diffusion of any evolved gases is easier with a flat shape.

1.4.4.7 Effects due to sample characteristics

The most important sample characteristics influencing TG curve are mass of the sample, particle size, type of packing in the crucible or holder and the nature of the reaction which it undergoes on heating. The mode of preparation (pre-history) of the sample also influences the TG curve. A large mass of sample may often create a deviation from linearity in the temperature rise which is particularly true for a fast exothermic reaction¹⁰⁶. A large sample can also impede the diffusion of evolved gases through the bulk of the solid crystals which may undergo decrepitation when heated. Some samples may swell, or foam or even bubble. Considering all this it is always better to use a small sample mass with a small particle size. Particle size causes a change in the diffusion of the product gases which will alter the reaction rate and the slope of the TG curve. Effect of particle size has been extensively studied by Coats and Redfern¹⁰⁶ and Sestak¹¹⁷. The smaller the particle size, the greater extent to which equilibrium is reached and at any given temperature the greater will be the extent of decomposition and the lower the temperature at the beginning and end of the reaction.

Dollimore has stressed the importance of surface state¹¹⁸ in solid state decomposition. The structure of interface of the solid face is represented by a distorted structure reflecting the unbalance of forces at the surface. This unbalanced forces of solid surface leads to changes both in the extent of the surface and the surface energetics. This results in sintering of the solid particles during decomposition. The effects of sintering causing a reduction of surface area are counteracted by thermal activation brought about by the shattering of particles due to a difference in density between solid reactant and solid product. Both sintering and reactivation process have rates which are temperature dependent¹¹⁹. These observations

underline the importance of surface parameters like particle size, particle size distribution and surface area in TG studies.

1.4.5 Study of reaction kinetics by thermogravimetry

Thermogravimetry has been widely used for the last more than fifty years to study the kinetics of thermal decompositions of solids and the determination of the basic kinetic constants such as rate constant, activation energy, order of the reaction and frequency factor. When the kinetic study is based on the observation of the mass change two approaches are possible as mentioned earlier (section 1.4.2). Generally it can be said that the static method is more suitable for obtaining information about the slowest process and also the reaction order and reaction mechanism. The dynamic method is more suitable for obtaining data on the kinetics of the reaction from a single curve for whole range of temperature. As pointed out by Doyle¹²⁰ one non-isothermal curve is equivalent to a large number of isothermal mass loss curves and so much of information is obtained from a single sample. The advantages of determining kinetic parameters by non-isothermal methods over isothermal methods as pointed out by Doyle are:

- i) Considerably fewer data are required
- ii) The kinetics can be calculated over an entire temperature range in a continuous manner
- iii) When a sample undergoes considerable reaction on raising to the required temperature the results obtained by isothermal methods are doubtful and often questionable.
- iv) Only a single sample is required.

1.4.6 Calculation of kinetic parameters from TG traces

The derivation of equations for calculating kinetic parameters from a TG curve is based on the fundamental kinetic equation.

$$-\frac{dx}{dt} = kx^n \quad 1.40$$

where x is the amount of the sample undergoing the reaction, n is the order of the reaction and k is the rate constant.

The dependence of temperature on the rate constant is given by Arrhenius equation

$$k = Ze^{-E/RT} \quad 1.41$$

where Z is the frequency factor, E is the energy of activation, R is the gas constant and T is the temperature.

According to Sestak¹²¹, in a thermogravimetric analysis, the amount of the sample undergoing decomposition, x , is related to the mass loss, w , by the equation

$$-dx = \frac{m_0}{w_\infty} dw \quad 1.42$$

where m_0 is the initial mass of the sample and w_∞ is the maximum mass loss. Integration of the equation 1.42 gives,

$$x = \frac{m_0}{w_\infty}(w_\infty - w) \quad 1.43$$

From the above three equations (1.40, 1.41 and 1.43) three types of equations have been derived which are extensively used in the evaluation of kinetic parameters.

1.4.6.1 Freeman-Carroll method - Differential method

Perhaps this is the most widely used kinetic equation. It was developed by Elis. Freeman and Benjamin Carroll¹⁰³ in 1958 from Sestak's relation (1.43) by differential method. Substitution of 1.43 and 1.41 into 1.40 gives

$$Ze^{-E/RT} = -\frac{dx}{dt} / x^n \quad 1.44$$

The logarithmic form of 1.44 is differentiated with respect to $\frac{dx}{dt}$, x and T to get

$$\frac{Edt}{RT^2} = d \ln \left(\frac{-dx}{dt} \right) - n d \ln x \quad 1.45$$

Integrating 1.45 and rearranging

$$\frac{EdT}{RT^2 d \ln x} = \frac{d \ln \left(\frac{-dx}{dt} \right)}{d \ln x} - n \quad 1.46$$

or

$$\frac{-E}{R} \Delta \left(\frac{1}{T} \right) = \frac{\Delta \ln \left(\frac{-dx}{dt} \right)}{\Delta \ln x} - n \quad 1.47$$

which may be written in the form

$$\frac{-E}{2.303R} \Delta \left(\frac{1}{T} \right) = -n + \frac{\Delta \log \left(\frac{dw}{dt} \right)}{\Delta \log w_r} \quad 1.48$$

or

$$\log \left[\frac{dw/dt}{w_r} \right] = \frac{-E}{2.303R} \left(\frac{1}{T} \right) + \log Z \quad 1.49$$

where w = mass loss, $w_r = w_\infty - w$, w_∞ = maximum mass loss. It follows from equation 1.49

that a plot of $\log \left[\frac{dw/dt}{w_r} \right]$ against $\left(\frac{1}{T} \right)$ will give a straight line with a slope equal to $-E/2.303R$ and intercept equal to $\log Z$.

1.4.6.2 Coats-Redfern method -Integral method

For a reaction $A_{(s)} \rightarrow B_{(s)} + C_{(g)}$, the rate of disappearance of A may be expressed by

$$\frac{dx}{dt} = k(1 - \alpha)^n \quad 1.50$$

where α is the fraction of A decomposed in time t , n is the order of the reaction and k is the rate constant, which according to Arrhenius is given by

$$k = Ze^{-\frac{E}{RT}} \quad 1.41$$

For a linear heating rate of a °C min⁻¹

$$a = \frac{dT}{dt} \quad 1.51$$

Starting with the three equations 1.50, 1.41 and 1.51 Coats and Redfern¹²² derived the equation

$$\int_0^a \frac{d\alpha}{(1 - \alpha)^n} = \frac{Z}{a} \int_0^T e^{-E/RT} dT \quad 1.52$$

from which we can get

$$\frac{1-(1-\alpha)^{1-n}}{T^2(1-n)} = \frac{ZR}{aE} \left(1 - \frac{2RT}{E}\right) e^{-E/RT} \quad 1.53$$

Taking logarithms on both sides,

$$\log \left[\frac{1-(1-\alpha)^{1-n}}{T^2(1-n)} \right] = \log \frac{ZR}{aE} \left(1 - \frac{2RT}{E}\right) - \frac{E}{2.303RT} \quad 1.54$$

for all values of n except n = 1

When n = 1

$$\log \left[\frac{-\ln(1-\alpha)}{T^2} \right] = \log \frac{ZR}{aE} \left(1 - \frac{2RT}{E}\right) - \frac{E}{2.303RT} \quad 1.55$$

A plot of $\log \left[\frac{1-(1-\alpha)^{1-n}}{T^2(1-n)} \right]$ versus $\frac{1}{T}$ when $n \neq 1$ and $\log \left[\frac{-\ln(1-\alpha)}{T^2} \right]$ versus $\frac{1}{T}$

when

$n = 1$ will give a straight line of slope $\frac{-E}{2.303RT}$ for the correct value of n. The first term on the RHS of equations 1.54 and 1.55 is considered to be reasonably constant and is equal to the intercept of the line from which Z can be calculated.

1.4.6.3 Horowitz and Metzger method-Approximation method

A still another mathematical interpretation of TG traces which enables the determination of kinetic parameters of pyrolysis reactions of many polymers and thermal decompositions of inorganic salts is the one proposed by Hugh H. Horowitz and Gershon Metzger²⁸ in 1962. It is called approximation method since its derivation involves an approximation using the peak temperature (T_s) of the TG curve. The final approximated equation is given as

$$\ln \ln \left(\frac{w_\infty}{w_r} \right) = \frac{E\theta}{RT_s^2} \quad 1.56$$

where $\theta = T - T_s$

The equation well duplicates the characteristic shape of the TG trace – a gradual mass loss followed by a sharp drop followed by a turning towards zero slope when the decomposition is complete.

A plot of $\log \ln \left(\frac{w_{\infty}}{w_r} \right)$ versus θ will give a straight line the slope of which is equal to $\frac{E}{2.303RT_s^2}$ from which E can be calculated. The frequency factor can be calculated using the equation.

$$Z = \frac{E / RT_s^2 \cdot a}{\exp \left(\frac{-E}{RT_s} \right)} \quad 1.57$$

apart from the above methods, methods due to Newkirk¹²³, Doyle¹²⁴, Ingraham and Marier¹²⁵, Vachuska and Voboril¹²⁶, Dave and Chopra¹²⁷, Achar et. al.¹²⁸, Flynn and Wall¹²⁹, Urbanovici and Segal¹³⁰ etc have also been used in various kinetic studies.

1.4.6.4 Relative merits of the methods

The most common methods used are Freeman-Carroll method, Coats-Redfern method, Horowitz-Metzer method and Doyle method. Sestak¹²¹ undertook a comparative study of the kinetic results calculated by various methods and had shown that the deviation of computed values of E did not differ by more than 10%. Thus all the methods appear to be satisfactory for calculating E within the limits of accuracy needed. In the case of differential methods, the most accurate results are obtained by calculation from the medium-steep parts of the curve. For the approximate method the accuracy depends on the determination of the curve inflection point temperature or peak temperature at which the rate of change of mass with temperature is maximum.

1.5 The Scope of the Present Investigation

Considerable amount of work has been done on the thermal decomposition of alkali and alkaline earth metal bromates^{26,29,33,35-38,43,45-48}. It was of interest therefore to extend the studies to other bromates. Literature survey revealed that no such detailed studies have been carried out in the case of bromates of the transition metal series and of metals of the lanthanide series. Nickel bromate, yttrium bromate and neodymium bromate were taken for the investigations in a programme of comparative study of the thermal decomposition behaviour of metal bromates.

Thermal decomposition reactions are very sensitive to the presence of impurities. Imperfections can be introduced into the crystal lattice by irradiation^{84-86, 88, 89, 91-96, 98, 133, 134}, application of high pressure^{82, 88}, crushing⁸⁹, doping^{31,54, 62-71, 73,74,131} or by the addition of other additives or intentional impurities^{75-79, 89}.

Impurities can produce vacancies or act as electron traps and can affect the thermal decomposition reaction. The added impurities may simply remain as heterogeneous mixture with the host material, can generate new phase, or may get incorporated into the lattice creating defects in the host crystal or may play a catalytic effect on the decomposition. It was of interest therefore to study variation of the decomposition of barium bromate, nickel bromate, neodymium bromate and yttrium bromate due to the addition of intentional impurities. Dynamic thermogravimetric method was used because of its advantages over the isothermal method³².

Chapter II

Materials & Experimental Methods

2.1 Materials

All chemicals and reagents used were of analytical reagent grade BDH (AR) or E. Merck (AR). Double distilled water, freshly boiled, was used throughout.

2.1.1 Preparation of barium bromate

Barium bromate was synthesized by the method already reported^{26,135} using potassium bromate and barium chloride. The stoichiometric amount of potassium bromate was added to a solution prepared by dissolving 100g of $\text{BaCl}_2 \cdot 2\text{H}_2\text{O}$ in water and the precipitated $\text{Ba}(\text{BrO}_3)_2$ was washed several times to eliminate any potassium chloride. The product was dried and recrystallised. It was analyzed for bromate purity iodometrically¹³⁴. 99.1 percent pure barium bromate monohydrate was obtained.

2.1.2 Preparation of nickel bromate

Nickel bromate was synthesized by the method already known²⁶ using barium bromate (prepared by the above method) and nickel sulphate. Stoichiometric amount of $\text{NiSO}_4 \cdot 7\text{H}_2\text{O}$ was added to a solution containing 10g of barium bromate dissolved in 500ml hot water. The precipitated barium sulphate was filtered off. The filtrate was carefully evaporated to 25ml. The excess barium bromate precipitated was filtered. The filtrate was now evaporated at 50°C under vacuum. The product was recrystallised from water and analyzed for bromate purity iodometrically¹³⁴. Nearly 10g of pure sample of composition $\text{Ni}(\text{BrO}_3) \cdot 6\text{H}_2\text{O}$ was obtained with 99% purity.

2.1.3. Preparation of yttrium bromate

For preparing yttrium bromate⁵⁷⁻⁵⁹, first yttrium sulfate was made by the following procedure. Stoichiometric amount of yttrium oxide was weighed and soaked in water and sulphuric acid solution was added slowly. The mixture was warmed and the temperature was gradually raised to 500°C to convert it to anhydrous yttrium sulphate. It was now dissolved in ice cold water and the resulting solution was poured into a slight excess of barium bromate solution. The precipitated barium sulphate was filtered off. The resulting solution was warmed on a hot plate overnight and then evaporated using a rotatory evaporator. The solution was concentrated to obtain crystals of yttrium bromate. The crystals were filtered, air dried at

room temperature and then recrystallised. 99% pure yttrium bromate of composition $Y(\text{BrO}_3)_3 \cdot 9\text{H}_2\text{O}$ was obtained.

2.1.4. Preparation of neodymium bromate

Neodymium bromate was synthesized by the method similar to the one used for yttrium bromate. The crystals were grown by solid evaporation of the aqueous solution of neodymium bromate prepared by double decomposition of neodymium sulphate and barium bromate in a hot aqueous solution¹³³. The recrystallised sample was analyzed for purity. Nearly 99% Neodymium bromate of composition $(\text{NdBrO}_3)_3 \cdot 9\text{H}_2\text{O}$ was obtained.

2.1.5. Preparation of magnesium bromate, cadmium bromate, zinc bromate and strontium bromate

The stoichiometric amount of MSO_4 ($M = \text{Mg}, \text{Cd}, \text{Zn}$) was added to a solution containing 4g of $\text{Ba}(\text{BrO}_3)_2 \cdot \text{H}_2\text{O}$ dissolved in 200ml hot water. The precipitated barium sulphate was filtered off and the filtrate was evaporated to about 10ml. Any excess barium bromate precipitated was also filtered off. The solution was then evaporated at 80°C under vacuum^{26,136} and about 4g of each bromate was obtained. The samples were recrystallised, dried and analysed for bromate purity iodometrically¹³⁴. Nearly 99% pure samples were obtained.

Strontium bromate^{136, 137} was prepared from strontium carbonate and bromic acid (obtained by reaction of barium bromate solution with sulphuric acid).

2.1.6 Preparation of samples of barium bromate, nickel bromate, neodymium bromate and yttrium bromate containing intentional impurities

Crystals of barium bromate containing NaBrO_3 , KBrO_3 , $\text{Mg}(\text{BrO}_3)_2$, $\text{Sr}(\text{BrO}_3)_2$, $\text{Zn}(\text{BrO}_3)_2$, $\text{Cd}(\text{BrO}_3)_2$, $\text{Ni}(\text{BrO}_3)_2$, $\text{Nd}(\text{BrO}_3)_3$, $\text{Y}(\text{BrO}_3)_3$, KBr and SrBr_2 respectively as intentional impurities in the mole fraction range 10^{-3} to 10^{-1} were prepared by very slow evaporation of solutions containing calculated amounts of barium bromate and the other salt. The crystals were separated under suction, washed with small amounts of cold water and dried over P_2O_5 .

Similarly samples of nickel bromate containing neodymium bromate, yttrium bromate and zinc bromate, yttrium bromate containing barium bromate and zinc bromate and neodymium bromate containing nickel bromate and barium bromate were also prepared by similar methods.

2.2. Analysis of Bromate – Iodometric Method

To a measured volume (20ml) of an approximately 0.1N standard solution of the bromate 2ml concentrated hydrochloric acid and 10ml of a 5 percent solution of KI were added and the liberated iodine was immediately titrated against standard sodium thiosulphate using starch as indicator¹³⁴.

2.3. Thermogravimetric Studies

Barium bromate(Sample 1) and samples of barium bromate containing intentional impurities (Samples 2-33) nickel bromate (Sample 34) and samples of nickel bromate containing intentional impurities (Samples 35-43), neodymium bromate (Sample 44) and neodymium bromate containing intentional impurities (Samples 45-48) and yttrium bromate (Sample 49) and yttrium bromate containing intentional impurities (Samples 50-52) in the form of fine powder (200-240 mesh) were used for TG studies.

In the first phase thermograms of Sample 1(i)-24 were recorded in air using Ulvac Sinku-Rio (Japan) TA 1500. In the second phase thermograms of Samples (25-27, 30, 34-52) were recorded in nitrogen using TAQ20 Thermogravimetric Analyser. In the third phase thermograms of samples (28, 29, 31-33) were recorded in nitrogen using Perkin Elmer Thermal Analyser. The heating rate was 5°C min⁻¹ in all the TG studies. In all experiments less than 10 mg of the sample was used and the data have all been normalized to a mass of 100 mg. The recorded total mass loss in samples (1-43) agreed almost satisfactorily with the theoretical mass loss confirming nearly complete conversion of the bromate to the bromide. In the case of neodymium and yttrium bromate there was no such agreement showing that the decomposition is not to the bromide alone but oxide formation is also possible. Earlier studies⁴⁵⁻⁴⁸ had revealed that replacement of air by nitrogen had no effect on the thermal

decomposition of barium bromate and so in the present studies for samples (1-24), air was used as atmosphere and the remaining samples were analysed in nitrogen atmosphere.

2.4. XRD Studies

With a view to investigate whether any possible change occurs in the crystal structure of the samples during the addition of intentional impurities some of the samples were subjected to X-ray diffraction studies.

Pure barium bromate, nickel bromate, zinc bromate, neodymium bromate and yttrium bromate and samples of barium bromate containing 0.1 mole % of neodymium bromate, nickel bromate containing 0.1 mole % of zinc bromate, neodymium bromate containing 0.1 mole % of nickel bromate, yttrium bromate containing 0.1 mole % nickel bromate and barium bromate containing 0.1 mole % yttrium bromate were subjected to XRD studies.

Wide angle X-ray diffractions of the finely powdered samples were recorded by Philips Analytical diffractometer using CuK-alpha emission. The spectra were recorded in the range of $2\theta = 0-50$ and analyzed using X' Pert software.

2.5. FTIR Studies

Fourier Transform Infrared Spectroscopy has been widely used in the study of inorganic compounds especially metal complexes. Hydrated salts of transition and inner transition metals have structures similar to coordination compounds with the water molecules of hydration functioning as ligands or coordinated to the metal ion. With a view to get any information relating to this and to explore the possible changes due to the addition of other metal ions as intentional impurities, some of the samples viz. nickel bromate, neodymium bromate, zinc bromate, nickel bromate containing 0.1 M neodymium bromate, nickel bromate containing 0.01M neodymium bromate, nickel bromate containing 0.001 M zinc bromate and nickel bromate containing 0.1 M yttrium bromate were subjected to FTIR studies. The samples were used in the powdered form in a Nicolet-380 FTIR spectrometer.

Chapter III

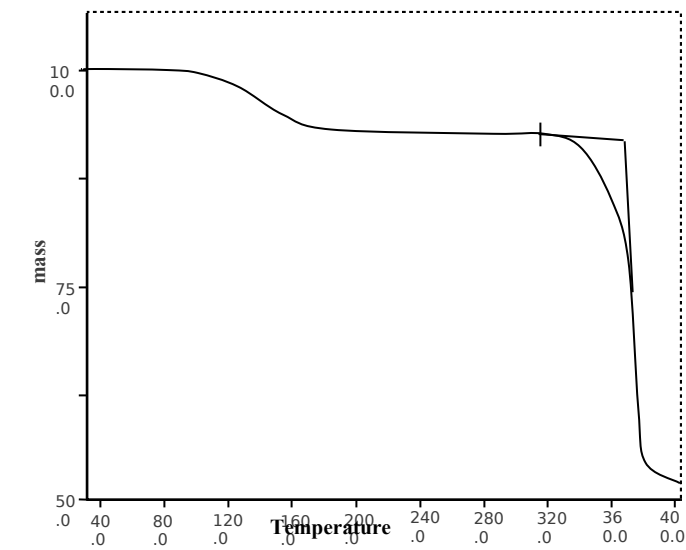
Results

3.1 TG Curves

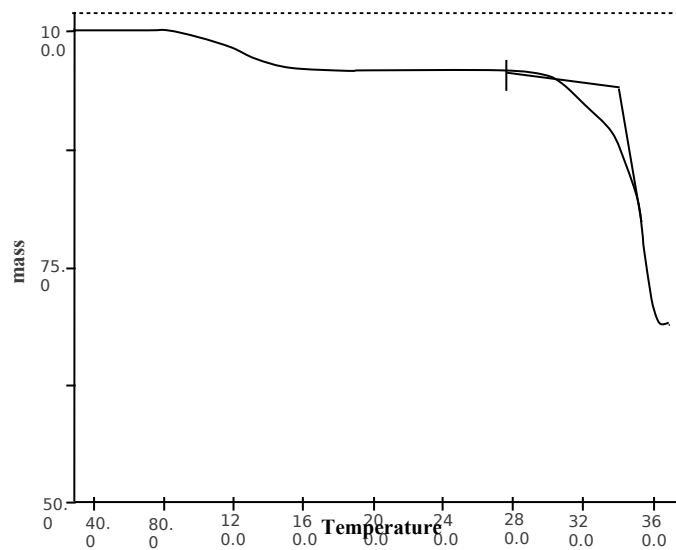
The recorded TG curves of all the samples(1-52) with mass plotted against temperature are presented in figures (2-19). TG curves of $\text{Ba}(\text{BrO}_3)_2 \cdot \text{H}_2\text{O}$ and samples of Barium bromate containing intentional impurities are of the same pattern showing similar decomposition in all cases. In all these curves there is an initial mass loss of nearly 4.5% indicating the loss of water of hydration and the final mass corresponds well with almost complete decomposition of the bromate to the bromide. The TG curve of pure Barium bromate - sample 1(ii) recorded in nitrogen atmosphere using Perkin Elmer Thermal analyzer - Fig.10(i) is analogous to that obtained for sample 1(i) recorded in air atmosphere using Ulvac Sinku-Riko TA 1500 studied earlier - Fig. 2(i). The sample of barium bromate containing 10^{-1} M yttrium bromate shows anomalous behaviour. Its decomposition shows two distinct stages - Fig. 12(iv).

The TG curves of nickel bromate and samples of nickel bromate containing intentional impurities are also of similar pattern showing that the impurities do not alter the mechanism or pathway of decomposition. The curves reveal that water of hydration in these samples are not lost entirely in one step but in two steps forming the anhydrous salt. Moreover, the decomposition of the anhydrous sample does not give entirely bromide but a mixture of bromide and oxide as is evident from the total mass loss at the completion of the reaction.

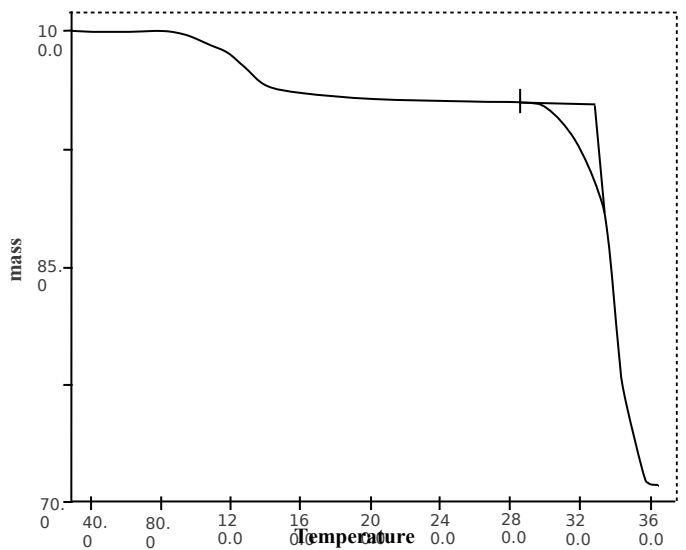
In the case of yttrium bromate and neodymium bromate and samples of these bromates containing intentional impurities the TG curves indicate two steps for the removal of water forming the anhydrous substance. The mass of the residue at the completion of the decomposition corresponds to neither completely to the oxide nor completely to the bromide showing that decomposition results in the formation of a mixture of oxide and bromide. In the case of these samples also the curves of the untreated samples and the treated samples are nearly of the same pattern.



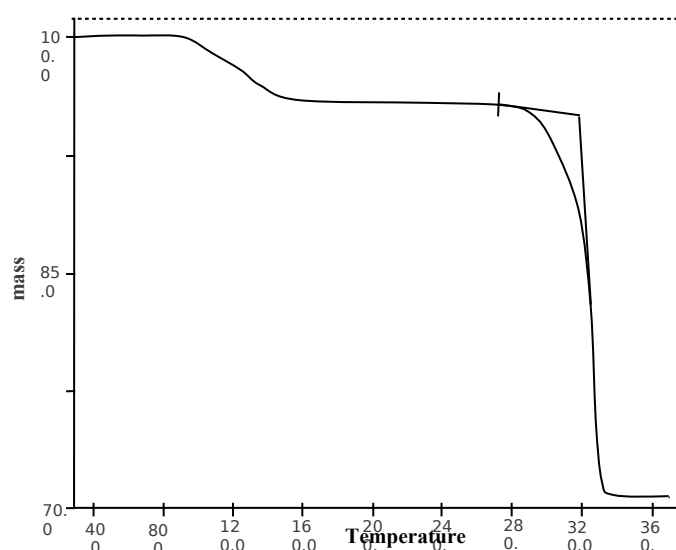
(i)



(ii)



(iii)



(iv)

Fig : 2 TG curves of barium bromate and samples of barium bromate containing sodium bromate
 (i) Pure
 (ii) 10^{-1} M sodium bromate
 (iii) 10^{-2} M sodium bromate
 (iv) 10^{-3} M sodium bromate

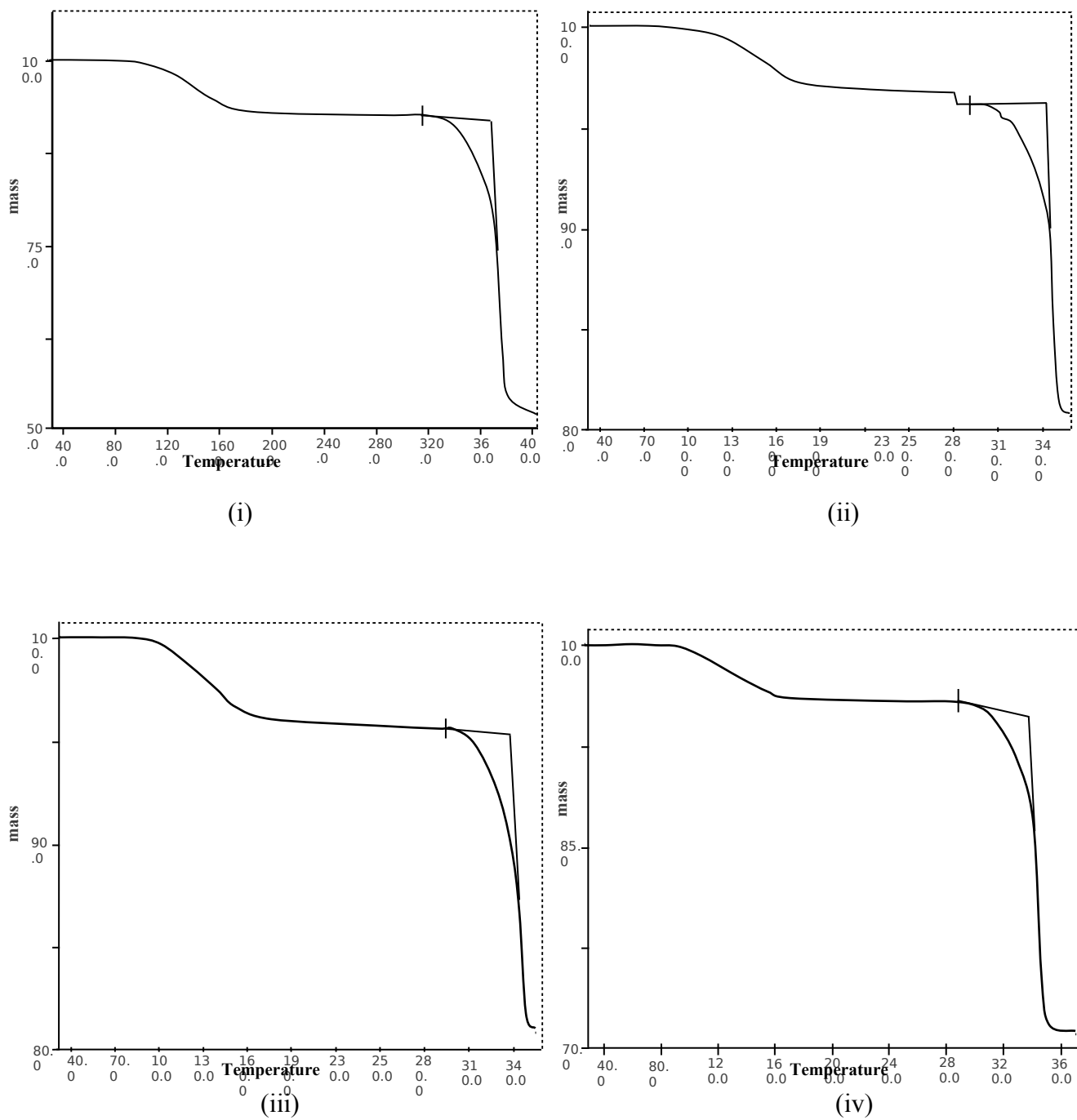
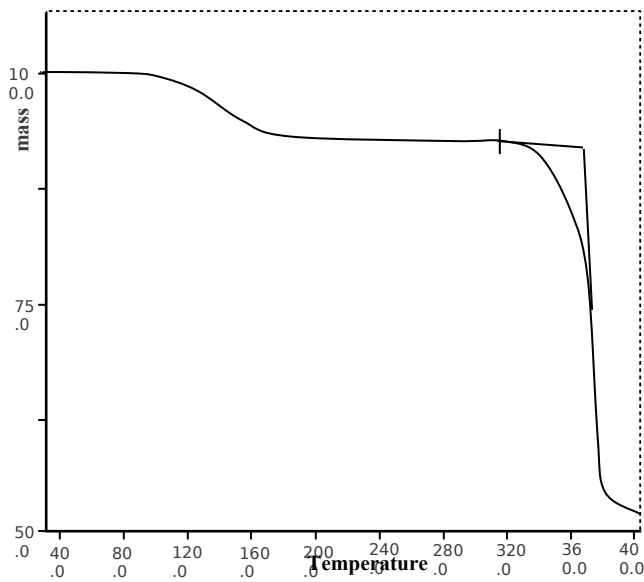
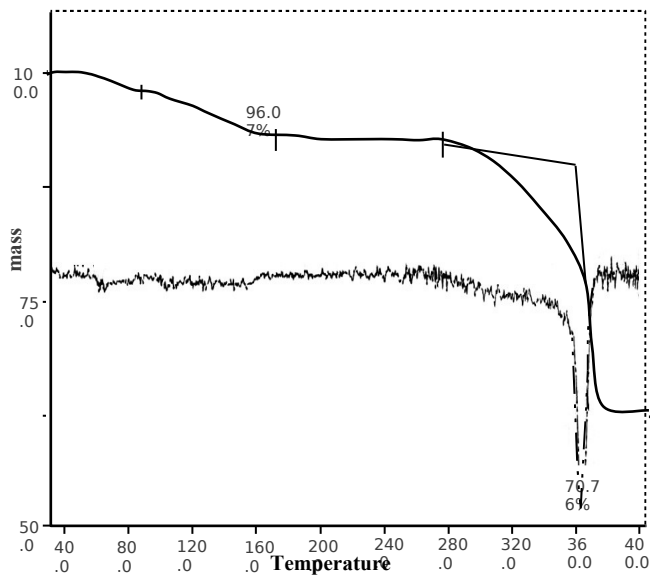


Fig : 3 TG curves of barium bromate and samples of barium bromate containing potassium bromate

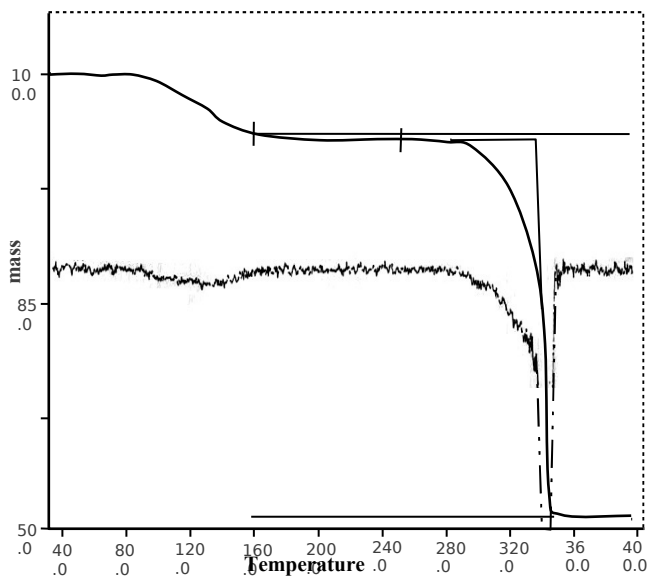
- (i) Pure
- (ii) 10⁻¹M potassium bromate
- (iii) 10⁻²M potassium bromate
- (iv) 10⁻³M potassium bromate



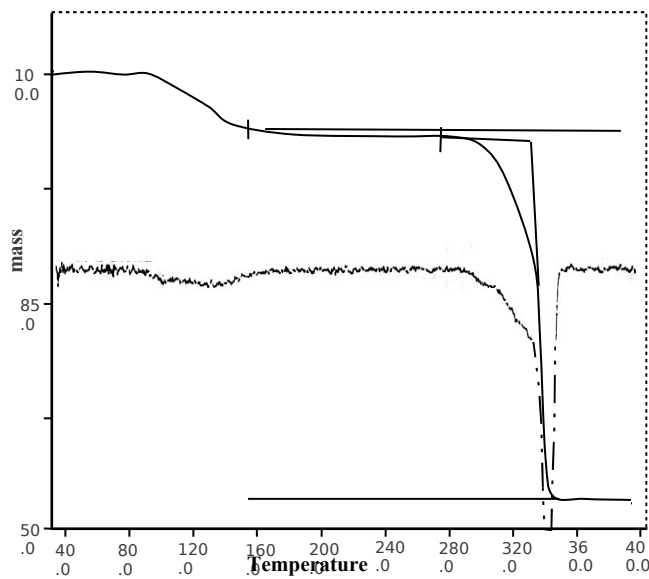
(i)



(ii)



(iii)

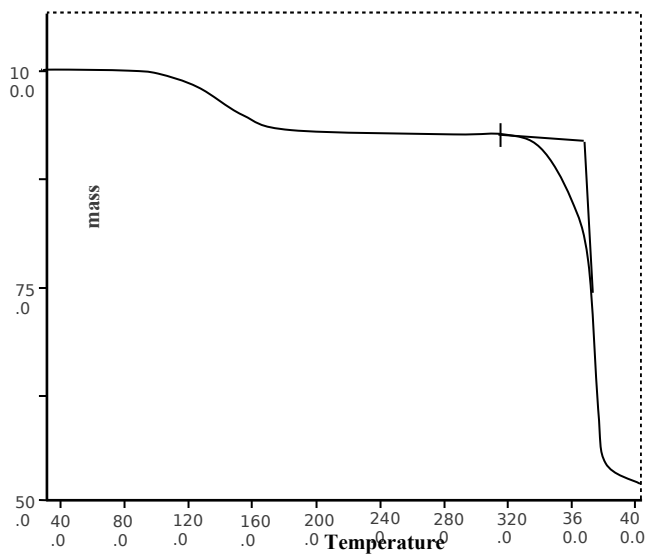


(iv)

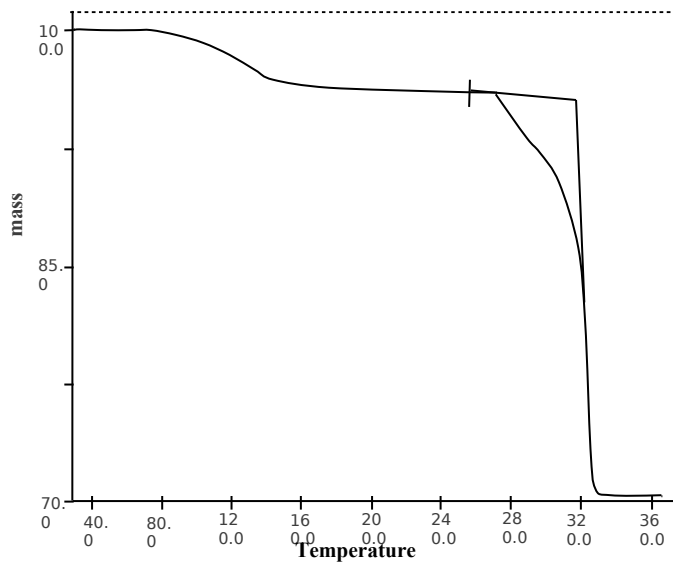
Fig : 4 TG curves of barium bromate and samples of barium bromate containing magnesium bromate

(i) Pure
(iii) 10^{-2} M magnesium bromate

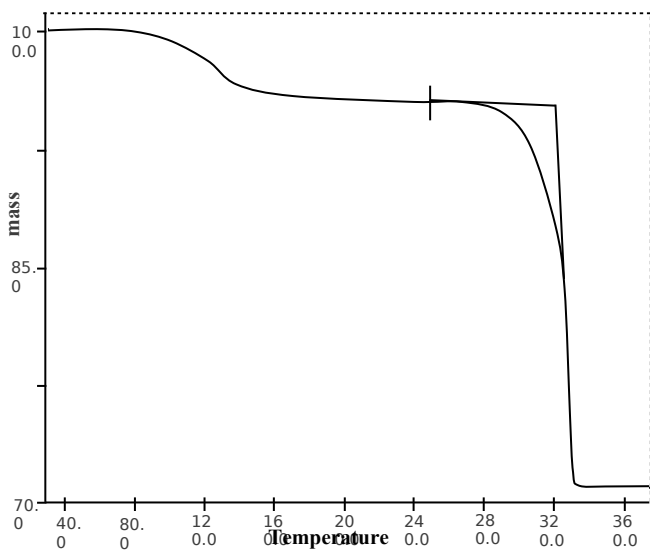
(ii) 10^{-1} M magnesium bromate
(iv) 10^{-3} M magnesium bromate



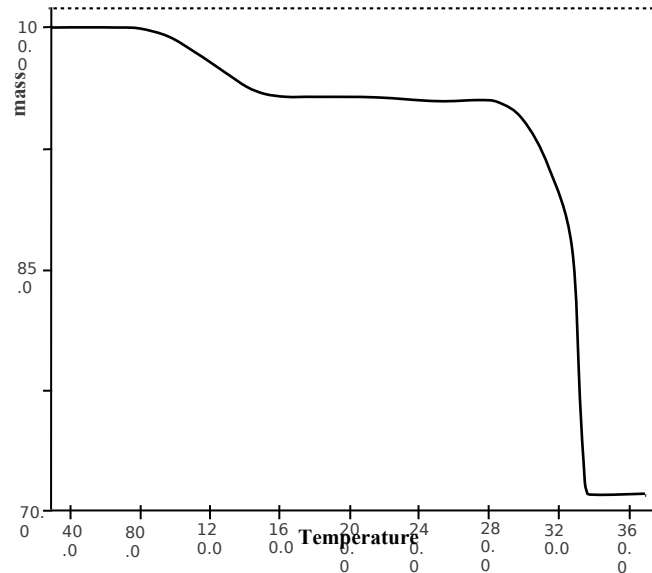
(i)



(ii)



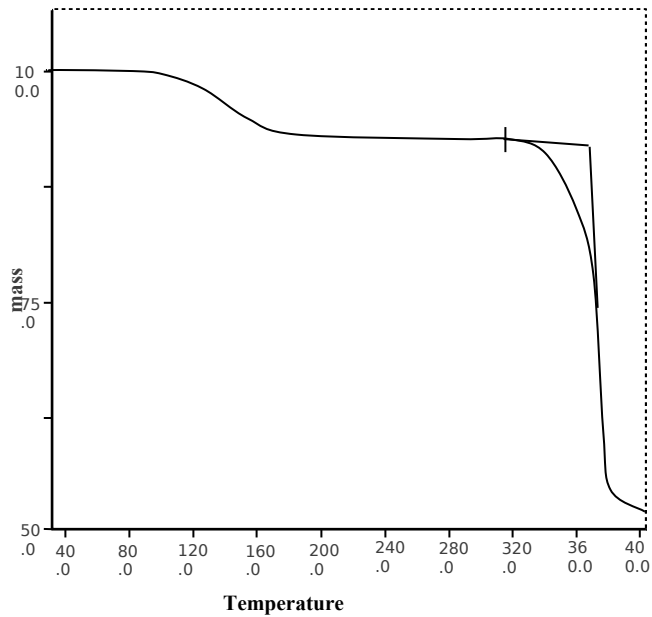
(iii)



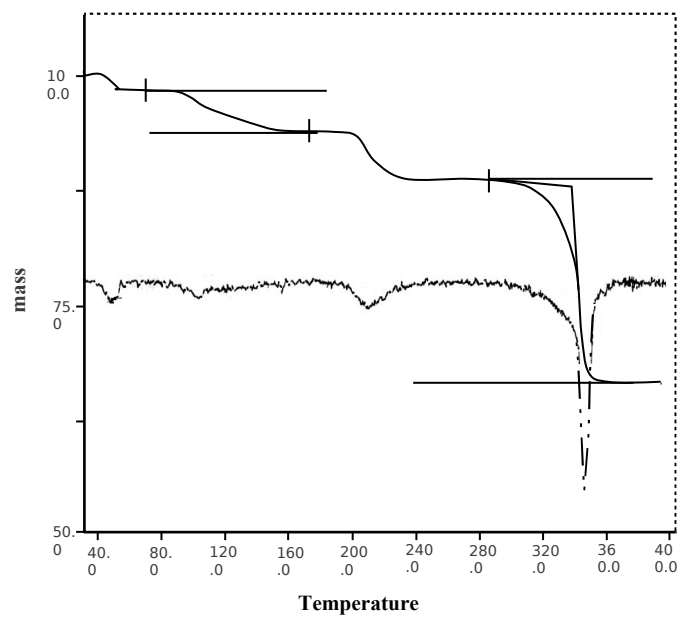
(iv)

Fig : 5 TG curves of barium bromate and samples of barium bromate containing strontium bromate

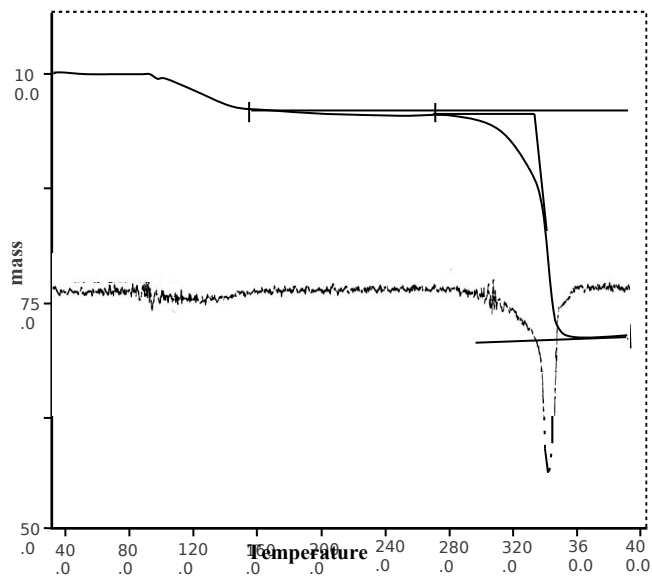
- (i) Pure (ii) 10^{-1} M strontium bromate
 (iii) 10^{-2} M strontium bromate (iv) 10^{-3} M strontium bromate



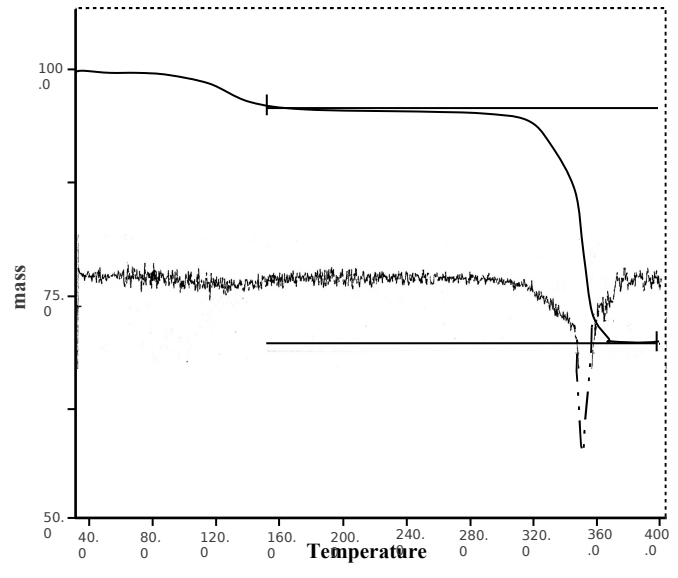
(i)



(ii)



(iii)

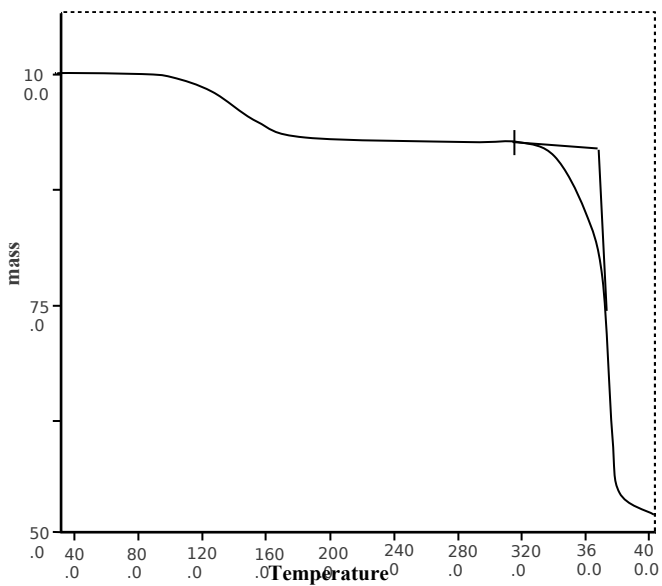


(iv)

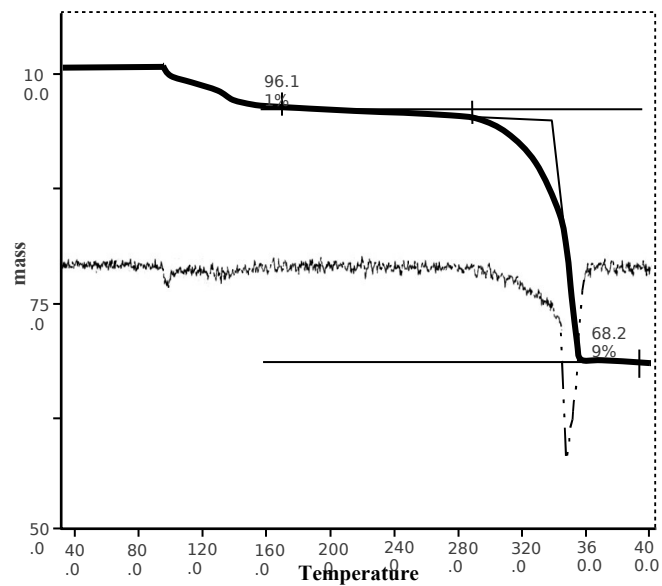
Fig : 6 TG curves of barium bromate and samples of barium bromate containing zinc bromate

(i) Pure
(iii) 10^{-2} M zinc bromate

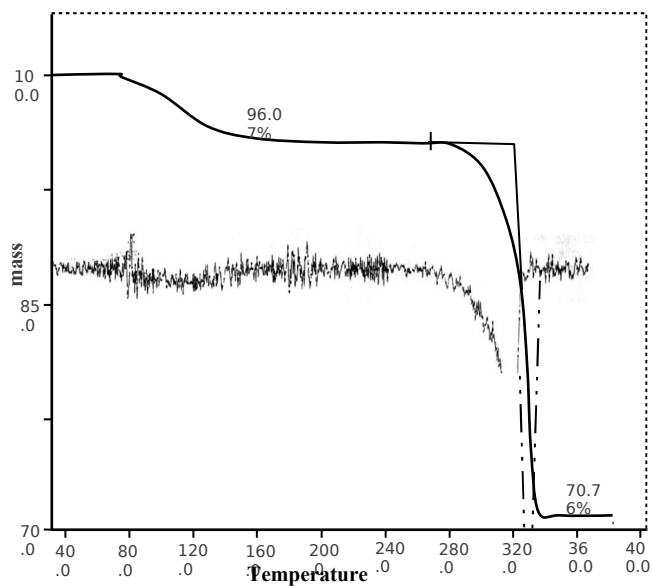
(ii) 10^{-1} M zinc bromate
(iv) 10^{-3} M zinc bromate



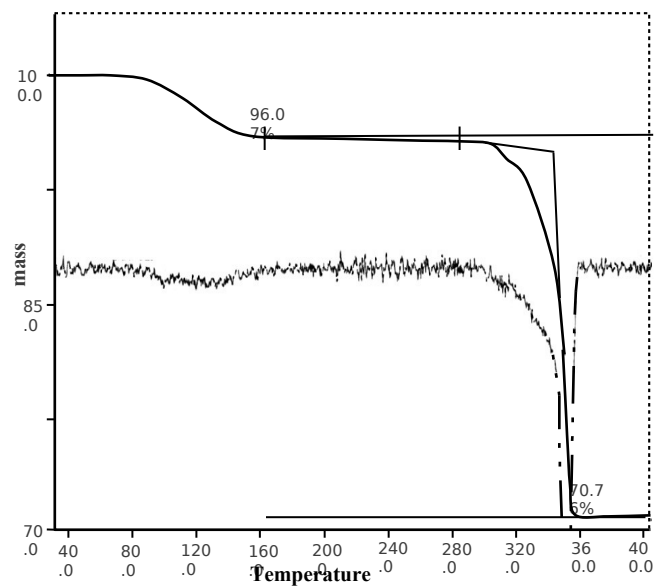
(i)



(ii)



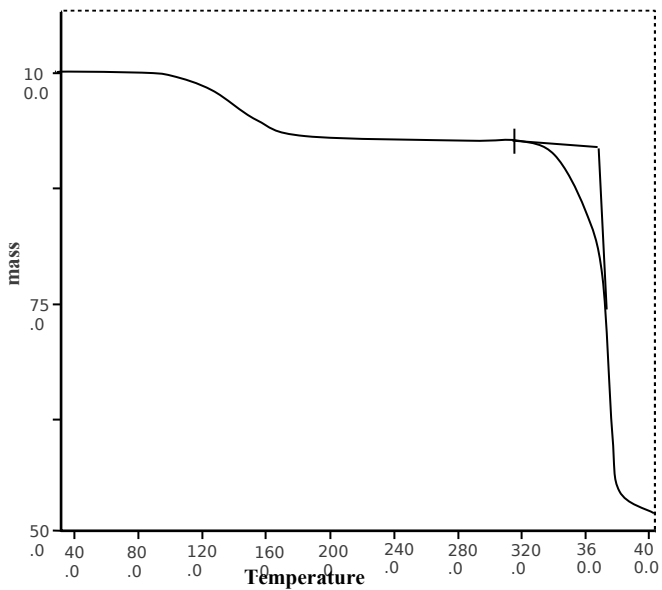
(iii)



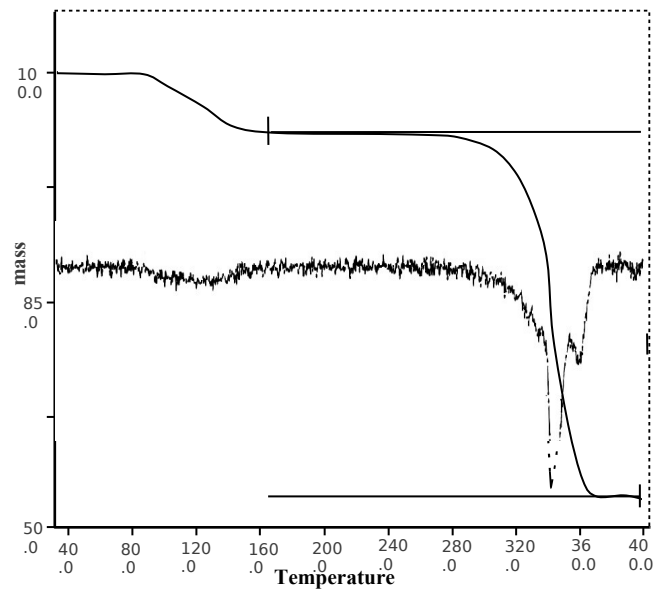
(iv)

Fig : 7 TG curves of barium bromate and samples of barium bromate containing cadmium bromate

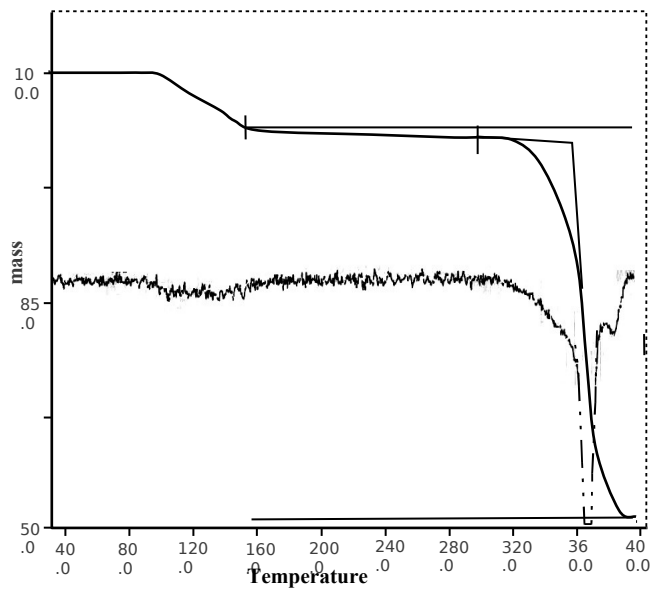
- (i) Pure (ii) 10^{-1} M cadmium bromate
 (iii) 10^{-2} M cadmium bromate (iv) 10^{-3} M cadmium bromate



(i)



(ii)



(iii)

(iv)

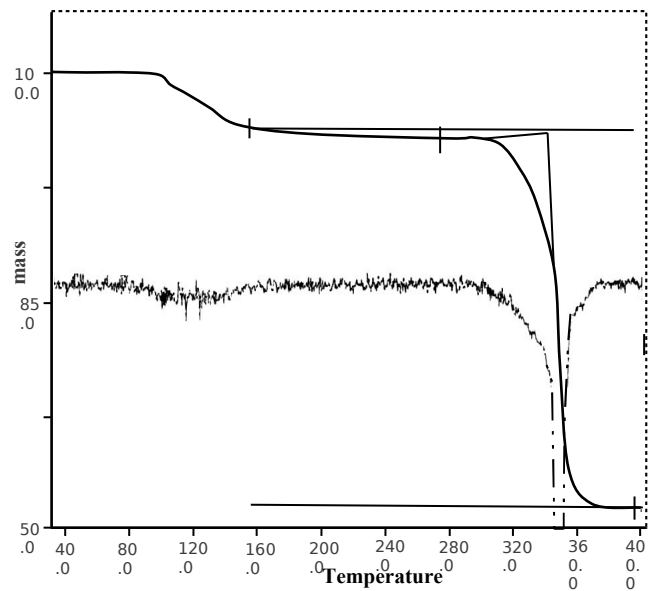
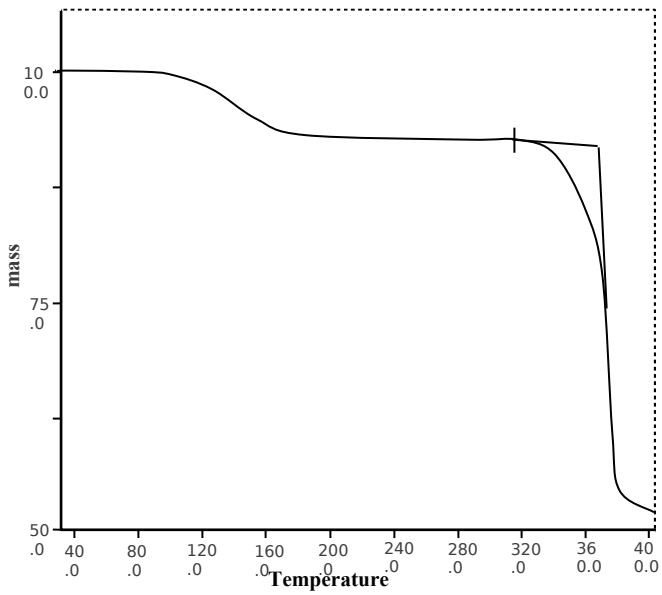
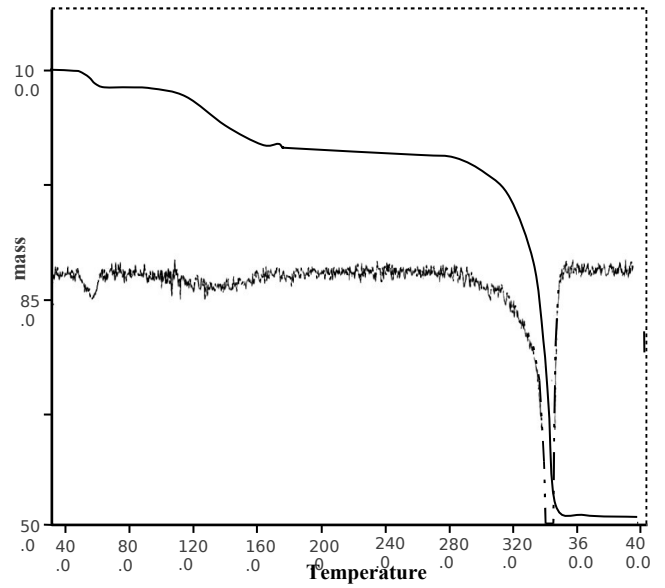


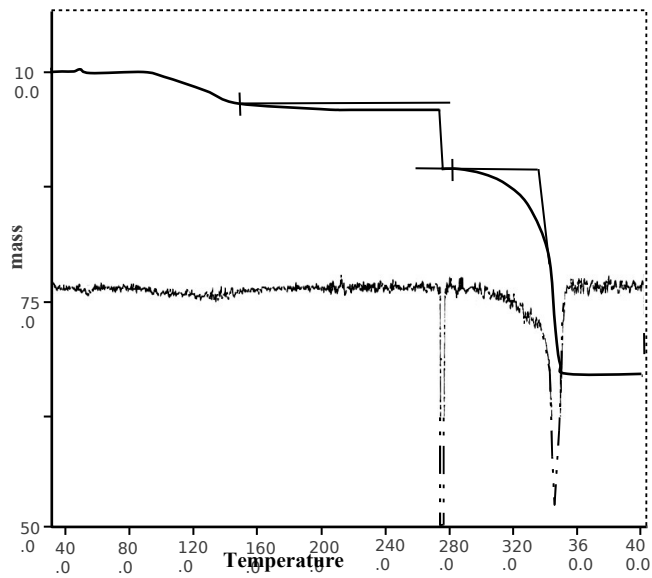
Fig : 8 TG curves of barium bromate and samples of barium bromate containing potassium bromide
 (i) Pure
 (ii) 10^{-1} M potassium bromide
 (iii) 10^{-2} M potassium bromide
 (iv) 10^{-3} M potassium bromide



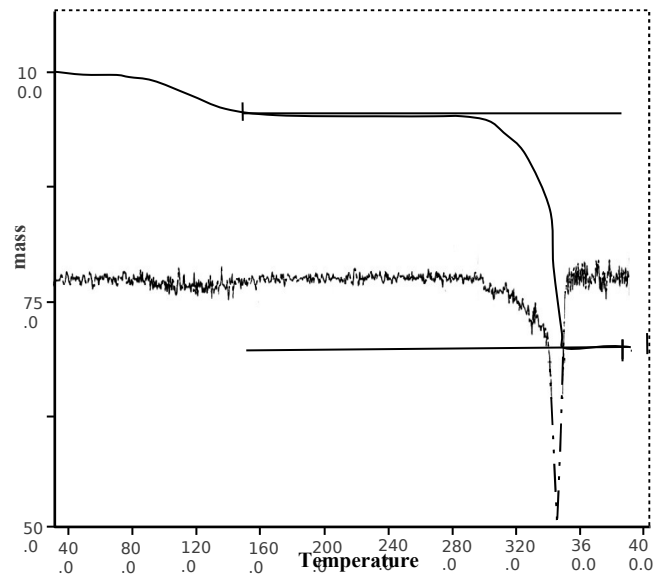
(i)



(ii)



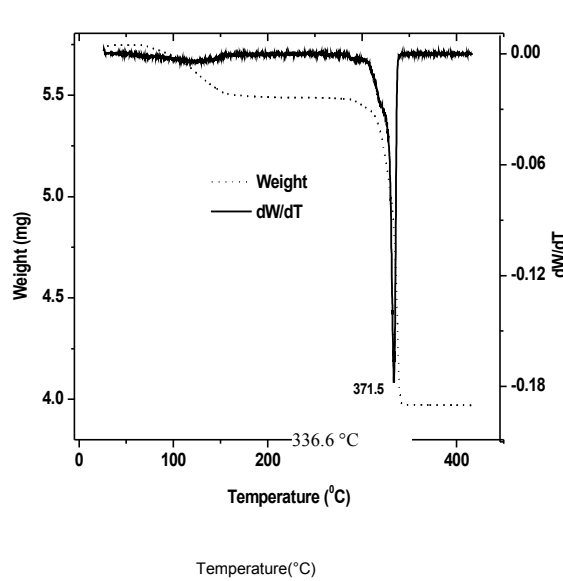
(iii)



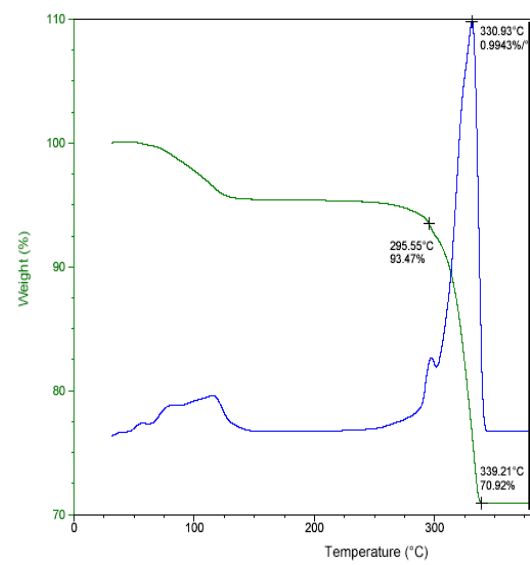
(iv)

Fig : 9 TG curves of barium bromate and samples of barium bromate containing strontium bromide

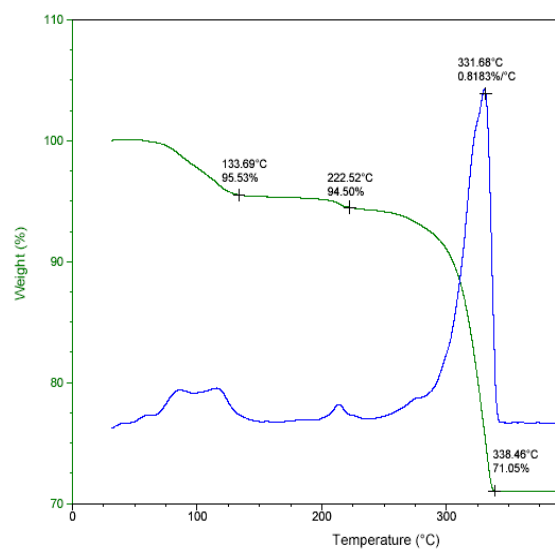
(i) Pure (ii) 10^{-1} M strontium bromide
 (iii) 10^{-2} M strontium bromide (iv) 10^{-3} M strontium bromide



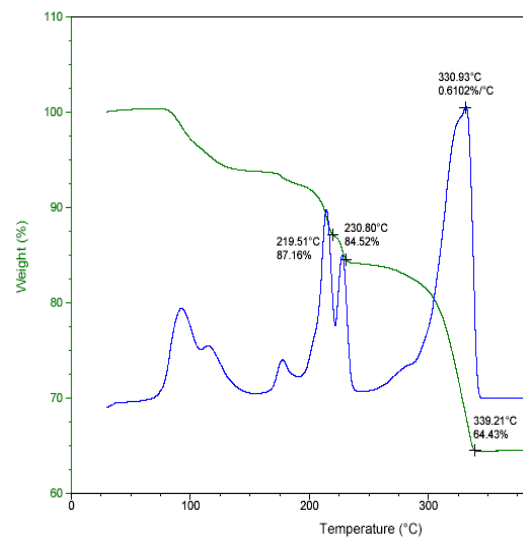
(i)



(ii)

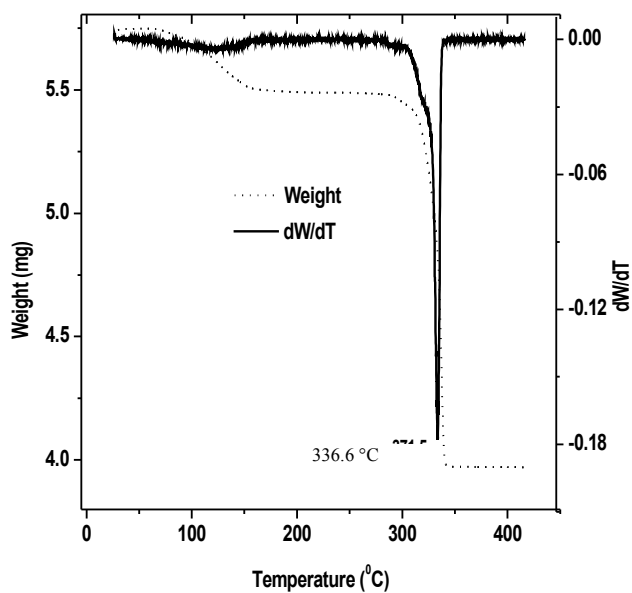


(iii)

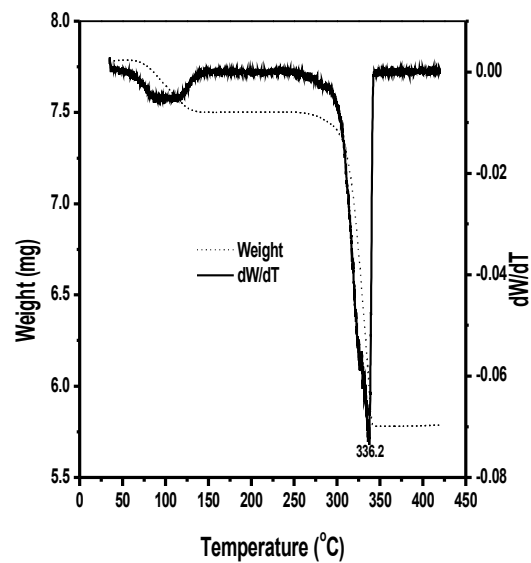


(iv)

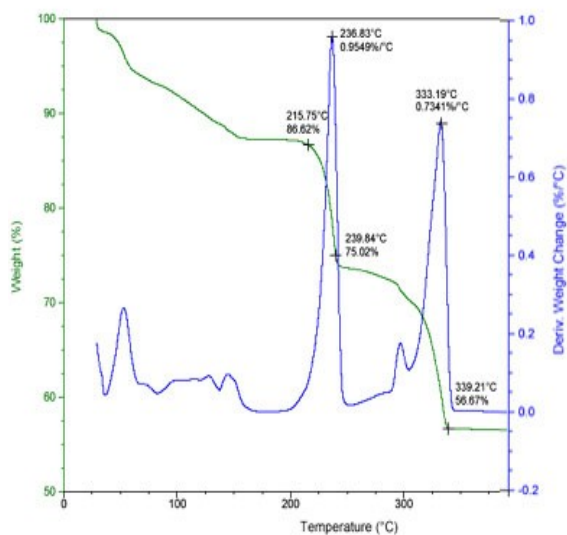
Fig : 10 TG curves of barium bromate and samples of barium bromate containing nickel bromate
 (i) Pure (ii) 10^{-3} M nickel bromate
 (iii) 10^{-2} M nickel bromate (iv) 10^{-1} M nickel bromate



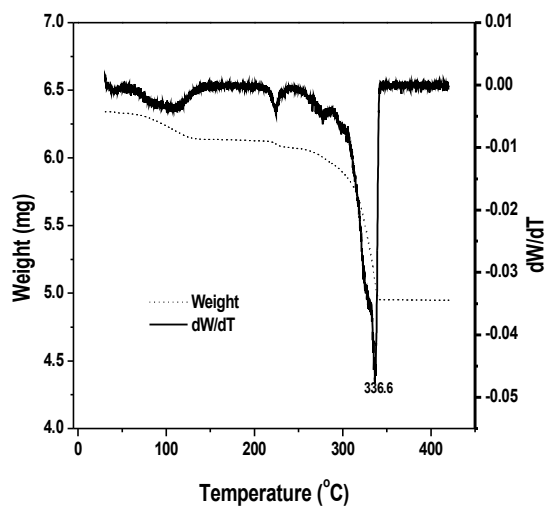
(i)



(ii)

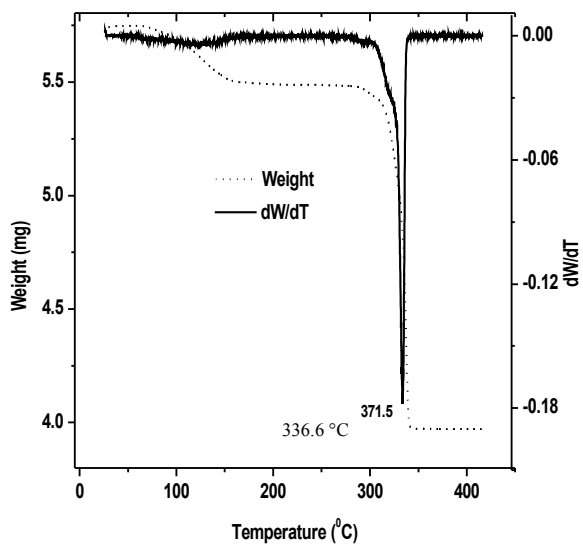


(iii)

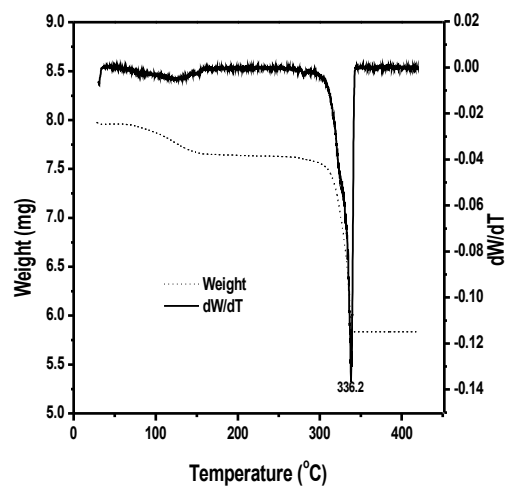


(iv)

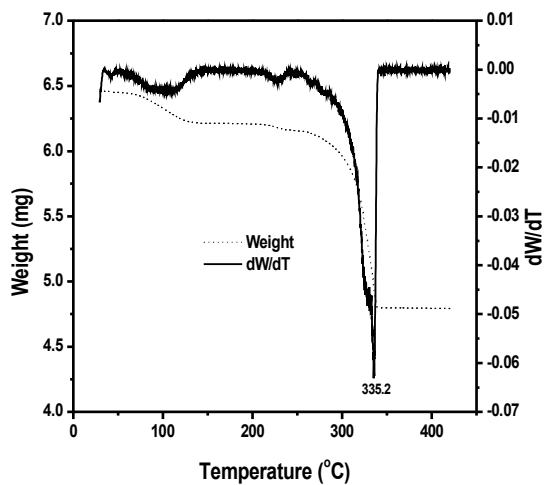
Fig : 11 TGA curves of barium bromate and samples of barium bromate containing neodymium bromate
 (i) Pure barium bromate (ii) 10^{-3} M neodymium bromate
 (iii) 10^{-2} M neodymium bromate (iv) 10^{-1} M neodymium bromate



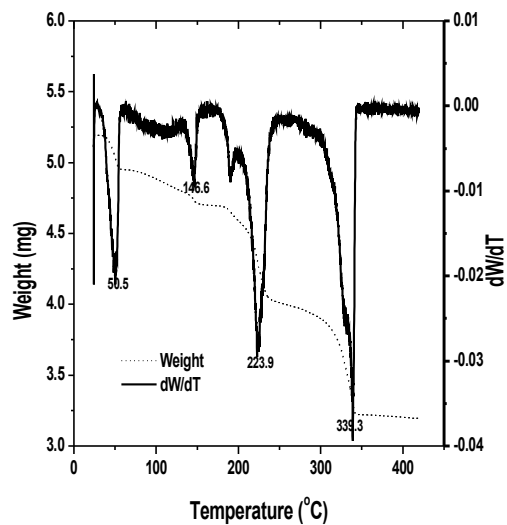
(i)



(ii)

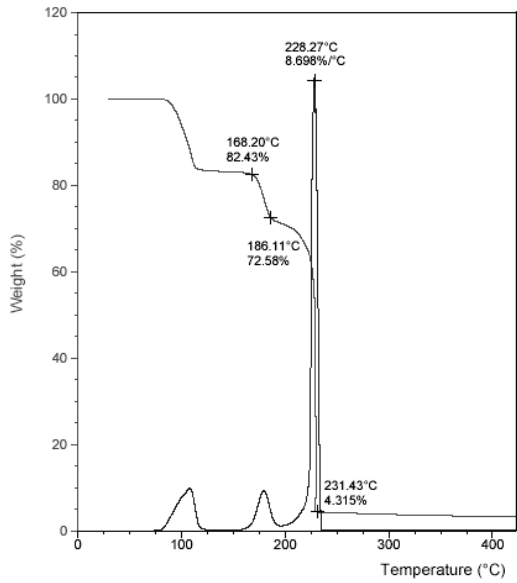


(iii)

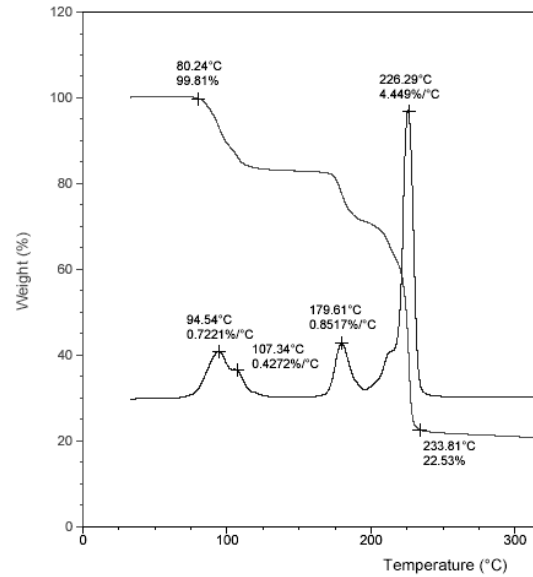


(iv)

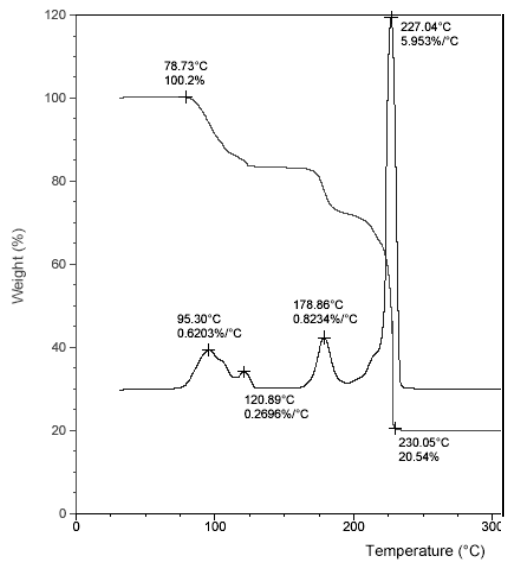
Fig : 12 TG curves of barium bromate and samples of barium bromate containing yttrium bromate
 (i) Pure barium bromate 1(ii) 10^{-3} M yttrium bromate
 (iii) 10^{-2} M yttrium bromate (iv) 10^{-1} M yttrium bromate



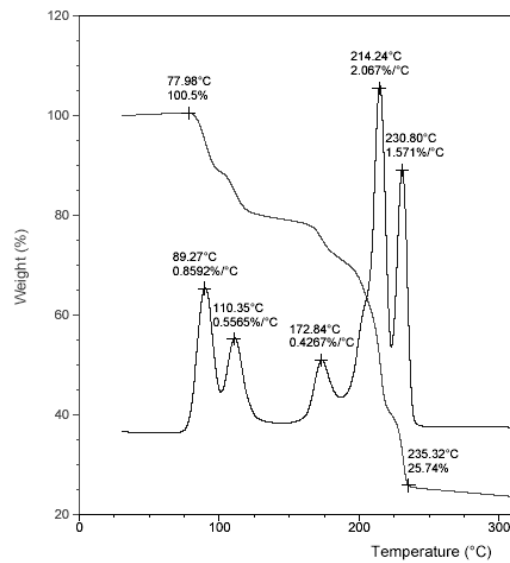
(i)



(ii)

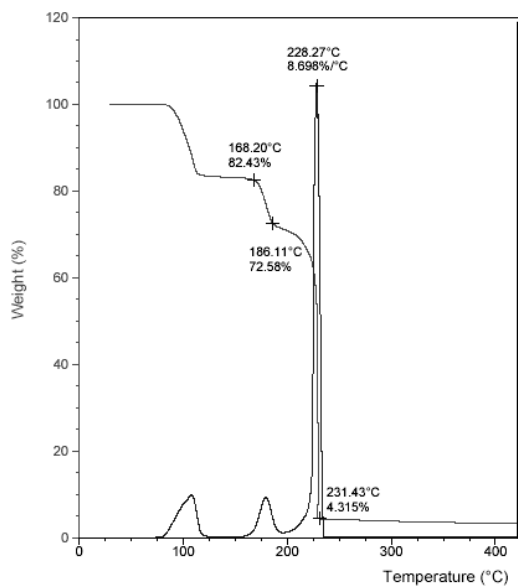


(iii)

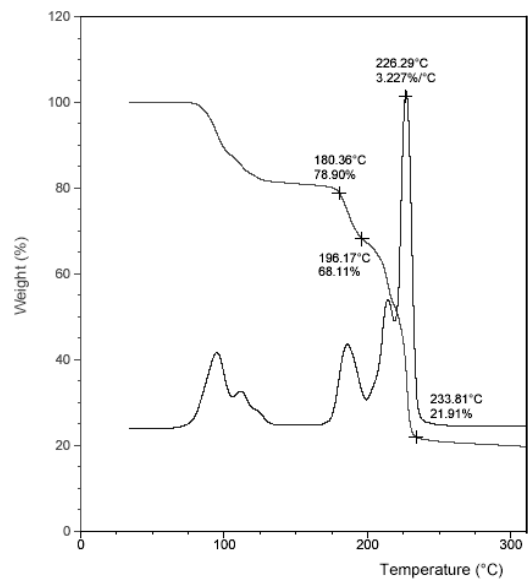


(iv)

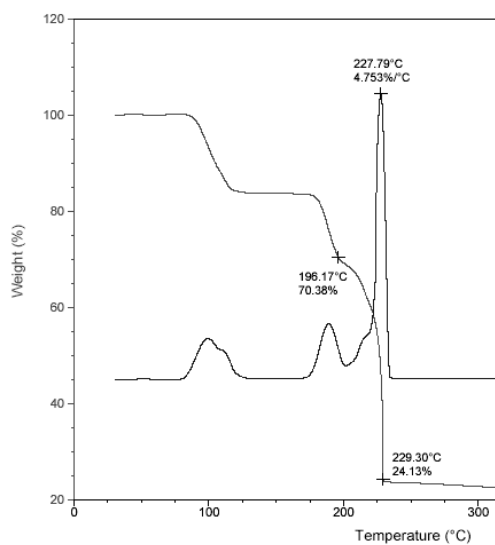
Fig : 13 TG curves of nickel bromate and samples of nickel bromate containing zinc bromate
 (i) Pure (ii) 10^{-3} M zinc bromate
 (iii) 10^{-2} M zinc bromate (iv) 10^{-1} M zinc bromate



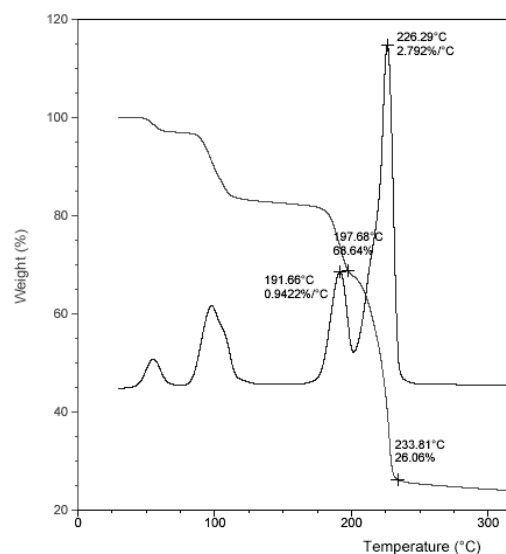
(i)



(ii)

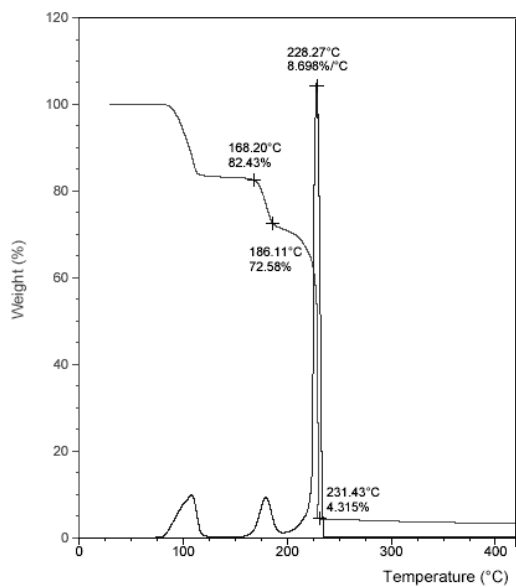


(iii)

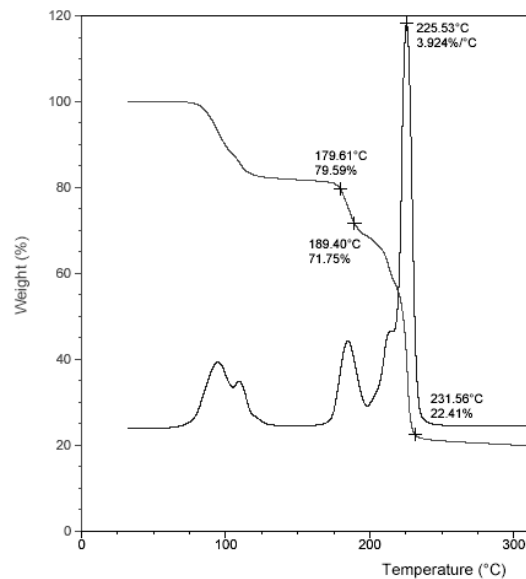


(iv)

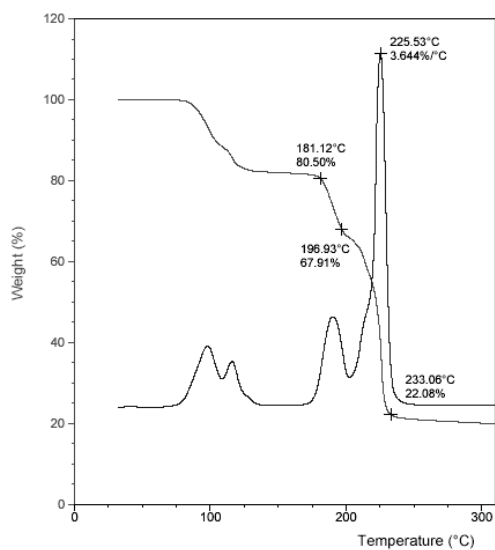
Fig : 14 TG curves of nickel bromate and samples of nickel bromate containing neodymium bromate
 (i) Pure (ii) 10^{-3} M neodymium bromate
 (iii) 10^{-2} M neodymium bromate (iv) 10^{-1} M neodymium bromate



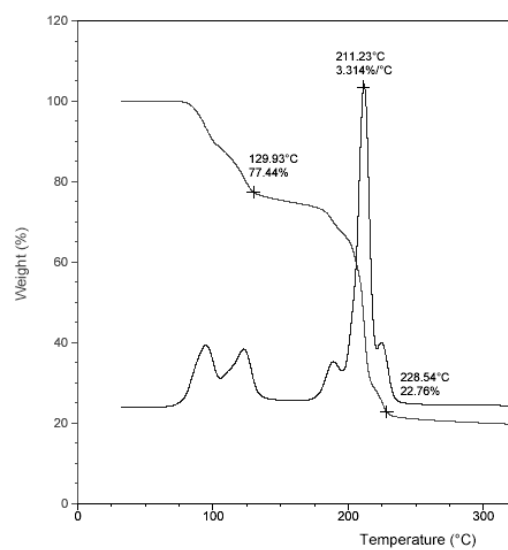
(i)



(ii)



(iii)



(iv)

Fig : 15 TG curves of nickel bromate and samples of nickel bromate containing yttrium bromate
 (i) Pure (ii) 10^{-3} M yttrium bromate
 (iii) 10^{-2} M yttrium bromate (iv) 10^{-1} M yttrium bromate

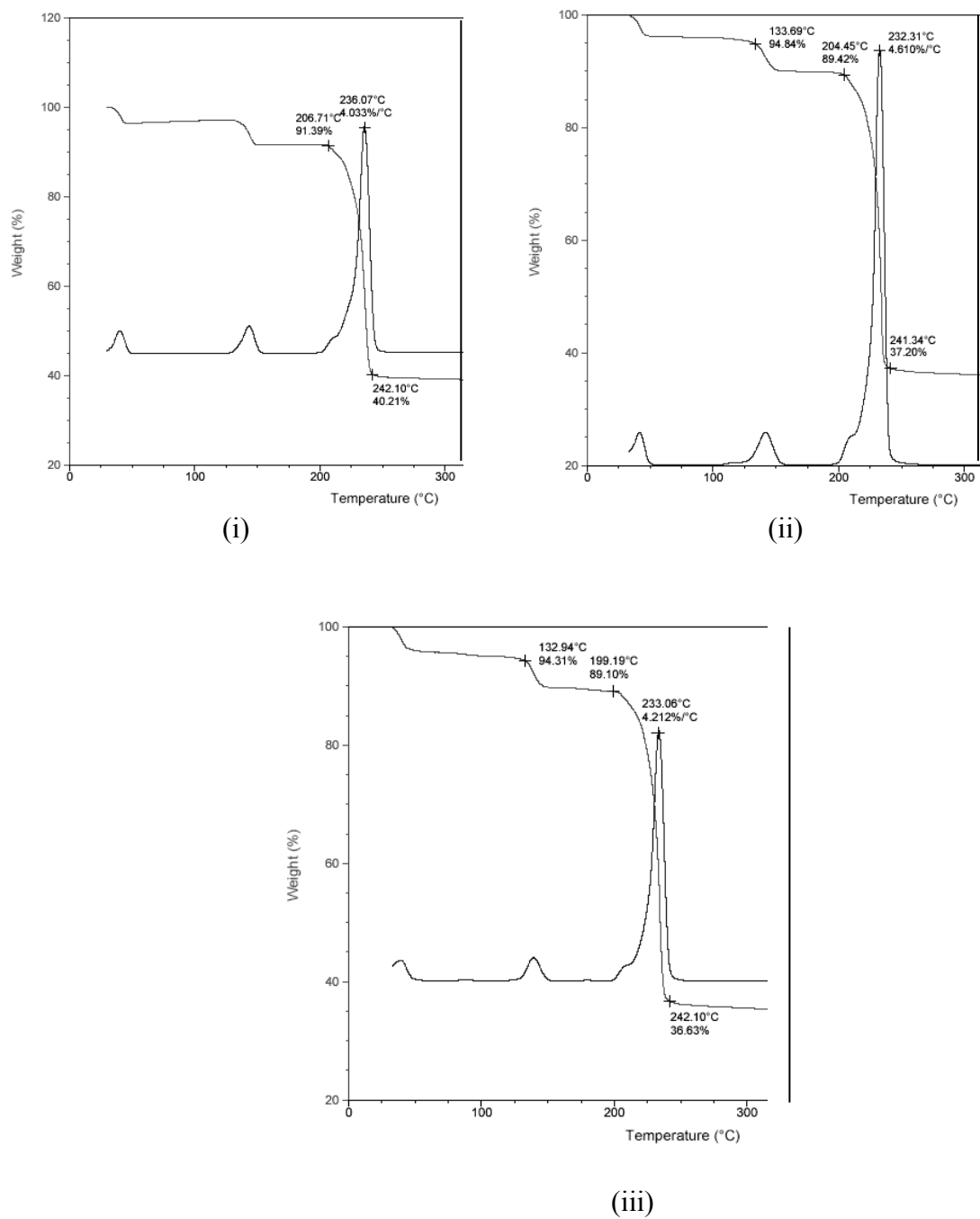


Fig : 16 TG curves of neodymium bromate and samples of neodymium bromate containing nickel bromate
 (i) Pure (ii) 10^{-2} M nickel bromate (iii) 10^{-1} M nickel bromate

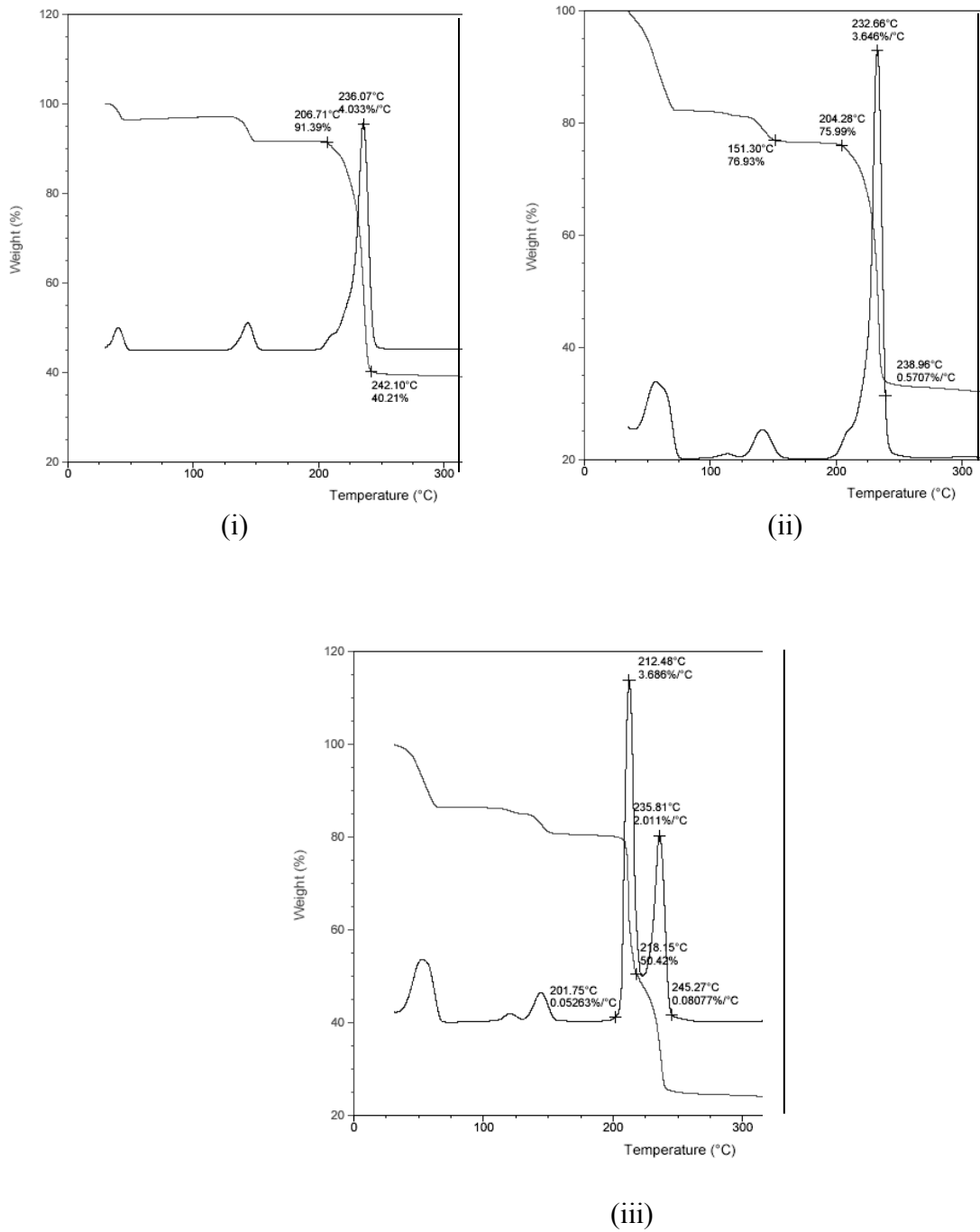
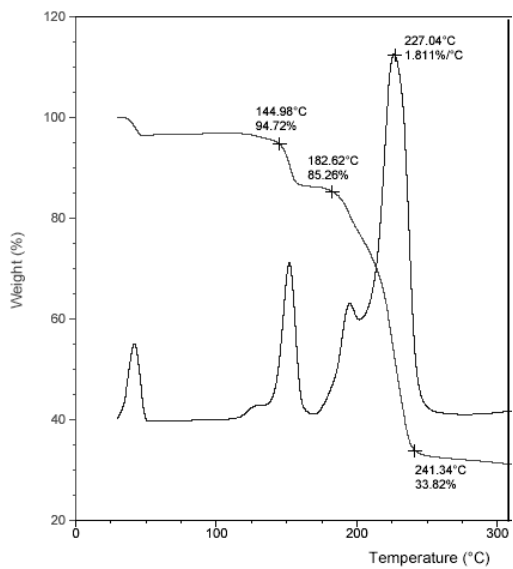
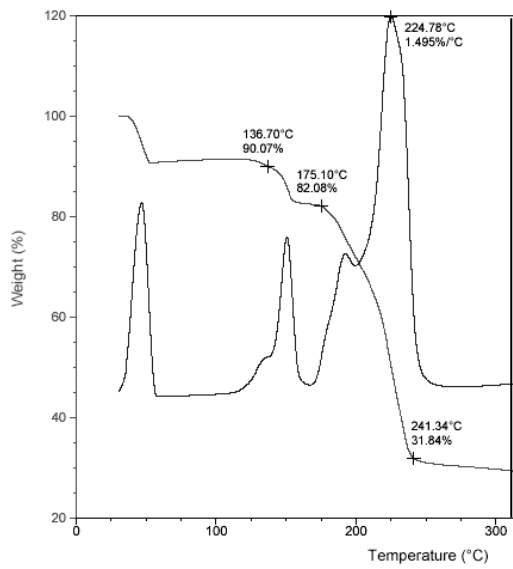


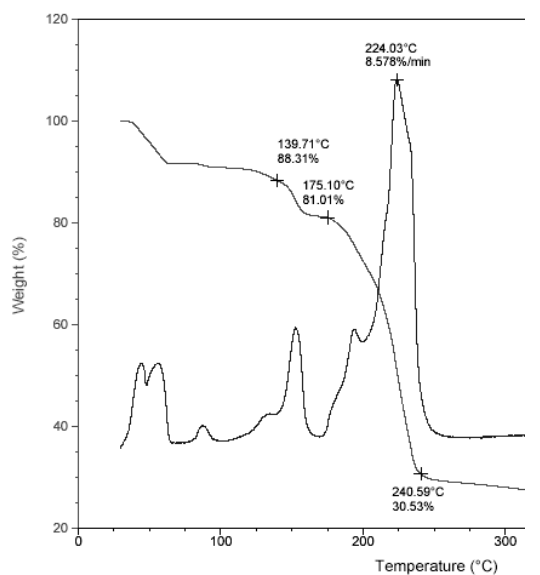
Fig : 17 TG curves of neodymium bromate and samples of neodymium bromate containing barium bromate
 (i) Pure (ii) 10^{-2} M barium bromate (iii) 10^{-1} M barium bromate



(i)

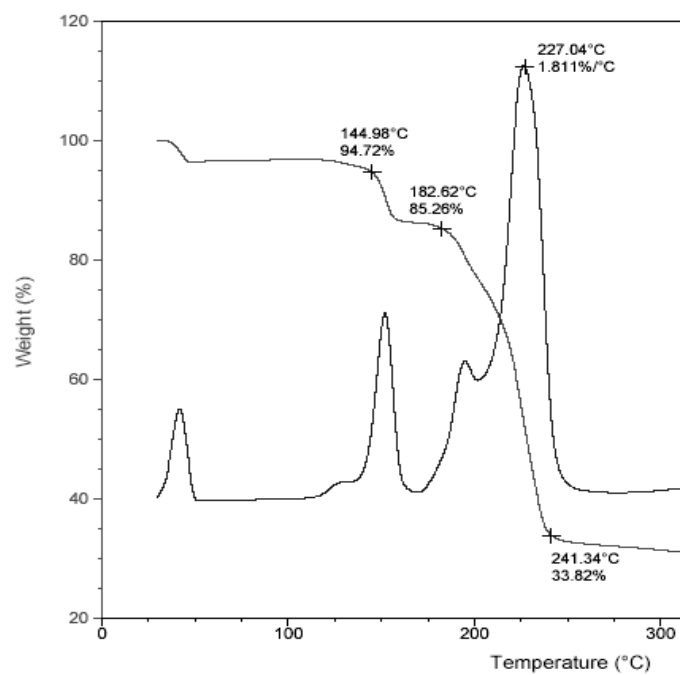


(ii)

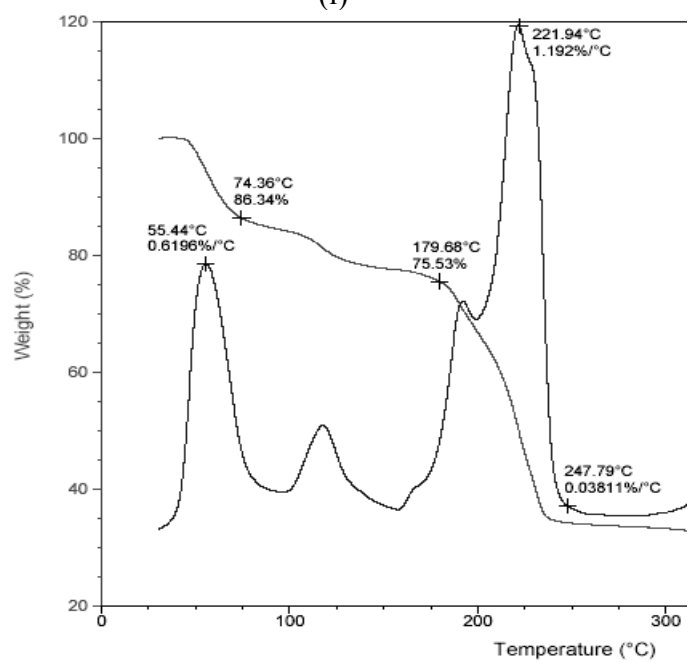


(iii)

Fig : 18 TG curves of yttrium bromate and samples of yttrium bromate containing nickel bromate
 (i) Pure (ii) 10^{-2} M nickel bromate (iii) 10^{-1} M nickel bromate



(i)



(ii)

Fig : 19 TG curves of yttrium bromate and sample of yttrium bromate containing barium bromate
 (i) Pure (ii) 10^{-1} M barium bromate

3.2 XRD Results

In all the samples studied wide angle X-ray diffraction patterns(WXRD) were obtained which clearly indicate highly crystalline nature of the samples. The plots also indicate that the intentional impurities in the treated samples remain as dopants(at least to a good extent). In the case of treated samples of nickel bromate containing zinc bromate, yttrium bromate containing nickel bromate and barium bromate containing yttrium bromate there is no indication of any new phase formation. However in the case of barium bromate containing neodymium bromate(10^{-1} M), a new peak of sufficiently good intensity at 2θ value of 48.2° is obtained pointing a chance of new phase formation. In the case of nickel bromate containing neodymium bromate(10^{-1} M) also some new peaks are observed at 2θ angles of 13.4° and 21.4° (Fig. 20-24).

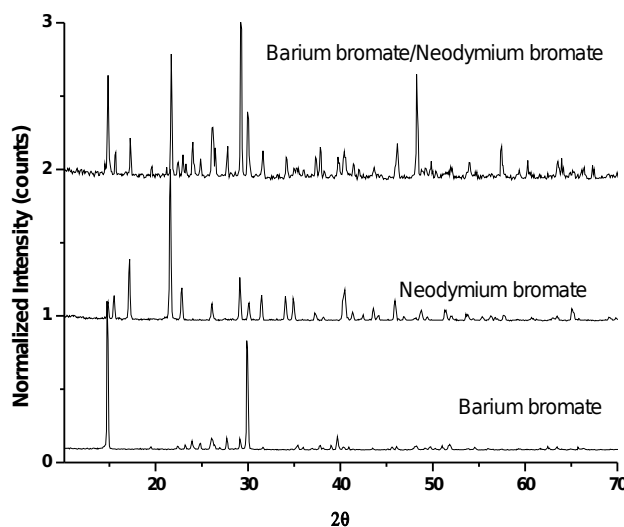


Fig. 20 : XRD plots for barium bromate, neodymium bromate and barium bromate containing neodymium bromate(10^{-1} M)

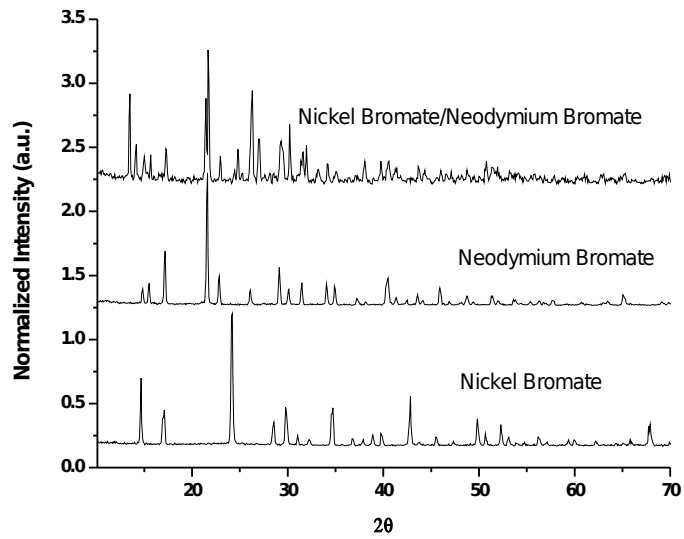


Fig 21 : XRD plots for neodymium bromate, nickel bromate and neodymium bromate containing nickel bromate(10^{-1} M)

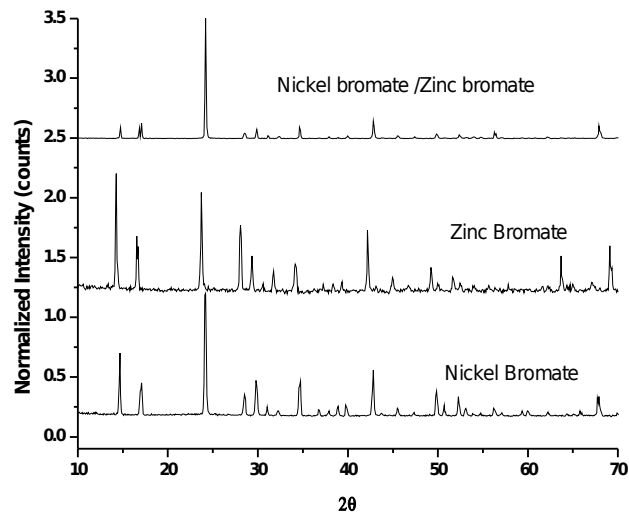


Fig 22 : XRD plots for nickel bromate, zinc bromate and nickel bromate containing zinc bromate(10^{-1} M)

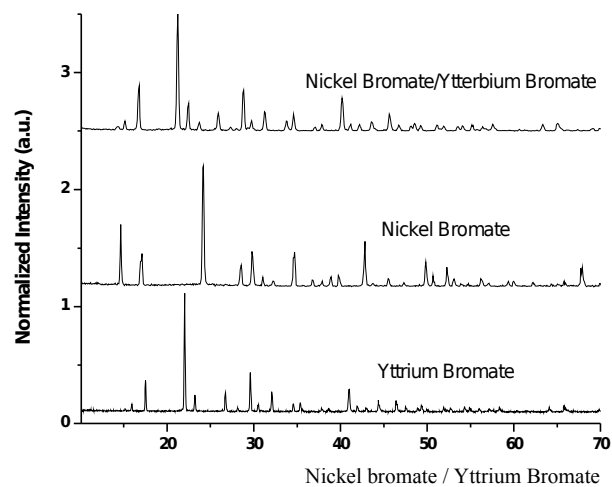


Fig 23 : XRD plots for yttrium bromate, nickel bromate and yttrium bromate containing nickel bromate(10^{-1} M)

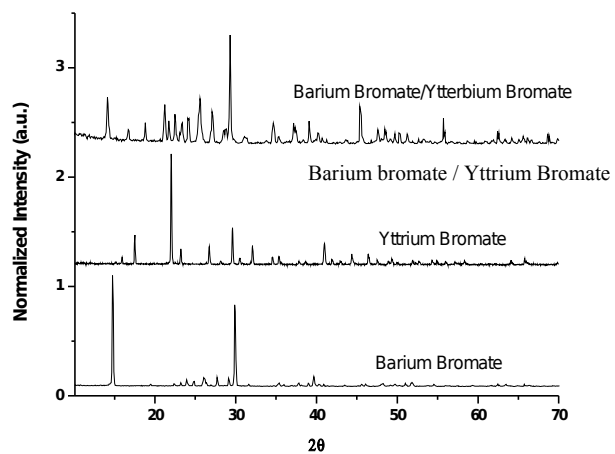


Fig 24 : XRD plots for barium bromate, yttrium bromate and barium bromate containing yttrium bromate(10^{-1} M)

3.3 FTIR Spectra

The Fourier Transform Infra Red spectra of the pure as well as those containing intentional impurities show prominent absorptions in the range 3450-3200 cm^{-1} , 1650-1600 cm^{-1} and around 800 cm^{-1} . Those in the range 3450-3200 cm^{-1} are the antisymmetric and symmetric – O-H stretching frequencies of ‘lattice water’ and those in the range 1630-1600 cm^{-1} are the characteristic bending vibrations of lattice water or coordinated water¹⁴⁶. Those vibrations in the vicinity of 800 cm^{-1} are the vibrational frequencies of the pyramidal BrO_3^- ion¹⁴⁶ in these compounds. In some spectra frequencies near to 600 cm^{-1} which is most probably due to lattice water exhibiting vibrations due to “librational oscillations” by interaction with neighbouring atoms¹⁴⁶ are seen (Fig. 25-27). The vibrations of BrO_3^- and the lattice water are altered in the treated samples to varying extents. The data relating to the prominent IR absorption frequencies as given by some of the samples studied are presented in Table 53.

Table 53 : FTIR spectral data
Prominent Vibrational Absorption Frequencies

Sample	O-H Stretching (Lattice water) cm^{-1}	H-O-H bending (Lattice water) cm^{-1}	Vibrations of BrO_3^-	
			$\nu_1(\text{A}_1)$ cm^{-1}	$\nu_3(\text{E})$ cm^{-1}
Nickel bromate $\text{Ni}(\text{BrO}_3)_2 \cdot 6\text{H}_2\text{O}$	3243.6	-	863.8 796.0	774.6 689.0 664.0
Neodymium bromate $\text{Nd}(\text{BrO}_3)_3 \cdot 9\text{H}_2\text{O}$	3447.0	1620.2	874.5 792.5	756.8
Zinc bromate $\text{Zn}(\text{BrO}_3)_2 \cdot 6\text{H}_2\text{O}$	3211.5	-	846.0 792.5	778.2 664.0
Nickel bromate containing 0.01 M Neodymium bromate	3247.2	1648.8	867.4 796.0	774.6 653.3
Nickel bromate containing 0.1 M Neodymium bromate	3225.8	1627.4	863.8 796.0	671.2 649.8
Nickel bromate containing 0.001 M Zinc bromate	3168.7	-	863.8 799.6	778.2 671.2
Nickel bromate containing 0.1 M Yttrium bromate	3222.2	1645.2	842.4 796.0	774.8 724.7

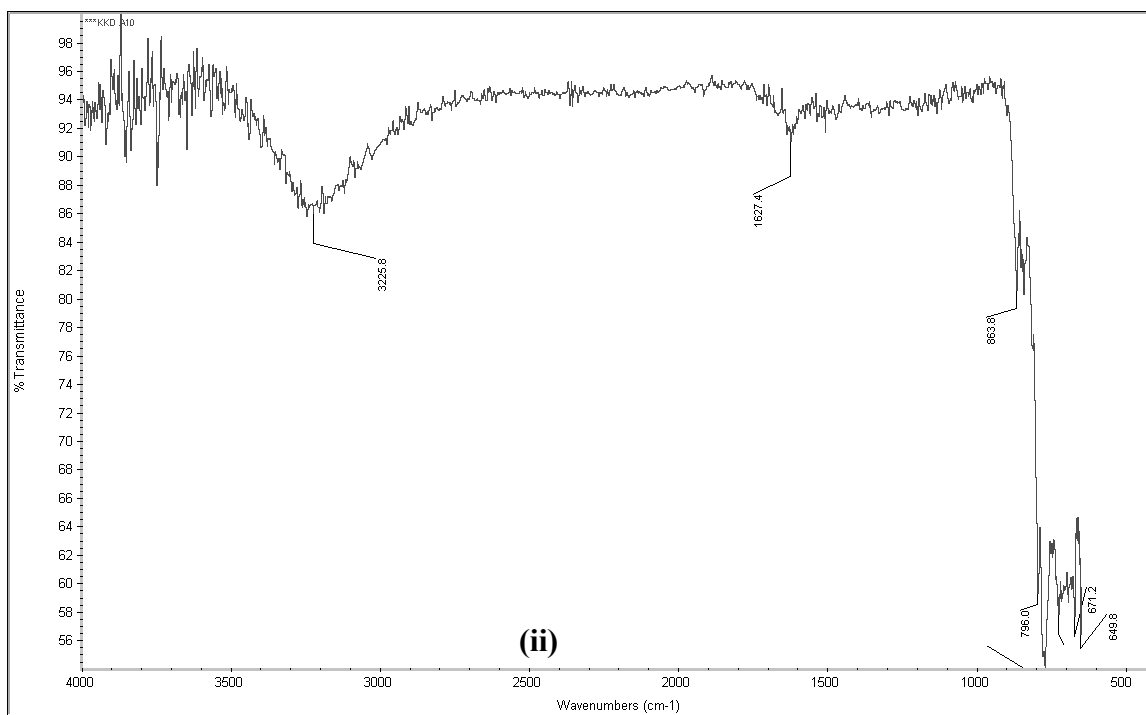
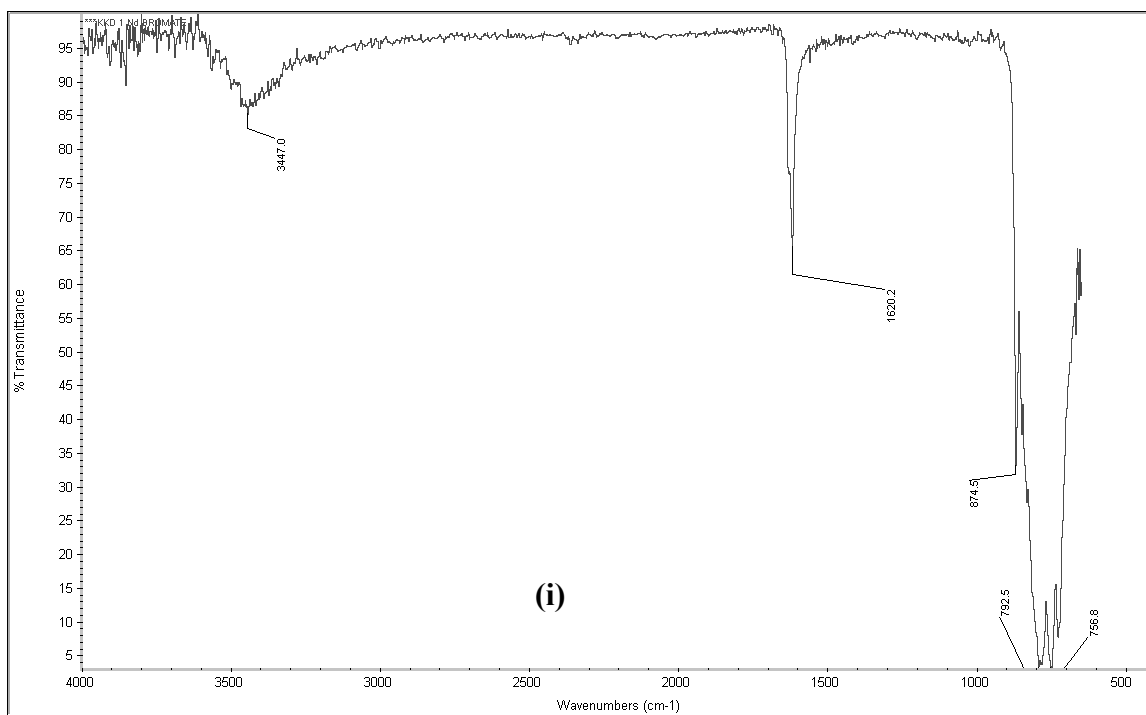


Fig. 25 : FTIR Spectrum of (i) neodymium bromate
(ii) nickel bromate containing 10^{-1} M neodymium bromate

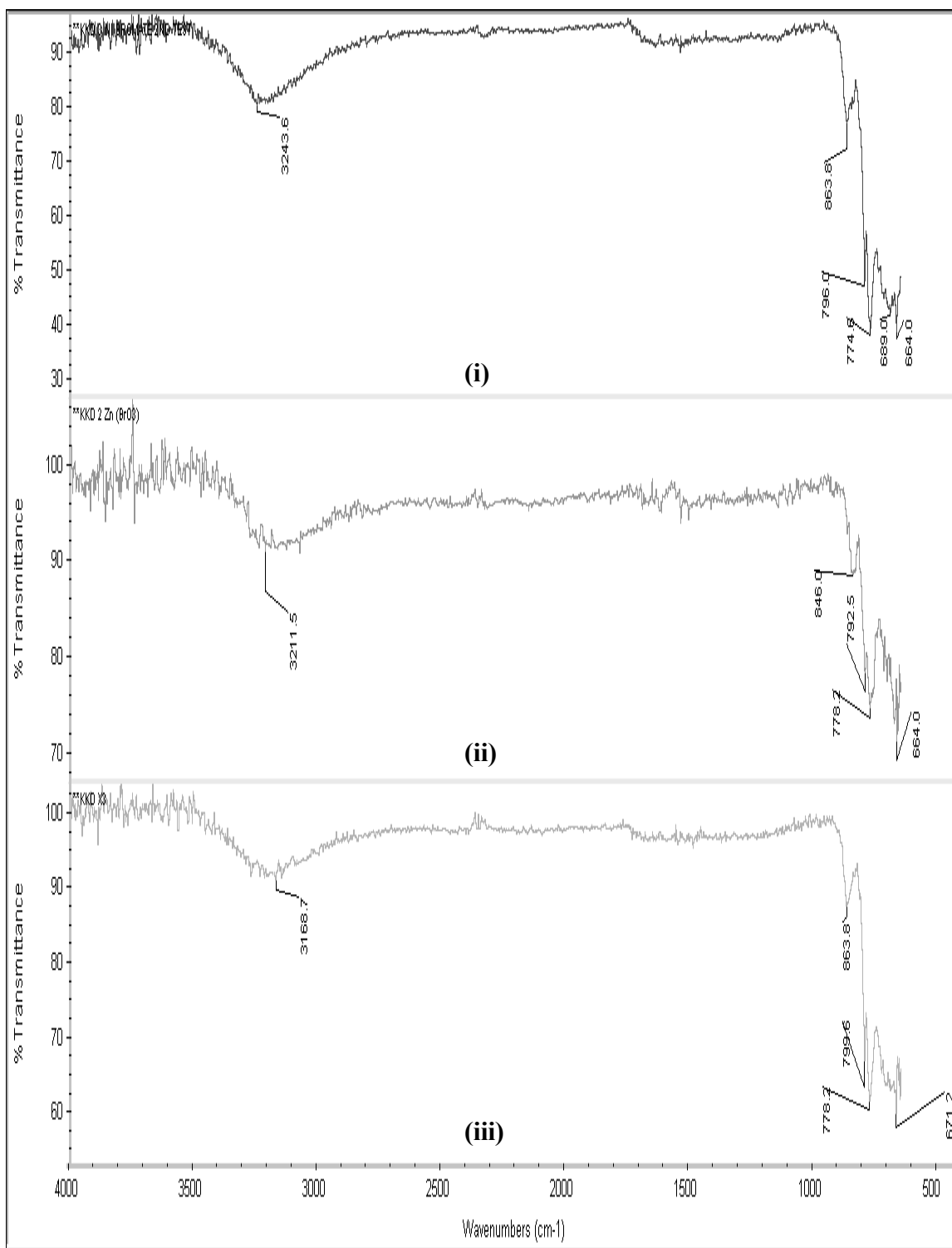


Fig. 26 : FTIR Spectrum of (i) nickel bromate (ii) zinc bromate (iii)nickel bromate containing 10⁻³ M zinc bromate

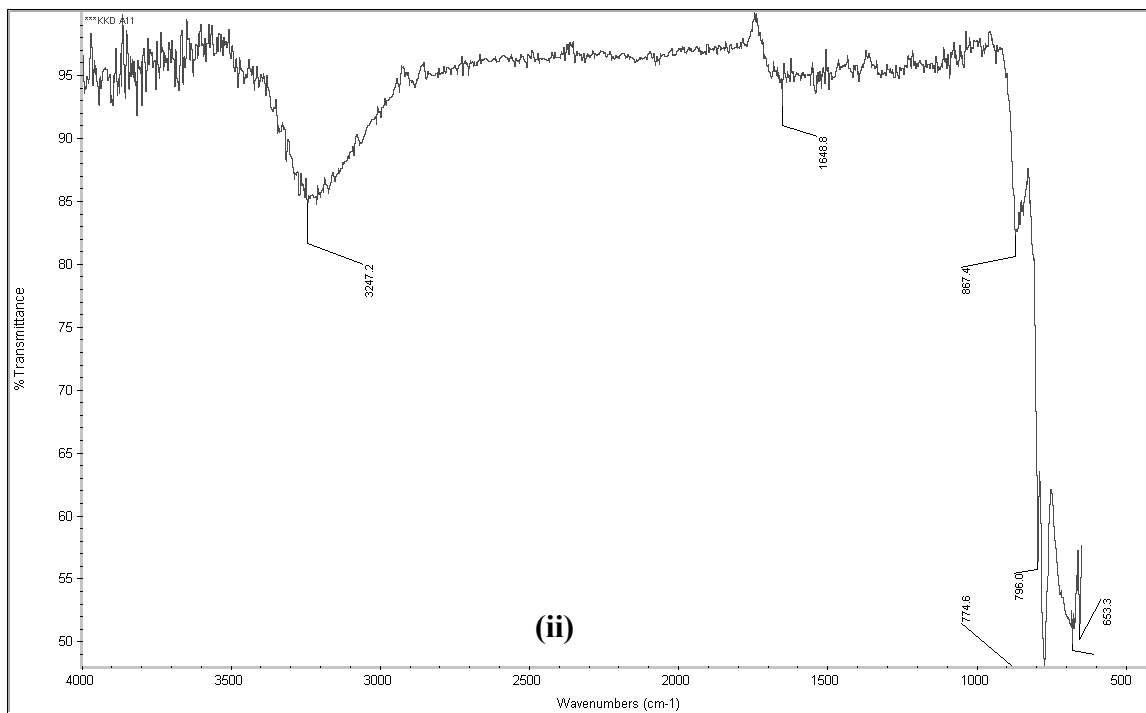
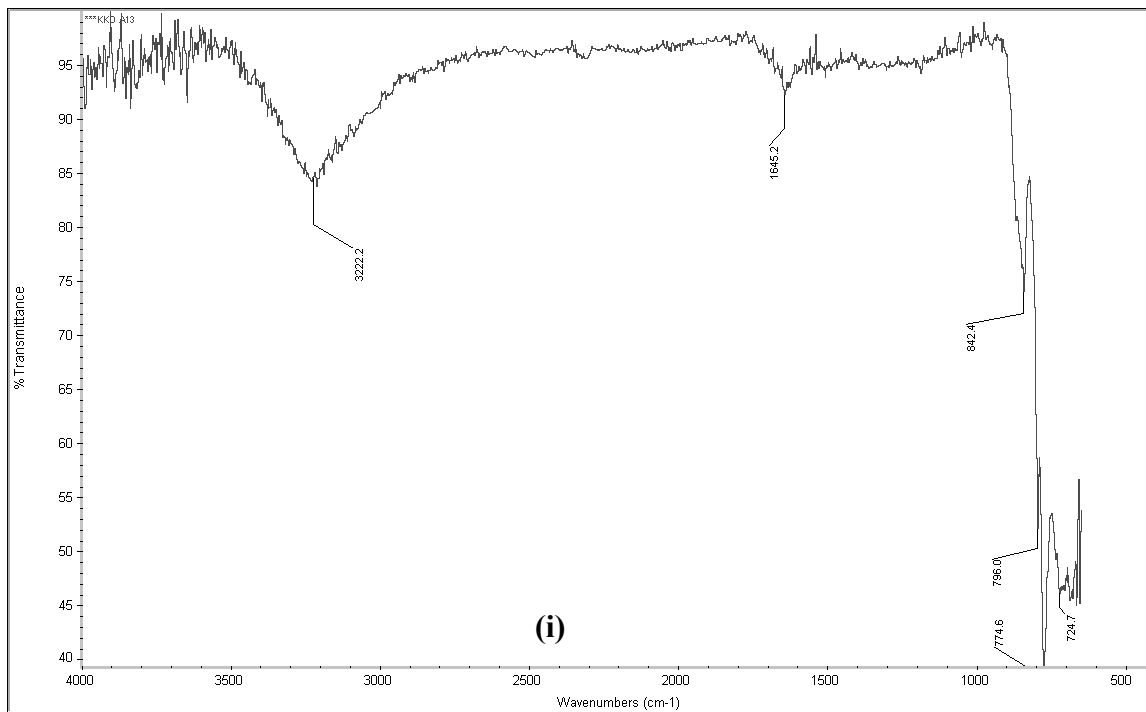


Fig. 27 : FTIR Spectrum of (i) nickel bromate containing 10^{-1} M yttrium bromate
(ii) nickel bromate containing 10^{-2} M neodymium bromate

3.4 Evaluation of Kinetic Parameters

It has been established in the previous investigation on the thermal decomposition of barium bromate²⁶ that the reaction follows first order kinetics and hence the kinetic parameters of the decompositions of pure barium bromate and samples of barium bromate containing intentional impurities (Na⁺, K⁺, Mg²⁺, Sr²⁺, Zn²⁺, Cd²⁺, Ni²⁺, Y³⁺ and Nd³⁺) each in 10⁻³ to 10⁻¹ M concentrations were evaluated using the Coats-Redfern¹²², Freeman-Carroll¹⁰³ and Horowitz-Metzger²⁸ equations in the form applicable to first order reactions and the results were compared. The kinetic parameters were also calculated for samples of barium bromate containing KBr and SrBr₂ as intentional impurities in 10⁻³ to 10⁻¹ M concentrations and the results were compared.

In the case of nickel bromate, neodymium bromate and yttrium bromate and samples containing intentional impurities the observed thermogravimetric data fit best with a first order process. The kinetic parameters of nickel bromate and samples of nickel bromate containing intentional impurities (Zn²⁺, Nd³⁺, Y³⁺ in 10⁻³ to 10⁻¹ M concentrations), neodymium bromate and samples of it containing intentional impurities (Ni²⁺, Ba²⁺ in 10⁻² to 10⁻¹ M concentrations) and yttrium bromate and samples of yttrium bromate containing Ni²⁺ and Ba²⁺ each in 10⁻² to 10⁻¹ M concentrations were calculated by Coats-Redfern¹²², Freeman-Carroll¹⁰³ and Horowitz-Metzger²⁸ methods in the form applicable to first order reactions and the results were compared.

3.4.1 The Coats-Redfern method

For a first order reaction the Coats-Redfern¹²² equation may be written in the form

$$\log \left[\frac{-\ln(1-\alpha)}{T^2} \right] = \frac{-E}{2.303 RT} + \log \frac{ZR}{aE} \left(1 - \frac{2RT}{E} \right) \quad 1.55$$

where α is the fractional decomposition at the temperature T and a is the heating rate. Z and E are the frequency factor and energy of activation respectively. Since E is large

$\frac{2RT}{E}$ is very small and as an approximation $1 - \frac{2RT}{E} \approx 1$. So the equation is used in the form

$$\log\left[\frac{-\ln(1-\alpha)}{T^2}\right] = \frac{-E}{2.303 RT} + \log\frac{ZR}{aE} \quad 3.1$$

Plot of L.H.S. of the equation 3.1 against $\frac{1}{T}$ was linear (in fairly good range of the mass loss – temperature data for all the samples). E and Z were calculated from the slope $\left(\frac{-E}{2.303 R}\right)$ and intercept $\left(\log\frac{ZR}{aE}\right)$ respectively. The results of the analysis of the data by this method are given in Tables 1-52.

3.4.2 The Freeman-Carroll method

The Freeman-Carroll equation¹⁰³ for the evaluation of kinetic parameters was used in the form

$$\log\left[\frac{(dw/dt)}{w_r}\right] = \frac{-E}{2.303 RT} + \log Z \quad 1.49$$

A plot of the L.H.S of equation 1.49 against $\frac{1}{T}$ was linear and E and Z were calculated from the slope $\left(\frac{-E}{2.303 R}\right)$ and intercept (log Z) respectively. The results of the analysis of data by this method are presented in the tables 1-52.

3.4.3 The Horowitz-Metzger method

The Horowitz-Metzger equation²⁸ applicable to a first order process is

$$\log\left[\log\left(\frac{w_\infty}{w_r}\right)\right] = \frac{E\theta}{2.303 RT_s^2} - \log 2.303 \quad 3.2$$

where $\theta = T-T_s$ and T_s is the peak temperature of decomposition (obtained from the TG curve). A plot of LHS of the equation versus θ was linear in a considerable good range of

mass loss-temperature data. E was calculated from the slope $\frac{E\theta}{2.303 RT_s^2}$

Table 1(i)
 Thermal decomposition of barium bromate - 1(i)
 Analysis of data by Coats-Redfern (C-R), Freeman-Carroll (F-C) and Horowitz-Metzger (H-M) methods
 Instrument: Ulvac Sinku-Riko (Japan) TA 1500, heating rate: 5° min⁻¹
 Peak temperature T_s: 621K, theoretical maximum mass loss w_∞: 24.4 mg, w_r = w_∞ - w

Temp K	(1/T) 10 ³	θ = T - T _s	Mass of sample mg	Mass loss w mg	Fraction decomposed	C-R $\log \left[\frac{-\log(1-\alpha)}{T^2} \right]$	F-C $\log \left[\frac{dw/dt}{w_r} \right]$	H-M $\log \left[\log \left(\frac{w_\infty}{w_r} \right) \right]$
565	1.7700	-56	100	--	--	--	--	--
571	1.7513	-50	99.89	0.11	0.0045	-8.2213	-2.4237	-2.7076
577	1.7331	-44	99.67	0.33	0.0135	-7.7510	-2.1205	-2.4056
583	1.7153	-38	99.34	0.66	0.0270	-7.4558	-1.9365	-1.9245
589	1.6978	-32	98.85	1.15	0.0471	-7.2191	-1.7558	-1.6788
595	1.6807	-26	97.98	2.02	0.0827	-6.9750	-1.4899	-1.4260
601	1.6639	-20	96.48	3.52	0.1441	-6.7278	-1.2232	-1.1701
607	1.6474	-14	94.94	5.06	0.2072	-6.5627	-1.1785	-0.9964
613	1.6313	-8	92.41	7.59	0.3108	-6.3660	-0.9021	-0.7914
619	1.6155	-2	87.67	12.3 3	0.5049	-6.0986	-0.4858	-0.5152
625	1.6000	+4	76.21	23.7 9	0.9742	-5.3908	+1.1807	+0.2010
			Intercept			17.65	22.07	0.4489
			Slope			14.68	14.01	0.0383
			Correlation coefficient			0.9936	0.9925	0.9885

Table 1(ii)
 Thermal Decomposition of barium bromate - 1(ii)
 Analysis of Data by Coats-Refern(C-R), Freeman-Carroll(F-C) and Horowitz-Metzger(H-M) Methods
 Instrument : Perkin Elmer Thermal Analyser Heating Rate : 5° min⁻¹
 Peak temperature : 609.6K, maximum mass loss w_∞ : 27.39mg, w_r = w_∞ - w

Temp K	(1/T) 10 ³	θ = T - T _s	Mass of Sample mg	Mass loss W mg	Fraction decompsd α	C-R	F-C	H-M
						$\log \left[\frac{-\log(1-\alpha)}{T^2} \right]$	$\log \left[\frac{dw/dt}{-1.0986} \right]$	$\log [\log(w_\infty/w_r)]$
562.81	1.7768	-46.79	100.00	--	--	--		--
567.81	1.7612	-41.79	99.79	0.21	0.0077	-7.9801		-2.4717
572.81	1.7458	-36.79	99.52	0.48	0.0177	-7.6263	-2.0087	-2.1102
577.88	1.7305	-31.72	99.25	0.75	0.0275	-7.4411	-1.9074	-1.9174
582.81	1.7158	-26.79	98.92	1.08	0.0393	-7.2898	-1.5984	-1.7587
587.82	1.7012	-21.78	98.26	1.74	0.0636	-7.0829	-1.2617	-1.5444
592.82	1.6868	-16.78	96.85	3.15	0.1149	-6.8216	-1.0155	-1.2757
597.84	1.6727	-11.76	94.51	5.49	0.2005	-6.5656	-0.8704	-1.0124
602.81	1.6589	-6.79	91.58	8.42	0.3076	-6.3572	-0.5571	-0.7969
607.85	1.6451	-1.75	86.27	13.73	0.5012	-6.0875	-0.0276	-0.5199
612.87	1.6317	3.27	73.40	26.60	0.9712	-5.3872	0.2895	0.1875
615.44	1.6249	5.84	72.61	27.39	1.0000	--	--	--
Intercept						19.2255	24.7114	-0.4923
Slope						-15.4222	-15.2791	0.0461
Correlation Coefficient						0.9956	0.9788	0.9968

Table 2
 Thermal decomposition of barium bromate containing sodium bromate (10^{-3})
 Analysis of data by Coats-Redfern (C-R), Freeman-Carroll (F-C) and Horowitz-Metzger (H-M) methods
 Instrument: Ulvac Sinku-Riko (Japan) TA 1500, heating rate: $5^{\circ} \text{ min}^{-1}$
 Peak temperature T_s : 621K, theoretical maximum mass loss w_{∞} : 24.4 mg, $w_r = w_{\infty} - w$

Temp K	$(1/T) 10^3$	$\theta = T - T_s$	Mass of sample mg	Mass loss w mg	Fraction decomposed	C-R $\log \left[\frac{-\log(1-\alpha)}{T^2} \right]$	F-C $\log \left[\frac{dw/dt}{w_r} \right]$	H-M $\log \left[\log \left(\frac{w_{\infty}}{w_r} \right) \right]$
573	1.7452	-48	100	--	--	--	--	--
578	1.7301	-43	99.73	0.27	0.0114	-7.8282	-1.9462	-2.3109
583	1.7153	-38	99.45	0.55	0.0224	-7.5384	-1.9416	-2.0076
593	1.7007	-33	98.91	1.09	0.0448	-7.2403	-1.6303	-1.7015
598	1.6863	-28	98.14	1.86	0.0761	-7.0100	-1.4697	-1.4639
603	1.6722	-23	97.21	2.79	0.1141	-6.8322	-1.3670	-1.2780
608	1.6584	-18	96.01	3.99	0.1634	-6.6716	-1.2303	-1.1109
613	1.6447	-13	94.75	5.25	0.2148	-6.5465	-1.1834	-0.9787
613	1.6313	-8	92.57	7.43	0.3043	-6.3774	-0.8905	-0.8024
618	1.6184	-3	89.18	10.8 2	0.4431	-6.1768	-0.6036	-0.5948
623	1.6051	+2	79.34	20.6 6	0.8459	-5.6794	+1.4171	-0.0904
			Intercept			16.70	19.63	0.4681
			Slope			14.12	12.55	0.0380
			Correlation coefficient			0.9923	0.9905	0.9935

Table 3
 Thermal decomposition of barium bromate containing sodium bromate (10^{-2} M)
 Analysis of data by Coats-Redfern (C-R), Freeman-Carroll (F-C) and Horowitz-Metzger (H-M) methods
 Instrument: Ulvac Sinku-Riko (Japan) TA 1500, heating rate: $5^{\circ} \text{ min}^{-1}$
 Peak temperature T_s : 627K, theoretical maximum mass loss w_{∞} : 24.4 mg, $w_r = w_{\infty} - w$

Temp K	$(1/T) 10^3$	$\theta = T - T_s$	Mass of sample mg	Mass loss W mg	Fraction decomposed	C-R $\log \left[\frac{-\log(1-\alpha)}{T^2} \right]$	F-C $\log \left[\frac{dw/dt}{w_r} \right]$	H-M $\log \left[\log \left(\frac{w_{\infty}}{w_r} \right) \right]$
573	1.7452	-54	100	--	--	--	--	--
578	1.7301	-49	99.84	0.16	0.0067	-8.0602	-2.1727	-2.5363
583	1.7153	-44	99.56	0.44	0.0179	-7.6380	-1.9390	-2.1066
588	1.7007	-39	99.35	0.65	0.0268	-7.4670	-2.0375	-1.9285
593	1.6863	-34	98.80	1.20	0.0491	-7.2064	-1.6303	-1.6606
598	1.6722	-29	98.04	1.96	0.0803	-6.9929	-1.4689	-1.4394
603	1.6584	-24	97.17	2.83	0.1160	-6.8319	-1.3942	-1.2714
608	1.6447	-19	95.97	4.03	0.1650	-6.6740	-1.2310	-0.1061
613	1.6313	-14	94.61	5.39	0.2290	-6.5221	-0.0811	-0.9471
618	1.6184	-9	92.81	7.19	0.2944	-6.4017	-0.0327	-0.8197
623	1.6051	-4	89.54	10.46	0.4283	-6.2037	-0.6307	-0.6148
628	1.5924	+1	83.01	16.99	0.6959	-5.8824	-0.0556	-0.2866
633	1.5798	+6	78.98	21.02	0.8609	-5.6699	-0.0745	-0.0671
638	1.5674	+11	76.80	23.20	0.9501	-5.4951	-0.2527	-0.1147
			Intercept			15.41	19.12	0.4189
			Slope			13.43	12.37	0.0363
			Correlation coefficient			0.9956	0.9735	0.9932

Table 4
 Thermal decomposition of barium bromate containing sodium bromate (10^{-1} M)
 Analysis of data by Coats-Redfern (C-R), Freeman-Carroll (F-C) and Horowitz-Metzger (H-M) methods
 Instrument: Ulvac Sinku-Riko (Japan) TA 1500, heating rate: $5^{\circ} \text{ min}^{-1}$
 Peak temperature T_s : 635.5K, theoretical maximum mass loss w_{∞} : 24.4 mg, $w_r = w_{\infty} - w$

Temp K	$(1/T) 10^3$	$\theta = T - T_s$	Mass of sample mg	Mass loss w mg	Fraction decomposed	C-R $\log \left[\frac{-\log(1-\alpha)}{T^2} \right]$	F-C $\log \left[\frac{dw/dt}{w_r} \right]$	H-M $\log \left[\log \left(\frac{w_{\infty}}{w_r} \right) \right]$
573	1.7452	-62.5	100	--	--	--	--	--
578	1.730	-57.5	99.82	0.18	0.0074	-8.0145	-2.1268	-2.4907
583	1.7153	-52.5	99.64	0.36	0.0149	-7.7183	-2.1212	-2.1868
588	1.7007	-47.5	99.27	0.73	0.0298	-7.4202	-1.8135	-1.8819
593	1.6863	-42.5	98.55	1.45	0.0596	-7.1200	-1.4989	-1.5738
598	1.6722	-37.5	98.18	1.82	0.0745	-7.0271	-1.7942	-1.4738
603	1.6584	-32.5	97.09	2.91	0.1191	-6.8196	-1.2948	-1.2590
608	1.6447	-27.5	96.00	4.00	0.1638	-6.6774	-1.2722	-0.1096
613	1.6313	-22.5	94.91	5.09	0.2085	-6.5683	-0.2484	-0.9934
618	1.6181	-17.5	93.82	6.18	0.2532	-6.4790	-0.2232	-0.8970
623	1.6051	-12.5	92.00	8.00	0.3276	-6.3525	-0.9558	-0.7635
628	1.5924	-7.5	89.46	10.5 4	0.4318	-6.2058	-0.7365	-0.6090
633	1.5798	-2.5	86.18	13.8 2	0.5659	-6.0437	-0.5104	-0.4409
638	1.5674	+2.5	81.89	18.9 1	0.7743	-5.7991	-0.0344	-0.1894
			Intercept			13.76	16.91	0.3306
			Slope			12.49	11.04	0.0305
			Correlation coefficient			0.9909	0.9601	0.9936

Table 5
 Thermal decomposition of barium bromate containing potassium bromate (10^{-3} M)
 Analysis of data by Coats-Redfern (C-R), Freeman-Carroll (F-C) and Horowitz-Metzger (H-M) methods
 Instrument: Ulvac Sinku-Riko (Japan) TA 1500, heating rate: $5^{\circ} \text{ min}^{-1}$
 Peak temperature T_s : 620.5K, theoretical maximum mass loss w_{∞} : 24.4 mg, $w_r = w_{\infty} - w$

Temp K	$(1/T) 10^3$	$\theta = T - T_s$	Mass of sample mg	Mass loss w mg	Fraction decomposed	C-R $\log \left[\frac{-\log(1-\alpha)}{T^2} \right]$	F-C $\log \left[\frac{dw/dt}{w_r} \right]$	H-M $\log \left[\log \left(\frac{w_{\infty}}{w_r} \right) \right]$
563	1.7762	-57.5	100	--	--	--	--	--
568	1.7606	-52.5	99.96	0.04	0.0018	-8.6148	-2.7435	-3.1061
573	1.7452	-47.5	99.87	0.13	0.0054	-8.1479	-2.4459	-2.6315
578	1.7301	-42.5	99.74	0.26	0.0105	-7.8634	-2.2863	-2.3394
583	1.7153	-37.5	99.51	0.49	0.0199	-7.5903	-2.0173	-2.0590
588	1.7007	-32.5	99.13	0.87	0.0358	-7.3398	-1.7842	-1.8011
593	1.6863	-27.5	98.36	1.64	0.0670	-7.0670	-1.4745	-1.5209
598	1.6722	-22.5	97.39	2.61	0.1070	-6.8617	-1.3487	-1.3083
603	1.6584	-17.5	96.30	3.70	0.1517	-6.7067	-1.2789	-1.1461
608	1.6447	-12.5	94.99	5.01	0.2053	-6.5686	-1.1707	-1.0008
613	1.6313	-7.5	93.35	6.65	0.32722	-6.4351	-1.0371	-0.8602
618	1.6181	-2.5	90.41	9.59	0.3926	-6.2465	-0.7029	-0.6646
623	1.6051	+2.5	81.59	18.4 1	0.7539	-5.8045	+0.1667	-0.2155
			Intercept			16.66	21.11	0.5262
			Slope			14.12	13.49	0.0385
			Correlation coefficient			0.9926	0.9901	0.9916

Table 6
 Thermal decomposition of barium bromate containing potassium bromate (10^{-2} M)
 Analysis of data by Coats-Redfern (C-R), Freeman-Carroll (F-C) and Horowitz-Metzger (H-M) methods
 Instrument: Ulvac Sinku-Riko (Japan) TA 1500, heating rate: $5^{\circ} \text{ min}^{-1}$
 Peak temperature T_s : 621K, theoretical maximum mass loss w_{∞} : 24.4 mg, $w_r = w_{\infty} - w$

Temp K	$(1/T) 10^3$	$\theta = T - T_s$	Mass of sample mg	Mass loss W mg	Fraction decomposed	C-R $\log \left[\frac{-\log(1-\alpha)}{T^2} \right]$	F-C $\log \left[\frac{dw/dt}{w_r} \right]$	H-M $\log \left[\log \left(\frac{w_{\infty}}{w_r} \right) \right]$
568	1.7606	-53	100	--	--	--	--	--
573	1.7452	-48	99.90	0.10	0.0043	-82482	-2.3686	-2.7320
578	1.7301	-43	99.68	0.32	0.0133	-7.7603	-2.0395	-2.2365
583	1.7153	-38	99.34	0.66	0.0270	-7.4571	-1.8580	-2.2232
588	1.7007	-33	98.02	0.98	0.0402	-7.2878	-1.8593	-1.7490
593	1.6863	-28	98.37	1.63	0.0668	-7.0690	-1.5462	-1.5229
598	1.6722	-23	97.44	2.56	0.1048	-6.8715	-1.3717	-1.3181
603	1.6584	-18	96.19	3.81	0.1561	-6.6931	-1.2161	-1.1325
608	1.6447	-13	94.56	5.44	0.2229	-6.5284	-1.0661	-0.9606
613	1.6313	-8	92.71	7.29	0.2986	-6.3874	-0.9668	-0.8124
618	1.6181	-3	90.42	9.58	0.3923	-6.2470	-0.8120	-0.6650
623	1.6051	+2	80.52	19.48	0.7978	-5.7475	+0.3022	-0.1558
			Intercept			15.33	18.82	0.5195
			Slope			13.30	12.10	0.0362
			Correlation coefficient			0.9966	0.9926	0.9971

Table 7
 Thermal decomposition of barium bromate containing potassium bromate (10^{-1} M)
 Analysis of data by Coats-Redfern (C-R), Freeman-Carroll (F-C) and Horowitz-Metzger (H-M) methods
 Instrument: Ulvac Sinku-Riko (Japan) TA 1500, heating rate: $5^{\circ} \text{ min}^{-1}$
 Peak temperature T_s : 621K, theoretical maximum mass loss w_{∞} : 24.4 mg, $w_r = w_{\infty} - w$

Temp K	$(1/T) 10^3$	$\theta = T - T_s$	Mass of sample mg	Mass loss w mg	Fraction decomposed	C-R $\log \left[\frac{-\log(1-\alpha)}{T^2} \right]$	F-C $\log \left[\frac{dw/dt}{w_r} \right]$	H-M $\log \left[\log \left(\frac{w_{\infty}}{w_r} \right) \right]$
565	1.7700	-56	100	--	--	--	--	--
571	1.7513	-50	99.92	0.08	0.0033	-8.2594	-2.5625	-2.8462
577	1.7331	-44	99.73	0.27	0.0111	-7.8384	-2.1833	-2.3162
583	1.7153	-38	99.30	0.70	0.0287	-7.4298	-1.8208	-1.8986
589	1.6978	-32	98.63	1.37	0.0561	-7.1410	-1.6158	-1.6008
595	1.6807	-26	97.74	2.26	0.0926	-6.9240	-1.4754	-1.3749
601	1.6639	-20	95.96	4.04	0.1654	-6.6626	-1.1379	-1.1049
607	1.6476	-14	93.97	6.03	0.2469	-6.4759	-1.0449	-0.9095
613	1.6313	-8	91.51	8.49	0.3477	-6.3065	-0.8905	-0.7316
619	1.6155	-2	87.96	12.0 4	0.4930	-6.1135	-0.6217	-0.5301
625	1.6000	+4	78.19	21.8 1	0.8931	-5.6045	-0.4941	-0.0127
631	1.5848	+10	76.85	23.1 5	0.9480	-5.4915	-0.0559	+0.1085
			Intercept			15.29	18.15	0.4366
			Slope			13.23	11.65	0.0356
			Correlation coefficient			0.9966	0.9953	0.9975

Table 8
 Thermal decomposition of barium bromate containing magnesium bromate (10^{-3} M)
 Analysis of data by Coats-Redfern (C-R), Freeman-Carroll (F-C) and Horowitz-Metzger (H-M) methods
 Instrument: Ulvac Sinku-Riko (Japan) TA 1500, heating rate: $5^{\circ} \text{ min}^{-1}$
 Peak temperature T_s : 617K, theoretical maximum mass loss w_{∞} : 24.4 mg, $w_r = w_{\infty} - w$

Temp K	$(1/T) 10^3$	$\theta = T - T_s$	Mass of sample mg	Mass loss w mg	Fraction decomposed	C-R $\log \left[\frac{-\log(1-\alpha)}{T^2} \right]$	F-C $\log \left[\frac{dw/dt}{w_r} \right]$	H-M $\log \left[\log \left(\frac{w_{\infty}}{w_r} \right) \right]$
568	1.7606	-49	100	--	--	--	--	--
573	1.7452	-44	99.67	0.33	0.0134	-7.4788	-1.8673	-2.2325
578	1.7301	-39	99.64	0.54	0.0223	-7.5327	-2.0401	-2.0090
583	1.7153	-34	98.91	1.09	0.0446	-7.2341	-1.6315	-1.7028
588	1.7007	-29	98.48	1.52	0.0583	-7.1220	-1.5366	-1.5833
593	1.6863	-24	97.49	2.51	0.1026	-6.8739	-1.3069	-1.3278
598	1.6722	-19	96.08	3.92	0.1606	-6.6724	-1.1607	-1.1190
603	1.6584	-14	94.34	5.66	0.2320	-6.5013	-1.0316	-0.9407
608	1.6447	-9	92.81	7.19	0.2944	-6.3875	-1.0532	-0.8197
613	1.6313	-4	89.98	10.0 2	0.4104	-6.2143	-0.7062	-0.6394
618	1.6184	+1	80.17	19.8 3	0.8119	-5.7213	+0.3292	-0.1394
			Intercept			15.80	21.14	0.4691
			Slope			13.47	13.40	0.0365
			Correlation coefficient			0.9964	0.9653	0.9957

Table 9
 Thermal decomposition of barium bromate containing magnesium bromate (10^{-2} M)
 Analysis of data by Coats-Redfern (C-R), Freeman-Carroll (F-C) and Horowitz-Metzger (H-M) methods
 Instrument: Ulvac Sinku-Riko (Japan) TA 1500, heating rate: $5^{\circ} \text{ min}^{-1}$
 Peak temperature T_s : 618K, theoretical maximum mass loss w_{∞} : 24.4 mg, $w_r = w_{\infty} - w$

Temp K	$(1/T) 10^3$	$\theta = T - T_s$	Mass of sample mg	Mass loss w mg	Fraction decomposed	C-R $\log \left[\frac{-\log(1-\alpha)}{T^2} \right]$	F-C $\log \left[\frac{dw/dt}{w_r} \right]$	H-M $\log \left[\log \left(\frac{w_{\infty}}{w_r} \right) \right]$
558	1.7921	-60	100	--	--	--	--	--
563	1.7762	-55	99.95	0.05	0.0022	-8.5156	-2.6520	-3.0147
568	1.7606	-50	99.78	0.22	0.0089	-7.9187	-2.1703	-2.4100
573	1.7452	-45	99.56	0.44	0.0178	-7.6231	-2.0415	-2.1068
578	1.7301	-40	99.13	0.87	0.0357	-7.3258	-1.7329	-1.8019
583	1.7153	-35	98.75	1.25	0.0514	-7.1712	-1.7835	-1.6407
588	1.7007	-30	98.04	1.96	0.0803	-6.9782	-1.5014	-1.4395
593	1.6863	-25	97.11	2.89	0.1182	-6.8086	-1.3664	-1.2625
598	1.6722	-20	95.86	4.14	0.1695	-6.6467	-1.2092	-1.0933
603	1.6584	-15	94.34	5.66	0.2320	-6.5013	-1.0898	-0.9405
608	1.6447	-10	92.37	7.63	0.3123	-6.3567	-0.9327	-0.7889
613	1.6313	-5	90.20	9.80	0.4015	-6.2267	0.2867	-0.6519
618	1.6184	0	82.79	17.2 1	0.7048	-5.8578	+0.0118	-0.2758
			Intercept			15.23	18.72	0.4191
			Slope			13.09	11.93	0.0354
			Correlation coefficient			0.9936	0.9891	0.9951

Table 10
 Thermal decomposition of barium bromate containing strontium bromate (10^{-3} M)
 Analysis of data by Coats-Redfern (C-R), Freeman-Carroll (F-C) and Horowitz-Metzger (H-M) methods
 Instrument: Ulvac Sinku-Riko (Japan) TA 1500, heating rate: $5^{\circ} \text{ min}^{-1}$
 Peak temperature T_s : 621K, theoretical maximum mass loss w_{∞} : 24.4 mg, $w_r = w_{\infty} - w$

Temp K	$(1/T) 10^3$	$\theta = T - T_s$	Mass of sample mg	Mass loss w mg	Fraction decomposed	C-R $\log \left[\frac{-\log(1-\alpha)}{T^2} \right]$	F-C $\log \left[\frac{dw/dt}{w_r} \right]$	H-M $\log \left[\log \left(\frac{w_{\infty}}{w_r} \right) \right]$
573	1.7452	-48	100	--	--	--	--	--
578	1.7301	-43	99.73	0.27	0.0111	-7.8368	-1.9483	-2.3130
583	1.7153	-38	99.35	0.65	0.0268	-7.4599	-1.7939	-1.9285
588	1.7007	-33	98.80	1.20	0.0491	-7.1994	-1.6303	-1.6606
593	1.6863	-28	98.15	1.85	0.0758	-7.0114	-1.5379	-1.4653
598	1.6722	-23	97.17	2.83	0.1166	-6.8248	-1.3430	-1.2714
603	1.6584	-18	95.86	4.14	0.1695	-6.6540	-1.1908	-1.0934
608	1.6447	-13	94.12	5.88	0.2409	-6.4898	-1.0268	-0.9220
613	1.6313	-8	92.16	7.84	0.3212	-6.3490	-0.9270	-0.7741
618	1.6184	-3	89.11	10.8 9	0.4461	-6.1728	-0.6467	-0.5908
623	1.6051	+2	78.00	22.0 0	0.9011	-5.5869	+0.6628	+0.0021
			Intercept			16.63	19.24	0.4516
			Slope			14.05	12.32	0.0372
			Correlation coefficient			0.9914	0.9921	0.9970

Table 11
 Thermal decomposition of barium bromate containing strontium bromate (10^{-2} M)
 Analysis of data by Coats-Redfern (C-R), Freeman-Carroll (F-C) and Horowitz-Metzger (H-M) methods
 Instrument: Ulvac Sinku-Riko (Japan) TA 1500, heating rate: $5^{\circ} \text{ min}^{-1}$
 Peak temperature T_s : 621K, theoretical maximum mass loss w_{∞} : 24.4 mg, $w_r = w_{\infty} - w$

Temp K	$(1/T) 10^3$	$\theta = T - T_s$	Mass of sample mg	Mass loss w mg	Fraction decomposed	C-R $\log \left[\frac{-\log(1-\infty)}{T^2} \right]$	F-C $\log \left[\frac{dw/dt}{w_r} \right]$	H-M $\log \left[\log \left(\frac{w_{\infty}}{w_r} \right) \right]$
573	1.7452	-48	100	--	--	--	--	--
578	1.7301	-43	99.67	0.33	0.0134	-7.7577	-1.8681	-2.2338
583	1.7153	-38	99.35	0.65	0.0268	-7.4599	-1.8622	-2.0127
588	1.7007	-33	98.91	1.09	0.0446	-7.2414	-1.7284	-1.7027
593	1.6863	-28	98.15	1.85	0.0758	-7.0114	-1.4715	-1.4509
598	1.6722	-23	97.17	2.83	0.1160	-6.8248	-1.3430	-1.2714
603	1.6584	-18	95.86	4.14	0.1695	-6.6540	-1.1908	-1.0934
608	1.6447	-13	94.23	5.77	0.2364	-6.4991	-1.0571	-0.9312
613	1.6313	-8	92.21	7.79	0.3190	-6.3527	-0.9166	-0.7777
618	1.6184	-3	89.11	10.8 9	0.4461	-6.1728	-0.6391	-0.5908
623	1.6051	+2	78.21	21.7 9	0.8921	-5.6035	-0.6165	0.0145
			Intercept			14.94	18.94	0.4711
			Slope			13.04	12.14	0.0359
			Correlation coefficient			0.9980	0.9940	0.9974

Table 12
 Thermal decomposition of barium bromate containing strontium bromate (10^{-1} M)
 Analysis of data by Coats-Redfern (C-R), Freeman-Carroll (F-C) and Horowitz-Metzger (H-M) methods
 Instrument: Ulvac Sinku-Riko (Japan) TA 1500, heating rate: $5^{\circ} \text{ min}^{-1}$
 Peak temperature T_s : 621K, theoretical maximum mass loss w_{∞} : 24.4 mg, $w_r = w_{\infty} - w$

Temp K	$(1/T) 10^3$	$\theta = T - T_s$	Mass of sample mg	Mass loss w mg	Fraction decomposed	C-R $\log \left[\frac{-\log(1-\alpha)}{T^2} \right]$	F-C $\log \left[\frac{dw/dt}{w_r} \right]$	H-M $\log \left[\log \left(\frac{w_{\infty}}{w_r} \right) \right]$
563	1.7762	-58	100	--	--	--	--	--
568	1.7606	-53	99.78	0.22	0.0090	-7.9163	-2.0434	-2.4076
573	1.7452	-48	99.91	1.09	0.0447	-7.2181	-1.4269	-1.7018
578	1.7301	-43	98.47	1.53	0.0626	-7.0755	-2.0632	-1.5516
583	1.7153	-38	97.71	2.29	0.0939	-6.8997	-1.4618	-1.3683
588	1.7007	-33	96.83	3.17	0.1297	-6.7584	-1.3864	-1.2196
593	1.6863	-28	95.96	4.04	0.1654	-6.6510	-1.3677	-1.1049
598	1.6722	-23	95.09	4.91	0.2012	-6.5641	-1.3492	-0.0108
603	1.6584	-18	93.45	6.55	0.2641	-6.4361	-0.0663	-0.8706
608	1.6447	-13	91.92	8.08	0.3308	-6.3261	-1.0014	-0.7583
613	1.6313	-8	89.74	10.6 6	0.4366	-5.1784	-0.7264	-0.6035
618	1.6184	-3	85.15	14.8 5	0.6080	-5.9727	-0.3594	-0.3907
			Intercept			11.94	16.34	0.3876
			Slope			11.06	10.45	0.0266
			Correlation coefficient			0.9606	0.9720	0.9970

Table 13
 Thermal decomposition of barium bromate containing zinc bromate (10^{-3} M)
 Analysis of data by Coats-Redfern (C-R), Freeman-Carroll (F-C) and Horowitz-Metzger (H-M) methods
 Instrument: Ulvac Sinku-Riko (Japan) TA 1500, heating rate: $5^{\circ} \text{ min}^{-1}$
 Peak temperature T_s : 620K, theoretical maximum mass loss w_{∞} : 24.4 mg, $w_r = w_{\infty} - w$

Temp K	$(1/T) 10^3$	$\theta = T - T_s$	Mass of sample mg	Mass loss w mg	Fraction decomposed	C-R $\log \left[\frac{-\log(1-\alpha)}{T^2} \right]$	F-C $\log \left[\frac{dw/dt}{w_r} \right]$	H-M $\log \left[\log \left(\frac{w_{\infty}}{w_r} \right) \right]$
563	1.7762	-57	100	--	--	--	--	--
568	1.7606	-52	99.91	0.09	0.0037	-8.3007	-2.4290	-2.7920
573	1.7452	-47	99.73	0.27	0.0111	-7.8298	-2.1250	-2.3134
578	1.7301	-37	99.46	0.54	0.0223	-7.5338	-1.9439	-2.0100
583	1.7153	-32	99.28	0.72	0.0297	-7.4147	-2.1165	-1.8833
588	1.7007	-33	98.73	1.27	0.0519	-7.1741	-1.6295	-1.6353
593	1.6863	-27	97.83	2.17	0.0890	-6.9387	-1.3902	-1.3926
598	1.6722	-22	96.74	3.26	0.1135	-6.8346	-1.2893	-1.0502
603	1.6584	-17	95.47	4.53	0.1855	-6.6108	-1.1955	-0.8699
608	1.6447	-12	93.48	6.52	0.2671	-6.4371	-0.9533	-0.7300
613	1.6313	-7	91.49	8.51	0.3489	-6.3049	-0.9021	-0.4433
618	1.6184	-2	86.23	13.7 7	0.5638	-6.0253	-0.3070	-0.0310
623	1.6051	+3	78.44	21.5 6	0.8828	-5.6200	-0.4349	
			Intercept			17.32	21.11	0.4156
			Slope			14.41	13.38	0.0380
			Correlation coefficient			0.9927	0.9810	0.9965

Table 14
 Thermal decomposition of barium bromate containing zinc bromate (10^{-2} M)
 Analysis of data by Coats-Redfern (C-R), Freeman-Carroll (F-C) and Horowitz-Metzger (H-M) methods
 Instrument: Ulvac Sinku-Riko (Japan) TA 1500, heating rate: $5^{\circ} \text{ min}^{-1}$
 Peak temperature T_s : 620K, theoretical maximum mass loss w_{∞} : 24.4 mg, $w_r = w_{\infty} - w$

Temp K	$(1/T) 10^3$	$\theta = T - T_s$	Mass of sample mg	Mass loss w mg	Fraction decomposed	C-R $\log \left[\frac{-\log(1-w)}{T^2} \right]$	F-C $\log \left[\frac{dw/dt}{w_r} \right]$	H-M $\log \left[\log \left(\frac{w_{\infty}}{w_r} \right) \right]$
563	1.7762	-57	100	--	--	--	--	--
568	1.7606	-52	99.82	0.18	0.0075	-7.9958	-2.1232	-2.4871
573	1.7452	-47	99.54	0.46	0.0187	-7.6030	-1.9423	-2.0867
578	1.7301	-42	99.36	0.64	0.0262	-7.4628	-2.1152	-1.9390
583	1.7153	-37	98.91	1.09	0.0448	-7.2320	-1.7056	-1.7007
588	1.7007	-32	98.54	1.46	0.0598	-7.1111	-1.7987	-1.5723
593	1.6863	-27	97.81	2.19	0.0897	-6.9354	-1.4837	-1.3893
598	1.6722	-22	96.90	3.10	0.1270	-6.7825	-1.3685	-1.2291
603	1.6584	-17	95.80	4.20	0.1719	-6.6473	-1.2665	-1.0867
608	1.6447	-12	93.80	6.20	0.2541	-6.4630	-0.9578	-0.8952
613	1.6313	-7	92.34	7.66	0.3139	-6.3612	-1.0598	-0.7863
618	1.6184	-2	88.50	11.5 0	0.4708	-6.1405	-0.5279	-0.5585
623	1.6051	+3	78.10	21.9 0	0.8967	-5.5951	+0.5838	-0.0061
			Intercept			15.04	20.11	0.4509
			Slope			13.03	12.82	0.0364
			Correlation coefficient			0.9852	0.9703	0.9907

Table 15
 Thermal decomposition of barium bromate containing zinc bromate (10^{-1} M)
 Analysis of data by Coats-Redfern (C-R), Freeman-Carroll (F-C) and Horowitz-Metzger (H-M) methods
 Instrument: Ulvac Sinku-Riko (Japan) TA 1500, heating rate: $5^{\circ} \text{ min}^{-1}$
 Peak temperature T_s : 618.5K, theoretical maximum mass loss w_{∞} : 24.4 mg, $w_r = w_{\infty} - w$

Temp K	$(1/T) 10^3$	$\theta = T - T_s$	Mass of sample mg	Mass loss w mg	Fraction decomposed	C-R $\log \left[\frac{-\log(1-\alpha)}{T^2} \right]$	F-C $\log \left[\frac{dw/dt}{w_r} \right]$	H-M $\log \left[\log \left(\frac{w_{\infty}}{w_r} \right) \right]$
568	1.7606	-50.5	100	--	--	--	--	--
573	1.7452	-45.5	99.80	0.20	0.0080	-8.9727	-2.0909	-2.4548
578	1.7301	-40.5	99.61	0.39	0.0161	-7.6760	-2.0876	-2.1522
583	1.7153	-35.5	99.41	0.59	0.0241	-7.5055	-2.0838	-1.9742
588	1.7007	-30.5	98.72	1.28	0.0523	-7.1709	-1.5271	-1.6322
593	1.6863	-25.5	98.23	1.77	0.0724	-7.0324	-1.6638	-1.4535
598	1.6722	-20.5	97.15	2.85	0.1167	-6.8221	-1.3002	-1.2687
603	1.6584	-15.5	95.87	4.13	0.1744	-6.6404	-1.2002	-1.0949
608	1.6447	-10.5	93.91	6.09	0.2494	-6.4651	-0.9926	-0.9045
613	1.6313	-5.5	91.36	8.64	0.3540	-6.2967	-0.7908	-0.7218
618	1.6184	-0.5	84.48	15.5 2	0.6356	-5.9401	-0.1120	-0.3581
623	1.6051	+4.5	76.23	23.7 7	0.9735	-5.3912	1.1050	+0.1976
			Intercept			14.71	18.72	0.5238
			Slope			12.88	11.88	0.0364
			Correlation coefficient			0.9889	0.9847	0.9999

Table 16
 Thermal decomposition of barium bromate containing cadmium bromate (10^{-3} M)
 Analysis of data by Coats-Redfern (C-R), Freeman-Carroll (F-C) and Horowitz-Metzger (H-M) methods
 Instrument: Ulvac Sinku-Riko (Japan) TA 1500, heating rate: $5^{\circ} \text{ min}^{-1}$
 Peak temperature T_s : 616K, theoretical maximum mass loss w_{∞} : 24.4 mg, $w_r = w_{\infty} - w$

Temp K	$(1/T) 10^3$	$\theta = T - T_s$	Mass of sample mg	Mass loss w mg	Fraction decomposed	C-R $\log \left[\frac{-\log(1-w)}{T^2} \right]$	F-C $\log \left[\frac{dw/dt}{w_r} \right]$	H-M $\log \left[\log \left(\frac{w_{\infty}}{w_r} \right) \right]$
568	1.7606	-48	100	--	--	--	--	--
573	1.7452	-43	99.67	0.33	0.0134	-7.7482	-1.8667	-2.2318
578	1.7301	-38	99.24	0.76	0.0313	-7.3842	-1.7347	-1.8604
583	1.7153	-33	98.85	1.15	0.0469	-7.2121	-1.7850	-1.6807
588	1.7007	-28	98.15	1.85	0.0759	-7.0036	-1.5030	-1.4646
593	1.6863	-23	97.38	2.62	0.1072	-6.8539	-1.4559	-1.3079
598	1.6722	-18	96.18	3.82	0.1563	-6.6853	-1.2352	-1.1319
603	1.6584	-13	94.44	5.56	0.2278	-6.5105	-1.0337	-1.9498
608	1.6447	-8	92.26	7.74	0.3171	-6.3487	-0.8835	-0.7809
613	1.6313	-3	89.20	10.8 0	0.4421	-6.1710	-0.6495	-0.5961
618	1.6184	+2	79.61	20.3 9	0.8351	-5.6884	-0.3770	-0.1064
			Intercept			17.04	20.39	0.4860
			Slope			14.16	12.98	0.0359
			Correlation coefficient			0.9883	0.9933	0.9996

Table 17
 Thermal decomposition of barium bromate containing cadmium bromate (10^{-2} M)
 Analysis of data by Coats-Redfern (C-R), Freeman-Carroll (F-C) and Horowitz-Metzger (H-M) methods
 Instrument: Ulvac Sinku-Riko (Japan) TA 1500, heating rate: $5^{\circ} \text{ min}^{-1}$
 Peak temperature T_s : 618K, theoretical maximum mass loss w_{∞} : 24.4 mg, $w_r = w_{\infty} - w$

Temp K	$(1/T) 10^3$	$\theta = T - T_s$	Mass of sample mg	Mass loss w mg	Fraction decomposed	C-R $\log \left[\frac{-\log(1-\alpha)}{T^2} \right]$	F-C $\log \left[\frac{dw/dt}{w_r} \right]$	H-M $\log \left[\log \left(\frac{w_{\infty}}{w_r} \right) \right]$
563	1.7762	-55	100	--	--	--	--	--
568	1.7606	-50	99.89	0.11	0.0045	-8.2203	-2.3484	-2.7116
573	1.7452	-45	99.78	0.22	0.0089	-7.9263	-2.3472	-2.4100
578	1.7301	-40	99.35	0.65	0.0268	-7.4526	-1.7367	-1.9288
583	1.7153	-35	98.91	1.09	0.0446	-7.2342	-1.7286	-1.7029
588	1.7007	-30	98.48	1.52	0.0624	-7.0915	-1.7207	-1.6417
593	1.6863	-25	97.71	2.29	0.0937	-6.9155	-1.4627	-1.3694
598	1.6722	-20	96.51	3.49	0.1427	-6.7280	-1.2423	-1.1746
603	1.6584	-15	95.21	4.79	0.1963	-6.5834	-1.1765	-0.9875
608	1.6447	-10	92.92	7.08	0.2900	-6.3946	-0.8797	-0.8277
613	1.6313	-5	90.63	9.37	0.3836	-6.2524	-0.8185	-0.6775
618	1.6184	0	82.92	17.08	0.0995	-5.8642	+0.0216	-0.2822
			Intercept			15.88	19.89	0.4730
			Slope			13.53	12.67	0.0357
			Correlation coefficient			0.9871	0.9902	0.9990

Table 18
 Thermal decomposition of barium bromate containing cadmium bromate (10^{-1} M)
 Analysis of data by Coats-Redfern (C-R), Freeman-Carroll (F-C) and Horowitz-Metzger (H-M) methods
 Instrument: Ulvac Sinku-Riko (Japan) TA 1500, heating rate: $5^{\circ} \text{ min}^{-1}$
 Peak temperature T_s : 620.5K, theoretical maximum mass loss w_{∞} : 24.4 mg, $w_r = w_{\infty} - w$

Temp K	$(1/T) 10^3$	$\theta = T - T_s$	Mass of sample mg	Mass loss w mg	Fraction decomposed	C-R $\log \left[\frac{-\log(1-\alpha)}{T^2} \right]$	F-C $\log \left[\frac{dw/dt}{w_r} \right]$	H-M $\log \left[\log \left(\frac{w_{\infty}}{w_r} \right) \right]$
558	1.7921	-62.5	100	--	--	--	--	--
563	1.7762	-57.5	99.82	0.18	0.0075	-7.9881	-2.1232	-2.4871
568	1.7606	-52.5	99.45	0.55	0.0224	-7.5154	-1.8158	-2.0067
573	1.7452	-47.5	99.27	0.73	0.0299	-7.3964	-2.1131	-1.8801
578	1.7301	-42.5	98.91	1.09	0.0448	-7.2245	-1.8057	-1.7006
583	1.7153	-37.5	98.36	1.64	0.0673	-7.0508	-1.6191	-1.5193
588	1.7007	-32.5	97.63	2.37	0.0971	-6.8916	-1.4801	-1.3528
593	1.6863	-27.5	96.90	3.10	0.1270	-6.7752	-1.4655	-1.2291
598	1.6722	-22.5	95.44	4.56	0.1868	-6.6001	-1.1336	-1.0467
603	1.6584	-17.5	93.89	6.11	0.2503	-6.4633	-1.0720	-0.9026
608	1.6447	-12.5	92.15	7.85	0.3213	-6.3416	-0.9805	-0.7738
613	1.6313	-7.5	90.15	9.85	0.4035	-6.2239	-0.8607	-0.6490
618	1.6184	-2.5	86.86	13.1 4	0.5380	-6.0564	-0.5359	-0.4745
623	1.6051	+2.5	79.20	20.8 0	0.8519	-5.6702	+0.3261	-0.0812
			Intercept			12.75	17.10	0.3852
			Slope			11.57	10.95	0.0307
			Correlation coefficient			0.9899	0.9885	0.9990

Table 19
 Thermal decomposition of barium bromate containing potassium bromate (10^{-3} M)
 Analysis of data by Coats-Redfern (C-R), Freeman-Carroll (F-C) and Horowitz-Metzger (H-M) methods
 Instrument: Ulvac Sinku-Riko (Japan) TA 1500, heating rate: $5^{\circ} \text{ min}^{-1}$
 Peak temperature T_s : 618K, theoretical maximum mass loss w_{∞} : 24.4 mg, $w_r = w_{\infty} - w$

Temp K	$(1/T) 10^3$	$\theta = T - T_s$	Mass of sample mg	Mass loss w mg	Fraction decomposed	C-R $\log \left[\frac{-\log(1-\alpha)}{T^2} \right]$	F-C $\log \left[\frac{dw/dt}{w_r} \right]$	H-M $\log \left[\log \left(\frac{w_{\infty}}{w_r} \right) \right]$
568	1.7606	-50	100	--	---	---	---	---
573	1.7452	-45	99.89	0.11	0.0044	-8.2295	-2.3500	-2.7132
578	1.7301	-40	99.67	0.33	0.0134	-7.7575	-2.0444	-2.2337
583	1.7153	-35	99.24	0.76	0.0312	-7.3932	-1.7358	-1.8618
588	1.7007	-30	98.70	1.30	0.0534	-7.1615	-1.6287	-1.6227
593	1.6863	-25	98.04	1.96	0.0801	-6.9866	-1.5371	-1.4405
598	1.6722	-20	96.96	3.04	0.1246	-6.7914	-1.2937	-1.2380
603	1.6584	-15	95.43	4.57	0.1870	-6.6070	-1.1155	-1.0463
608	1.6447	-10	93.70	6.30	0.2582	-6.4549	-1.0177	-0.8871
613	1.6313	-5	91.07	8.93	0.3658	-6.2787	-0.7701	-0.7038
618	1.6184	0	84.35	5.65	0.6410	-5.9338	-0.1156	-0.3518
623	1.6051	+5	77.61	22.3 9	0.9169	-5.5553	+0.5214	+0.0336
628	1.5924	+10	75.65	24.3 5	0.9970	-5.4116	+1.4329	+0.4030
			Intercept			16.76	20.20	0.4944
			Slope			14.08	12.86	0.0381
			Correlation coefficient			0.9913	0.9913	0.9987

Table 20
 Thermal decomposition of barium bromate containing potassium bromate (10^{-2} M)
 Analysis of data by Coats-Redfern (C-R), Freeman-Carroll (F-C) and Horowitz-Metzger (H-M) methods
 Instrument: Ulvac Sinku-Riko (Japan) TA 1500, heating rate: $5^{\circ} \text{ min}^{-1}$
 Peak temperature T_s : 620.5K, theoretical maximum mass loss w_{∞} : 24.4 mg, $w_r = w_{\infty} - w$

Temp K	$(1/T) 10^3$	$\theta = T - T_s$	Mass of sample mg	Mass loss w mg	Fraction decomposed	C-R $\log \left[\frac{-\log(1-w)}{T^2} \right]$	F-C $\log \left[\frac{dw/dt}{w_r} \right]$	H-M $\log \left[\log \left(\frac{w_{\infty}}{w_r} \right) \right]$
563	1.7762	-57.5	100	--	---	---	---	---
568	1.7606	-52.5	99.89	0.11	0.0045	-8.2211	-2.3492	-2.7124
573	1.7452	-47.5	99.83	0.17	0.0071	-8.0234	-2.5084	-2.5071
578	1.7301	-42.5	99.67	0.33	0.0134	-7.7566	-2.1986	-2.2328
583	1.7153	-37.5	99.34	0.66	0.0268	-7.4601	-1.7343	-1.9288
588	1.7007	-32.5	98.80	1.20	0.0491	-7.1993	-1.6298	-1.6606
593	1.6863	-27.5	98.15	1.85	0.0758	-7.0115	-1.5382	-1.4654
598	1.6722	-22.5	97.17	2.83	0.1160	-6.8247	-1.3428	-1.2713
603	1.6584	-17.5	95.97	4.03	0.1650	-6.6667	-1.2308	-1.1057
608	1.6447	-12.5	94.34	5.66	0.2320	-6.5086	-1.0599	-0.9408
613	1.6313	-7.5	92.37	7.63	0.3123	-6.3639	-0.9327	-0.7890
618	1.6184	-2.5	88.89	11.1 1	0.4550	-6.1610	-0.5818	-0.5790
623	1.6051	+2.5	80.39	19.6 1	0.8029	-5.7405	+0.2469	-0.1516
628	1.5924	+7.5	76.47	23.5 3	0.9635	-5.4381	+0.6438	+0.1578
			Intercept			14.62	18.60	0.5000
			Slope			12.84	11.92	0.0352
			Correlation coefficient			0.9978	0.9865	0.9991

Table 21
 Thermal decomposition of barium bromate containing potassium bromate (10^{-1} M)
 Analysis of data by Coats-Redfern (C-R), Freeman-Carroll (F-C) and Horowitz-Metzger (H-M) methods
 Instrument: Ulvac Sinku-Riko (Japan) TA 1500, heating rate: $5^{\circ} \text{ min}^{-1}$
 Peak temperature T_s : 615.5K, theoretical maximum mass loss w_{∞} : 24.4 mg, $w_r = w_{\infty} - w$

Temp K	$(1/T) 10^3$	$\theta = T - T_s$	Mass of sample mg	Mass loss w mg	Fraction decomposed	C-R $\log \left[\frac{-\log(1-\alpha)}{T^2} \right]$	F-C $\log \left[\frac{dw/dt}{w_r} \right]$	H-M $\log \left[\log \left(\frac{w_{\infty}}{w_r} \right) \right]$
553	1.8083	-62.5	100	--	---	---	---	---
558	1.7921	-57.5	99.89	0.11	0.0044	-8.2064	-2.3500	-2.7132
563	1.7762	-52.5	99.78	0.22	0.0089	-7.9118	-1.3390	-2.4108
568	1.7606	-47.5	99.57	0.43	0.0178	-7.6166	-2.0429	-2.1079
573	1.7452	-42.5	99.46	0.54	0.0223	-7.5263	-1.4226	-2.0010
578	1.7301	-37.5	99.13	0.87	0.0356	-7.3267	-1.8587	-1.8028
583	1.7153	-32.5	98.70	1.30	0.0534	-7.1541	-1.5791	-1.6227
588	1.7007	-27.5	98.26	1.74	0.0712	-7.0325	-1.7174	-1.4937
593	1.6863	-22.5	97.61	2.39	0.0979	-6.8953	-1.5287	-1.3492
598	1.6722	-17.5	96.63	3.37	0.1380	-6.7439	-1.3327	-1.1905
603	1.6584	-12.5	95.38	4.62	0.1892	-6.6012	-1.2000	-1.0406
608	1.6447	-7.5	93.70	6.30	0.2582	-6.4549	-1.0316	-0.8871
613	1.6313	-2.5	91.30	8.70	0.3561	-6.2935	-0.8179	-0.7186
618	1.6184	+2.5	85.00	15.0 0	0.6143	-5.9653	-0.1744	-0.3833
623	1.6051	+7.5	81.30	18.7 0	0.7656	-5.7896	-0.1920	-0.2020
628	1.5924	+12.5	79.35	20.6 5	0.8452	-5.6866	-0.2846	-0.0906
			Intercept			13.24	18.33	0.5541
			Slope			11.91	11.66	0.0342
			Correlation			0.9953	0.9711	0.9934

			coefficient					
--	--	--	-------------	--	--	--	--	--

Table 22
 Thermal decomposition of barium bromate containing strontium bromide (10^{-3} M)
 Analysis of data by Coats-Redfern (C-R), Freeman-Carroll (F-C) and Horowitz-Metzger (H-M) methods
 Instrument: Ulvac Sinku-Riko (Japan) TA 1500, heating rate: $5^{\circ} \text{ min}^{-1}$
 Peak temperature T_s : 617K, theoretical maximum mass loss w_{∞} : 24.4 mg, $w_r = w_{\infty} - w$

Temp K	$(1/T) 10^3$	$\theta = T - T_s$	Mass of sample mg	Mass loss w mg	Fraction Decomposed α	C-R $\log \left[\frac{-\log(1-\alpha)}{T^2} \right]$	F-C $\log \left[\frac{dw/dt}{w_r} \right]$	H-M $\log \left[\log \left(\frac{w_{\infty}}{w_r} \right) \right]$
563	1.7762	-54	100	--	---	---	---	---
568	1.7606	-49	100	--	--	--	--	--
573	1.7452	-44	99.82	0.18	0.0075	-8.0026	-2.1225	-2.4864
578	1.7301	-39	99.73	0.27	0.0112	-7.8332	-2.4219	-2.3094
583	1.7153	-34	98.81	1.19	0.0487	-7.1956	-1.4051	-1.6642
588	1.7007	-29	97.99	2.01	0.0824	-6.9668	-1.4352	-1.4280
593	1.6863	-24	97.07	2.93	0.1198	-6.8025	-1.3713	-1.2564
598	1.6722	-19	95.80	4.20	0.1722	-6.6392	-1.1986	-1.0858
603	1.6584	-14	93.60	6.40	0.2620	-6.4402	-0.9146	-0.8796
608	1.6447	-9	91.68	8.32	0.3406	-6.3104	-0.9236	-0.7426
613	1.6313	-4	88.48	11.5 2	0.4716	-6.1324	-0.6058	-0.5595
618	1.6184	+1	79.71	20.2 9	0.8310	-5.6943	+0.3276	-0.1123
			Intercept			16.84	20.94	0.4000
			Slope			14.02	13.20	0.0362
			Correlation coefficient			0.9857	0.9946	0.9984

Table 23
 Thermal decomposition of barium bromate containing strontium bromide (10^{-2} M)
 Analysis of data by Coats-Redfern (C-R), Freeman-Carroll (F-C) and Horowitz-Metzger (H-M) methods
 Instrument: Ulvac Sinku-Riko (Japan) TA 1500, heating rate: $5^{\circ} \text{ min}^{-1}$
 Peak temperature T_s : 618K, theoretical maximum mass loss w_{∞} : 24.4 mg, $w_r = w_{\infty} - w$

Temp K	$(1/T) 10^3$	$\theta = T - T_s$	Mass of sample mg	Mass loss w mg	Fraction decomposed	C-R $\log \left[\frac{-\log(1-\alpha)}{T^2} \right]$	F-C $\log \left[\frac{dw/dt}{w_r} \right]$	H-M $\log \left[\log \left(\frac{w_{\infty}}{w_r} \right) \right]$
563	1.7762	-55	100	--	---	---	---	---
568	1.7606	-50	99.42	0.58	0.0238	-7.4890	-1.6128	-1.9803
573	1.7452	-45	99.22	0.78	0.0317	-7.3699	-2.0866	-1.8536
578	1.7301	-40	98.84	1.16	0.0476	-7.1978	-1.7782	-1.6739
583	1.7153	-35	98.45	1.55	0.0635	-7.0767	-1.7708	-1.5454
588	1.7007	-30	97.87	2.13	0.0873	-6.9403	-1.5836	-1.4015
593	1.6863	-25	97.09	2.91	0.1190	-6.8054	-1.4440	-1.2593
598	1.6722	-20	95.74	4.26	0.1746	-6.6326	-1.1720	-1.0792
603	1.6584	-15	93.80	6.20	0.2540	-6.4560	-0.9732	-0.8954
608	1.6447	-10	92.25	7.75	0.3174	-6.3481	-1.0314	-0.7803
613	1.6313	-5	89.15	10.8 5	0.4444	-6.1680	-0.6410	-0.5930
618	1.6184	0	80.62	19.3 8	0.7936	-5.7461	+0.2284	-0.1641
			Intercept			13.42	20.41	0.3648
			Slope			11.96	12.92	0.0335
			Correlation coefficient			0.9816	0.9960	0.9900

Table 24
 Thermal decomposition of barium bromate containing strontium bromide (10^{-1} M)
 Analysis of data by Coats-Redfern (C-R), Freeman-Carroll (F-C) and Horowitz-Metzger (H-M) methods
 Instrument: Ulvac Sinku-Riko (Japan) TA 1500, heating rate: $5^{\circ} \text{ min}^{-1}$
 Peak temperature T_s : 619.5K, theoretical maximum mass loss w_{∞} : 24.4 mg, $w_r = w_{\infty} - w$

Temp K	$(1/T) 10^3$	$\theta = T - T_s$	Mass of sample mg	Mass loss w mg	Fraction decomposed	C-R $\log \left[\frac{-\log(1-\alpha)}{T^2} \right]$	F-C $\log \left[\frac{dw/dt}{w_r} \right]$	H-M $\log \left[\log \left(\frac{w_{\infty}}{w_r} \right) \right]$
558	1.7921	-61.5	100	--	---	---	---	---
563	1.7762	-56.5	99.89	0.11	0.0045	-8.2059	-2.3416	-2.7084
568	1.7606	-51.5	99.67	0.33	0.0134	-7.7347	-2.0370	-2.2260
573	1.7452	-46.5	99.34	0.66	0.0272	-7.4383	-1.8549	-1.9920
578	1.7301	-41.5	99.00	1.00	0.0408	-7.2667	-1.8485	-1.7428
583	1.7153	-36.5	98.45	1.55	0.0634	-7.0772	-1.6165	-1.5458
558	1.7007	-31.5	97.90	2.10	0.0861	-6.9467	-1.6059	-1.4080
593	1.6863	-26.5	97.35	2.65	0.1087	-6.8473	-1.5940	-1.3012
598	1.6722	-21.5	96.24	3.76	0.1540	-6.6922	-1.2713	-1.1388
603	1.6584	-16.5	94.69	5.31	0.2211	-6.5252	-1.0643	-0.9727
608	1.6447	-11.5	93.25	6.75	0.2763	-6.4203	-1.0895	-0.8525
613	1.6313	-6.5	90.49	9.51	0.3896	-6.2438	-0.7316	-0.6688
618	1.6154	-1.5	84.62	15.3 7	0.6297	-5.9471	-0.1882	-0.3651
623	1.6051	+3.5	75.66	24.3 4	0.9966	-5.1972	+2.0296	+0.3918
			Intercept			12.04	18.28	0.4219
			Slope			11.18	11.59	0.0321
			Correlation coefficient			0.9937	0.9779	0.9950

Table 25

Thermal Decomposition of barium bromate containing nickel bromate(10^{-3} M)
 Analysis of Data by Coats-Refern(C-R), Freeman-Carroll(F-C) and Horowitz-Metzger(H-M) Methods
 Instrument : TAQ 20 Thermogravimetric Analyser Heating Rate : $5^{\circ} \text{ min}^{-1}$
 Peak temperature :603.9K, maximum mass loss w_{∞} :24.1155mg, $w_r = w_{\infty} - w$

Temp K	$(1/T) 10^3$	$\theta = T - T_s$	Mass of Sample mg	Mass loss W mg	Fraction decompsed α	C-R $\log \left[\frac{-\log(1-\alpha)}{T^2} \right]$	F-C $\log \left[\frac{dw/dt}{w_r} \right]$	H-M $\log [\log(w_{\infty}/w_r)]$
568.56	1.7588	-35.37	100.00	--	--	--	--	--
572.56	1.7466	-31.37	99.17	0.83	0.0344	-7.3335	-1.4748	-1.8178
576.56	1.7344	-27.37	98.55	1.45	0.0603	-7.0901	-1.3430	-1.5684
580.56	1.7225	-23.37	97.72	2.28	0.0944	-6.8934	-1.1761	-1.3657
584.56	1.7107	-19.37	96.56	3.44	0.1428	-6.7083	-1.0138	-1.1746
588.52	1.6992	-15.41	94.97	5.03	0.2085	-6.5327	-0.8189	-0.9932
592.52	1.6877	-11.41	92.65	7.35	0.3046	-6.3474	-0.6151	-0.8020
596.52	1.6764	-7.41	89.40	10.60	0.4396	-6.1507	-0.4576	-0.5995
600.52	1.6652	-3.41	85.63	14.37	0.5959	-5.9621	-0.2810	-0.4050
604.52	1.6542	0.59	81.55	18.45	0.7652	-5.7640	-0.0114	-0.2012
608.55	1.6432	4.62	77.10	22.90	0.9496	-5.4555	0.1347	0.1131
612.22	1.6334	8.29	75.88	24.12	1.0000	--	--	--
Intercept						20.7161	25.5625	-0.2475
Slope						-16.0318	-15.5216	0.0481

Correlation
Coefficient

0.9998

0.9989

0.9999

Table 26

Thermal Decomposition of barium bromate containing nickel bromate(10⁻² M)

Analysis of Data by Coats-Refern(C-R), Freeman-Carroll(F-C) and Horowitz-Metzger(H-M) Methods

Instrument : TAQ 20 Thermogravimetric Analyser Heating Rate : 5° min⁻¹

Peak temperature : 604.7K, maximum mass loss w_∞ : 24.82mg, w_t = w_∞ - w

Temp K	(1/T) 10 ³	θ = T - Ts	Mass of Sample mg	Mass loss W mg	Fraction decompsed α	C-R $\log \left[\frac{-\log(1-\alpha)}{T^2} \right]$	F-C $\log \left[\frac{dw/dt}{w} \right]$	H-M $\log [\log(w_\infty/w_t)]$
495.50	2.0182	-109.18	100.00	--	--	--		--
500.50	1.9980	-104.18	99.90	0.10	0.0040	-8.1570		-2.7582
505.49	1.9783	-99.19	99.83	0.17	0.0068	-7.9376		-2.5301
510.50	1.9589	-94.18	99.78	0.22	0.0088	-7.8323		-2.4163
515.50	1.9399	-89.18	99.73	0.27	0.0110	-7.7417		-2.3173
520.50	1.9212	-84.18	99.66	0.34	0.0136	-7.6598		-2.2269
525.50	1.9030	-79.18	99.58	0.42	0.0171	-7.5663		-2.1252
530.50	1.8850	-74.18	99.46	0.54	0.0216	-7.4724		-2.0231
535.50	1.8674	-69.18	99.31	0.69	0.0277	-7.3711		-1.9136
540.50	1.8501	-64.18	99.11	0.89	0.0357	-7.2678		-1.8022
545.50	1.8332	-59.18	98.85	1.15	0.0462	-7.1611		-1.6875
550.50	1.8165	-54.18	98.53	1.47	0.0591	-7.0592		-1.5777
555.50	1.8002	-49.18	98.21	1.79	0.0722	-6.9767		-1.4873
560.50	1.7841	-44.18	97.84	2.16	0.0871	-6.8996		-1.4025
565.50	1.7683	-39.18	97.38	2.62	0.1056	-6.8195		-1.3147
570.50	1.7528	-34.18	96.74	3.26	0.1315	-6.7256		-1.2131
575.50	1.7376	-29.18	95.83	4.17	0.1680	-6.6177		-1.0976
580.50	1.7226	-24.18	94.63	5.37	0.2165	-6.5025		-0.9749

585.50	1.7079	-19.18	92.86	7.14	0.2878	-6.3665	-0.8527	-0.8315
590.50	1.6935	-14.18	90.37	9.63	0.3878	-6.2138	-0.6446	-0.6713
595.50	1.6792	-9.18	86.93	13.07	0.5266	-6.0382	-0.4700	-0.4884
600.51	1.6653	-4.17	82.95	17.05	0.6870	-5.8542	-0.2480	-0.2971
605.51	1.6515	0.83	78.56	21.44	0.8638	-5.6268	-0.0107	-0.0625
610.49	1.6380	5.81	75.27	24.73	0.9964	-5.1834	0.6978	0.3880
611.50	1.6353	6.82	75.18	24.82	1.0000	--	--	--
Intercept						16.6377	28.5889	-0.0388
Slope						-13.4490	-17.2288	0.0399
Correlation Coefficient						0.9736	0.9649	0.9786

Table 27

Thermal Decomposition of barium bromate containing nickel bromate(10^{-1} M)
 Analysis of Data by Coats-Refern(C-R), Freeman-Carroll(F-C) and Horowitz-Metzger(H-M) Methods
 Instrument : TAQ 20 Thermogravimetric Analyser Heating Rate : $5^{\circ} \text{ min}^{-1}$
 Peak temperature :603.9K, maximum mass loss w_{∞} : 23.77mg, $w_r = w_{\infty} - w$

Temp K	$(1/T) 10^3$	$\theta = T - T_s$	Mass of Sample mg	Mass loss W mg	Fraction decomposed α	C-R $\log \left[\frac{-\log(1-\alpha)}{T^2} \right]$	F-C $\log \left[\frac{dw/dt}{w} \right]$	H-M $\log [\log(w_{\infty}/w_r)]$
503.77	1.9850	-100.16	100.00	--	--	--	--	--
508.78	1.9655	-95.15	99.58	0.42	0.0177	-7.5233	-2.4314	-2.1103
513.78	1.9463	-90.15	99.49	0.51	0.0213	-7.4498	-2.4873	-2.0283
518.78	1.9276	-85.15	99.42	0.58	0.0245	-7.3971	-2.4570	-1.9671
523.78	1.9092	-80.15	99.34	0.66	0.0279	-7.3482	-2.3954	-1.9099
528.78	1.8911	-75.15	99.24	0.76	0.0318	-7.2987	-2.2843	-1.8521
533.78	1.8734	-70.15	99.12	0.88	0.0369	-7.2420	-2.1501	-1.7873
538.78	1.8560	-65.15	98.96	1.04	0.0437	-7.1750	-2.0084	-1.7121
543.78	1.8390	-60.15	98.74	1.26	0.0531	-7.0964	-1.8718	-1.6255
548.78	1.8222	-55.15	98.44	1.56	0.0658	-7.0081	-1.7890	-1.5293
553.78	1.8058	-50.15	98.07	1.93	0.0810	-6.9223	-1.7334	-1.4356
558.78	1.7896	-45.15	97.67	2.33	0.0980	-6.8435	-1.6963	-1.3490
563.78	1.7737	-40.15	97.24	2.76	0.1161	-6.7730	-1.5692	-1.2708
568.79	1.7581	-35.14	96.67	3.33	0.1400	-6.6938	-1.4196	-1.1839
573.79	1.7428	-30.14	95.89	4.11	0.1727	-6.6019	-1.2614	-1.0844

578.78	1.7278	-25.15	94.82	5.18	0.2180	-6.4965	-1.0619	-0.9715	
583.79	1.7130	-20.14	93.20	6.80	0.2858	-6.3675	-0.8809	-0.8350	
588.79	1.6984	-15.14	90.97	9.03	0.3798	-6.2230	-0.6966	-0.6831	
593.79	1.6841	-10.14	88.01	11.99	0.5045	-6.0630	-0.5384	-0.5158	
598.79	1.6700	-5.14	84.59	15.41	0.6480	-5.8980	-0.3806	-0.3435	
603.79	1.6562	-0.14	81.11	18.89	0.7946	-5.7246	-0.1201	-0.1628	
608.78	1.6426	4.85	77.41	22.59	0.9502	-5.4541	0.1603	0.1149	
612.24	1.6333	8.31	76.23	23.77	1.0000	--	--	--	
						Intercept	15.2316	22.3387	-0.1363
						Slope	-12.6307	-13.5568	0.0335
						Correlation Coefficient	0.9925	0.9944	0.9928

Table 28

Thermal Decomposition of barium bromate containing neodymium bromate(10^{-3} M)
 Analysis of Data by Coats-Referrn(C-R), Freeman-Carroll(F-C) and Horowitz-Metzger(H-M) Methods

Instrument : Perkin Elmer Thermal Analyser Heating Rate : $5^{\circ} \text{ min}^{-1}$

Peak temperature :608.6K, maximum mass loss w_{∞} : 21.10mg, $w_r = w_{\infty} - w$

Temp K	$(1/T) 10^3$	$\theta = T - T_s$	Mass of Sample mg	Mass loss W mg	Fraction decompsed α	C-R $\log \left[\frac{-\log(1-\alpha)}{T^2} \right]$	F-C $\log \left[\frac{dw/dt}{\bar{w}_r} \right]$	H-M $\log [\log(w_{\infty}/w_r)]$
528.05	1.8938	-80.54	100.00	--	--	--		--
535.04	1.8690	-73.55	99.95	0.05	0.0024	-8.4305	-2.4689	-2.9738
542.08	1.8447	-66.51	99.85	0.15	0.0072	-7.9704	-2.4085	-2.5022
549.02	1.8214	-59.57	99.73	0.27	0.0126	-7.7384	-2.1224	-2.2593
556.02	1.7985	-52.57	99.51	0.49	0.0230	-7.4852	-2.0285	-1.9950
563.08	1.7759	-45.51	99.24	0.76	0.0360	-7.2997	-1.8913	-1.7986
570.01	1.7544	-38.58	98.88	1.12	0.0531	-7.1371	-1.6301	-1.6253
577.02	1.7331	-31.57	98.22	1.78	0.0842	-6.9403	-1.3039	-1.4179
584.04	1.7122	-24.55	96.88	3.12	0.1481	-6.6903	-0.9694	-1.1574
591.06	1.6919	-17.53	94.17	5.83	0.2765	-6.3955	-0.6848	-0.8522
598.06	1.6721	-10.53	89.75	10.25	0.4858	-6.0927	-0.4472	-0.5392
605.06	1.6527	-3.53	84.33	15.67	0.7428	-5.7930	-0.0792	-0.2294
611.06	1.6365	2.47	78.90	21.10	1.0000	--	--	--
Intercept						12.6054	18.2474	-0.1833
Slope						-11.2094	-11.2157	0.0362
Correlation Coefficient						0.9940	0.9828	0.9953

Table 29
 Thermal Decomposition of barium bromate containing neodymium bromate(10^{-2} M)
 Analysis of Data by Coats-Refern(C-R), Freeman-Carroll(F-C) and Horowitz-Metzger(H-M) Methods
 Instrument : Perkin Elmer Thermal Analyser Heating Rate : $5^{\circ} \text{ min}^{-1}$
 Peak temperature :606.2K, maximum mass loss w_{∞} : 24.47mg, $w_r = w_{\infty} - w$

Temp K	$(1/T) 10^3$	$\theta = T - T_s$	Mass of Sample mg	Mass loss W mg	Fraction decompsd α	C-R $\log \left[\frac{-\log(1-\alpha)}{T^2} \right]$	F-C $\log \left[\frac{dw/dt}{w} \right]$	H-M $\log [\log(w_{\infty}/w_r)]$
512.82	1.9500	-93.37	100.00	--	--	--	--	--
517.83	1.9312	-88.36	98.29	1.71	0.0700	-6.9301	-2.136474	-1.5017
522.83	1.9127	-83.36	98.12	1.88	0.0768	-6.8966	-2.276007	-1.4599
527.83	1.8945	-78.36	98.00	2.00	0.0817	-6.8769	-2.202989	-1.4319
532.83	1.8768	-73.36	97.86	2.14	0.0874	-6.8542	-2.105150	-1.4010
537.83	1.8593	-68.36	97.69	2.31	0.0946	-6.8264	-2.023024	-1.3651
542.83	1.8422	-63.36	97.48	2.52	0.1032	-6.7946	-1.943375	-1.3253
547.83	1.8254	-58.36	97.23	2.77	0.1134	-6.7591	-1.862802	-1.2819
552.83	1.8089	-53.36	96.93	3.07	0.1255	-6.7199	-1.804037	-1.2347
557.83	1.7927	-48.36	96.59	3.41	0.1393	-6.6792	-1.800613	-1.1862
562.83	1.7767	-43.36	96.26	3.74	0.1529	-6.6431	-1.535232	-1.1423
567.83	1.7611	-38.36	95.65	4.35	0.1776	-6.5795	-1.183167	-1.0710
572.83	1.7457	-33.36	94.34	5.66	0.2315	-6.4577	-1.413618	-0.9417
577.84	1.7306	-28.36	93.61	6.39	0.2612	-6.4048	-1.381963	-0.8812
582.83	1.7158	-23.36	92.86	7.14	0.2918	-6.3554	-1.199448	-0.8243
587.84	1.7012	-18.35	91.76	8.24	0.3366	-6.2875	-0.969828	-0.7490
592.84	1.6868	-13.35	90.02	9.98	0.4078	-6.1889	-0.700133	-0.6430
597.84	1.6727	-8.35	87.13	12.87	0.5258	-6.0425	-0.473962	-0.4894

602.84	1.6588	-3.35	83.24	16.76	0.6851	-5.8598	-0.173296	-0.2994	
607.84	1.6452	1.65	78.07	21.93	0.8965	-5.5742	0.058518	-0.0066	
612.21	1.6334	6.02	75.53	24.47	1.0000	--	--	--	
						Intercept	12.0349	13.7340	-0.1553
						Slope	-10.7652	8.5734	0.0319
						Correlation			
						Coefficient	0.9677	0.9476	0.9733

Table 30

Thermal Decomposition of barium bromate containing neodymium bromate(10^{-1} M)
 Analysis of Data by Coats-Referrn(C-R), Freeman-Carroll(F-C) and Horowitz-Metzger(H-M) Methods

Instrument : Perkin Elmer Thermal Analyser Heating Rate : $5^{\circ} \text{ min}^{-1}$

Peak temperature :608.8K, l maximum mass loss w_{∞} : 18.59mg, $w_r = w_{\infty} - w$

Temp K	$(1/T) 10^3$	$\theta = T - T_s$	Mass of Sample mg	Mass loss W mg	Fraction decompsd α	C-R $\log \left[\frac{-\log(1-\alpha)}{T^2} \right]$	F-C $\log \left[\frac{dw/dt}{w} \right]$	H-M $\log [\log(w_{\infty}/w_r)]$
502.77	1.9890	-106.00	100.00	--	--	--	--	--
512.78	1.9502	-95.99	99.82	0.18	0.0094	-7.8054	-2.5317	-2.3856
522.79	1.9128	-85.98	99.72	0.28	0.0153	-7.6120	-2.2785	-2.1753
532.76	1.8770	-76.01	99.52	0.48	0.0256	-7.4014	-1.9603	-1.9483
542.80	1.8423	-65.97	99.13	0.87	0.0470	-7.1486	-1.7102	-1.6793
552.76	1.8091	-56.01	98.44	1.56	0.0840	-6.9039	-1.6877	-1.4188
562.73	1.7770	-46.04	97.74	2.26	0.1216	-6.7502	-1.5436	-1.2496
572.80	1.7458	-35.97	96.80	3.20	0.1721	-6.6020	-1.3627	-1.0860
582.77	1.7160	-26.00	95.47	4.53	0.2437	-6.4470	-1.0304	-0.9161
592.78	1.6870	-15.99	92.84	7.16	0.3850	-6.2213	-0.6602	-0.6755
602.76	1.6590	-6.01	87.85	12.15	0.6535	-5.8973	-0.3120	-0.3370
612.72	1.6321	3.95	81.59	18.41	0.9901	-5.2729	0.6147	0.3016
613.94	1.6288	5.17	81.41	18.59	1.0000	--	--	--
Intercept						9.9987	13.3911	-0.1265
Slope						-9.5120	-8.2498	0.0241
Correlation Coefficient						0.9492	0.9481	0.9858

Table 31

Thermal Decomposition of barium bromate containing yttrium bromate(10^{-3} M)
 Analysis of Data by Coats-Referrn(C-R), Freeman-Carroll(F-C) and Horowitz-Metzger(H-M) Methods

Instrument : Perkin Elmer Thermal Analyser Heating Rate : $5^{\circ} \text{ min}^{-1}$

Peak temperature :608.9K,maximum mass loss w_{∞} : 23.14mg, $w_r = w_{\infty} - w$

Temp K	$(1/T) 10^3$	$\theta = T - T_s$	Mass of Sample mg	Mass loss W mg	Fraction decompsd α	C-R	F-C	H-M
						$\log \left[\frac{-\log(1-\alpha)}{T^2} \right]$	$\log \left[\frac{dw/dt}{w} \right]$	$\log [\log(w_{\infty}/w_r)]$
552.73	1.8092	-56.1898	100.00	--	--	--		--
557.74	1.7930	-51.1833	99.87	0.13	0.0055	-8.1161		-2.6232
562.75	1.7770	-46.1729	99.76	0.24	0.0103	-7.8464		-2.3458
567.77	1.7613	-41.1499	99.62	0.38	0.0166	-7.6479		-2.1395
572.75	1.7460	-36.1709	99.41	0.59	0.0255	-7.4652		-1.9493
577.75	1.7308	-31.1665	99.09	0.91	0.0394	-7.2817		-1.7583
582.72	1.7161	-26.1998	98.56	1.44	0.0625	-7.0836		-1.5527
587.77	1.7013	-21.1481	97.52	2.48	0.1072	-6.8461		-1.3077
592.77	1.6870	-16.1458	95.62	4.38	0.1892	-6.5864		-1.0406
597.75	1.6729	-11.1693	92.64	7.36	0.3181	-6.3323		-0.7792
602.79	1.6590	-6.1308	88.87	11.13	0.4813	-6.1054		-0.5451
607.73	1.6455	-1.1851	83.49	16.51	0.7138	-5.8324		-0.2650
612.86	1.6317	3.9390	76.86	23.14	1.0000	--	--	--
Intercept						18.9015	26.0242	-0.2771
Slope						-15.0907	-15.9039	0.0461
Correlation Coefficient						0.9967	0.9932	0.9983

Table 32

Thermal Decomposition of barium bromate containing yttrium bromate(10^{-2} M)
 Analysis of Data by Coats-Refern(C-R), Freeman-Carroll(F-C) and Horowitz-Metzger(H-M) Methods

Instrument : Perkin Elmer Thermal Analyser Heating Rate : $5^{\circ} \text{ min}^{-1}$

Peak temperature :607.7K, maximum mass loss w_{∞} : 21.60mg, $w_r = w_{\infty} - w$

Temp K	(1/T) 10^3	$\theta = T - T_s$	Mass of Sample mg	Mass loss W mg	Fraction decompsd α	C-R $\log \left[\frac{-\log(1-\alpha)}{T^2} \right]$	F-C $\log \left[\frac{dw}{dt} \right]$	H-M $\log [\log(w_{\infty}/w_r)]$
514.95	1.9419	-92.70	100.00	--	--	--		--
523.96	1.9086	-83.69	99.91	0.09	0.0042	-8.1811		-2.7425
532.97	1.8763	-74.68	99.77	0.23	0.0106	-7.7866		-2.3332
542.00	1.8450	-65.65	99.41	0.59	0.0273	-7.3884		-1.9204
550.99	1.8149	-56.66	98.92	1.08	0.0502	-7.1327		-1.6504
559.98	1.7858	-47.67	98.22	1.78	0.0825	-6.9237		-1.4274
568.98	1.7575	-38.67	97.28	2.72	0.1258	-6.7437		-1.2335
577.96	1.7302	-29.69	95.92	4.08	0.1888	-6.5654		-1.0416
586.93	1.7038	-20.72	93.78	6.22	0.2880	-6.3684		-0.8312
595.98	1.6779	-11.67	89.84	10.16	0.4707	-6.1091		-0.5587
604.96	1.6530	-2.69	83.28	16.72	0.7742	-5.7531		-0.1896
610.57	1.6378	2.92	78.40	21.60	1.0000	--		--
Intercept						8.5303	13.4548	-0.1461
Slope						-8.6890	-8.3460	0.0289
Correlation Coefficient						0.9934	0.9776	0.9919

Table 33(i)

Thermal Decomposition of barium bromate containing yttrium bromate(10^{-1} M)
 Analysis of Data by Coats-Refern(C-R), Freeman-Carroll(F-C) and Horowitz-Metzger(H-M) Methods

Instrument : Perkin Elmer Thermal Analyser Heating Rate : $5^{\circ} \text{ min}^{-1}$

Peak temperature : 496.2K, maximum mass loss w_{∞} : 13.91mg, $w_r = w_{\infty} - w$

Temp K	$(1/T) 10^3$	$\theta = T - T_s$	Mass of Sample mg	Mass loss W mg	Fraction decompsd α	C-R	F-C	H-M
						$\log \left[\frac{-\log(1-\alpha)}{T^2} \right]$	$\log \left[\frac{dw}{dt} \right]$	$\log [\log(w_{\infty}/w_r)]$
451.06	2.2170	-45.18	100.00	--	--	--		--
456.00	2.1930	-40.24	99.84	0.16	0.0115	-7.6185	-1.5622	-2.3006
461.07	2.1689	-35.17	99.46	0.54	0.0389	-7.0913	-1.2122	-1.7638
466.06	2.1456	-30.18	98.64	1.36	0.0978	-6.6865	-1.2815	-1.3496
471.01	2.1231	-25.23	97.99	2.01	0.1445	-6.5150	-1.2922	-1.1689
476.06	2.1006	-20.18	97.38	2.62	0.1886	-6.3974	-1.2045	-1.0421
481.06	2.0788	-15.18	96.67	3.33	0.2392	-6.2898	-1.0414	-0.9254
486.01	2.0576	-10.23	95.72	4.28	0.3077	-6.1699	-0.8127	-0.7966
491.02	2.0366	-5.22	94.23	5.77	0.4146	-6.0157	-0.5207	-0.6335
496.02	2.0160	-0.22	91.78	8.22	0.5910	-5.8018	-0.3079	-0.4108
501.00	1.9960	4.76	88.99	11.01	0.7916	-5.5665	-0.1423	-0.1668
506.01	1.9762	9.77	86.89	13.11	0.9419	-5.3163	0.0435	0.0920
510.53	1.9587	14.29	86.09	13.91	1.0000	--	--	--
Intercept						12.5230	14.0536	-0.3292
Slope						-9.0520	-7.1606	0.0409
Correlation Coefficient						0.9776	0.9571	0.9769

Table 33(ii)

Thermal Decomposition of barium bromate containing yttrium bromate(10^{-1} M)

Analysis of Data by Coats-Referrn(C-R), Freeman-Carroll(F-C) and Horowitz-Metzger(H-M) Methods

Instrument : Perkin Elmer Thermal Analyser Heating Rate : 5° min⁻¹

Peak temperature :603.93K, maximum mass loss w_{∞} : 20.16mg, $w_r = w_{\infty} - w$

Temp K	(1/T) 10 ³	$\theta = T - T_s$	Mass of Sample mg	Mass loss W mg	Fraction decomposed α	C-R $\log \left[\frac{-\log(1-\alpha)}{T^2} \right]$	F-C $\log \left[\frac{dw/dt}{w_r} \right]$	H-M $\log [\log(w_{\infty}/w_r)]$
510.53	1.9587	-100.34	100.00	--	--	--	--	--
520.52	1.9212	-90.35	99.36	0.64	0.0315	-7.2897	-1.9937	-1.8568
530.52	1.8849	-80.35	98.97	1.03	0.0512	-7.0912	-1.9730	-1.6418
540.52	1.8501	-70.35	98.56	1.44	0.0714	-6.9584	-1.9208	-1.4928
550.51	1.8165	-60.36	98.11	1.89	0.0936	-6.8512	-1.7527	-1.3696
560.51	1.7841	-50.36	97.47	2.53	0.1256	-6.7314	-1.6549	-1.2343
570.57	1.7526	-40.30	96.68	3.32	0.1646	-6.6199	-1.4871	-1.1073
580.51	1.7226	-30.36	95.59	4.41	0.2187	-6.4975	-1.1914	-0.9698
590.52	1.6934	-20.35	93.56	6.44	0.3194	-6.3195	-0.8296	-0.7771
600.58	1.6651	-10.29	89.47	10.53	0.5221	-6.0511	-0.4712	-0.4940
610.59	1.6377	-0.28	82.95	17.05	0.8456	-5.6623	0.0313	-0.0908
615.25	1.6254	4.38	79.84	20.16	1.0000	--	--	--
Intercept						2.3006	10.7944	-0.3117
Slope						-5.0246	-6.8358	0.0175
Correlation Coefficient						0.9691	0.9343	0.9810

Table 34
Thermal Decomposition of nickel bromate

Analysis of Data by Coats-Referrn(C-R), Freeman-Carroll(F-C) and Horowitz-Metzger(H-M) Methods

Instrument : TAQ 20 Thermogravimetric Analyser Heating Rate : 5° min-1

Peak temperature :501.3K, maximum mass loss w_{∞} : 94.06mg, $w_r = w_{\infty} - w$

Temp K	(1/T) 10 ³	$\theta = T - T_s$	Mass of Sample mg	Mass loss W mg	Fraction decompsd α	C-R $\log \left[\frac{-\log(1-\alpha)}{T^2} \right]$	F-C $\log \left[\frac{dw/dt}{w_r} \right]$	H-M $\log [\log(w_{\infty}/w_r)]$	
459.10	2.1782	-42.17	100.00	--	--	--		--	
463.09	2.1594	-38.18	98.91	1.09	0.0116	-7.6276		-2.2962	
467.11	2.1408	-34.16	98.34	1.66	0.0176	-7.4506		-2.1118	
471.12	2.1226	-30.15	97.87	2.13	0.0227	-7.3484		-2.0021	
475.08	2.1049	-26.19	97.32	2.68	0.0285	-7.2542		-1.9007	
479.08	2.0873	-22.19	96.59	3.41	0.0363	-7.1554		-1.7946	
483.09	2.0700	-18.18	95.66	4.34	0.0461	-7.0561		-1.6881	
487.09	2.0530	-14.18	94.26	5.74	0.0610	-6.9382		-1.5630	
491.08	2.0363	-10.19	92.12	7.88	0.0837	-6.8028		-1.4205	
495.09	2.0198	-6.18	89.31	10.69	0.1136	-6.6702		-1.2808	
499.09	2.0036	-2.18	83.07	16.93	0.1800	-6.4609		-1.0645	
501.05	1.9958	-0.22	75.08	24.92	0.2649	-6.2738		-0.8740	
503.10	1.9877	1.83	6.11	93.89	0.9982	-4.9654		0.4380	
504.46	1.9823	3.19	5.94	94.06	1.0000	0.0000		--	
				Intercept		15.8420		21.1100	0.9461
				Slope		11.1150		11.0100	0.0433
				Correlation Coefficient		0.9801		0.9821	0.9840

Table 35

Thermal Decomposition of nickel bromate containing zinc bromate(10⁻³ M)

Analysis of Data by Coats-Referrn(C-R), Freeman-Carroll(F-C) and Horowitz-Metzger(H-M) Methods

Instrument : TAQ 20 Thermogravimetric Analyser Heating Rate : 5° min⁻¹
 Peak temperature : 499.3K, maximum mass loss w_∞ : 69.42mg, w_r = w_∞ - w

Temp K	(1/T) 10 ³	θ = T - T _s	Mass of Sample mg	Mass loss W mg	Fraction decomposed α	C-R	F-C	H-M
						$\log \left[\frac{-\log(1-\alpha)}{T^2} \right]$	$\log \left[\frac{dw/dt}{w} \right]$	$\log [\log(w_\infty/w_r)]$
458.03060	2.1833	-41.26	100.00	--	--	--	--	--
463.25950	2.1586	-36.03	97.71	2.29	0.0330	-7.1685	-1.8776	-1.8368
468.01110	2.1367	-31.28	96.74	3.26	0.0470	-7.0206	-1.8769	-1.6801
473.22050	2.1132	-26.07	95.83	4.17	0.0601	-6.9198	-1.6135	-1.5697
478.01080	2.0920	-21.28	94.30	5.70	0.0821	-6.7885	-1.4073	-1.4296
483.22220	2.0694	-16.07	91.70	8.30	0.1195	-6.6257	-1.0667	-1.2574
488.00790	2.0491	-11.28	86.69	13.31	0.1918	-6.4108	-1.0501	-1.0339
493.22210	2.0275	-6.07	81.47	18.53	0.2669	-6.2563	-0.4657	-0.8702
498.01500	2.0080	-1.28	64.78	35.22	0.5074	-5.9066	-0.0398	-0.5122
503.21620	1.9872	3.93	32.32	67.68	0.9750	-5.1988	0.1402	0.2047
506.83630	1.9730	7.55	30.58	69.42	1.0000	-4.3476	--	--
Intercept						14.2053	24.6435	-0.3834
Slope						-9.9853	-12.3909	0.0449
Correlation Coefficient						0.9417	0.9711	0.9522

Table 36
 Thermal Decomposition of nickel bromate containing zinc bromate(10⁻² M)

Analysis of Data by Coats-Refern(C-R), Freeman-Carroll(F-C) and Horowitz-Metzger(H-M) Methods

Instrument : TAQ 20 Thermogravimetric Analyser Heating Rate : 5° min⁻¹

Peak temperature : 500.0K, maximum mass loss w_{∞} : 72.93mg, $w_r = w_{\infty} - w$

Temp K	(1/T) 10 ³	$\theta = T - T_s$	Mass of Sample mg	Mass loss W mg	Fraction decompsed α	C-R	F-C	H-M
						$\log \left[\frac{-\log(1-\alpha)}{T^2} \right]$	$\log \left[\frac{dw/dt}{w} \right]$	$\log [\log(w_{\infty}/w_r)]$
457.03	2.1881	-43.01	100.00	--	--	--	$\log \left[\frac{dw/dt}{w} \right]$	--
462.03	2.1644	-38.01	98.46	1.54	0.0193	-7.4013		-2.0024
467.02	2.1412	-33.02	97.75	2.25	0.0282	-7.2438	-2.0859	-1.8670
472.03	2.1185	-28.01	97.17	2.83	0.0355	-7.1516	-1.8797	-1.7654
477.03	2.0963	-23.01	96.25	3.75	0.0472	-7.0351	-1.7163	-1.6396
482.03	2.0746	-18.01	94.92	5.08	0.0639	-6.9086	-1.3933	-1.5036
487.03	2.0532	-13.01	92.17	7.83	0.0984	-6.7218	-1.2246	-1.3071
492.03	2.0324	-8.01	88.30	11.70	0.1472	-6.5442	-0.9688	-1.1194
497.01	2.0120	-3.03	81.74	18.26	0.2297	-6.3383	-0.0105	-0.9025
502.01	1.9920	1.97	28.44	71.56	0.9000	-5.4013	-0.0011	0.2371
507.02	1.9723	6.98	27.07	72.93	0.9173	-5.3757	--	--
Intercept						12.7521	25.1385	-0.8621
Slope						-9.3935	-12.7125	0.0323
Correlation Coefficient						0.9101	0.9180	0.9028

Table 37

Thermal Decomposition of nickel bromate containing zinc bromate(10⁻¹ M)

Analysis of Data by Coats-Refern(C-R), Freeman-Carroll(F-C) and Horowitz-Metzger(H-M) Methods

Instrument : TAQ 20 Thermogravimetric Analyser Heating Heating Rate : 5° min⁻¹

Peak temperature : 487.2K, maximum mass loss w_∞ : 64.35mg, w_r = w_∞ - w

Temp K	(1/T) 10 ³	θ = T - T _s	Mass of Sample mg	Mass loss W mg	Fraction decompsd α	C-R	F-C	H-M
						$\log \left[\frac{-\log(1-\alpha)}{T^2} \right]$	$\log \left[\frac{dw/dt}{w} \right]$	$\log [\log(w_\infty/w_r)]$
455.03	2.1977	-32.21	100.00	--	--	--		--
460.00	2.1739	-27.24	98.58	1.42	0.0221	-7.3387	$\log \left[\frac{dw/dt}{w} \right]$	-2.0131
465.01	2.1505	-22.23	97.15	2.85	0.0443	-7.0413	-1.4976	-1.7064
470.01	2.1276	-17.23	95.19	4.81	0.0747	-6.8164	-1.2037	-1.4722
475.02	2.1052	-12.22	91.47	8.53	0.1326	-6.5626	-1.0136	-1.2092
480.01	2.0833	-7.23	86.07	13.93	0.2165	-6.3372	-0.8330	-0.9747
485.02	2.0618	-2.22	78.65	21.35	0.3319	-6.1281	-0.4219	-0.7566
490.04	2.0407	2.80	62.32	37.68	0.5856	-5.7977	-0.6243	-0.4173
495.04	2.0200	7.80	55.98	44.02	0.6841	-5.6899	-0.7676	-0.3006
500.02	1.9999	12.78	52.52	47.48	0.7379	-5.6335	-0.1706	-0.2355
505.02	1.9801	17.78	41.13	58.87	0.9149	-5.3771	0.1774	0.0295
508.35	1.9672	21.11	35.65	64.35	1.0000	--	--	--
Intercept						13.2742	17.3664	-0.6644
Slope						-9.4058	-8.7418	0.0403
Correlation Coefficient						0.9808	0.9747	0.9865

Table 38

Thermal Decomposition of nickel bromate containing neodymium bromate(10⁻³M)
 Analysis of Data by Coats-Refern(C-R), Freeman-Carroll(F-C) and Horowitz-Metzger(H-M) Methods

Instrument : TAQ 20 Thermogravimetric Analyser Heating Rate : 5° min⁻¹

Peak temperature : 500.8K, maximum mass loss w_∞ : 65.52mg, w_r = w_∞ - w

Temp K	(1/T) 10 ³	θ = T - T _s	Mass of Sample mg	Mass loss W mg	Fraction decompsd α	C-R $\log \left[\frac{-\log(1-\alpha)}{T^2} \right]$	F-C $\log \left[\frac{dw/dt}{w_r} \right]$	H-M $\log [\log(w_\infty/w_r)]$
469.16	2.1315	-31.63	100.00	--	--	--	--	--
473.16	2.1135	-27.64	98.32	1.68	0.0257	-7.2972	-1.6252	-1.9472
477.15	2.0958	-23.64	97.11	2.89	0.0441	-7.0650	-1.4921	-1.7077
481.15	2.0783	-19.64	95.49	4.51	0.0688	-6.8740	-1.3590	-1.5094
485.16	2.0612	-15.63	93.36	6.64	0.1014	-6.7049	-1.0710	-1.3331
489.16	2.0443	-11.63	89.36	10.64	0.1624	-6.4926	-1.0456	-1.1137
493.16	2.0278	-7.63	85.41	14.59	0.2227	-6.3468	-0.8488	-0.9609
497.17	2.0114	-3.62	79.61	20.39	0.3112	-6.1838	-0.3122	-0.7908
501.16	1.9954	0.37	62.07	37.93	0.5789	-5.8252	0.6408	-0.4252
502.31	1.9908	1.52	34.48	65.52	1.0000	0.0000	--	--
Intercept						17.2933	32.6831	-0.5300
Slope						-11.6351	-16.3492	0.0509
Correlation Coefficient						0.9943	0.9102	0.9953

Table 39

Thermal Decomposition of nickel bromate containing neodymium bromate(10⁻² M)
Analysis of Data by Coats-Refern(C-R), Freeman-Carroll(F-C) and Horowitz-Metzger(H-M) Methods

Instrument : TAQ 20 Thermogravimetric Analyser Heating Rate : 5° min⁻¹

Peak temperature : 499.3K, maximum mass loss w_{∞} : 67.84mg, $w_r = w_{\infty} - w$

Temp K	$(1/T) 10^3$	$\theta = T - T_s$	Mass of Sample mg	Mass loss W mg	Fraction decomposed α	C-R	F-C	H-M
						$\log \left[\frac{-\log(1-\alpha)}{T^2} \right]$	$\log \left[\frac{dw/dt}{w_r} \right]$	$\log [\log(w_{\infty}/w_r)]$
469.16	2.1315	-30.13	100.00	--	--	--	--	--
473.15	2.1135	-26.14	98.57	1.43	0.0212	-7.3822	-1.4409	-2.0322
477.15	2.0958	-22.14	96.64	3.36	0.0495	-7.0136	-1.2593	-1.6563
481.15	2.0784	-18.14	93.80	6.20	0.0914	-6.7454	-1.0288	-1.3808
485.16	2.0612	-14.13	89.17	10.83	0.1596	-6.4938	-0.7216	-1.1220
489.18	2.0442	-10.11	80.48	19.52	0.2878	-6.2105	-0.8737	-0.8316
493.14	2.0278	-6.15	75.35	24.65	0.3633	-6.0935	-0.6501	-0.7076
497.16	2.0114	-2.13	67.58	32.42	0.4779	-5.9423	-0.0937	-0.5493
501.16	1.9954	1.87	44.76	55.24	0.8142	-5.5360	0.0698	-0.1361
505.15	1.9796	5.86	32.95	67.05	0.9884	-5.1201	0.4760	0.2867
506.82	1.9731	7.53	32.16	67.84	1.0000	0.0000	--	--
Intercept						22.4842	26.9910	-0.2315
Slope						-14.0845	-13.4970	0.0663
Correlation Coefficient						0.9896	0.9664	0.9918

Table 40

Thermal Decomposition of nickel bromate containing neodymium bromate(10^{-1} M)
 Analysis of Data by Coats-Refern(C-R), Freeman-Carroll(F-C) and Horowitz-Metzger(H-M) Methods

Instrument : TAQ 20 Thermogravimetric Analyser Heating Rate : 5° min⁻¹
 Peak temperature : 499.3K, maximum mass loss w_∞ : 62.03mg, w_r = w_∞ - w

Temp K	(1/T) 10 ³	θ = T - T _s	Mass of Sample mg	Mass loss W mg	Fraction decomposed α	C-R	F-C	H-M
						$\log\left[\frac{-\log(1-\alpha)}{T^2}\right]$	$\log\left[\frac{dw/dt}{w_r}\right]$	$\log[\log(w_\infty/w_r)]$
470.69	2.1245	-28.60	100.00	--	--	--	--	--
475.67	2.1023	-23.62	98.10	1.90	0.0306	-7.2238	-1.3511	-1.8692
480.67	2.0804	-18.62	95.42	4.58	0.0738	-6.8410	-1.0520	-1.4773
485.68	2.0590	-13.61	90.32	9.68	0.1561	-6.5053	-0.8023	-1.1326
490.67	2.0380	-8.62	82.08	17.92	0.2888	-6.2113	-0.6040	-0.8297
495.68	2.0174	-3.61	71.08	28.92	0.4662	-5.9548	-0.2170	-0.5644
500.68	1.9973	1.39	50.96	49.04	0.7905	-5.5674	-0.0092	-0.1683
505.67	1.9776	6.38	38.28	61.72	0.9949	-5.0469	0.6305	0.3608
506.84	1.9730	7.55	37.97	62.03	1.0000	0.0000	--	0.0000
Intercept						24.9436	29.6219	-0.2038
Slope						-15.2886	-14.7673	0.0705
Correlation Coefficient						0.9984	0.9833	0.9956

Table 41
 Thermal Decomposition of nickel bromate containing yttrium bromate(10⁻³M)
 Analysis of Data by Coats-Referrn(C-R), Freeman-Carroll(F-C) and Horowitz-Metzger(H-M) Methods
 Instrument : TAQ 20 Thermogravimetric Analyser Heating Rate : 5° min⁻¹

Peak temperature : 498.5K, maximum mass loss w_{∞} : 68.78mg, $w_r = w_{\infty} - w$

Temp K	(1/T) 10 ³	$\theta = T - T_s$	Mass of Sample mg	Mass loss W mg	Fraction decompsed α	C-R	F-C	H-M
						$\log \left[\frac{-\log(1-\alpha)}{T^2} \right]$	$\log \left[\frac{dw}{dt} \right]$	$\log [\log(w_{\infty}/w_r)]$
462.37	2.1628	-36.16	100.00	--	--	--	$\log \left[\frac{dw}{dt} \right]$	--
467.40	2.1395	-31.13	96.68	3.32	0.0483	-7.0074	-1.0755	-1.6680
472.39	2.1169	-26.14	95.30	4.70	0.0683	-6.8612	-1.5300	-1.5126
477.39	2.0947	-21.14	93.41	6.59	0.0958	-6.7169	-1.3415	-1.3591
482.39	2.0730	-16.14	90.58	9.42	0.1370	-6.5607	-0.9613	-1.1939
487.39	2.0517	-11.14	84.09	15.91	0.2313	-6.3179	-0.9512	-0.9422
492.39	2.0309	-6.14	78.17	21.83	0.3173	-6.1651	-0.5464	-0.7805
497.40	2.0104	-1.13	64.80	35.20	0.5117	-5.9002	-0.0295	-0.5067
502.38	1.9905	3.85	33.57	66.43	0.9658	-5.2358	0.3585	0.1662
504.57	1.9819	6.04	31.22	68.78	1.0000	0.0000	--	--
Intercept						15.5856	26.9067	-0.3298
Slope						-10.6283	-13.4440	0.0473
Correlation Coefficient						0.9562	0.9732	0.9640

Table 42

Thermal Decomposition of nickel bromate containing yttrium bromate(10⁻²M)
 Analysis of Data by Coats-Referrn(C-R), Freeman-Carroll(F-C) and Horowitz-Metzger(H-M) Methods
 Instrument : TAQ 20 Thermogravimetric Analyser Heating Rate : 5° min⁻¹

Peak temperature : 498.5K, maximum mass loss w_{∞} : 72.60mg, $w_r = w_{\infty} - w$

Temp K	(1/T) 10 ³	$\theta = T - T_s$	Mass of Sample mg	Mass loss W mg	Fraction decomposed α	C-R	F-C	H-M
						$\log \left[\frac{-\log(1-\alpha)}{T^2} \right]$	$\log \left[\frac{dw/dt}{w_r} \right]$	$\log [\log(w_{\infty}/w_r)]$
453.87	2.2033	-44.66	100.00	--	--	--		--
457.90	2.1839	-40.63	97.41	2.59	0.0357	-7.1235		-1.8019
461.89	2.1650	-36.64	93.10	6.90	0.0951	-6.6918	-1.0465	-1.3627
465.90	2.1464	-32.63	88.36	11.64	0.1603	-6.4565	-1.0788	-1.1199
469.90	2.1281	-28.63	84.30	15.70	0.2163	-6.3194	-1.3556	-0.9754
473.93	2.1100	-24.60	82.28	17.72	0.2441	-6.2667	-1.5116	-0.9153
477.92	2.0924	-20.61	80.93	19.07	0.2627	-6.2370	-1.3445	-0.8783
481.92	2.0750	-16.61	78.99	21.01	0.2894	-6.1946	-1.1193	-0.8287
485.90	2.0580	-12.63	75.87	24.13	0.3324	-6.1289	-0.8797	-0.7558
489.90	2.0412	-8.63	70.75	29.25	0.4029	-6.0301	-0.7939	-0.6499
493.91	2.0247	-4.62	65.17	34.83	0.4797	-5.9344	-0.3860	-0.5471
497.93	2.0083	-0.60	52.68	47.32	0.6518	-5.7334	0.0348	-0.3390
501.92	1.9924	3.39	30.83	69.17	0.9528	-5.2788	0.0910	0.1225
505.91	1.9766	7.38	27.45	72.55	0.9993	-4.9116	1.4632	0.4965
506.08	1.9760	7.55	27.40	72.60	1.0000	-4.3820	--	--
Intercept						16.2101	23.7858	-0.1126
Slope						-10.8263	-11.9509	0.0468
Correlation Coefficient						0.9201	0.9424	0.9311

Table 43

Thermal Decomposition of nickel bromate containing yttrium bromate(10⁻¹M)
 Analysis of Data by Coats-Referrn(C-R), Freeman-Carroll(F-C) and Horowitz-Metzger(H-M) Methods
 Instrument : TAQ 20 Thermogravimetric Analyser Heating Rate : 5° min⁻¹

Peak temperature : 484.2K, maximum mass loss w_{∞} : 69.14mg, $w_r = w_{\infty} - w$

Temp K	(1/T) 10 ³	$\theta = T - T_s$	Mass of Sample mg	Mass loss W mg	Fraction decompsd α	C-R $\log \left[\frac{-\log(1-\alpha)}{T^2} \right]$	F-C $\log \left[\frac{dw/dt}{w_r} \right]$	H-M $\log [\log(w_{\infty}/w_r)]$
447.92	2.2326	-36.31	100.00	--	--	--	--	--
452.91	2.2079	-31.32	99.23	0.77	0.0112	-7.6235	-1.0012	-2.3115
457.92	2.1838	-26.31	97.51	2.49	0.0360	-7.1196	-1.3177	-1.7980
462.90	2.1603	-21.33	94.32	5.68	0.0822	-6.7598	-1.3524	-1.4289
467.91	2.1371	-16.32	91.49	8.51	0.1231	-6.5843	-1.3805	-1.2439
472.91	2.1145	-11.32	88.97	11.03	0.1596	-6.4716	-0.9962	-1.1221
477.92	2.0924	-6.31	83.09	16.91	0.2445	-6.2731	-0.6419	-0.9144
482.92	2.0707	-1.31	71.19	28.81	0.4167	-5.9984	-0.1824	-0.6306
487.91	2.0496	3.68	44.76	55.24	0.7988	-5.5338	-0.3421	-0.1571
492.90	2.0288	8.67	38.44	61.56	0.8903	-5.4033	-0.2742	-0.0178
497.93	2.0083	13.70	34.38	65.62	0.9490	-5.2830	0.1378	0.1114
501.57	1.9937	17.34	30.86	69.14	1.0000	--	--	--
Intercept						17.4169	17.5698	-0.4930
Slope						-11.2675	-8.7230	0.0478
Correlation Coefficient						0.9890	0.9578	0.9862

Table 44
Thermal Decomposition of neodymium bromate
Analysis of Data by Coats-Refern(C-R), Freeman-Carroll(F-C) and Horowitz-Metzger(H-M) Methods
Instrument : TAQ 20 Thermogravimetric Analyser Heating Rate : 5° min-1

Peak temperature : 509.1K, maximum mass loss w_{∞} : 56.11mg, $w_r = w_{\infty} - w$

Temp K	(1/T) 10 ³	$\theta = T - T_s$	Mass of Sample mg	Mass loss W mg	Fraction decompsd α	C-R	F-C	H-M
						$\log \left[\frac{-\log(1-\alpha)}{T^2} \right]$	$\log \left[\frac{dw/dt}{w_r} \right]$	$\log [\log(w_{\infty}/w_r)]$
479.71	2.0846	-29.36	100.00	--	--	--	$\log \left[\frac{dw/dt}{w_r} \right]$	--
483.70	2.0674	-25.37	98.86	1.14	0.0204	-7.4182	-1.5469	-2.0490
487.70	2.0504	-21.37	97.61	2.39	0.0426	-7.0996	-1.3950	-1.7233
491.70	2.0338	-17.37	95.88	4.12	0.0734	-6.8632	-1.1247	-1.4798
495.70	2.0173	-13.37	92.76	7.24	0.1291	-6.6121	-0.9793	-1.2217
499.70	2.0012	-9.37	88.66	11.34	0.2022	-6.4058	-0.7586	-1.0084
503.71	1.9853	-5.36	82.40	17.60	0.3136	-6.1910	-0.3822	-0.7866
507.69	1.9697	-1.38	69.68	30.32	0.5403	-5.8829	0.0195	-0.4717
511.69	1.9543	2.62	48.07	51.93	0.9254	-5.3660	0.0956	0.0520
515.71	1.9391	6.64	43.89	56.11	1.0000	0.0000	--	--
Intercept						27.0517	30.3255	-0.2989
Slope						-16.6830	-15.4655	0.0692
Correlation Coefficient						0.9897	0.9880	0.9915

Table 45

Thermal Decomposition of neodymium bromate containing nickel bromate(10⁻² M)
 Analysis of Data by Coats-Refern(C-R), Freeman-Carroll(F-C) and Horowitz-Metzger(H-M) Methods

Instrument : TAQ 20 Thermogravimetric Analyser Heating Rate : 5° min⁻¹

Peak temperature : 505.3K, maximum mass loss w_∞ : 58.40mg, w_r = w_∞ - w

Temp K	(1/T) 10 ³	θ = T - Ts	Mass of Sample mg	Mass loss W mg	Fraction decompsed α	C-R $\log \left[\frac{-\log(1-\alpha)}{T^2} \right]$	F-C $\log \left[\frac{dw}{dt} \right]$	H-M $\log [\log(w_\infty/w_r)]$
477.43	2.0946	-27.88	100.00	--	--	--	--	--
481.42	2.0772	-23.89	98.66	1.34	0.0229	-7.3617	-1.5039	-1.9966
485.46	2.0599	-19.85	97.22	2.78	0.0477	-7.0457	-1.4349	-1.6734
489.42	2.0432	-15.89	95.60	4.40	0.0754	-6.8473	-1.2195	-1.4680
493.42	2.0267	-11.89	92.99	7.01	0.1201	-6.6418	-0.9861	-1.2553
497.42	2.0104	-7.89	88.75	11.25	0.1927	-6.4251	-0.7574	-1.0317
501.44	1.9942	-3.87	82.11	17.89	0.3062	-6.1996	-0.3158	-0.7992
505.42	1.9785	0.11	66.54	33.46	0.5730	-5.8397	0.0727	-0.4324
509.43	1.9630	4.12	42.90	57.10	0.9777	-5.1964	0.0619	0.2177
513.44	1.9477	8.13	41.70	58.30	0.9983	-4.9778	0.7263	0.4432
514.38	1.9441	9.07	41.60	58.40	1.0000	0.0000	--	--
Intercept						22.7900	30.7930	0.5653
Slope						14.5100	15.6270	0.0580
Correlation Coefficient						0.9954	0.9803	0.9976

Table 46

Thermal Decomposition of neodymium bromate containing nickel bromate(10⁻¹ M)
Analysis of Data by Coats-Refern(C-R), Freeman-Carroll(F-C) and Horowitz-Metzger(H-M) Methods

Instrument : TAQ 20 Thermogravimetric Analyser Heating Rate : 5° min⁻¹

Peak temperature : 506.1K, maximum mass loss w_∞ : 58.89mg, w_r = w_∞ - w

Temp K	(1/T) 10 ³	θ = T - T _s	Mass of Sample mg	Mass loss W mg	Fraction decompsd α	C-R	F-C	H-M
						$\log \left[\frac{-\log(1-\alpha)}{T^2} \right]$	$\log \left[\frac{dw/dt}{w_r} \right]$	$\log [\log(w_\infty/w_r)]$
472.19	2.1178	-33.87	100.00	--	--	--	--	--
476.19	2.1000	-29.87	99.82	0.18	0.0031	-8.2288	-1.6707	-2.8732
480.19	2.0825	-25.87	98.82	1.18	0.0201	-7.4175	-1.5794	-2.0547
484.19	2.0653	-21.87	97.60	2.40	0.0407	-7.1132	-1.5153	-1.7432
488.19	2.0484	-17.87	96.22	3.78	0.0642	-6.9176	-1.3357	-1.5404
492.19	2.0317	-13.87	94.19	5.81	0.0987	-6.7297	-1.0731	-1.3454
496.19	2.0154	-9.87	90.60	9.40	0.1596	-6.5131	-0.8557	-1.1218
500.19	1.9992	-5.87	85.07	14.93	0.2534	-6.2947	-0.5566	-0.8964
504.16	1.9835	-1.90	75.39	24.61	0.4179	-6.0341	-0.0882	-0.6290
508.16	1.9679	2.10	52.99	47.01	0.7981	-5.5700	0.0736	-0.1580
512.17	1.9525	6.11	41.71	58.29	0.9898	-5.1196	0.2320	0.2993
515.10	1.9414	9.04	41.11	58.89	1.0000	0.0000	--	--
Intercept						23.7760	27.8190	0.5410
Slope						14.9960	14.1537	0.0571
Correlation Coefficient						0.9845	0.9797	0.9982

Table 47

Thermal Decomposition of neodymium bromate containing barium bromate(10⁻² M)
 Analysis of Data by Coats-Refern(C-R), Freeman-Carroll(F-C) and Horowitz-Metzger(H-M) Methods

Instrument : TAQ 20 Thermogravimetric Analyser Heating Rate : 5° min⁻¹

Peak temperature : 505.7K, maximum mass loss w_{∞} : 55.35mg, $w_r = w_{\infty} - w$

Temp K	(1/T) 10 ³	$\theta = T - T_s$	Mass of Sample mg	Mass loss W mg	Fraction decomposed α	C-R	F-C	H-M
						$\log \left[\frac{-\log(1-\alpha)}{T^2} \right]$	$\log \left[\frac{dw/dt}{-1.4935} \right]$	$\log [\log(w_{\infty}/w_r)]$
477.26	2.0953	-28.40	100.00	--	--	--		--
481.26	2.0779	-24.40	98.88	1.12	0.0202	-7.4180		-2.0533
485.26	2.0608	-20.40	97.49	2.51	0.0453	-7.0679	-1.4080	-1.6959
489.26	2.0439	-16.40	95.84	4.16	0.0752	-6.8484	-1.2021	-1.4693
493.26	2.0273	-12.40	93.27	6.73	0.1217	-6.6353	-0.9891	-1.2492
497.26	2.0110	-8.40	89.28	10.72	0.1936	-6.4225	-0.7673	-1.0293
501.27	1.9949	-4.39	83.16	16.84	0.3042	-6.2029	-0.3277	-0.8027
505.29	1.9791	-0.37	68.61	31.39	0.5672	-5.8464	0.0616	-0.4393
509.28	1.9635	3.62	46.54	53.46	0.9659	-5.2476	0.2663	0.1664
511.99	1.9532	6.33	44.65	55.35	1.0000	0.0000	--	--
Intercept						23.5870	26.8300	0.4668
Slope						14.90	13.68	0.0631
Correlation Coefficient						0.9958	0.9736	0.9961

Table 48

Thermal Decomposition of neodymium bromate containing barium bromate(10⁻¹ M)
 Analysis of Data by Coats-Refern(C-R), Freeman-Carroll(F-C) and Horowitz-Metzger(H-M) Methods

Instrument : TAQ 20 Thermogravimetric Analyser Heating Rate : 5° min⁻¹

Peak temperature : 485.5K, maximum mass loss w_{∞} : 68.54mg, $w_r = w_{\infty} - w$

Temp K	(1/T) 10 ³	$\theta = T - T_s$	Mass of Sample mg	Mass loss W mg	Fraction decomposed α	C-R	F-C	H-M
						$\log \left[\frac{-\log(1-\alpha)}{T^2} \right]$	$\log \left[\frac{dw}{dt} \right]$	$\log [\log(w_{\infty}/w_r)]$
474.72	2.1065	-10.76	100.00	--	--	--	$\log \left[\frac{dw}{dt} \right]$	--
478.73	2.0889	-6.75	99.65	0.35	0.0051	-8.0178	-1.3491	-2.6576
482.73	2.0715	-2.75	97.21	2.79	0.0407	-7.1106	-0.3247	-1.7432
486.72	2.0546	1.24	72.39	27.61	0.4029	-6.0244	-0.5551	-0.6499
490.76	2.0377	5.28	63.19	36.81	0.5371	-5.8573	-0.9797	-0.4756
494.72	2.0213	9.24	60.55	39.45	0.5756	-5.8179	-0.9997	-0.4292
498.72	2.0051	13.24	58.22	41.78	0.6096	-5.7845	-0.8213	-0.3888
502.73	1.9891	17.25	54.98	45.02	0.6568	-5.7357	-0.5218	-0.3331
506.74	1.9734	21.26	49.31	50.69	0.7395	-5.6430	-0.0863	-0.2334
510.74	1.9579	25.26	37.60	62.40	0.9105	-5.3960	0.0671	0.0204
514.74	1.9427	29.26	31.87	68.13	0.9940	-5.0760	0.1463	0.3472
518.31	1.9293	32.83	31.46	68.54	1.0000	0.0000	--	--
Intercept						16.6290	27.56	-1.6587
Slope						11.23	14.08	0.0741
Correlation Coefficient						0.9442	0.9695	0.9468

Table 49
 Thermal Decomposition of yttrium bromate
 Analysis of Data by Coats-Refern(C-R), Freeman-Carroll(F-C) and Horowitz-Metzger(H-M) Methods
 Instrument : TAQ 20 Thermogravimetric Analyser Heating Rate : 5° min-1

Peak temperature : 500.0K, maximum mass loss w_{∞} : 60.34mg, $w_r = w_{\infty} - w$

Temp K	(1/T) 10 ³	$\theta = T - T_s$	Mass of Sample mg	Mass loss W mg	Fraction decomposed α	C-R	F-C	H-M
						$\log \left[\frac{-\log(1-\alpha)}{T^2} \right]$	$\log \left[\frac{dw/dt}{w_r} \right]$	$\log [\log(w_{\infty}/w_r)]$
455.60	2.1949	-44.44	100.00	--	--	--		--
460.60	2.1711	-39.44	98.70	1.30	0.0215	-7.3516		-2.0249
465.61	2.1477	-34.43	96.18	3.82	0.0633	-6.8830	-1.2082	-1.5470
470.60	2.1250	-29.44	92.69	7.31	0.1212	-6.5964	-1.2602	-1.2511
475.60	2.1026	-24.44	89.77	10.23	0.1695	-6.4479	-1.2259	-1.0934
480.60	2.0807	-19.44	86.80	13.20	0.2188	-6.3331	-1.1281	-0.9696
485.60	2.0593	-14.44	83.28	16.72	0.2770	-6.2237	-0.9607	-0.8512
490.61	2.0383	-9.43	78.51	21.49	0.3562	-6.0999	-0.6849	-0.7184
495.61	2.0177	-4.43	70.48	29.52	0.4892	-5.9252	-0.4565	-0.5350
500.59	1.9976	0.55	59.74	40.26	0.6673	-5.7196	-0.2972	-0.3207
505.59	1.9779	5.55	49.61	50.39	0.8351	-5.5139	-0.1026	-0.1063
510.62	1.9584	10.58	41.71	58.29	0.9661	-5.2489	0.1287	0.1673
514.34	1.9442	14.30	39.66	60.34	1.0000	0.0000	--	--
Intercept						11.3528	13.9170	-0.2928
Slope						-8.5210	-7.1287	0.0380
Correlation Coefficient						0.9849	0.9589	0.9852

Table 50

Thermal Decomposition of yttrium bromate containing nickel bromate(10⁻² M)
 Analysis of Data by Coats-Referrn(C-R), Freeman-Carroll(F-C) and Horowitz-Metzger(H-M) Methods
 Instrument : TAQ 20 Thermogravimetric Analyser Heating Rate : 5° min⁻¹

Peak temperature : 497.0K, maximum mass loss w_{∞} : 62.32mg, $w_r = w_{\infty} - w$

Temp K	(1/T) 10 ³	$\theta = T - T_s$	Mass of Sample mg	Mass loss W mg	Fraction decompsd α	C-R	F-C	H-M
						$\log \left[\frac{-\log(1-\alpha)}{T^2} \right]$	$\log \left[\frac{dw/dt}{w} \right]$	$\log [\log(w_{\infty}/w_r)]$
448.08	2.2318	-48.95	100.00	--	--	--		--
453.08	2.2071	-43.95	99.08	0.92	0.0148	-7.5013	-1.6246	-2.1889
458.08	2.1830	-38.95	97.62	2.38	0.0382	-7.0939	-1.4636	-1.7720
463.08	2.1595	-33.95	95.56	4.44	0.0713	-6.8247	-1.2699	-1.4934
468.07	2.1364	-28.96	92.45	7.55	0.1211	-6.5920	-1.2556	-1.2514
473.07	2.1139	-23.96	89.41	10.59	0.1699	-6.4422	-1.2285	-1.0923
478.07	2.0917	-18.96	86.36	13.64	0.2189	-6.3283	-1.1290	-0.9693
483.08	2.0701	-13.95	82.74	17.26	0.2770	-6.2192	-0.9386	-0.8512
488.07	2.0489	-8.96	77.55	22.45	0.3603	-6.0892	-0.7461	-0.7122
493.08	2.0281	-3.95	70.39	29.61	0.4751	-5.9388	-0.5087	-0.5529
498.11	2.0076	1.08	60.19	39.81	0.6389	-5.7489	-0.3564	-0.3542
503.11	1.9877	6.08	50.29	49.71	0.7977	-5.5619	-0.1632	-0.1586
508.10	1.9681	11.07	41.64	58.36	0.9365	-5.3338	-0.0413	0.0781
513.60	1.9470	16.57	37.68	62.32	1.0000	0.0000	--	--
Intercept						10.3660	12.7535	-0.3434
Slope						-8.0020	-6.5502	0.0365
Correlation Coefficient						0.9889	0.9791	0.9878

Table 51

Thermal Decomposition of yttrium bromate containing nickel bromate(10⁻¹ M)
 Analysis of Data by Coats-Refern(C-R), Freeman-Carroll(F-C) and Horowitz-Metzger(H-M) Methods

Instrument : TAQ 20 Thermogravimetric Analyser Heating Rate : 5° min⁻¹

Peak temperature : 497.8K, maximum mass loss w_∞ : 61.21mg, w_r = w_∞ - w

Temp K	(1/T) 10 ³	θ = T - T _s	Mass of Sample mg	Mass loss W mg	Fraction decompsed α	C-R $\log \left[\frac{-\log(1-\alpha)}{T^2} \right]$	F-C $\log \left[\frac{dw/dt}{w_r} \right]$	H-M $\log [\log(w_\infty/w_r)]$
448.09	2.2317	-49.69	100.00	--	--	--		--
454.10	2.2022	-43.68	98.36	1.64	0.0268	-7.2430	-1.4387	-1.9287
460.10	2.1735	-37.68	95.76	4.24	0.0693	-6.8317	-1.2396	-1.5060
466.09	2.1455	-31.69	91.82	8.18	0.1336	-6.5426	-1.2237	-1.2057
472.09	2.1182	-25.69	88.02	11.98	0.1957	-6.3723	-1.1988	-1.0242
478.09	2.0916	-19.69	84.28	15.72	0.2568	-6.2488	-1.1027	-0.8898
484.09	2.0657	-13.69	79.97	20.03	0.3272	-6.1341	-0.9431	-0.7642
490.10	2.0404	-7.68	74.34	25.66	0.4193	-6.0076	-0.6574	-0.6271
496.09	2.0158	-1.69	64.96	35.04	0.5725	-5.8240	-0.4576	-0.4329
502.09	1.9917	4.31	54.01	45.99	0.7513	-5.6202	-0.2659	-0.2187
508.09	1.9682	10.31	44.10	55.90	0.9132	-5.3860	-0.0993	0.0258
514.38	1.9441	16.60	38.79	61.21	1.0000	0.0000	--	--
Intercept						8.3691	10.9361	-0.3214
Slope						-7.0102	-5.6690	0.0321
Correlation Coefficient						0.9867	0.9643	0.9860

Table 52

Thermal Decomposition of yttrium bromate containing barium bromate(10⁻¹ M)
Analysis of Data by Coats-Refern(C-R), Freeman-Carroll(F-C) and Horowitz-Metzger(H-M) Methods

Instrument : TAQ 20 Thermogravimetric Analyser Heating Rate : 5° min⁻¹

Peak temperature : 494.7K, maximum mass loss w_{∞} : 55.83mg, $w_r = w_{\infty} - w$

Temp K	(1/T) 10 ³	$\theta = T - T_s$	Mass of Sample mg	Mass loss W mg	Fraction decomposed α	C-R	F-C	H-M
						$\log \left[\frac{-\log(1-\alpha)}{T^2} \right]$	$\log \left[\frac{dw/dt}{w} \right]$	$\log [\log(w_{\infty}/w_r)]$
435.49	2.2963	-59.45	100.00	--	--			--
441.49	2.2651	-53.45	99.38	0.62	0.0111	-7.6044	-1.9461	-2.3146
447.48	2.2347	-47.46	98.63	1.37	0.0245	-7.2690	-1.7514	-1.9674
453.48	2.2052	-41.46	97.47	2.53	0.0453	-7.0095	-1.4487	-1.6964
459.48	2.1764	-35.46	95.20	4.80	0.0861	-6.7326	-1.1858	-1.4080
465.48	2.1483	-29.46	91.21	8.79	0.1574	-6.4642	-1.1614	-1.1284
471.47	2.1210	-23.47	87.32	12.68	0.2271	-6.2981	-1.1321	-0.9512
477.47	2.0944	-17.47	83.50	16.50	0.2955	-6.1757	-1.0256	-0.8178
483.48	2.0683	-11.46	79.05	20.95	0.3753	-6.0584	-0.8212	-0.6896
489.48	2.0430	-5.46	72.73	27.27	0.4885	-5.9154	-0.5718	-0.5359
495.47	2.0183	0.53	63.55	36.45	0.6529	-5.7277	-0.4236	-0.3377
501.47	1.9941	6.53	54.78	45.22	0.8099	-5.5425	-0.2009	-0.1420
507.47	1.9706	12.53	46.77	53.23	0.9534	-5.2864	-0.1815	0.1244
513.48	1.9475	18.54	44.72	55.28	0.9903	-5.1175	-0.1340	0.3035
519.48	1.9250	24.54	44.24	55.76	0.9988	-4.9630	0.5735	0.4682
520.81	1.9201	25.87	44.17	55.83	1.0000	0.0000	--	--
Intercept						9.1151	12.2083	-0.3063
Slope						-7.3181	-6.2415	0.0336
Correlation Coefficient						-0.9953	-0.9768	0.9934

and Z was calculated using the equation

$$Z = \frac{E / RT_s^2 \cdot a}{\exp(-E / RT_s)} \quad 1.57$$

The results are presented in tables 1-52.

The slopes and intercepts of all the plots by the three methods given above were calculated by the least squares linear regression method by Excel data calculation and E and Z were calculated therefrom. The correlation coefficients r, in most cases, were in the range 0.96 to 0.99.

In all cases the entropy of activation(ΔS) was also calculated using the equation

$$\Delta S = 2.303 R \left[\log Z - \log \left(\frac{kT_s}{h} \right) \right] \quad 3.3$$

where k is Boltzmann constant, h is Planck's constant and T_s is the peak temperature.

E, Z and ΔS calculated by the three methods are given in Tables 53 to 60. The E and Z values obtained by the three methods show good agreement, within ± 10 percent.

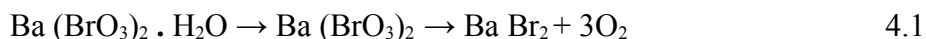
The initial temperature of decomposition (T_i), final temperature(T_f) and peak temperature(T_s) characteristic of each sample were noted down from the TG and DTG curves and the results were compared.

Chapter IV
Discussion

4.1 Thermal Decomposition Patterns

4.1.1 Thermal decomposition of barium bromate

Ba(BrO₃)₂.H₂O was converted to the anhydrous salt at 170°C (with a mass loss of nearly 4.5% corresponding to the loss of one molecule of water of hydration) in both studies (sample 1(i) in air and sample 1(ii) in nitrogen atmosphere). The result is in agreement with the earlier work^{135,138,139}. Barium bromate decomposes entirely in the solid state¹⁴⁰ to give bromide in accordance with the reaction



The decomposition of sample 1(i) of barium bromate in air starts at 565 K and is complete at 625 K (Table 54). The decomposition of sample 1(ii) of barium bromate in nitrogen atmosphere starts at 562.8 K and is complete at 615.4 K (Table 58).

As we can see, temperature zone of decomposition in nitrogen atmosphere has shifted to slightly lower values showing that decomposition is slightly faster in nitrogen atmosphere. $T_f - T_i$ is 60 K in air atmosphere and is 52.6 K in N₂ atmosphere. This, however, is only a very small difference.

Analysis of the effect of addition of intentional impurities to barium bromate shows that the presence of impurity generally lowers the initial temperature of decomposition (T_i). Similarly the temperature of completion of decomposition (T_f) and peak temperature (T_s) are also lowered in samples of barium bromate containing intentional impurities. It can also be noted that all these temperatures, in general, are lowered to larger extent as the concentration of the impurity is increased.

The activation energy for the decomposition of Ba(BrO₃)₂ - sample 1(i) in the present study is 281.1 KJ mol⁻¹ by Coats-Redfern method, 268.3 KJmol⁻¹ by Freeman-Carroll method and 282.7 KJmol⁻¹ by Horowitz-Metzger method. These values are quite close to one another and they are comparable to that obtained in the earlier work (277.0 KJmol⁻¹ by Horowitz-Metzger method)¹³⁵. The activation energy is lowered in samples containing the impurities, the lowering increases with increase in the concentration of the impurity (Tables 54-58).

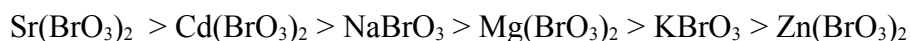
The activation energy for the decomposition of $\text{Ba}(\text{BrO}_3)_2$ - sample 1(ii) - in nitrogen is $295.3 \text{ KJ mol}^{-1}$ by Coats-Redfern method, 292.6 KJmol^{-1} by Freeman-Carroll method and 327.9 KJmol^{-1} by Horowitz-Metzger method. These values are slightly higher than those obtained in the decomposition of sample 1(i) in air. However this difference is small (only $\approx 5\%$ higher).

Table 54 gives a comparison of the lowering of activation energy due to the addition of NaBrO_3 and KBrO_3 each in 10^{-3} to 10^{-1} M concentrations. The effect due to NaBrO_3 is higher than that due to KBrO_3 . This is possibly due to the varying extents of defects created on adding the impurities. Though both the added ions are monovalent, they have different size and different surface charge densities (Table 73).

Table 55 gives a comparison of the lowering of activation energy due to the addition of $\text{Mg}(\text{BrO}_3)_2$ and $\text{Sr}(\text{BrO}_3)_2$ in 10^{-3} to 10^{-1} M concentrations. Here the decrease due to the addition of Sr^{2+} is found to be higher than that due to Mg^{2+} .

Table 56 gives the effect of adding zinc bromate and cadmium bromate as intentional impurities in 10^{-3} to 10^{-1} M concentrations to barium bromate. The effect of lowering of activation energy due to the addition of Cd^{2+} is found to be higher than that caused by adding Zn^{2+} .

A comparison of the results of Tables 54-56 shows that the effect of decreasing the activation energy is the highest in the case of barium bromate containing $\text{Sr}(\text{BrO}_3)_2$ and the effect decreases in the order



The variation of activation energy with concentration of the impurity for barium bromate is represented graphically in Figures 28-30.

Table 54

Kinetic parameters of decomposition of barium bromate and barium bromate containing sodium bromate and potassium bromate as intentional impurities calculated using Coats-Redfern, Freeman-Carroll and Horowitz-Metzger methods

Sample No	Sample Ba(BrO ₃) ₂	T _i	T _f	T _s	Kinetic parameters											
					Coats-Redfern				Freeman-Carroll				Horowitz-Metzger			
					E	Z	ΔS	r	E	Z	ΔS	r	E	Z	ΔS	r
kJmol ⁻¹	Min ⁻¹	JK ⁻¹ mol ⁻¹		kJmol ⁻¹	Min ⁻¹	JK ⁻¹ mol ⁻¹		kJmol ⁻¹	Min ⁻¹	JK ⁻¹ mol ⁻¹						
1(i)	Untreated Ba(BrO ₃) ₂	565.0	625.0	621.0	281.1	7.9 x 10 ²²	187.4	0.9936	268.3	1.2 x 10 ²²	171.5	0.9925	282.7	2.7 x 10 ²³	197.4	0.9985
2	Containing NaBrO ₃ 10 ⁻³ M	573.0	628.0	621.0	270.3	8.5 x 10 ²¹	168.9	0.9923	240.2	4.3 x 10 ¹⁹	124.9	0.9905	280.7	1.8 x 10 ²³	194.1	0.9935
3	10 ⁻² M	573.0	646.0	627.0	257.2	4.2 x 10 ²⁰	143.7	0.9976	236.8	1.3 x 10 ¹⁹	115.0	0.9735	273.4	2.5 x 10 ²²	177.7	0.9932
4	10 ⁻¹ M	573.0	647.0	635.5	239.1	8.6 x 10 ¹⁸	111.3	0.9909	211.3	8.2 x 10 ¹⁶	72.6	0.9601	236.0	8.9 x 10 ¹⁸	111.5	0.9936
5	Containing KBrO ₃ 10 ⁻³ M	563.0	626.0	620.5	270.4	7.8 x 10 ²¹	168.1	0.9926	258.4	1.3 x 10 ²¹	153.1	0.9901	283.7	3.4 x 10 ²²	180.4	0.9916
6	10 ⁻² M	568.0	626.0	621.0	254.7	3.4 x 10 ²⁰	142.1	0.9966	231.6	6.6 x 10 ¹⁸	109.3	0.9926	267.1	1.2 x 10 ²²	171.8	0.9971
7	10 ⁻¹ M	565.0	627.0	621.0	253.4	3.1 x 10 ²⁰	141.4	0.9966	223.0	1.4 x 10 ¹⁸	99.5	0.9952	262.9	5.3 x 10 ²¹	165.0	0.9975

Table 55

Kinetic parameters of decomposition of barium bromate and barium bromate containing magnesium bromate and strontium bromate as intentional impurities calculated using Coats-Redfern, Freeman-Carroll and Horowitz-Metzger methods

Sample No	Sample Ba(BrO ₃) ₂	T _i	T _f	T _s	Kinetic parameters											
					Coats-Redfern				Freeman-Carroll				Horowitz-Metzger			
					E kJmol ⁻¹	Z Min ⁻¹	ΔS JK ⁻¹ mol ⁻¹	r	E kJmol ⁻¹	Z Min ⁻¹	ΔS JK ⁻¹ mol ⁻¹	r	E kJmol ⁻¹	Z Min ⁻¹	ΔS JK ⁻¹ mol ⁻¹	r
1(i)	Untreated Ba(BrO ₃) ₂	565.0	625.0	621.0	281.1	7.9 x 10 ²²	187.4	0.9936	268.3	1.2 x 10 ²²	171.5	0.9925	282.7	2.7 x 10 ²³	197.4	0.9985
8	Containing Mg(BrO ₃) ₂ 10 ⁻³ M	568.0	623.0	617.0	257.9	1.0 x 10 ²¹	151.3	0.9964	256.5	1.4 x 10 ²¹	153.7	0.9638	265.7	1.3 x 10 ²²	172.6	0.9957
9	10 ⁻² M	558.0	623.0	618.0	250.6	2.7 x 10 ²⁰	140.1	0.9936	228.5	5.3 x 10 ¹⁸	107.5	0.9891	258.5	2.9 x 10 ²¹	158.9	0.9951
10	Containing Sr(BrO ₃) ₂ 10 ⁻³ M	573.0	631.0	621.0	269.0	7.2 x 10 ²¹	167.5	0.9914	235.8	1.7 x 10 ¹⁹	117.3	0.9921	274.3	5.1 x 10 ²²	183.7	0.9970
11	10 ⁻² M	573.0	628.0	621.0	249.6	1.4 x 10 ²⁰	134.5	0.9980	232.4	8.7 x 10 ¹⁸	111.6	0.9940	264.9	7.9 x 10 ²¹	168.2	0.9974
12	10 ⁻¹ M	563.0	627.0	621.0	211.8	1.2 x 10 ¹⁷	75.8	0.9606	200.0	2.2 x 10 ¹⁶	61.8	0.9720	196.3	1.0 x 10 ¹⁶	55.3	0.9970

Table 56

Kinetic parameters of decomposition of barium bromate and barium bromate containing zinc bromate and cadmium bromate as intentional impurities calculated using Coats-Redfern, Freeman-Carroll and Horowitz-Metzger methods

Sample No	Sample Ba(BrO ₃) ₂	T _i	T _f	T _s	Kinetic parameters											
					Coats-Redfern				Freeman-Carroll				Horowitz-Metzger			
					E kJmol ⁻¹	Z Min ⁻¹	ΔS JK ⁻¹ mol ⁻¹	r	E kJmol ⁻¹	Z Min ⁻¹	ΔS JK ⁻¹ mol ⁻¹	r	E kJmol ⁻¹	Z Min ⁻¹	ΔS JK ⁻¹ mol ⁻¹	r
1(i)	Untreated Ba(BrO ₃) ₂	565.0	625.0	621.0	281.1	7.9 x 10 ²²	187.4	0.9936	268.3	1.2 x 10 ²²	171.5	0.9925	282.7	2.7 x 10 ²³	197.4	0.9985
13	10 ⁻³ M Containing Zn(BrO ₃) ₂	563.0	638.0	620.0	275.9	3.6 x 10 ²²	180.9	0.9927	256.2	1.3 x 10 ²¹	153.2	0.9810	279.8	1.6 x 10 ²³	193.5	0.9965
14	10 ⁻² M	563.0	633.0	620.0	249.5	1.7 x 10 ²⁰	136.3	0.9852	245.4	1.3 x 10 ²⁰	134.1	0.9703	267.9	1.6 x 10 ²²	173.9	0.9907
15	10 ⁻¹ M	568.0	631.0	618.5	246.5	7.9 x 10 ¹⁹	130.0	0.9989	238.5	3.3 x 10 ¹⁸	103.6	0.9847	266.7	1.4 x 10 ²²	173.0	0.9999
16	10 ⁻³ M Containing Cd(BrO ₃) ₂	568.0	628.0	616.0	273.2	1.8 x 10 ²²	175.3	0.9883	247.4	2.5 x 10 ²⁰	139.5	0.9933	260.7	5.3 x 10 ²¹	164.9	0.9996
17	10 ⁻² M	563.0	625.0	618.0	259.1	1.2 x 10 ²¹	152.8	0.9871	242.5	7.8 x 10 ¹⁹	129.8	0.9902	261.2	4.9 x 10 ²¹	164.3	0.9990
18	10 ⁻¹ M	553.0	630.0	620.5	221.6	7.8 x 10 ¹⁷	91.5	0.9899	209.6	1.3 x 10 ¹⁷	76.3	0.9885	226.6	4.2 x 10 ¹⁸	105.5	0.9990

Table 57

Kinetic parameters of decomposition of barium bromate and barium bromate containing potassium bromide and strontium bromide as intentional impurities calculated using Coats-Redfern, Freeman-Carroll and Horowitz-Metzger methods

Sample No	Sample Ba(BrO ₃) ₂	T _i	T _f	T _s	Kinetic parameters											
					Coats-Redfern				Freeman-Carroll				Horowitz-Metzger			
					E	Z	ΔS	r	E	Z	ΔS	r	E	Z	ΔS	r
kJmol ⁻¹	Min ⁻¹	JK ⁻¹ mol ⁻¹		kJmol ⁻¹	Min ⁻¹	JK ⁻¹ mol ⁻¹		kJmol ⁻¹	Min ⁻¹	JK ⁻¹ mol ⁻¹						
1(i)	Untreated Ba(BrO ₃) ₂	565.0	625.0	621.0	281.1	7.9 x 10 ²²	187.4	0.9936	268.3	1.2 x 10 ²²	171.5	0.9925	282.7	2.7 x 10 ²³	197.4	0.9985
19	Containing KBr 10 ⁻³ M	568.0	638.0	618.0	261.6	9.4 x 10 ²¹	169.7	0.9945	246.3	1.6 x 10 ²⁰	135.8	0.9913	278.9	1.6 x 10 ²³	193.5	0.9987
20	10 ⁻² M	563.0	641.0	620.5	245.9	6.4 x 10 ¹⁹	128.2	0.9978	228.3	3.9 x 10 ¹⁸	105.0	0.9865	259.5	2.8 x 10 ²¹	159.7	0.9991
21	10 ⁻¹ M	553.0	640.0	615.5	228.1	2.5 x 10 ¹⁸	101.2	0.9953	223.2	2.2 x 10 ¹⁸	100.0	0.9711	248.4	7.1 x 10 ²⁰	148.3	0.9934
22	Containing SrBr ₂ 10 ⁻³ M	568.0	621.0	617.0	268.5	1.1 x 10 ²²	171.4	0.9857	252.8	8.7 x 10 ²⁰	149.9	0.9946	263.8	9.1 x 10 ²¹	169.4	0.9984
23	10 ⁻² M	563.0	624.0	618.0	229.0	3.8 x 10 ¹⁸	104.7	0.9811	247.3	2.6 x 10 ²⁰	139.9	0.9960	245.0	1.9 x 10 ²⁰	137.5	0.9900
24	10 ⁻¹ M	558.0	626.0	619.5	214.1	1.5 x 10 ¹⁷	77.8	0.9937	221.8	1.9 x 10 ¹⁸	98.9	0.9779	235.7	2.8 x 10 ¹⁹	121.2	0.9950

Table 58

Kinetic parameters of decomposition of barium bromate and barium bromate containing nickel bromate, neodymium bromate and yttrium bromate as intentional impurities calculated using Coats-Redfern, Freeman-Carroll and Horowitz-Metzger methods

Sample No	Sample Ba(BrO ₃) ₂	T _i	T _f	T _s	Kinetic parameters											
					Coats-Redfern				Freeman-Carroll				Horowitz-Metzger			
					E	Z	ΔS	r	E	Z	ΔS	r	E	Z	ΔS	r
kJmol ⁻¹	Min ⁻¹	JK ⁻¹ mol ⁻¹		kJmol ⁻¹	Min ⁻¹	JK ⁻¹ mol ⁻¹		kJmol ⁻¹	Min ⁻¹	JK ⁻¹ mol ⁻¹						
1(ii)	Untreated Ba(BrO ₃) ₂	562.8	615.4	609.6	295.3	4.98 x 10 ¹⁹	126.2	0.9956	292.6	5.15 x 10 ²⁴	222.2	0.9788	327.9	1.1 x 10 ²⁶	247.7	0.9968
25	Containing Ni(BrO ₃) ₂ 10 ⁻³ M	568.6	612.2	603.9	306.5	1.6 x 10 ²¹	155.1	0.9998	297.2	3.65 x 10 ²⁵	238.6	0.9989	335.9	1.04 x 10 ²⁷	264.4	0.9998
26	10 ⁻² M	495.5	611.5	604.7	257.5	1.1 x 10 ¹⁷	75.6	0.9736	329.9	3.9 x 10 ²⁸	296.5	0.9649	279.2	9.9 x 10 ²¹	170.4	0.9786
27	10 ⁻¹ M	503.8	612.2	603.9	241.8	4.1 x 10 ¹⁵	48.2	0.9925	259.6	2.2 x 10 ²²	176.9	0.9944	234.1	1.1 x 10 ¹⁸	94.9	0.9928
28	Containing Nd(BrO ₃) ₃ 10 ⁻³ M	528.0	611.0	608.6	214.6	8.67 x 10 ¹²	3.2	0.9940	214.8	1.77 x 10 ¹⁸	98.5	0.9828	256.5	7.16 x 10 ¹⁹	129.3	0.9953
29	10 ⁻² M	512.8	612.2	606.2	206.1	2.2 x 10 ¹²	14.4	0.9677	164.0	5.42 x 10 ¹³	12.1	0.9476	224.7	1.4 x 10 ¹⁷	77.5	0.9733
30	10 ⁻¹ M	502.7	613.9	608.8	182.1	1.82 x 10 ¹⁰	54.4	0.9492	157.9	2.46 x 10 ¹³	05.5	0.9481	170.7	2.08 x 10 ¹²	15.04	0.9858
31	Containing Y(BrO ₃) ₃ 10 ⁻³ M	552.7	612.8	608.9	288.9	2.31 x 10 ¹⁹	119.8	0.9967	304.5	1.06 x 10 ²⁶	247.4	0.9932	327.0	1.0 x 10 ²⁶	246.9	0.9983
32	10 ⁻² M	514.9	610.5	607.7	166.4	5.65 x 10 ⁸	83.3	0.9934	159.8	2.85 x 10 ¹³	6.7	0.9776	204.1	1.96 x 10 ¹⁵	41.9	0.9919
33(i) (Stage -1)	10 ⁻¹ M	451.0	510.0	496.2	173.3	5.79 x 10 ¹²	4.8	0.9776	137.1	1.13 x 10 ¹⁴	19.9	0.9571	192.9	1.59 x 10 ¹⁸	99.3	0.9769
33(ii) (Stage -2)	10 ⁻¹ M	510.0	615.2	610.9	96.2	1.92 x 10 ²	207.1	0.9691	130.9	6.23 x 10 ¹⁰	44.2	0.9343	124.8	1.57 x 10 ⁸	94.0	0.9810

Table 59

Kinetic parameters of decomposition of nickel bromate and nickel bromate containing zinc bromate, neodymium bromate and yttrium bromate as intentional impurities calculated using Coats-Redfern, Freeman-Carroll and Horowitz-Metzger methods

Sample No	Sample Ni(BrO ₃) ₂	T _i	T _f	T _s	Kinetic parameters											
					Coats-Redfern				Freeman-Carroll				Horowitz-Metzger			
					E	Z	ΔS	r	E	Z	ΔS	r	E	Z	ΔS	r
kJmol ⁻¹	Min ⁻¹	JK ⁻¹ mol ⁻¹		kJmol ⁻¹	Min ⁻¹	JK ⁻¹ mol ⁻¹		kJmol ⁻¹	Min ⁻¹	JK ⁻¹ mol ⁻¹						
34	Untreated Ni(BrO ₃) ₂	459.1	504.4	501.3	212.8	2 x 10 ⁶	62.9	0.9801	210.8	1.3 x 10 ²¹	154.9	0.9821	208.3	4.25 x 10 ¹⁹	126.5	0.9839
35	Containing Zn(BrO ₃) ₂	458.0	506.8	499.3	191.2	3.1 x 10 ¹⁴	28.2	0.9416	237.3	4.4x 10 ²⁴	222.6	0.9711	214.5	2.38 x 10 ²⁰	140.9	0.9522
36	10 ⁻³ M	457.0	507.0	500.0	179.9	1.0 x 10 ¹³	0.20	0.9100	226.7	1.97 x 10 ²³	196.7	0.9180	154.6	8.6 x 10 ¹³	17.6	0.9027
37	10 ⁻² M	455.0	508.3	487.2	180.1	3.4 x 10 ¹³	10.0	0.9807	167.4	2.32 x 10 ¹⁷	53.5	0.9747	183.2	8.4 x 10 ¹⁷	86.6	0.9864
38	Containing Nd(BrO ₃) ₃	469.2	502.3	500.8	222.8	4.4 x 10 ¹⁷	88.5	0.9943	313.0	4.8 x 10 ³²	376.5	0.9102	244.3	3.0 x 10 ²³	200.2	0.9953
39	10 ⁻³ M	469.2	506.8	499.3	269.7	8.2 x 10 ²²	189.5	0.9896	258.4	9.8 x 10 ²⁶	267.5	0.9664	316.4	1.6 x 10 ³¹	348.3	0.9918
40	10 ⁻² M	470.7	506.8	499.3	292.7	2.6 x 10 ²⁵	237.3	0.9984	282.8	4.2 x 10 ²⁹	317.9	0.9833	336.7	2.3 x 10 ³³	389.4	0.9956
41	Containing Y(BrO ₃) ₃	462.4	504.6	498.5	203.5	7.9 x 10 ¹⁵	55.1	0.9562	257.4	8.1 x 10 ²⁶	265.9	0.9732	225.0	3.4 x 10 ²¹	163.0	0.9640
42	10 ⁻³ M	454.1	506.1	498.5	207.3	3.5 x 10 ¹⁶	67.6	0.9201	228.8	6.1 x 10 ²³	206.1	0.9424	222.7	1.9 x 10 ²¹	158.4	0.9310
43	10 ⁻² M	447.9	501.5	484.2	215.7	5.6 x 10 ¹⁷	90.9	0.9889	167.0	2.7 x 10 ¹⁷	87.4	0.9577	214.6	1.3x 10 ²¹	155.2	0.9862

Table 60

Kinetic parameters of decomposition of neodymium bromate and neodymium bromate containing nickel bromate and barium bromate as intentional impurities calculated using Coats-Redfern, Freeman-Carroll and Horowitz-Metzger methods

Sample No	Sample Nd(BrO ₃) ₃	T _i	T _f	T _s	Kinetic parameters											
					Coats-Redfern				Freeman-Carroll				Horowitz-Metzger			
					E	Z	ΔS	r	E	Z	ΔS	r	E	Z	ΔS	r
kJmol ⁻¹	Min ⁻¹	JK ⁻¹ mol ⁻¹		kJmol ⁻¹	Min ⁻¹	JK ⁻¹ mol ⁻¹		kJmol ⁻¹	Min ⁻¹	JK ⁻¹ mol ⁻¹						
44	Untreated Nd(BrO ₃) ₃	479.7	515.1	509.1	319.4	3.6 x 10 ²⁷	278.2	0.9897	296.1	2.1 x 10 ³⁰	331.2	0.9880	343.6	2.4 x 10 ³³	389.6	0.9915
45	Containing Ni(BrO ₃) ₂ 10 ⁻² M	477.4	514.4	505.4	277.8	1.7 x 10 ²³	195.5	0.9953	299.2	6.7 x 10 ³⁰	340.2	0.9803	283.6	2.29 x 10 ²⁷	274.5	0.9976
46	Containing Ni(BrO ₃) ₂ 10 ⁻¹ M	472.2	515.1	506.1	287.1	1.7 x 10 ²⁴	214.6	0.9845	271.0	6.6 x 10 ²⁷	283.2	0.9797	279.0	8.7 x 10 ²⁶	266.4	0.9982
47	Containing Ba(BrO ₃) ₂ 10 ⁻² M	477.3	512.0	505.7	285.3	1.1 x 10 ²⁴	211.0	0.9958	262.0	6.7 x 10 ²⁶	264.3	0.9736	308.9	9.9 x 10 ²⁹	324.9	0.9961
48	Containing Ba(BrO ₃) ₂ 10 ⁻¹ M	474.8	518.3	485.5	214.9	2.8 x 10 ¹⁶	65.9	0.9442	269.6	3.6 x 10 ²⁷	278.6	0.9694	286.7	1.3 x 10 ²⁴	304.9	0.9468

Table 61

Kinetic parameters of decomposition of yttrium bromate and yttrium bromate containing nickel bromate and barium bromate as intentional impurities calculated using Coats-Redfern, Freeman-Carroll and Horowitz-Metzger methods

Sample No	Sample $Y(BrO_3)_3$	T_i	T_f	T_s	Kinetic parameters											
					Coats-Redfern				Freeman-Carroll				Horowitz-Metzger			
					E	Z	ΔS	r	E	Z	ΔS	r	E	Z	ΔS	r
					$kJmol^{-1}$	Min^{-1}	$JK^{-1}mol^{-1}$		$kJmol^{-1}$	Min^{-1}	$JK^{-1}mol^{-1}$		$kJmol^{-1}$	Min^{-1}	$JK^{-1}mol^{-1}$	
49	Untreated $Y(BrO_3)_3$	455.6	514.3	500.0	163.2	3.7×10^{11}	27.8	0.9849	136.5	8.3×10^{13}	17.2	0.9589	181.8	7.1×10^{16}	73.4	0.9852
50	Containing $Ni(BrO_3)_2$ $10^{-2} M$	448.0	513.6	497.0	153.2	3.6×10^{10}	47.1	0.9889	125.4	5.7×10^{12}	5.0	0.9791	172.5	9.5×10^{15}	56.7	0.9878
51	$10^{-1} M$	448.1	514.3	497.8	134.2	3.2×10^8	86.5	0.9867	108.5	8.6×10^{10}	39.8	0.9643	152.3	6.0×10^{13}	14.5	0.9860
52	Containing $Ba(BrO_3)_2$ $10^{-1} M$	435.5	520.8	494.7	140.1	1.8×10^9	71.8	0.9953	119.5	1.6×10^{12}	15.4	0.9768	157.6	2.8×10^{14}	27.4	0.9934

A comparison of the effect of adding nickel bromate, neodymium bromate and yttrium bromate in 10^{-3} to 10^{-1} M concentrations to barium bromate shows that the effect is highest for Nd^{3+} and the effect decreases in the order (Table 58 and Fig. 31).



Further, the presence of strontium bromide as impurity lowers E to a greater extent than that produced by potassium bromide (Table 57).

In the present investigations cationic impurities with surface charge density both greater and smaller than that of the host ion have been tried. The surface charge density (σ) of an ion is

given by $\frac{Ze}{4\pi r^2}$ where Ze is the numerical value of the charge of the ion and r is the ionic radius. Table 62 gives the radii and surface charge densities of different ions (radius substituted in pm units and charge in atomic units).

Table 62 : Ionic radii and surface charge densities of ions

Ion	Ionic radius in pm	Surface charge density
Ba^{2+}	135	0.0874
K^+	133	0.0450
Na^+	95	0.0882
Sr^{2+}	113	0.1247
Cd^{2+}	109	0.1340
Zn^{2+}	74	0.2907
Mg^{2+}	65	0.3769
Y^{3+}	104	0.2208
Nd^{3+}	100	0.2388
Ni^{2+}	72	0.3071

Incorporation of a cationic impurity having a surface charge density different from that of the corresponding ion in the host lattice generates defects in the host lattice¹⁴¹. It has also been

found that homovalent impurities can produce vacancies¹⁴² or act as electron traps¹⁴³ and affect the sensitivity towards decomposition.²⁶ The defects generated due to the introduction of the impurity cation into the lattice sites may create local strain due to which there may happen distortions in the structure of host crystal and may cause alterations in the lattice vibrations¹⁴⁴.

The cumulative effect of these changes will certainly decrease the electron charge symmetry of the host ion and weaken the chemical bonds in the vicinity of the defect thereby enhancing the chances of decomposition at these sites.

The greater susceptibility of barium bromate containing intentional impurities arises from the presence of lattice defects in large concentrations. The intensity of the lattice defects increases with increase in the concentration of the added impurity.

In an earlier study⁷³ on the addition of cationic impurity in strontium bromate it has been reported that the thermal stability of the treated samples decreases with increase in the surface charge density of the added cation. However, in the present study, the observed order of decrease of the thermal stability is not exactly the same as the order of increasing surface charge density (Table-62). Probably the added ion may be causing variation in parameters like lattice energy¹⁴⁵, extent of co-ordination of lattice water with the cation, extent of hydrogen bonding of lattice water with the anion and the electron charge distribution of the anion. These factors, however, have to be investigated in detail.

Jach³² has suggested that the bromide ion produced during the decomposition of bromide catalyses the decomposition by donating an electron to an oxygen atom of a bromate ion that has still to be decomposed, thereby enhancing the cleavage of the latter. This effect, however, is equally probable in the pure bromates as well as those containing other bromates as added impurities. However this becomes quite significant in the case of a bromide impurity added. Thus in sample of barium bromate containing potassium bromide or strontium bromide, in addition to the effect of the defects generated by the cationic impurity, the presence of bromide ions in large concentration facilitates the formation of a eutectic with the bromate

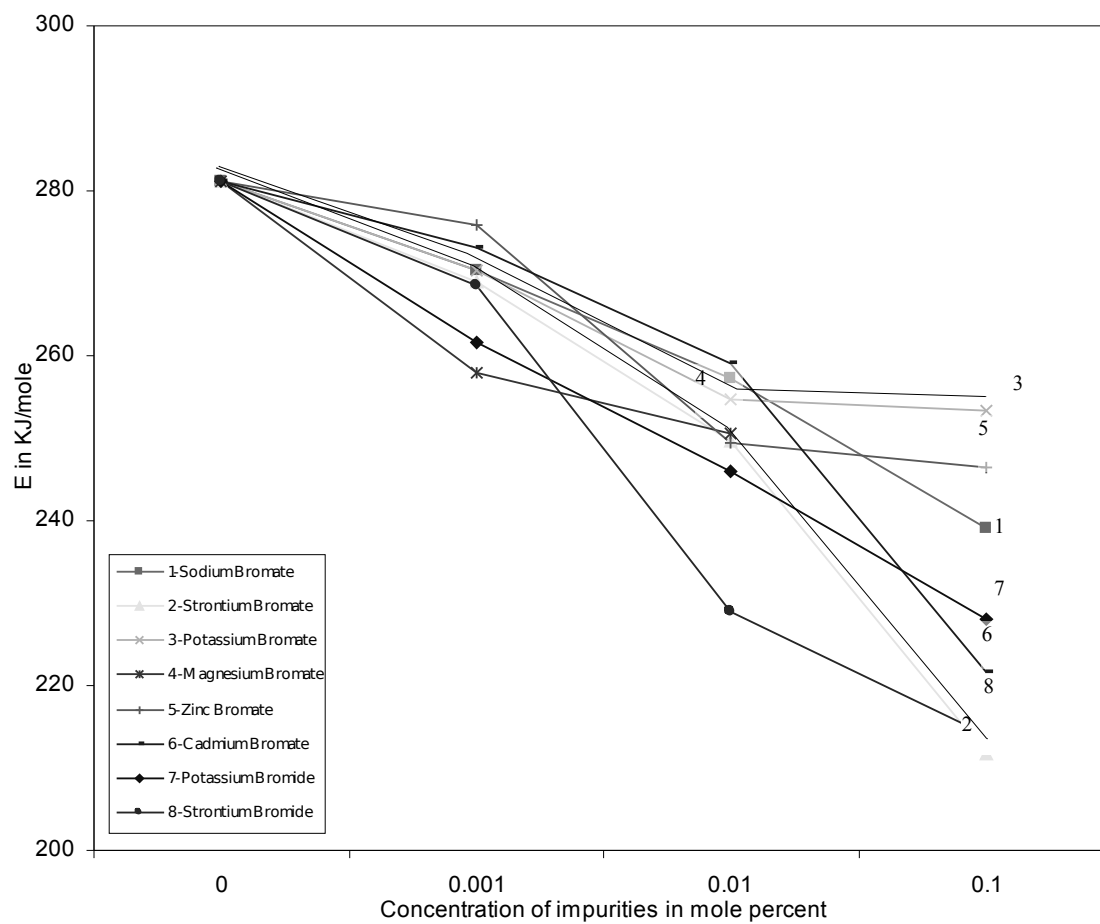


Fig : 28 Variation of E with concentration of impurities - barium bromate containing Na, K, Mg, Sr, Zn, Cd bromates and K, Sr bromides – Coats-Redfern method

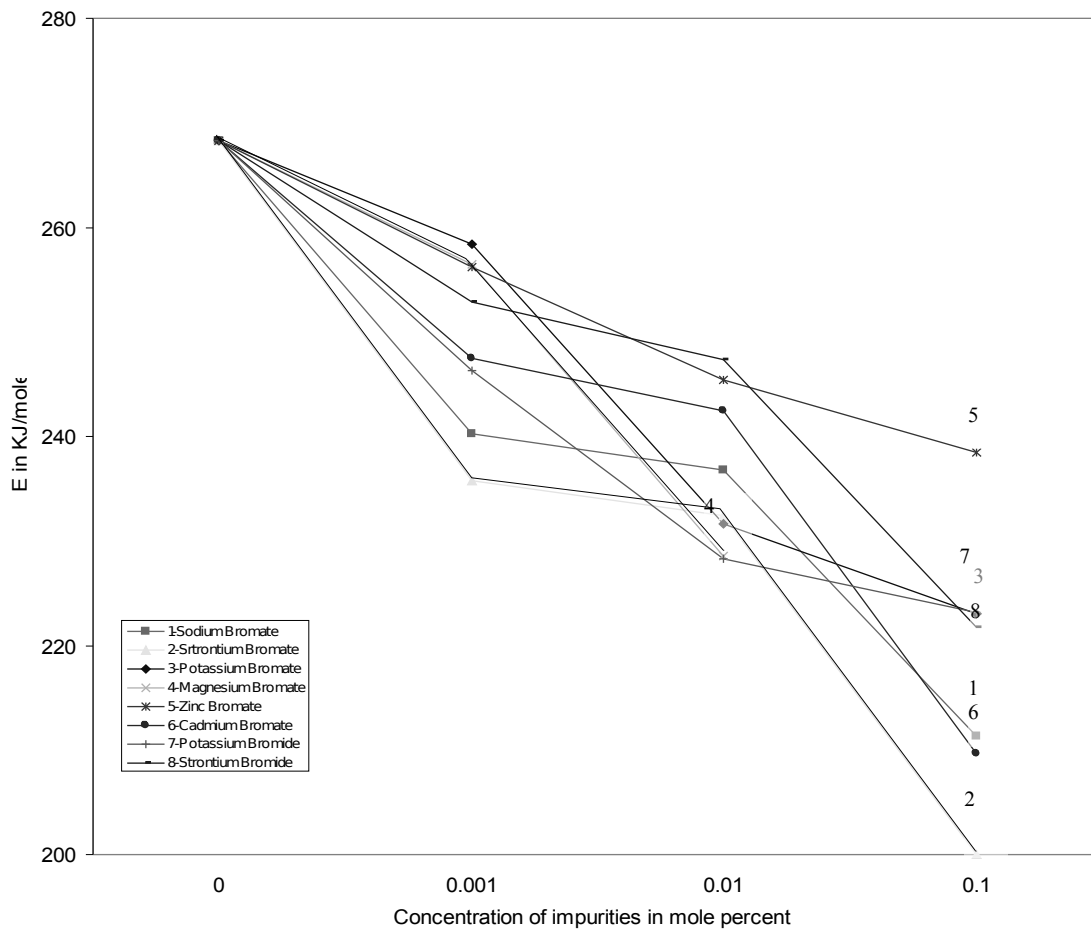


Fig 29 : Variation of E with concentration of impurities - barium bromate containing Na, K, Mg, Sr, Zn, Cd bromates and K, Sr bromides – Freeman-Carroll method

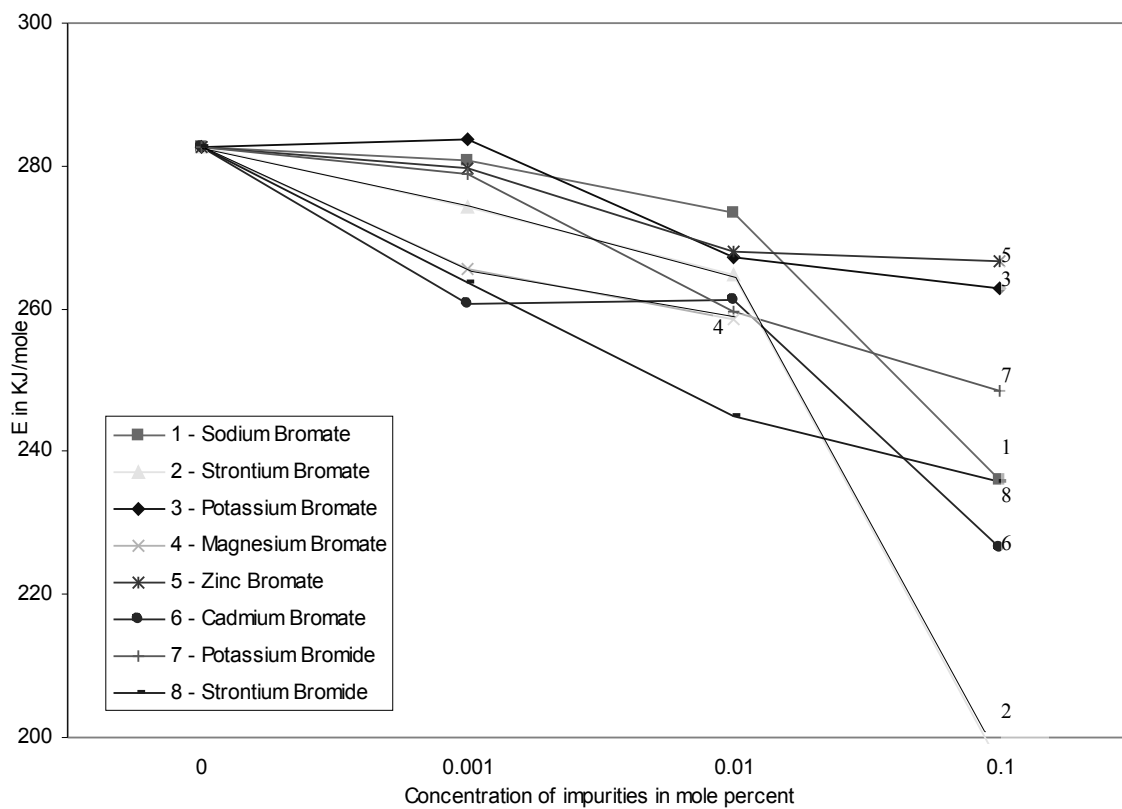
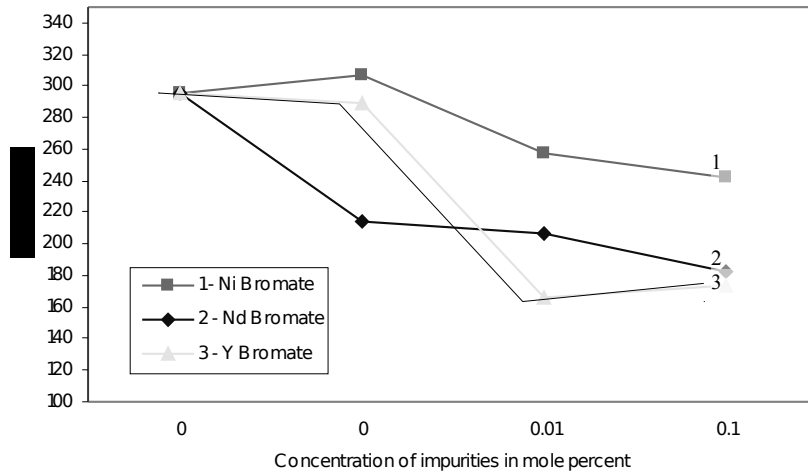
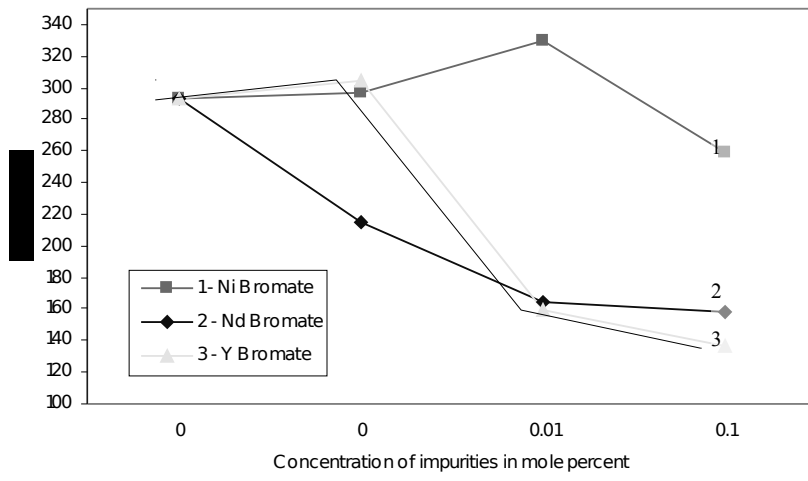


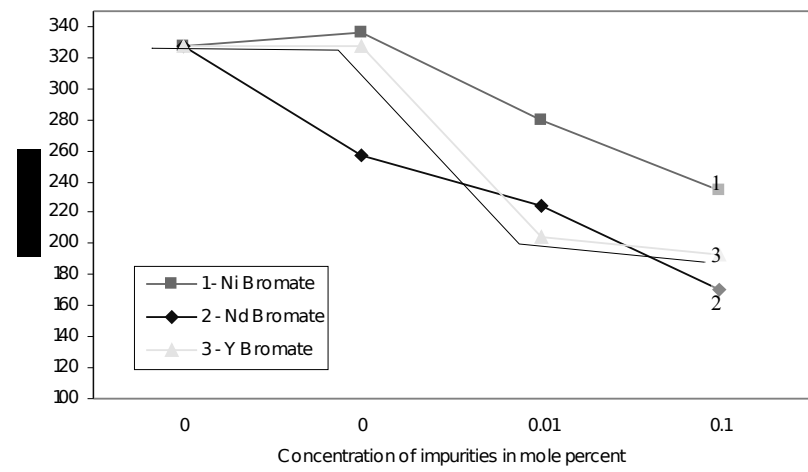
Fig 30 : Variation of E with concentration of impurities - barium bromate containing Na, K, Mg, Sr, Zn, Cd bromates and K, Sr bromides – Horowitz-Metzger method



(i)

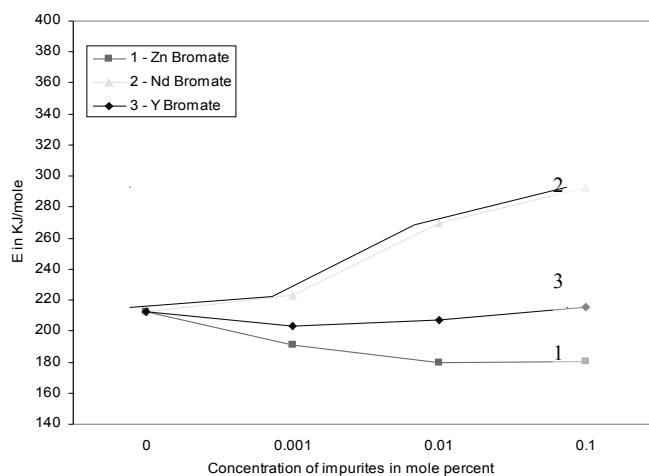


(ii)

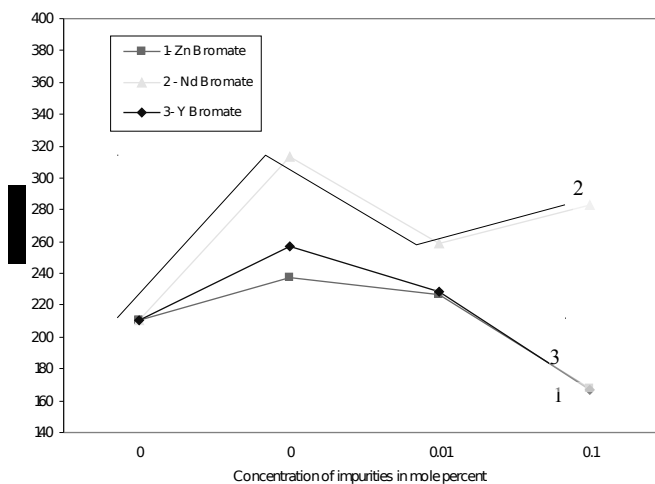


(iii)

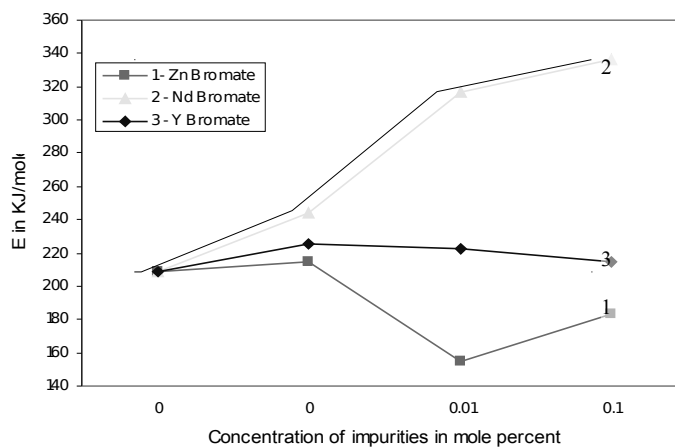
Fig 31 : Variation of E with concentration of impurities – barium bromate containing Ni, Nd and Y Bromates - (i) Coats-Redfern (ii) Freeman-Carroll (iii)Horowitz-Metzger



(i)

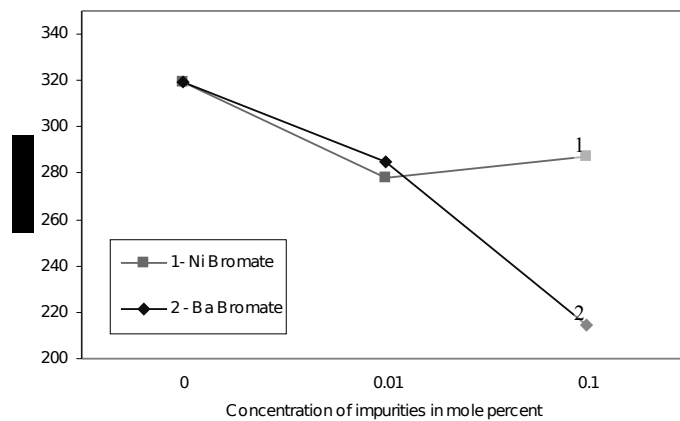


(ii)

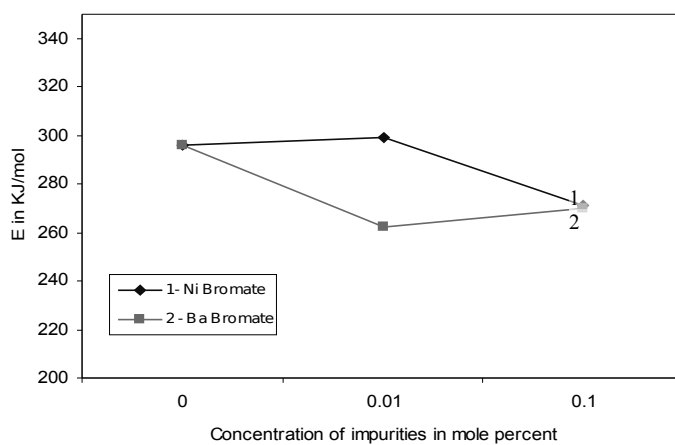


(iii)

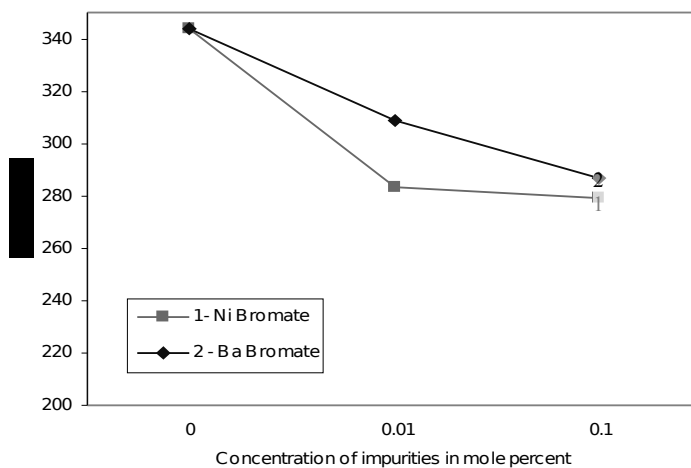
Fig 32 : Variation of E with concentration of impurities - nickel bromate containing Zn, Nd and Y bromates - (i) Coats-Redfern (ii) Freeman-Carroll (iii) Horowitz-Metzger



(i)



(ii)



(iii)

Fig 33 : Variation of E with concentration of impurities - neodymium bromate containing Ni and Ba bromates - (i) Coats-Redfern (ii) Freeman-Carroll (iii)Horowitz-Metzger

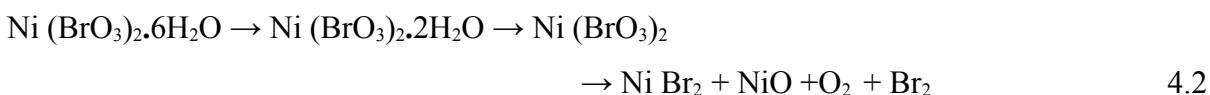
ions and this enhances the susceptibility to decomposition to a larger extent. The effect due to strontium bromide is seen to be greater than that produced by potassium bromide as the former provides two moles of bromide ions per mole of the added impurity while the latter provides only one mole of bromide ions per mole of the added impurity.

A somewhat interesting but abnormal result is obtained for barium bromate containing 10⁻¹ mole percent of Y(BrO₃)₃. In this case the TG curve - Fig. 12(iv) shows two distinct stages during the decomposition of the anhydrous bromate. The energy of activation for both the steps were calculated separately and it is found that the sum of the activation energies of these two steps is less than the energy of activation for the untreated sample. Probably at the higher concentration of 10⁻¹ M yttrium bromate in barium bromate some new stable intermediate phase may be formed between the two, but this has to be confirmed by more detailed studies.

The presence of impurities also lowers Z and ΔS (Table 54 to 61). Here also in majority of cases the lowering in Z and ΔS increases with the concentration of the impurity. The decrease in ΔS suggests that the decomposition is catalysed by the presence of the impurities.

4.1.2 Thermal decomposition of nickel bromate

As indicated in 3.1 nickel bromate loses water of hydration in two stages to form anhydrous bromate which decomposes to a mixture of NiBr₂ and NiO. The observed mass percentage of the residue is about 21%. If it were NiBr₂ alone it would be 51.8%. If it were NiO alone it would be 17.7%. As the residue is 21%, it follows that the residue contains a greater proportion of the oxide than of the bromide.



The decomposition of nickel bromate starts at 459.1 K and is complete at 504.4 K. These values are considerably less than those for barium bromate showing that nickel bromate is thermally less stable. It is found that the addition of Zn(BrO₃)₂ to Ni(BrO₃)₂ lowers T_i and T_s but increases T_f whereas addition of Nd (BrO₃)₃ increases both T_i and T_f. T_s changes only

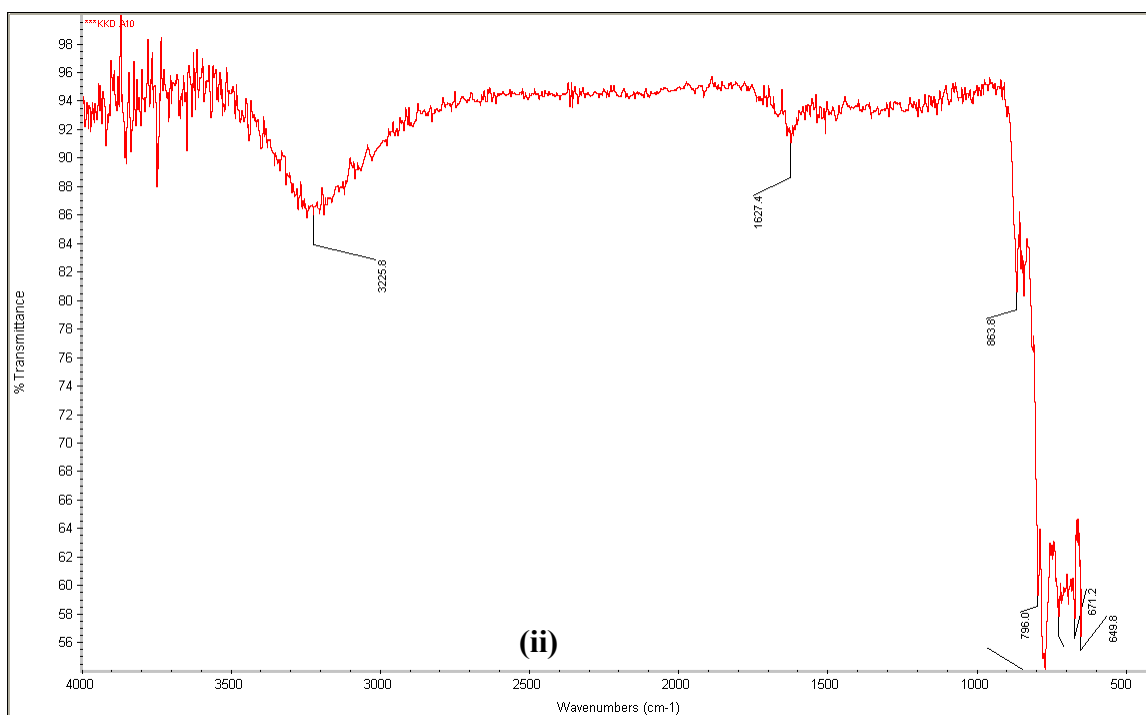
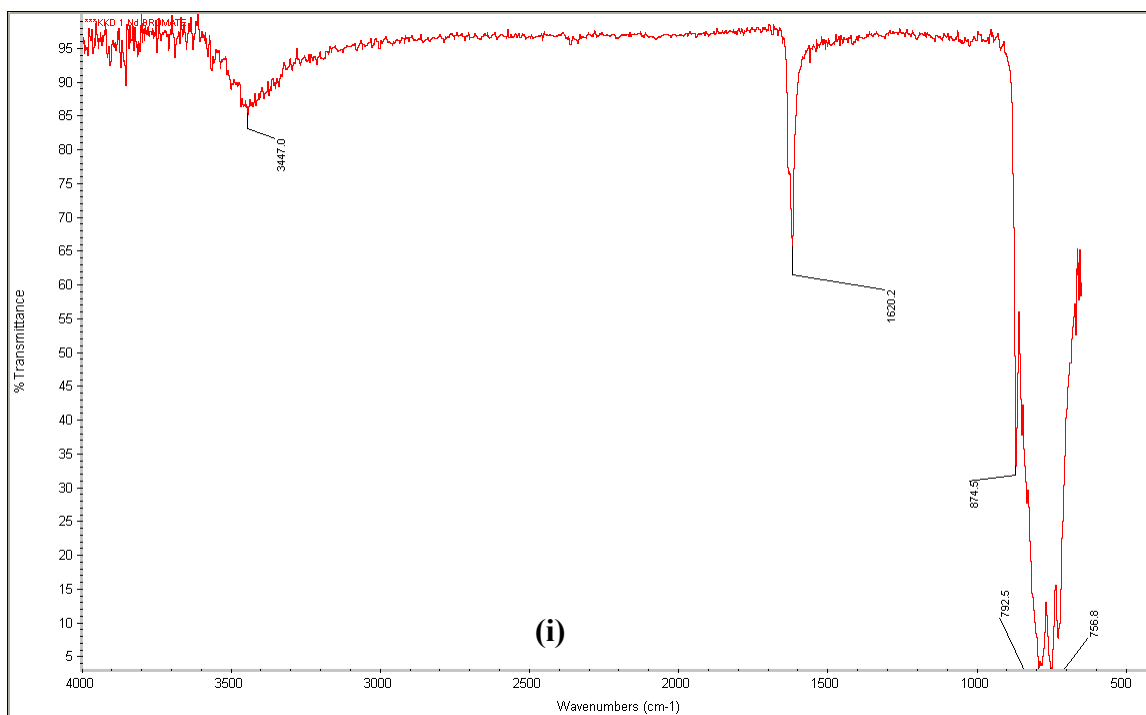


Fig. 31 : FTIR Spectrum of (i) neodymium bromate
(ii) nickel bromate containing 10^{-1} M neodymium bromate

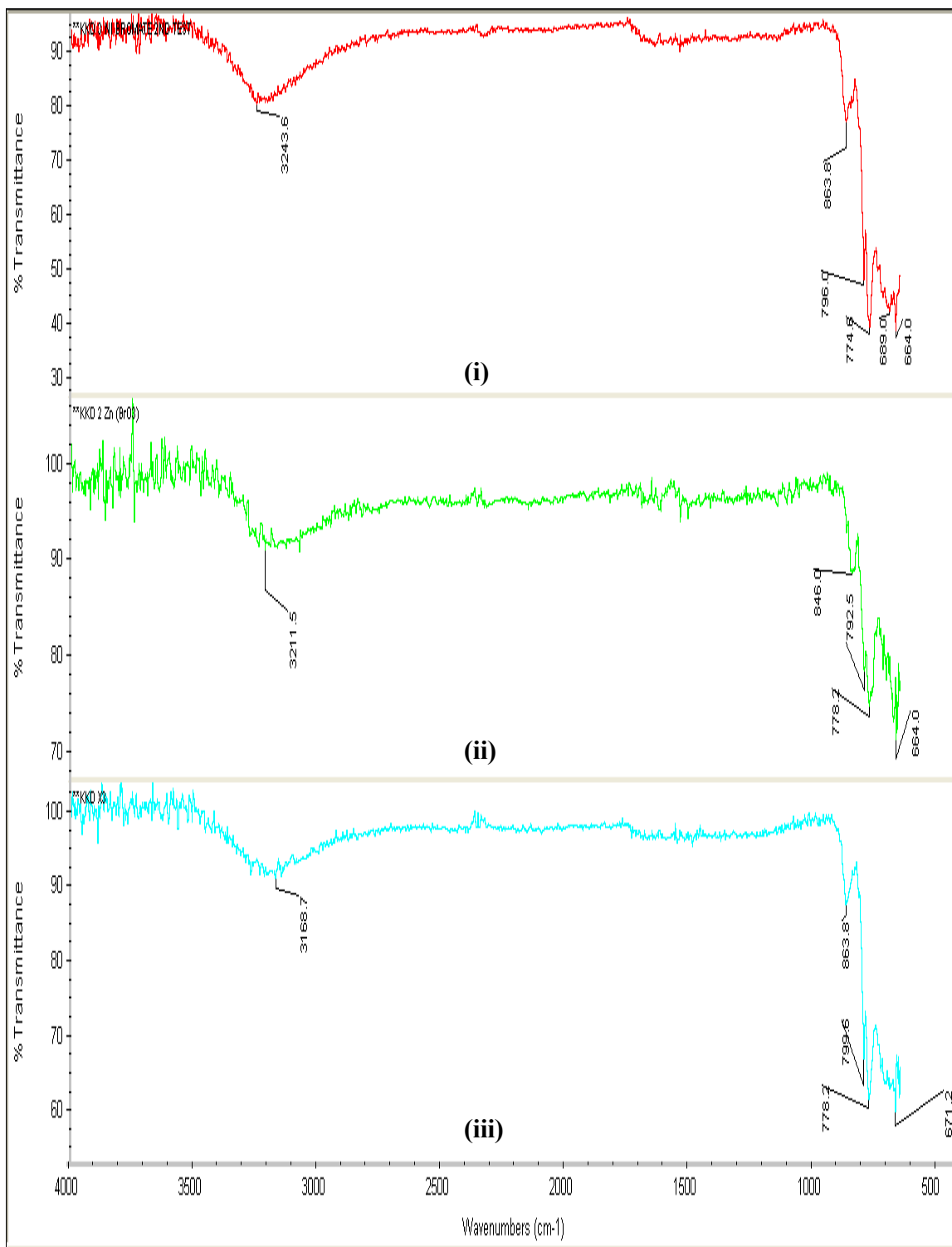


Fig. 32 : FTIR Spectrum of (i) nickel bromate (ii) zinc bromate (iii)nickel bromate containing 10⁻³ M zinc bromate

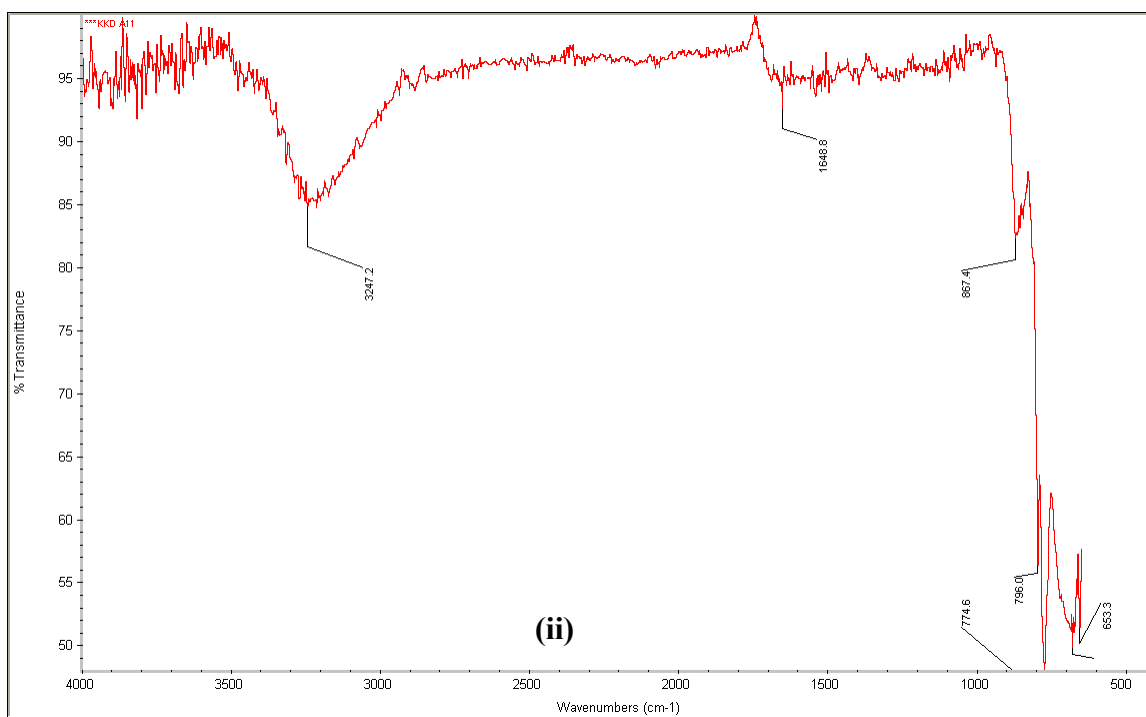
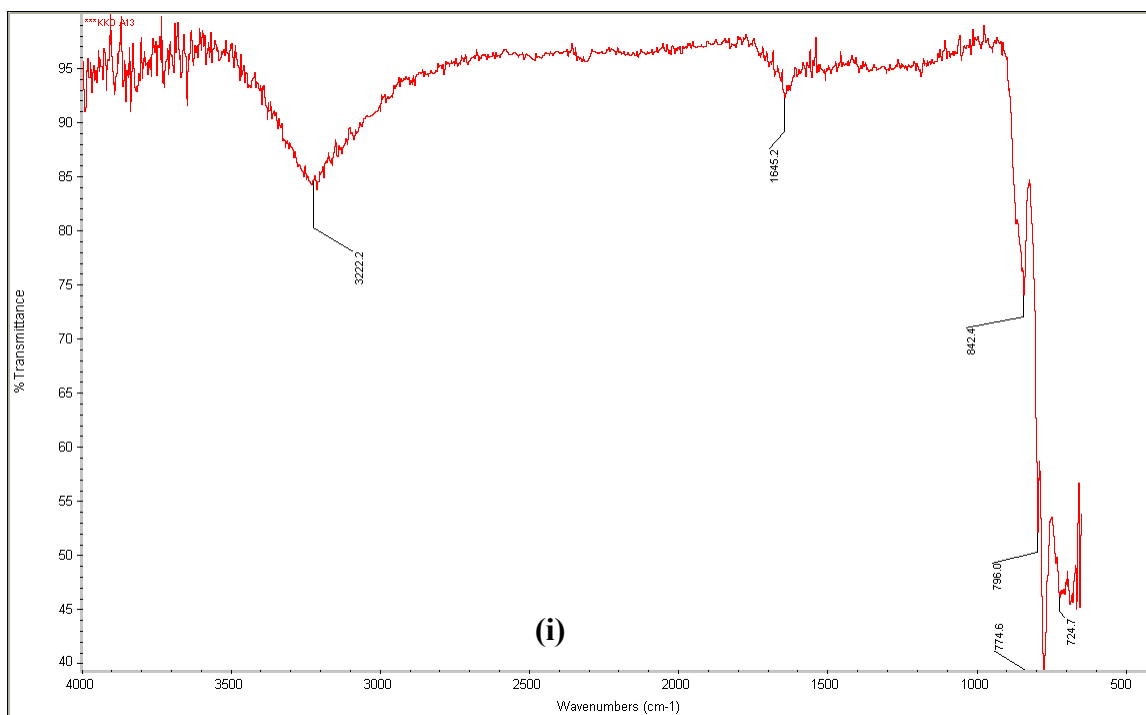


Fig. 33 : FTIR Spectrum of (i) nickel bromate containing 10^{-1} M yttrium bromate
(ii) nickel bromate containing 10^{-2} M neodymium bromate

to a negligible extent for 10^{-3} and 10^{-2} M concentrations but decreases appreciably in the case of 10^{-1} M concentration of added $\text{Zn}(\text{BrO}_3)_2$. Presence of $\text{Y}(\text{BrO}_3)_3$ as impurity lowers T_i , T_f and T_s to an appreciable extent. The activation energy of decomposition is lowered in samples of nickel bromate containing zinc bromate and yttrium bromate as intentional impurities whereas it is increased in samples containing neodymium bromate. The variation of activation energy with concentration of impurities in the case of nickel bromate are represented graphically in Fig 32.

It must be noted that in the case of transition and inner transition metal bromates, the decomposition takes place with the formation of the oxide and these oxides, as is well known, are extremely good catalysts. Thus the variation in activation energy for these decompositions can be explained as due to the combined effects of the lattice defects generated due to impurities, eutectic formation between bromide ion and bromate, catalytic effect of the bromide ion in causing the cleavage of bromate ion and also due to the catalytic effect of the metal oxide formed.

The higher value of activation energy of nickel bromate containing neodymium bromate appears to be due to the greater thermal stability of the added impurity. T_i , T_f and T_s of $\text{Nd}(\text{BrO}_3)_3$ are higher than that of $\text{Ni}(\text{BrO}_3)_2$ and the activation energy is also higher.

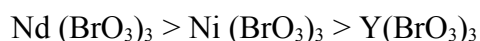
The decrease in Z is almost in tune with the lowering of activation energy but the variation in ΔS is not very regular. This is probably due to the fact that the decomposition forms the oxide and bromide in varying proportions in the presence of the added impurities and the evolution of Br_2 and O_2 during decomposition may be in varying proportions making the entropy changes irregular.

4.1.3 Thermal decomposition of neodymium bromate and yttrium bromate

The decomposition of neodymium bromate starts at 479.7 K and is complete at 515.7 K. T_i , T_f and T_s of neodymium bromate are found to be higher than that of nickel bromate.

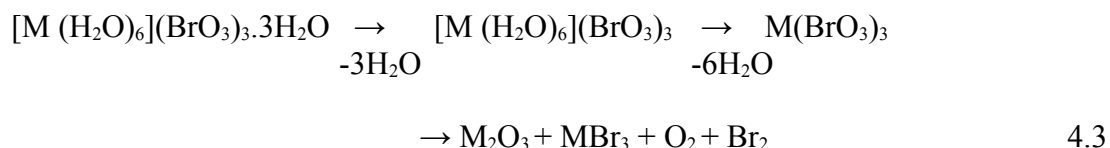
Activation energy for the decomposition of neodymium bromate is $319.4 \text{ kJ mol}^{-1}$ while it is $212.8 \text{ kJ mol}^{-1}$ for nickel bromate (Coats-Redfern method). This very clearly shows that neodymium bromate is thermally more stable than nickel bromate. Addition of nickel bromate and barium bromate to neodymium bromate lowers T_i , T_f and T_s and the activation energy of the latter, the effect being more pronounced for the added impurity nickel bromate. This also may be due to the lower thermal stability of the added impurity apart from the generated crystal defects, eutectic formation and catalytic effect of the oxide formed. The variation of activation energy with concentration of impurities for neodymium bromate is represented graphically in Fig 33.

The energy of activation for the decomposition of yttrium bromate is $163.2 \text{ kJ mol}^{-1}$, much lower than that for neodymium bromate and nickel bromate. The decomposition starts at 455.6 K and is complete at 514.3 K. T_i , T_f and T_s values for yttrium bromate are lower than those for neodymium bromate and nickel bromate. Thus the observed order of thermal stability is



Addition of nickel bromate and barium bromate as intentional impurities to yttrium bromate lowers T_i , T_f and T_s and activation energy of the latter. The effect is more with nickel bromate than with barium bromate.

For both neodymium bromate and yttrium bromate the water of hydration is lost in two stages and subsequent decomposition to a mixture of oxide and bromide (possibly through intermediate hypobromite). The scheme of decomposition thus appears to be



The residual mass after complete decomposition as read from the TG curves for neodymium bromate and yttrium bromate justify the above formulation.

4.1.4 XRD results

X-ray diffraction studies do not indicate the formation of any new phase in samples of nickel bromate treated with zinc bromate, yttrium bromate treated with nickel bromate and barium bromate treated with yttrium bromate. However in the case of barium bromate treated with neodymium bromate and nickel bromate treated with neodymium bromate there are some new peaks observed in the XRD plots indicating new phase formation. The plots also indicate that the added impurity cations get doped in the host crystal to a good extent. Thus the impurities function as dopants, create defects in crystals and catalyse the decomposition by lowering the activation energy.

4.1.5 FTIR results

Regarding IR studies, all the samples studied give characteristic absorptions due to –O–H symmetric and antisymmetric stretching, H–O–H bending and the $\nu_1(A_1)$ and $\nu_3(E)$ characteristic of the vibrations of the pyramidal BrO_3^- ion¹⁴⁶ ion where A_1 and E refer to the symmetry of the vibrational modes. It is found that these absorptions get shifted to slightly lower or higher values in the treated samples. However, any quantitative conclusion cannot be arrived at relating to the extent of the shift in frequencies and the nature and concentration of the cationic impurity added. Water in inorganic salts may remain as lattice water, that is, water trapped in the crystalline lattice either by weak hydrogen bonds to the anion or by weak ionic bonds to the metal or both or as coordinated water.

The shift in absorption frequencies of lattice water and coordinated water takes place as they are highly sensitive to the changes in their surrounding as brought about by the addition of the impurity cations. However, a quantitative conclusion cannot be arrived at on the basis of the available results in the present studies.

4.2 Mechanism of Thermal Decomposition

The mechanism of the thermal decomposition of bromates was established by following the non-isothermal method proposed by Sestak and Berggren^{147,148}, Satava¹⁴⁹⁻¹⁵³, and Somasekharan and Kalpagam¹⁵⁴. The procedure adopted by Satava¹⁴⁹ in unraveling the mechanism is based on the argument that the non-isothermal decomposition proceeds in an infinitesimal time interval isothermally where the rate of decomposition may be expressed as

$$\frac{d\alpha}{dt} = Z e^{\frac{-E}{RT}} \cdot f(\alpha) \quad 4.4$$

where α is the fraction decomposed in time t and $f(\alpha)$ is a function of α which depends on the mechanism of the decomposition. With a constant temperature increase $\frac{dT}{dt} = a$, the heating rate, the integration of (4.4) gives

$$g(\alpha) = \int_0^{\alpha} \frac{d\alpha}{f(\alpha)} = \frac{ZE}{aR} p(x) \quad 4.5$$

where $g(\alpha)$ is a new function of α which depends on the mechanism of the process and $p(x)$ is a function defined by

$$p(x) = \frac{e^{-x}}{x} - \int_x^{\infty} \frac{e^{-u}}{u} du \quad 4.6$$

or,

$$p(x) = \frac{e^{-x}}{x} + Ei(-x) \quad 4.7$$

where $u = \frac{E}{RT}$ and $x = \frac{E}{RT_{\alpha}}$ where T_{α} is the temperature at which the fraction α of the sample has reacted.

Writing (4.5) in the logarithmic form

$$\ln g(\alpha) - \ln p(x) = \ln \frac{ZE}{Ra} \quad 4.8$$

The LHS of the equation (4.8) is temperature dependent while the RHS is temperature independent. When x is sufficiently large, to a first approximation, the function $\ln p(x)$ is

linear with respect to $\frac{1}{T}$ and so for the correct mechanism, $\ln g(\alpha)$ versus $\frac{1}{T}$ should be a straight line. E is related to the slope(S) of the straight line in the form

Table 63
Computation of E & Z using the mechanism based equation for barium bromate

Temp K	(1/T)10 ³	Mass of sample	Mass loss	Fraction decompsed α	lnD ₁	lnD ₂	lnD ₃	lnD ₄	lnF ₁	lnA ₂	lnA ₃	lnR ₂	lnR ₃
565	1.77	100	---	----	---	---	----	----	----	----	----	----	-----
571	1.7153	99.89	0.11	0.005	-10.59663	-11.28754	-12.79051	-12.66526	-6.29582	-2.64791	-1.76527	-5.99023	-6.3952
577	1.7331	99.67	0.33	0.014	-8.5374	-9.22583	-10.72524	-10.6849	-4.26165	-213082	-1.42055	-4.95834	-5.3626
583	1.7153	99.34	0.66	0.027	-7.22384	-7.90778	-9.40288	-9.38773	-3.59827	-1.79915	-1.19942	-4.29827	-4.7014
589	1.6978	99.85	1.15	0.047	-6.11522	-6.79246	-8.2805	-8.27873	-3.03364	-1.51681	-1.01121	-3.73878	-4.1402
595	1.6807	97.98	2.02	0.083	-4.97783	-5.6425	-7.11785	-7.13006	-2.4459	-1.22295	-0.81529	-3.16063	-3.5589
601	1.6639	96.48	3.52	0.144	-3.87588	-4.51853	-5.97123	-6.00164	-1.86124	-0.93059	-0.6204	-2.59298	-2.9856
607	1.6474	94.94	5.06	0.207	-3.15007	-3.78888	-5.19666	-5.24493	-1.46132	-0.73066	-0.48711	-2.21192	-2.5983
613	1.6313	92.41	7.59	0.311	-2.33592	-2.91253	-4.29504	-4.37446	-0.98749	-0.49359	-0.32916	-1.77231	-2.1476
619	1.6155	87.67	12.33	0.505	-1.36639	-1.85202	-3.13128	-3.28041	-0.35211	-0.17606	-0.11738	-1.21591	-1.5657
625	1.6	76.21	23.79	0.974	-0.05269	-0.12885	-0.70267	-1.33572	1.29464	0.64731	0.43152	-0.17584	-0.3513
631	1.5848	75.88	24.12	0.988	-0.02414	-0.06728	-0.51998	-1.2414	1.48677	0.74341	0.49561	-0.11602	-0.26
Intercept					99.3975	104.681	112.22	105.2583	67.1736	31.2905	20.86	54.2782	56.1097
Slope					-62.3122	-65.8045	-71.096	-66.9974	-41.5054	-19.3467	-12.8976	-34.2388	-35.548
Correlation coefficient					0.9928	0.9947	0.9941	0.9954	0.9823	0.9811	0.9891	0.9949	0.9941

Computation of E & Z using mechanism based equation for nickel bromate

Temp K	(1/T) 10 ³	Mass of Sample mg	Mass loss W mg	Fraction decomposed α	ln D ₁	ln D ₂	ln D ₃	ln D ₄	ln F ₁	ln A ₂	ln A ₃	ln R ₂	ln R ₃
459.10	2.1782	100.00	--	--	--	--	--	--	--	--	--	--	--
463.09	2.1594	98.91	1.09	0.01	-8.84570	-9.53431	-11.03489	-10.99009	-4.41678	-2.21338	-1.47219	-5.11298	-5.51744
467.11	2.1408	98.34	1.66	0.02	-8.03477	-8.72158	-10.21993	-10.19298	-4.00831	-2.00419	-1.33610	-4.70601	-5.10996
471.12	2.1226	97.87	2.13	0.02	-7.54452	-8.23164	-9.72628	-9.70601	-3.76063	-1.88033	-1.25355	-4.45960	-4.86314
475.08	2.1049	97.32	2.68	0.03	-7.08092	-7.76429	-9.25860	-9.24535	-3.52577	-1.76288	-1.17526	-4.22625	-4.62930
479.08	2.0873	96.59	3.41	0.04	-6.64847	-7.32941	-8.82134	-8.81311	-3.30596	-1.65323	-1.10199	-4.00826	-4.41067
483.09	2.0700	95.66	4.34	0.05	-6.15823	-6.83571	-8.32422	-8.32216	-3.05565	-1.52781	-1.01827	-3.76055	-4.16209
487.09	2.0530	94.26	5.74	0.06	-5.59376	-6.26611	-7.74933	-7.75384	-2.76557	-1.38278	-0.92186	-3.47441	-3.87468
491.08	2.0363	92.12	7.88	0.08	-4.95388	-5.61819	-7.09318	-7.10586	-2.43339	-1.21669	-0.81112	-3.14839	-3.54658
495.09	2.0198	89.31	10.69	0.11	-4.34311	-4.99672	-6.46076	-6.48255	-2.11163	-1.05581	-0.70388	-2.83491	-3.23037
499.09	2.0036	83.07	16.93	0.18	-3.42960	-4.05878	-5.49745	-5.53802	-1.61722	-0.80860	-0.53907	-2.35957	-2.74872
501.05	1.9958	75.08	24.92	0.26	-2.65605	-3.25179	-4.65503	-4.72030	-1.17805	-0.58902	-0.39267	-1.94715	-2.32751
503.10	1.9877	6.11	93.89	1.00	-0.00400	-0.01454	-0.26933	-1.14300	1.82690	0.91345	0.60895	-0.04575	-0.13466
504.46	1.9823	5.94	94.06	1.00	$\log \left[\frac{\alpha \log(1-\alpha)}{w_r T^2} \right]$								
Intercept					78.7129	81.6376	86.2244	81.5267	48.2917	24.1718	16.0969	41.9768	49.8365
Slope					-40.7503	-42.4624	-45.3487	-43.1104	-24.6094	-12.3175	-8.2029	-21.9442	-25.9894
Correlation Coefficient					0.9432	0.9279	0.8979	0.9180	0.8572	0.8576	0.8572	0.9131	0.8746

Table 65

Computation of E & Z using mechanism based equation for neodymium bromate

Temp K	(1/T) 10 ³	Mass of Sample mg	Mass loss W mg	Fraction decomposed α	ln D ₁	ln D ₂	ln D ₃	ln D ₄	ln F ₁	ln A ₂	ln A ₃	ln R ₂	ln R ₃
479.71	2.0846	100.00	--	--	--	--	--	--	--	--	--	--	--
483.70	2.0674	98.86	1.14	0.02	-7.82405	-8.51042	-10.00783	-9.98266	-3.90192	-1.95094	-1.30063	-4.60018	-5.00392
487.70	2.0504	97.61	2.39	0.04	-6.29311	-6.97170	-8.46119	-8.45718	-3.12466	-1.56232	-1.04115	-3.82879	-4.23058
491.70	2.0338	95.88	4.12	0.07	-5.23459	-5.90276	-7.38172	-7.39069	-2.57963	-1.28982	-0.85989	-3.29166	-3.69084
495.70	2.0173	92.76	7.24	0.13	-4.09589	-4.74404	-6.20463	-6.22855	-1.97970	-0.98983	-0.65989	-2.70716	3.10123
499.70	2.0012	88.66	11.34	0.20	-3.19898	-3.81972	-5.24955	-5.29638	-1.48877	-0.74440	-0.49627	-2.23783	-2.62478
503.71	1.9853	82.40	17.60	0.31	-2.31672	-2.89206	-4.27321	-4.35556	-0.97583	-0.48792	-0.32527	-1.76172	-2.13656
507.69	1.9697	69.68	30.32	0.54	-1.23237	-1.69936	-2.95364	-3.12047	-0.25292	-0.12646	-0.08431	-1.33392	-1.47815
511.69	1.9543	48.07	51.93	0.93	-0.15542	-0.31371	-1.09539	-1.58207	0.95177	0.47584	0.31729	0.32001	-0.54770
515.71	1.9391	43.89	56.11	1.00									
Intercept					127.5674	134.4262	142.6168	135.6538	77.6667	38.8325	25.8862	74.4277	71.3315
Slope					-65.3565	-69.0490	-73.7941	-70.3787	-39.4720	-19.7356	-13.1560	-38.2393	-36.9103
Correlation Coefficient					0.9982	0.9980	0.9954	0.9974	0.9902	0.9902	0.9902	0.9787	0.9954

Table 66

Computation of E & Z using mechanism based equation for yttrium bromate

Temp K	(1/T) 10 ³	Mass of Sample mg	Mass loss W mg	Fraction decompd α	$\log \left[\frac{w_0 \log(1-\alpha)}{w_r T^2} \right]$	ln D ₁	ln D ₂	ln D ₃	ln D ₄	ln F ₁	ln A ₂	ln A ₃	ln R ₂	ln R ₃
455.60	2.1949	100.00	--	--	--	--	--	--	--	--	--	--	--	--
460.60	2.1711	98.70	1.30	0.02	-7.63343	-8.32105	-9.81586	-9.79499	-3.80559	-1.90280	-1.26855	-4.50433	-4.90793	
465.61	2.1477	96.18	3.82	0.06	-5.52924	-6.20090	-7.68339	-7.68864	-2.73226	-1.36614	-0.91076	-3.44164	-3.84170	
470.60	2.1250	92.69	7.31	0.12	-4.22393	-4.87500	-6.33644	-6.36021	-2.04818	-1.02410	-0.68272	-2.77339	-3.16821	
475.60	2.1026	89.77	10.23	0.17	-3.54391	-4.17690	-5.61949	-5.65725	-1.68024	-0.84012	-0.56009	-2.41960	-2.80975	
480.60	2.0807	86.80	13.20	0.22	-3.03737	-3.65151	-5.07433	-5.12606	-1.39764	-0.69882	-0.46588	-2.15193	-2.53717	
485.60	2.0593	83.28	16.72	0.28	-2.56748	-3.15830	-4.55628	-4.62515	-1.12593	-0.56298	-0.37532	-1.89906	-2.27809	
490.61	2.0383	78.51	21.49	0.36	-2.06565	-3.62274	-3.98384	-4.07778	-0.82084	-0.41042	-0.27362	-1.62202	-1.99194	
495.61	2.0177	70.48	29.52	0.49	-1.43079	-1.92470	-3.21366	-3.35624	-0.39841	-0.19921	-0.13280	-1.25470	-1.60684	
500.59	1.9976	59.74	40.26	0.67	-0.80993	-1.20121	-2.36266	-2.59096	0.09495	0.04746	0.03169	-0.86052	-1.18133	
505.59	1.9779	49.61	50.39	0.84	-0.36065	-0.62045	-1.59027	-1.94799	0.58879	0.29438	0.19622	-0.52121	-0.79514	
510.62	1.9584	41.71	58.29	0.97										
514.34	1.9442	39.66	60.34	1.00										
Intercept					65.9081	67.3914	72.6519	69.2257	39.9781	19.9890	13.3261	35.5358	37.3458	
Slope					-33.3183	-34.3504	-37.4920	-35.8860	-19.9396	-9.9698	-6.6466	-18.1875	-19.259	
Correlation Coefficient					0.9703	0.9631	0.9804	0.9778	0.9835	0.9835	0.9835	0.9784	0.9883	

$$E = \frac{(-449 + S/2.303)}{217} \times 4.184 \text{ KJ mol}^{-1} \quad 4.9$$

or by the method due to Satava¹⁵⁰

$$E = \frac{1.987 \left(-S + \sqrt{S^2 + 8ST_s} \right)}{2 \times 10^3} \times 4.184 \text{ KJ mol}^{-1} \quad 4.10$$

In the present study, the equation 4.9 has been used for the calculation of E for all the samples. The intercept of the line gives ln Z from which Z can be calculated.

The equations relating to the different types of mechanisms discussed for solid state decompositions are given in Table 67. Tables 63 to 66 illustrate the computational approach to obtain E and Z for the decomposition of the various samples citing untreated barium bromate, nickel bromate, neodymium bromate and yttrium bromate as examples. The functional values of ln g(α) required for this purpose were taken from the table of Nair and James¹⁵⁵ and E was calculated using equation (4.9). For almost the same value of correlation coefficient, r, the operating mechanism was chosen by comparison of the values with non-mechanistic equation. It was found that mechanism taking the function ln R₃ gives very good correlation in the case of barium bromate (Table 63) and the E value calculated agrees with that obtained by Coats-Redfern method (Tables 54 and 68). Thus the thermal decomposition of Ba(BrO₃)₂ and the samples containing the intentional impurities corresponds to the Avrami equation¹⁵⁶,

$$1 - (1 - \alpha)^{1/3} = kt \quad 1.25$$

suggesting that the rate controlling process is a phase boundary reaction assuming spherical symmetry. Though the impurities do influence the rate of the decomposition and alters the thermodynamic parameters vital for the reaction, the mechanism of the reaction remains unaltered.

Table 67

Solid state decomposition – Mechanistic Equations

Function	Equation	Rate controlling process
D ₁	$x^2 = kt$	One-dimensional diffusion
D ₂	$(1 - \alpha) \ln(1 - \alpha) + \alpha = kt$	Two-dimensional diffusion, cylindrical symmetry
D ₃	$[1 - (1 - \alpha)^{1/3}]^2 = kt$	Three-dimensional diffusion, spherical symmetry; Jander equation
D ₄	$[1 - 2/3 \alpha] - (1 - \alpha)^{2/3} = kt$	Three-dimensional diffusion, spherical symmetry; Ginstling-Brounshtein equation
F ₁	$-\ln(1 - \alpha) = kt$	Random nucleation, one nucleus on each particle
A ₂	$[-\ln(1 - \alpha)]^{1/2} = kt$	Random nucleation; Avrami equation I
A ₃	$[-\ln(1 - \alpha)]^{1/3} = kt$	Random nucleation; Avrami equation II
R ₂	$1 - (1 - \alpha)^{1/2} = kt$	Phase boundary reaction, cylindrical symmetry
R ₃	$1 - (1 - \alpha)^{1/3} = kt$	Phase boundary reaction, spherical symmetry

Table 68

Kinetic parameters calculated using the mechanism based equation $1-(1-\alpha)^{1/3} = kt$

Sample No	Sample Ba(BrO ₃) ₂	Parameters				
		Intercept	Slope	Correlation co-efficient	E (kJ mol ⁻¹)	Z (min ⁻¹)
1(i)	Untreated Ba(BrO ₃) ₂	56.11	-35.55	0.9941	284.8	2.3 ' 10 ²⁴
	Containing NaBrO ₃					
2	10 ⁻³ M	52.05	-33.16	0.9911	264.5	4.0 ' 10 ²²
3	10 ⁻² M	48.73	-31.37	0.9972	249.9	1.5 ' 10 ²¹
4	10 ⁻¹ M	40.56	-26.51	0.9881	209.2	4.1 ' 10 ¹⁷
	Containing KBrO ₃					
5	10 ⁻³ M	55.12	-35.09	0.9910	281.0	7.4 ' 10 ²³
6	10 ⁻² M	51.72	-32.95	0.9935	263.2	2.9 ' 10 ²²
7	10 ⁻¹ M	52.58	-33.40	0.9944	266.9	6.8 ' 10 ²²
	Containing Mg(BrO ₃) ₂					
8	10 ⁻³ M	52.78	-33.32	0.9935	276.0	8.4 ' 10 ²²
9	10 ⁻² M	46.78	-29.70	0.9930	236.2	2.1 ' 10 ²⁰
	Containing Sr(BrO ₃) ₂					
10	10 ⁻³ M	51.55	-32.83	0.9904	262.2	2.4 ' 10 ²²
11	10 ⁻² M	47.28	-30.25	0.9977	240.7	3.4 ' 10 ²⁰
12	10 ⁻¹ M	32.09	20.75	0.9975	161.5	8.7 ' 10 ¹³

Table 69

Kinetic parameters calculated using the mechanism based equation $1-(1-\alpha)^{1/3} = kt$

Sample No	Sample Ba(BrO ₃) ₂	Parameters				
		Intercept	Slope	Correlation co-efficient	E (kJ mol ⁻¹)	Z (min ⁻¹)
1(i)	Untreated Ba(BrO ₃) ₂	56.11	-35.55	0.9941	284.8	2.3 × 10 ²⁴
	Containing Zn(BrO ₃) ₂					
13	10 ⁻³ M	53.18	-33.72	0.9931	269.6	1.2 × 10 ²³
14	10 ⁻² M	48.30	-30.72	0.9887	244.6	9.5 × 10 ²⁰
15	10 ⁻¹ M	46.84	-29.94	0.9990	238.1	2.2 × 10 ²⁰
	Containing Cd(BrO ₃) ₂					
16	10 ⁻³ M	51.40	-32.44	0.9919	259.0	2.1 × 10 ²²
17	10 ⁻² M	49.84	-31.63	0.9869	252.3	4.4 × 10 ²¹
18	10 ⁻¹ M	42.25	-26.91	0.9910	212.9	2.2 × 10 ¹⁸
	Containing KBr					
19	10 ⁻³ M	56.33	-35.58	0.9943	285.1	2.9 × 10 ²⁴
20	10 ⁻² M	53.90	-34.20	0.9944	273.8	2.5 × 10 ²³
21	10 ⁻¹ M	41.92	-26.88	0.9840	212.7	1.6 × 10 ¹⁸
	Containing SrBr ₂					
22	10 ⁻³ M	49.62	-31.32	0.9918	249.7	3.6 × 10 ²¹
23	10 ⁻² M	40.46	-25.80	0.9913	203.7	3.7 × 10 ¹⁷
24	10 ⁻¹ M	40.93	-26.19	0.9951	206.9	6.0 × 10 ¹⁶

Table 70

Kinetic parameters calculated using the mechanism based equation $1-(1-\alpha)^{1/3} = kt$

Sample No	Sample Ba(BrO ₃) ₂	Parameters				
		Intercept	Slope	Correlation co-efficient	E (kJ mol ⁻¹)	Z (min ⁻¹)
1(ii)	Untreated Ba(BrO ₃) ₂	57.07	-35.71	0.9965	290.3	6.0 x 10 ²⁴
	Containing Ni(BrO ₃) ₂					
25	10 ⁻³ M	61.37	-37.65	0.9994	306.5	4.4 x 10 ²⁶
26	10 ⁻² M	40.39	-24.87	0.9594	199.6	3.4 x 10 ¹⁷
27	10 ⁻¹ M	28.04	-17.57	0.9863	138.4	1.5 x 10 ¹²
	Containing Nd(BrO ₃) ₃					
28	10 ⁻³ M	42.07	-26.21	0.9928	210.8	1.9 x 10 ¹⁸
29	10 ⁻² M	28.22	-17.69	0.9739	156.8	1.8 x 10 ¹²
30	10 ⁻¹ M	26.50	-16.68	0.9692	131.0	3.2 x 10 ¹¹
	Containing Y(BrO ₃) ₃					
31	10 ⁻³ M	56.70	-35.19	0.9981	286.0	4.2 x 10 ²⁴
32	10 ⁻² M	33.14	-20.66	0.9937	164.3	2.5 x 10 ¹⁴
33(i)	10 ⁻¹ M	42.47	-21.58	0.9630	159.1	1.0 x 10 ¹⁷
33(ii)	10 ⁻¹ M	18.31	-11.98	0.9812	91.6	9.5 x 10 ⁷

Table 71

Kinetic parameters calculated using the mechanism based equation $1-(1-\alpha)^{1/3} = kt$

Sample No	Sample Ni(BrO ₃) ₂	Parameters				
		Intercept	Slope	Correlation co-efficient	E (kJ mol ⁻¹)	Z (min ⁻¹)
34	Untreated Ni(BrO ₃) ₂	43.11	-22.67	0.8746	208.9	4.4 x 10 ²¹
	Containing Zn(BrO ₃) ₂					
35	10 ⁻³ M	42.57	-21.96	0.9640	175.2	3.1 x 10 ¹⁸
36	10 ⁻² M	41.00	-21.40	0.9325	170.0	6.4 x 10 ¹⁷
37	10 ⁻¹ M	42.20	-21.56	0.9908	171.8	2.3 x 10 ¹⁸
	Containing Nd(BrO ₃) ₃					
38	10 ⁻³ M	51.84	-26.77	0.9961	215.4	3.2 x 10 ²²
39	10 ⁻² M	68.46	-32.93	0.9943	267.0	1.5 x 10 ²⁸
40	10 ⁻¹ M	67.47	-34.22	0.9989	277.9	2.0 x 10 ²⁹
	Containing Y(BrO ₃) ₃					
41	10 ⁻³ M	47.50	-24.26	0.9784	194.4	4.2 x 10 ²⁰
42	10 ⁻² M	43.70	-22.25	0.9657	177.6	9.4 x 10 ¹⁸
43	10 ⁻¹ M	45.89	-22.99	0.9903	183.8	8.5 x 10 ¹⁹

Table 72

Kinetic parameters calculated using the mechanism based equation $1-(1-\alpha)^{1/3} = kt$

Sample No	Sample Nd(BrO ₃) ₃	Parameters				
		Intercept	Slope	Correlation co-efficient	E (kJ mol ⁻¹)	Z (min ⁻¹)
44	Untreated Nd(BrO ₃) ₃	71.33	-36.91	0.9954	300.4	9.4 x 10 ³⁰
	Containing Ni(BrO ₃) ₂					
45	10 ⁻² M	64.18	-33.22	0.9966	269.4	7.4 x 10 ²⁷
46	10 ⁻¹ M	59.78	-31.07	0.9982	251.5	9.1 x 10 ²⁵
	Containing Ba(BrO ₃) ₂					
47	10 ⁻² M	72.30	-37.20	0.9916	302.8	2.5 x 10 ³¹
48	10 ⁻¹ M	66.80	-34.22	0.8767	277.8	1.02 x 10 ²⁹

Table 73

Kinetic parameters calculated using the mechanism based equation $1-(1-\alpha)^{1/3} = kt$

Sample No	Sample Y(BrO ₃) ₃	Parameters				
		Intercept	Slope	Correlation co-efficient	E (kJ mol ⁻¹)	Z (min ⁻¹)
49	Untreated Y(BrO ₃) ₃	37.35	-19.26	0.9883	152.6	1.6 x 10 ¹⁶
	Containing Ni(BrO ₃) ₂					
50	10 ⁻² M	35.03	-18.03	0.9878	142.3	1.6 x 10 ¹⁵
51	10 ⁻¹ M	30.54	-15.80	0.9856	123.6	1.8 x 10 ¹³
	Containing Ba(BrO ₃) ₂					
52	10 ⁻¹ M	30.28	-15.61	0.9891	122.0	1.4 x 10 ¹³

In the case of nickel bromate fairly good correlation is obtained in the case of the functions $\ln D_1$ (one dimensional diffusion), $\ln D_2$ (two dimensional diffusion with cylindrical symmetry), $\ln D_4$ (three dimensional diffusion with spherical symmetry), $\ln D_4$ (three dimensional diffusion with cylindrical symmetry). However, the correlation is less for $\ln R_3$ (phase boundary reaction with spherical symmetry) - Table 64. Thus it becomes difficult to propose the exact mechanism of decomposition. Such instances do happen as reported in literature that in some cases it is difficult to distinguish between certain mechanisms¹⁵⁷. Sometimes we may have different models giving the same equation and the same model giving perhaps two or three alternative expressions¹⁵⁸. For instance, according to Dollimore, in both ‘contracting area’ and ‘contracting sphere’ models as the particle size diminishes the model predicts first a zero order, then a first order relationship and finally a contracting area or contracting volume equation.¹⁵⁸.

The calculated values of E and Z for nickel bromate and samples of nickel bromate containing intentional impurities based on $\ln R_3$ are given in Table 71. Except for some cases, the values agree with that calculated by Coats-Redfern equation. On the basis of all the above discussion it may be concluded that thermal decomposition of nickel bromate fits somewhat fairly well with the equation of “contracting cube”,

$$1 - (1 - \alpha)^{1/3} = kt \quad 1.25$$

and the rate controlling process is most probably a phase boundary reaction with spherical symmetry.

For yttrium bromate good correlation is observed for functions $\ln D_3$, $\ln F_1$, $\ln A_2$, $\ln A_3$ and $\ln R_3$ (Table 66). But the calculated values of E and Z based on $\ln R_3$ suit well with the values obtained by Coats-Redfern method (Table 73). Thus it is concluded that the rate controlling process in the thermal decomposition of yttrium bromate too is most probably a phase boundary reaction with spherical symmetry and obeying the equation of contracting cube (1.25).

For neodymium bromate good correlation is obtained for almost all the functions (Table 65). However calculation of E and Z using $\ln R_3$ gives values very close to the experimental values computed using Coats-Redfern method (Table 72).

This indicates that the thermal decomposition of neodymium bromate and samples of neodymium bromate containing impurities also obey the equation of contracting cube (1.25). Consolidation of the findings lead to the conclusion that the presence of impurities, though does tune the rate of decomposition, does not alter the mechanism of decomposition of barium bromate, nickel bromate, neodymium bromate and yttrium bromate. In other words, the mechanistic pathway of the decomposition of BrO_3^- ion virtually remains unchanged irrespective of cation (or cations) with which it is associated in the solid state.

4.3 Conclusion

The investigations reported in this thesis are concerned with the thermal decomposition of barium bromate, nickel bromate, neodymium bromate and yttrium bromate and the effect of intentional impurities thereon. It is observed that the presence of intentional impurities enhances the thermal decomposition and decreases the energy of activation, E . The small change in the value of E suggests that the same chemical process govern the decomposition of the pure and the treated salts. The decrease in ΔS suggests that the decomposition is catalysed in the treated samples. The thermal stability of the bromate has been found to be dependent on the surface charge density of the cation of the impurity. Further studies with other homovalent and heterovalent impurities will be of use in determining the role of ionic properties in the thermal decomposition of bromates.

Deduction of mechanism of the decomposition reaction from non-isothermal kinetic data has shown that the decomposition of barium, nickel, neodymium and yttrium bromates follows the Avrami equation $1 - (1 - \alpha)^{1/3} = kt$ and the rate controlling process is a phase boundary reaction assuming spherical symmetry. Addition of impurities does not change the mechanism of decomposition.

It will be of interest to extend the studies on the effect of crystal defects introduced by irradiation, precompression, crushing or doping on the thermal decomposition of the bromates included in the present studies.

References

References

- 1-5 Young D.A., *Decomposition of Solids*, Pergamon Press, First edition, ch. 1, pages 1-4 (1966).
6. Rees, *Chemistry of the Defect Solid State*, Methuen, London, pp. 64, 114(1954).
7. Roginskii and Schultz, *Zeit. Phy. Chem.*, A 138.21(1928).
8. Kohlschutter, *Helv. Chim. Acta.*, 13, 978 (1930).
9. Garner and Maggs, *Proc. Roy. Soc.*, A 172, 299 (1939).
10. Bradley, Colvin and Hume, *Phil. Mag.*, 14 1102(1932); *Proc. Roy. Soc.*, A 137, 531 (1932).
11. Bright and Garner, *J. Che. Soc.*, 1872 (1934).
12. Cooper and Garner, *Trans. Faraday Soc.*, 32, 1739 (1936).
13. Bartlett.B.E., Tompkins.F.C. and Young.D.A., *Nature* 179, 365 (1957).
14. Bagdassarian, *Acta. Phy. Chim. URSS*, 20, 441(1945).
15. Thomas and Tompkins, *Proc. Roy. Soc.*, A 210, 111(1951).
16. Cooper and Garner, *Proc. Roy. Soc.*, A 174, 487(1940).
17. Garner and Hailes, *Proc. Roy. Soc.*, A 139, 576(1933).
18. Avrami, *J. Chem. Phys.*, 7, 1103 (1939); 8, 212 (1940); 9, 177 (1941).
19. Erofejev, *Compt. Rend. Acad. Sci. URSS*, 52, 511 (1946).
20. Prout and Tompkins, *Trans. Faraday Soc.*, 40, 488 (1944).
21. Eckhardt and Flanagan, *Trans Faraday Soc.*, 60, 1289 (1964).
22. Hanny N. B, *Solid State Chemistry*, Prentice Hall, Inc. New Jersey, Ch.3(1967).
23. Leonid V. Azaroff., *Introduction to Solids*, McGraw Hill Inc., New York, Ch.5(1977).
24. Thomas and Tompkins, *Proc. Roy. Soc.* A 210, 111(1951).
25. Garner W.E. and Tanner M.G., *J. Chem. Soc.*, 47 (1930).

26. Bancroft G.M. and Gesser H.D., *J. Inorg. Nucl. Chem.*, 27, 1545(1965).
27. Markowitz M.M, *J. Inorg. Nucl. Chem.*, 25, 407 (1963).
28. Horowitz H.H. and Metzger G., *Anal. Chem.*, 35, 1464(1963).
29. Erdey L., Simon J. and Gal S., *Talanta*, 15, 653 (1968).
30. Simon J, Gal S. and Erdey L., *Acta. Chim. Acad. Sci. Hung.*, 66, 175 (1970).
31. Sahoo. K.K., Bose.S., Misra.S, Bhatta. D., *Radiochim.Acta.*, 65(2), 141-8(1994)
32. Jach J., *Reactivity of Solids* (Ed. DeBoer J.H.), Elsevier Publication Co., Amsterdam, p. 334 (1961).
33. Arnikar H.J. and Patnaik S.K., *J. Univ. Poona Sci. Technol.*, 50, 163-70 (1977).
34. Venugopalan C.R., Radhakrishnan Nair T.D., *J. Indian Che. Soc.*, 57 (12), 1191-3 (1980).
35. Nair S.M.K., Malayil Koshykunju, Daisamma Jacob P., *Thermochim. Acta.*, 141, 61-80 (1989).
36. Nair S.M.K., James C., *Thermochim. Acta.*, 96(1) 27-36 (1985).
37. Diefallah, EL. H.M., Basahl, Suliman N., Obaid Abdullah Y, *J. Radioanal, Nucl. Chem.* 109(1) 177-81 (1987).
38. Diefallah, EL. H.M., Basahl, Suliman N., Obaid Abdullah Y, Abu-Eittah, Rafie H., *Thermochim. Acta.*, 111, 49-56 (1987).
39. Sahoo Mihir K., Bhatta D., *Radiat. Phys. Chem.* 39(4) 367-73 (1992).
40. Simpson, J., Taylor D, Fanshaw R.S., Horburg J.M. and Watson W.J., *J. Chem. Soc*, 3323 (1958).
41. John Simpson, Duncan Taylor, Fanshawe R.S., Miss Norbury and Watson W.J., *J. Chem. Soc.*, 3323 – 3328(1958).
42. Solymosi .F., *Structure and Stability of Salts of Halogen Oxyacids in the Solid Phase*, John Wiley and Sons.
43. Solymosi .F. and Bansagi T., *J. Phys. Chem.*, 74, 15(1970).

44. Luto Slawksa – Rogoz, J., Kapturkiewicz – Kowal E., Hodorowicz, S. A., *Cryst. Res. Technol.*, 30(2), 255-62(1995).
45. Bhattamisra S.D. and Mohanty S.R., *I. Inorg. Nucl. Chem.*, 39(12), 2103-9 (1977).
46. Bhattamisra S.D. and Mohanty S.R., *Indian J. Chem.*, 15A, 350 (1977).
47. Mohanty. S.R., and Satapathy.M., *Radio Chem. Radioanal. Lett.*, 37, 345 (1979).
48. Jena B., Mohanty S.R. and Satapathy M., *Indian J. Chem.*, 19A, 1139 (1980).
49. Gavande A.M. and Ray M.N., *Indian J. Chem.*, 20A, 326 (1981).
50. Glassner A. and Weidenfield L., *J. Amer. Chem. Soc.*, 74, 2467 (1952).
51. Nair S.M.K., Daisamma Jacob P., *Thermochim. Acta.*, 157(1), 67-76 (1990).
52. Nair S.M.K., Daisamma Jacob P., *Radioanal. Nucl. Chem.*, 137(2), 113-25 (1989).
53. Gavande A.M., Ray M.N., *Indian J. Chem.*, 18A(1), 16-18 (1979).
54. Sasmitha Dash, *Thermal Annealing and Thermal Decomposition of Irradiated Inorganic salts*, Ph.D. thesis, Calicut University (1992).
55. Gavande A.M., Ray M.N., *Indian J. Chem.*, 2A(3), 287-8 (1982).
56. Nair S.M.K., Daisamma Jacob P., *J. Radioanal. Nucl. Chem.*, 145(2), 103-11 (1990).
57. Yukiko Nishimura, *J. Chem Eng. Data*, 46(2), 299-307(2001).
58. Abbasi A, Eriksson L., *Acta. Crystallogr. Ser. E.*, 62 p.m. 126 (2006).
59. Abbasi, Alireza, Badiei Alireza, *Iran J. Chem. Chem. Eng.*, Vol. 26 No. 4(2007).
60. Mayor I. and Glassner Y., *J. Inorg. Nucl. Chem.*, 29, 1605 (1967).
61. Weigel F. and Engelhardt L.W.H, *Journal of the Less Common Metals*, 91 339-350(1983).
62. Nair S.M.K., Daisamma Jacob P., *Thermochim. Acta.*, 181, 269-76(1991).

63. Sasmitha Dash, *Thermal Annealing and Thermal Decomposition of Irradiated Inorganic salts*, Ph.D. thesis, Calicut University (1992).
64. Mohanty S.R., Patnaik D., *J. Therm. Anal.*, 35(7), 2153-9 (1989).
65. Kannan M.P and Abdul Mujeeb V.M, *Reaction Kinetics and Catalysis Letters*(Ausgabe), 00002(2001).
66. Das B.C., Patnaik D., *J. Therm. Anal. Calorimetry*, 61(3), 879-883(2000).
67. Patnaik. D., Pradhan. G.B., Patra. P., *Proc. Natl. Symp. Therm. Anal.*, 8th, 109-12 (1991).
68. Bhatta D., Jena B., Mohanty S.R., *Indian J. Chem.*, 27A(8), 661-5 (1988).
69. Mohanty S.R., Satapathy M., *Radiochem . Radional Lett.*,57(6), 345-8 (1979).
70. Jena B., Mohanty S.R., *Indian J.Chem.*, 19 A(12), 1139-41A (1980).
71. Jena B., Mohanty S.R., *Indian J.Chem.*, 20A(7), 717-18,A (1981).
72. Sahish T.S., *Themal Decomposition and Thermal Annealing of Irradiated Strontium Bromate* , Ph.D. Thesis, Calicut University (1993).
73. Nair S.M.K, Sahish. T.S, *Thermochim. Acta*, 250(1), 207-12(1995).
74. Sahoo. Mihir. K., Bhatta. D., *Thermochim. Acta.*, 197(2), 391-7(1992).
75. Bhatta D., Sahoo M.K., Jena B., *Thermochim. Acta.*, 132, 7-13 (1988).
76. Das B.C., Sethi K.K., *J. Teach. Res. Chem.*, 6(2), 41-46(1999).
77. Sahu K.K., Bose S., Bhatta D., *React-Kinet-Catal. Lett.*, 52(1), 149-54(1994).
78. Bhatta D., Mishra S., Sahu K.K., *J. Therm. Anal.*, 39(3), 275-80(1993).
79. Shoba U.S., Udupa M.R., *Proc. Natl. Symp.Ther. Anal.*, 9th 395-8(1993).
80. Shoba U.S., Udupa M.R.,*Thermochim. Acta.*, 242(1-2), 215-21 (1994).
81. Pramod G., Kannan M.P., *J. Indian Chem. Soc.*, 77(5), 261-263(2000).
82. Kannan M.P., Devi T. Ganga, *Thermochim. Acta.*, 292 (1-2), 105-109(1997).
83. Mohanty S.R., Patnaik D., *J. Indian Counc. Chem.*, 11(1) 47-51 (1995).

84. Mohanty, S.R., Patnaik S.K., *Indian J. Chem.*, Vol II No. 9, p 95(Sept. **1973**).
85. Bhatta D., Padhee G., *J. Therm Anal.*, 37 (11-12), 2693-9(**1991**).
86. Bhatta D., Sahoo M.K., Sahu K.K., *Radiochim Acta.*, 56(2), 105-9(**1992**).
87. Bhatta D., Mishra S., Sahu K.K., *Radiat. Eff. Defects Solids*, 143(1), 95-101 (**1997**).
88. Nair S.M.K., Sahish T.S., *J. Radio and Nucl. Chem.*,188(1), 73-82(**1994**).
89. Nair S.M.K., Sahish T.S., *J. Radional Nucl. Chem. Letters*, 176 (4) 345-352 (**1993**).
90. Nair S.M.K., Sahish T.S., *J. Radional Nucl. Chem. Letters*, 154(3) 163-181 (**1991**).
91. Nair S.M.K., Sahish T.S., *J. Radional Nucl. Chem. Letters*, 155(5), 351-357 (**1991**).
92. Nair S.M.K., Dash Susmita, *J. Radional Nucl. Chem.*,187(4), 313-23(June **1994**).
93. Sahu K.K., Bose S., Bhatta D., *Radiat Eff. Defects Solids*, 132(2), 179-85(**1994**).
94. Sahu K.K., Bose S., Bhatta D., *J. Radional Nucl. Chem.*, 176(1), 37-43(**1993**).
95. Nair S.M.K., Sahish T.S., Sasmita Dash, *J. Radional Nucl. Chem. Letters*, 187(5) 325-337 (**1994**).
96. Otta S., Bhattamisra S.D., Mishra S.R., *Proc. Natl. Symp. Therm. Anal.*, 9th 530(**1993**).
97. Otta S., Bhattamisra S.D., Mishra S.R., *Radiat Eff. Defects Solids*, 132(3), 265-73 (**1994**).
98. Nair S.M.K., Daisamma Jacob P., *Journal of Radioanalytical & Nuclear Chemistry*, Vol. 137, No. 2(Sept. **1989**).
99. Wesley W.M. Wendlandt, '*Thermal Methods of Analysis*', Chapter 11, John Wiley and Sons (Second Edition).
100. Brill O., *Z. Anorg. Chem.*, 45,275 (**1905**).

101. Dual C., *Inorganic Thermal Analysis*, 2nd Ed. Elsevier, London(1963).
102. Newkirk A.E. and Simons, E.L. ., *Talanta*, 9, 489 (1962).
103. Freeman E.S. and Carroll B., *J. Phys. Chem.*, 62, 394 (1958).
104. Bradley W.S. and Wendlandt W.W. ., *Anal. Chem.*, 43(2), 223-227 (1971).
105. Hill. J.O., *J. Therm. Anal.*, 42,607-621(1994).
106. Coats A.W. and Redfern J.P, *Analyst*, 88, 906(1963).
107. Newkirk A.E., *Anal. Chem.*, 32, 1558 (1960).
108. Dual C., *Anal. Chim. Acta.*, 31 (1964)
109. Simmons E.L. and Wendlandt W.W., *Thermochim. Acta.*, 3,171(1972).
110. Boldyrev V.V., *Thermochim. Acta.*, 388, 63 (2002).
111. Mohamed M. Mohamed, Andrew K. Galwey, Samith A. Halaway, *Thermochim. Acta.*, 429, 57(2005).
112. Galwey A.K., *Thermochim. Acta*, 397, 249(2003).
113. Galwey A.K., *Thermochim. Acta*, 399,1(2003).
114. Galwey A.K., *Thermochim. Acta*, 413,139(2004).
115. Simmons E.L. and Newkirk A.E., *Talanta* ,549(1964).
116. Garn P.D. and Kessler J.E., *Anal. Chem.*, 32,1563,1900(1960).
117. Sestak J., *Talanta* 32(1960).
118. Dollimore.D. and Pearce. J., *J. Therm. Anal.*, 6,321(1974).
119. Dollimore.D. *Thermochim. Acta.*, 38,1 (1980).
120. Doyle C.D. in “ *Techniques and methods of polymer evaluation*” Slade P.E. and Jenkins L.T., eds., Marcel- Dekker, New York, Chap.4 (1966).
121. Sestak J., *Talanta* , 13, 567 (1966).
122. Coats A.W. and Redfern J.P., *Nature*, 201,68 (1964).
123. Newkirk A.E., *Anal. Chem.*, 32, 1558 (1960).

124. Doyle C.D., *J. Appl. Poly. Sci.*, 5,285 (1961).
125. Ingraham T.R. and P. Marier, *Can. J. Chem. Eng.* ,161 (1964).
126. Vachuska J. and Voboril M., *Thermochim. Acta.*, 4, 97 (1972).
127. Dave N.G. and Chopra S.K., *Z. Physik. Chem.* 48, 257 (1966).
128. Achar B.N.N., Brindley G.W. and Sharp J.H., *Proc. Int. clay Conf. Jerusalem*, 1, 67 (1966).
129. Flynn. J.H and Wall. L.A, *Polym. Lett.*, 4,323 (1966)
130. Urbanovici. E. and Segal. E., *Thermochim. Acta.*, 80,379 (1984).
131. Maycock S.N ., Pai Verneker V.R. and Gorzynski C.S., *J. Phys. Chem.*, 72, 4015 (1968).
132. Wesley W.M. Wendlandt, '*Thermal Methods of Analysis*', Wiley, New York, 2nd edn., p.45 (1974).
133. Chatterji .A, Chattopadhyay K.N, Neogy .D, Paul .P, Reba Chatterjee, Chatterjee S., *Journal of Magnetism and Magnetic materials*, 271, 1-8 (2004).
134. Jeffery G.H. *et al*(revised by), *Vogel's Text book of Quantitative Chemical Analysis*, page 405,5th edn.(1989).
135. Nair S.M.K. and Daisamma Jacob P., *Thermochim. Acta.*, 179, 273-280 (1991).
136. Linke, W.F, *J. Am. Chem. Soc.*,77, 866-867 (1955).
137. Vernon A. Stenger, Richard M. Van Effen and Nile N. Frawley, *J. Chem. Eng. Data* , 45,1160-1161(2000).
138. Sidgwick N.V., *Chemical Elements and their Compounds*, Vol. I, Oxford University Press, London, p.258 (1950).
139. Lange N.A. and Forker G.M. (Eds.), *Handbook of Chemistry*, McGraw-Hill, New york , 10th edn., p. 224 (1961).
140. Bhattamisra S.D and Mohanty S.R., *Indian J. Chem.*, 15, 350(1977).

141. Pick H. and Weber W.I., *Z. Physik.*, 128, 409 (1950).
142. Delbeeq C.J., Hayes W. and Yuster P.H., *Phys. Rev.*, 121, 1043 (1961).
143. Johnson P.D. and Williams F.E., *Phys. Rev.*, 117, 964 (1960).
144. Maradudin, A.A, in F. Seitz and D. Turnbull(Eds), *Solid State Physics*, Vol. 16, Academic press, New York, Page 273(1966).
145. Dedgaonkar, V.G., Apte, R.G., Bhagwat, D.A., *J. Radioanal. Nucl. Chem.*, 239(1), 197-199 (1999).
146. Kazuo Nokomoto, *Infrared and Raman spectra of inorganic and coordination compounds*, 3rd edition, John Wiley & Sons, New York(1970).
147. Sestak. J., *Thermochim. Acta.*, 3,150(1971).
148. Sestak J. and Berggren G., *Thermochim. Acta.*, 3,1 (1971).
149. Satava V., *Thermochim Acta*, 2, 423 (1971).
150. Satava. V. and Skvara, F., *J. Am. Ceram. Soc.* 52, 591(1996).
151. Satava. V. and Skvara, F., *J. Therm. Anal.* 2,325(1970).
152. Satava. V. and Sestak. J., *Anal. Chem.* 45, 154(1973).
153. Sestak. J., Satava. V. and Wendlandt. W.W., *Thermochim. Acta.* 7,333(1973).
154. Somasekharan. K.N and Kalpagam. V., *J. Therm. Anal.*, 34,777-781(1988).
155. Nair S.M.K. and James C., *Thermochim. Acta.*, 83, 387-389 (1985).
156. Avrami M., *J. Chem. Phys.*, 7, 1103 (1939).
157. Galwey. A.K., Brown. M.E., *Thermochim. Acta.* 269,270(1995).
158. Dollimore D, in *Thermal Analysis-Techniques and Applications*, edited by E. L. Charsley and S. B. Warrington, Royal Society of Chemistry,(1992).